2015

A Mathematical Framework of Human Thought Process: Rectifying Software Construction Inefficiency and Identifying Characteristic Efficiencies of Networked Systems Via Problem-solution Cycle

Jonathan Sarbah-Yalley
Andrews University, yalley@andrews.edu

ABSTRACT

A MATHEMATICAL FRAMEWORK OF HUMAN THOUGHT PROCESS: RECTIFYING SOFTWARE CONSTRUCTION INEFFICIENCY AND IDENTIFYING CHARACTERISTIC EFFICIENCIES OF NETWORKED SYSTEMS VIA PROBLEM-SOLUTION CYCLE

by

Jonathan Sarbah-Yalley

Chair: Hyun Kwon, Ph.D.

ABSTRACT OF GRADUATE STUDENT RESEARCH

THESIS

Andrews University

College of Arts and Sciences

Title: A MATHEMATICAL FRAMEWORK OF HUMAN THOUGHT PROCESS: RECTIFYING SOFTWARE CONSTRUCTION INEFFICIENCY AND IDENTIFYING CHARACTERISTIC EFFICIENCIES OF NETWORKED SYSTEMS VIA PROBLEM-SOLUTION CYCLE

Date Name of researcher: Jonathan Sarbah-Yalley

Name and degree of faculty chair: Hyun Kwon, Ph.D.

Date completed: August, 2015

Problem

The lack of a theory to explain human thought process latently affects the general perception of problem solving activities. This present study was to theorize human thought process (HTP) to ascertain in general the effect of problem solving inadequacy on efficiency.

Method

To theorize human thought process (HTP), basic human problem solving activities were investigated through the vein of

problem-solution cycle (PSC). The scope of PSC investigation was focused on the inefficiency problem in software construction and latent characteristic efficiencies of a similar networked system. In order to analyze said PSC activities, three mathematical quotients and a messaging wavefunction model similar to Schrodinger's electronic wavefunction model are respectively derived for four intrinsic brain traits namely intelligence, imagination, creativity and language. These were substantiated using appropriate empirical verifications. Firstly, statistical analysis of intelligence, imagination and creativity quotients was done using empirical data with global statistical views from:

1. 1994–2004 CHAOS report Standish Group International's software development projects success and failure survey.
2. 2000–2009 Global Creativity Index (GCI) data based on 3Ts of economic development (technology, talent and tolerance indices) from 82 nations.
3. Other varied localized success and failure surveys from 1994–2009/1998–2010 respectively.

These statistical analyses were done using spliced decision Sperner system (SDSS) to show that the averages of all empirical scientific data on successes and failures of software production within specified periods are in excellent agreement with theoretically derived values. Further, the catalytic effect of creativity (thought catalysis) in human thought process is outlined and shown to be in agreement with newly discovered

branch-like nerve cells in brain of mice (similar to human brain). Secondly, the networked communication activities of the language trait during PSC was scrutinized statistical using journal-journal citation data from 13 randomly selected 1984 major chemistry journals. With the aid of aforementioned messaging wave formulation, computer simulation of message-phase "thermogram" and "chromatogram" were generated to provide messaging line spectra relative to the behavioral messaging activities of the messaging network under study.

Results

Theoretical computations stipulated 66.67% efficiency due to intelligence, imagination and creativity traits interactions (multi-computational skills) was 33.33% due to networked linkages of language trait (aggregated language skills).

The worldwide software production and economic data used were normally distributed with significance level α of 0.005. Thus, there existed a permissible error of 1% attributed to the significance level of said normally distributed data. Of the brain traits quotient statistics, the imagination quotient (IMGQ) score was 52.53% from 1994-2004 CHAOS data analysis and that from 2010 GCI data was 54.55%. Their average reasonably approximated 50th percentile of the cumulative distribution of problem-solving skills. On the other hand, the creativity quotient score from 1994-2004 CHAOS data was 0.99% and that from 2010 GCI data was 1.17%. These averaged to a near 1%. The chances of creativity

and intelligence working together as joint problem-solving skills was consistently found to average at 11.32%(1994-2004 CHAOS: 10.95%, 2010 GCI: 11.68%). Also, the empirical data analysis showed that the language inefficiency of thought flow $\eta'(\tau)$ from 1994-2004 CHAOS data was 35.0977% and that for 2010 GCI data was 34.9482%. These averaged around 35%. On the success and failure of software production, statistical analysis of empirical data showed 63.2% average efficiency for successful software production (1994 - 2012) and 33.94% average inefficiency for failed software production (1998 - 2010). On the whole, software production projects had a bound efficiency approach level (BEAL) of 94.8%.

In the messaging wave analysis of 13 journal-to-journal citations, the messaging phase space graph(s) indicated a fundamental frequency (probable minimum message state) of 11.

Conclusions

By comparison, using cutoff level of printed editions of Journal Citation Reports to substitute for missing data values is inappropriate. However, values from optimizing method(s) harmonized with the fundamental frequency inferred from message wave analysis using informatics wave equation analysis (IWEA).

Due to its evenly spaced chronological data snapshot, the application of SDSS technique inherently does diminish the difficulty associated with handling large data volume (big data)

for analysis. From CHAOS and GCI data analysis, the averaged CRTQ scores indicate that only 1 percent (on the average) of the entire human race can be considered exceptionally creative. However in the art of software production, the siphoning effect of existing latent language inefficiency suffocates its processes of solution creation to an efficiency bound level of 66.67%. With a BEAL value of 94.8% and basic human error of 5.2%, it can be reasonable said that software production projects have delivered efficiently within existing latent inefficiency. Consequently, by inference from the average language inefficiency of thought flow, an average language efficiency of 65% exists in the process of software production worldwide. Reasonably, this correlates very strongly with existing average software production efficiency of 63.2% around which software crisis has averagely stagnated since the inception of software creation.

The persistent dismal performance of software production is attributable to existing central focus on the usage of multiplicity of programming languages. Acting as an "efficiency buffer", the latter minimizes changes to efficiency in software production thereby limiting software production efficiency theoretically to 66.67%. From both theoretical and empirical perspective, this latently shrouds software production in a deficit maximum attainable efficiency (DMAE).

Software crisis can only be improved drastically through policy-driven adaptation of a universal standard supporting very

minimal number of programming languages. On the average, the proposed universal standardization could save the world an estimated 6 trillion US dollars per year which is lost through existing inefficient software industry.

Andrews University

College of Arts and Sciences

A Mathematical Framework of Human Thought Process: Rectifying Software Construction Inefficiency and Identifying characteristic efficiencies of networked systems via Problem-Solution Cycle

A Thesis

Presented in Partial Fulfillment

of the Requirements for the Degree

Master of Science

By

Jonathan Sarbah-Yalley

2015.

TABLE OF CONTENTS

LIST OF ILLUSTRATIONS

LIST OF TABLES

LIST OF ABBREVIATIONS

AGI	Artificial General Intelligence
AMP	Auxiliary Mixed-Skills Phases
BAC	Binary Asymmetric Channel
BEAL	Bound Efficiency Approach Level
BSCp	Binary Symmetric Channel
BVSR	Blind Variation and Selective Retention
CCN	Cognitive Control Network
CIFE	Creativity-Imagination Free Entropy
CIT	Constant Information-Theoretic
CMS	Constant Message Span
CPU	Central Processing Unit
DIDMT	Data-Information Driven Message Transmission
DMAE	Deficit Maximum Attainable Efficiency
DMGT	Differentiated Model of Giftedness and Talent
DMN	Default Mode Network
DMN	Default Mode Network
DSS	Decision Sperner System
DT	Divergent Thinking
EEG	Electroencephalographic
fMRI	functional Magnetic Resonance Imaging
GCI	Global Creativity Index
GCI	Global Creativity Index
HTP	Human Thought Process

HTPP	Human Thought Procedural Phases
ICCC	Intelli-creativity cumulative constant
IE	Ionization Energy
IEW	Inforentropic Waves
IWEA	Informatics Wave Equation Analysis
LTCSR	Language to Computational Skills Ratio
LYM	Lubell-Yamamoto-Meshalkin
MiDEOM	Missed Data Estimation Optimizer Method
mPFC	Medial Prefrontal Cortex
mPFC	medial Prefrontal Cortex
OPP	Objective Prior Probability
PDF	Strategies for Project Recovery
PSC	Problem-Solution Cycle
rFC	Functional Connectivity at Rest
RPSE	Random Pure State Ensemble
RPSE	Random Pure State Ensemble
SCP	Spontaneous Creativity Phase
SDSS	Spliced Decision Sperner System
SIC-POVMs	Symmetric, Informationally-Complete, Positive Operator-Valued Measures
SIRE	Standard Index of Recurrent Error
SNPs	Single Nucleotide Polymorphisms
TOF	Turn Over Frequency
TON	Turn Over Number
UNIQOD	Universal Quantization of Dimensional
wff	Well-formed formulas

CHAPTER 1

INTRODUCTION

Historical Perspective

For a computer to truly have a human-like brain in the future there is the need for a theory to facilitate understanding of the thinking processes of humans. One fundamental conundrum that is preventing a realistic artificial general intelligence (AGI) is the lack of understanding of how the human brain operates (Deutsch, 2012).

Basically, this inherent problem-solving routine concerns how in the absence of information the human brain is able to come up with theories concerning how things work in the environment. In order to achieve said understanding, what is really needed is a theory capable of defining or explaining how the human brain creates new explanations through creativity as its core functionality. Also, the very thinking of computer scientists and/or engineers who will be able to develop a realistic computer based AGI must pragmatically mimic said fundamental human thought process (HTP).

In isolation, inherent brain processes must include analytic abilities not only of itself but of its surroundings where an unexplained phenomenon originates a problem. As such,

the key to defining HTP is a process involving problem definition followed by solution search interactions from which an explanative answer of the unexplained problem is derived. This constitutes a problem-solution cycle (PSC). The basic codified rules (theory) of HTP embodied in PSC are founded on four intrinsic brain traits namely language, intelligence, imagination and creativity (LIIC). These will facilitate critical analysis of software construction inefficiency. Essentially rendered, the human thought process can be described as a theory of all theories or a theory about how theories are created.

CHAPTER 2

PROBLEM-SOLUTION CYCLE WITHIN THE PURVIEW OF HUMAN THOUGHT PROCESS

The art of mathematically modeling problems leads reasonably to solutions. This must be the core activity and thus the substantive cake of computing. Unfortunately, the art of transferring mathematical models via computer languages into computer programs, which forms the icing of the computing cake, has rather become the most desire computing endeavor. But the latter is merely a tool for problem-solving. If one must ascertain the truth of problem-solving activities, it is imperative that the quality characteristics of computing solutions are fundamentally sort.

Global Perspective of Problem-Solution Cycle

The British scientist, Lord Kelvin (Kelvin, 1883) once said:

> "In physical science the first essential step in the direction of learning any subject is to find principles of numerical reckoning and practicable methods for measuring some quality connected with it. I often say that when you can measure what you are speaking about, and express it in numbers, you know something about it; but when you cannot measure it, when you cannot express it in numbers, your knowledge is of a meagre and unsatisfactory kind; it may be the beginning of knowledge, but you have scarcely in your thoughts advanced to the state of Science, whatever the matter may be."

Without human thought process (HTP), problem-solving activities and hence communication thereof cannot take place. Using process-solution cycle (PSC) within the purview of HTP, the latter is mathematically modeled to facilitate measurements of PSC activities involving fundamental brain traits namely intelligence, imagination and creativity together with language during solution phase. Varied and valid mathematical theorems together with other necessary status quo mathematical or physics concepts are brought together to help derive new mathematical formulations to quantify each of the brain traits. Three mathematical quotients and a wave equation are derived and substantiated using appropriate empirical verifications. By definition, a model is primarily evaluated by its consistency to empirical data. So, firstly, statistical analysis of intelligence, imagination and creativity quotients based on two different sets of worldwide data namely CHAOS and GCI datasets is done. Of these worldwide survey data, the software production based CHAOS dataset represents a sample of HTP endeavor while the economic activity based GCI dataset generally represents the population of HTP endeavor. Statistically, consistency of the measured brain traits must prevail if the sample dataset is truly representative of the population dataset. This will be spearheaded by the vital role of creativity in problem-solving. Secondly, without communication, the brain traits cannot function to bring about solution in PSC and hence HTP cannot take place.

To facilitate statistical analysis of said inherent communication linkages networking intelligence, imagination and creativity via language, the aforementioned wave formulation is subjected to empirical scrutiny using dataset from journal-to-journal citation of 13 chemistry journals. The results thereof are compared to results from conventional analysis of the same dataset for the purpose of verification. In the words of Lord Kelvin (Kelvin, 1883), "to measure is to know" but "if you cannot measure it, you cannot improve it."

The Process of Problem-Solution Cycle

The processes involved in problem-solution cycle (PSC) are based on 4 basic characteristics of the human brain namely intelligence, imagination, creativity and language. Firstly, the defining phase expresses specific recognition of existing problem. Secondly, the derivation phase seeks for precise and accurate outcome (solution). Lastly, the interpretation phase involves analysis of the outcome to bring about a much needed candid understanding to facilitate the explanation(s) for why the recognized problem existed.

In defining a problem, firstly one has to practically solve any misconception of any presiding phenomenon which constitutes a problem, in order to clearly describe the problem. This means, a misconception represents a problem of the problem within scope. Secondly, a properly defined problem must be solved to create a

solution (which entails understanding) that works. This meta-solution gives understanding to the presiding phenomenon that initially needed a primo understanding for its definition. Thus, in general, a defined problem which is a solution from a presiding phenomenon also has a solution. In software development, such scenario has been its motherhood and apple pie. Hitherto, such scenario has been seen as 'solving' a problem once in order to define it and then solving the same problem again to create a workable solution (Peters & Tripp, 1976). Both solutions seemingly contradict each other and so came to be

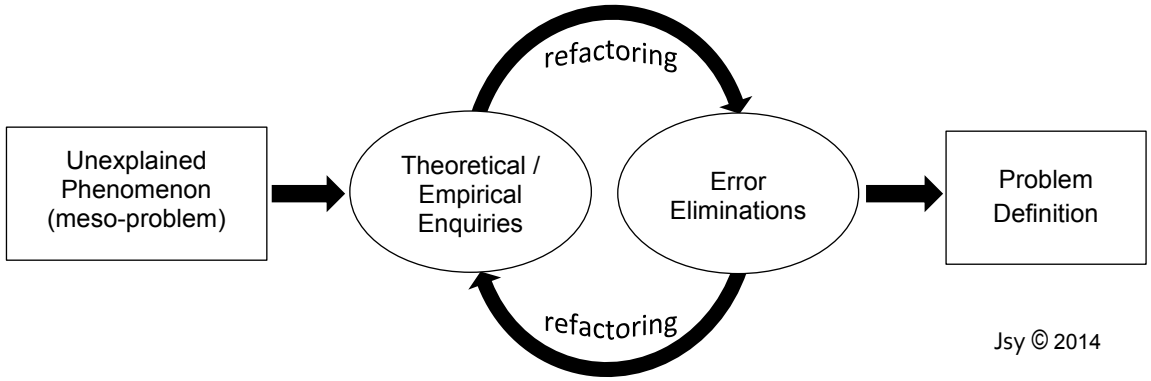

Figure 1. An unexplained phenomenon subjected to evolutionary problem formulation process to hone it into a problem definition.

called the paradox of design being 'wicked'. When an unexplained phenomenon in an environment is identified, the process of problem formulation which must adequately define the problem, leads to an ongoing cycle of hypothetical explanations as shown in figure 1. It involves refactoring of meso-problem (unexplained phenomenon) by subjecting it to

tentative theoretical enquiries which repeatedly brings about error elimination as further observations and/or measurements of the resident phenomenon are enquired until a meso-solution brings about a reasonable problem definition (see figure 2). This evolutionary honing process somewhat mimics Sir Karl Popper's theory on empirical falsification (deriving new explanations through the method of trial and the elimination of error) as applied to an unexplained problem.

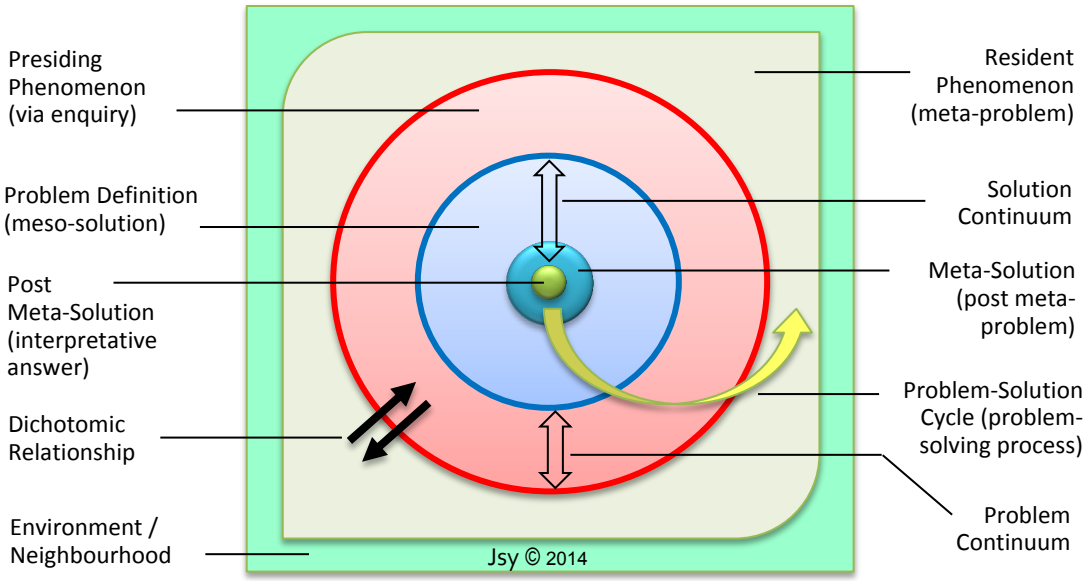

Figure 2. Depiction of problem-solution cycle in a general problem-solving process within an environment acting as a truth-functional system.

The hypothetical explanations of said unexplained phenomenon involve a reasoned proposal suggesting a possible correlation between the resident phenomenon and the presiding phenomenon within the neighbourhood of the environment. The

resident phenomenon which is the unexplained phenomenon identified, is the subject of enquiry. On the other hand, through further investigations, the characterizations (observations, definitions and measurements) of the resident phenomenon are encapsulated as presiding phenomenon which leads to a reasonable problem definition. The diagram in figure 2, explains the interlaced transitivity of a general problem-solving process. This involves problem definition, its meta-solution and post meta-solution together with their problem and solution continuums in an environment acting as a functional system. In order to bring about an understanding of the subject of enquiry (unexplained phenomenon), the meta-solution of the problem-solving process must be subjected to interpretation. This constitutes a post meta-problem. In general, solutions to problems should bring definitive understanding to the unexplained environmental phenomenon else they are of no importance or use. The work done in interpreting meta-solution, leads to an interpretative answer for the quest to understand the unexplained phenomenon. The successful result of this work constitutes a post meta-solution. Thus, the meta-solution automatically reconnects to the unexplained phenomenon through post meta-solution thereby elucidating it in a crystal clear fashion to complete the problem-solving process making it a problem-solution cycle. In general, the problem-solution cycle is an incremental integration of sub problem-solutions namely meta-problem/meso-

solution, problem definition/meta-solution, and post meta-problem/interpretative answer.

The efficient path for an excellent computer solution sort (see figure 3) must be based on both programming language and computational truth-functionality. But rather, a state of inefficiency brought about by a trend of multiple programing language knowledge acquisition (see figure 3), leads to a distorted language to computational skills ratio (LTCSR) which is ideally defined as

$$1{:}X \;\; where \;\; X > 1$$

and X is the number of multiple ideal algorithmic skills (see figure 3) namely intelligence, imagination and creativity which constitute computational skills. Note that language is classified as ideal communication skill. Within the sub units of programming languages namely internet authoring, artificial intelligence (AI), and general-purpose, each sub-unit consists of multiple programming languages due to the lack of certain capabilities. The existing deficiency in any of the programming languages implies none of them actually possess truth-functionality (absolute) to satisfy a self-sufficient language.

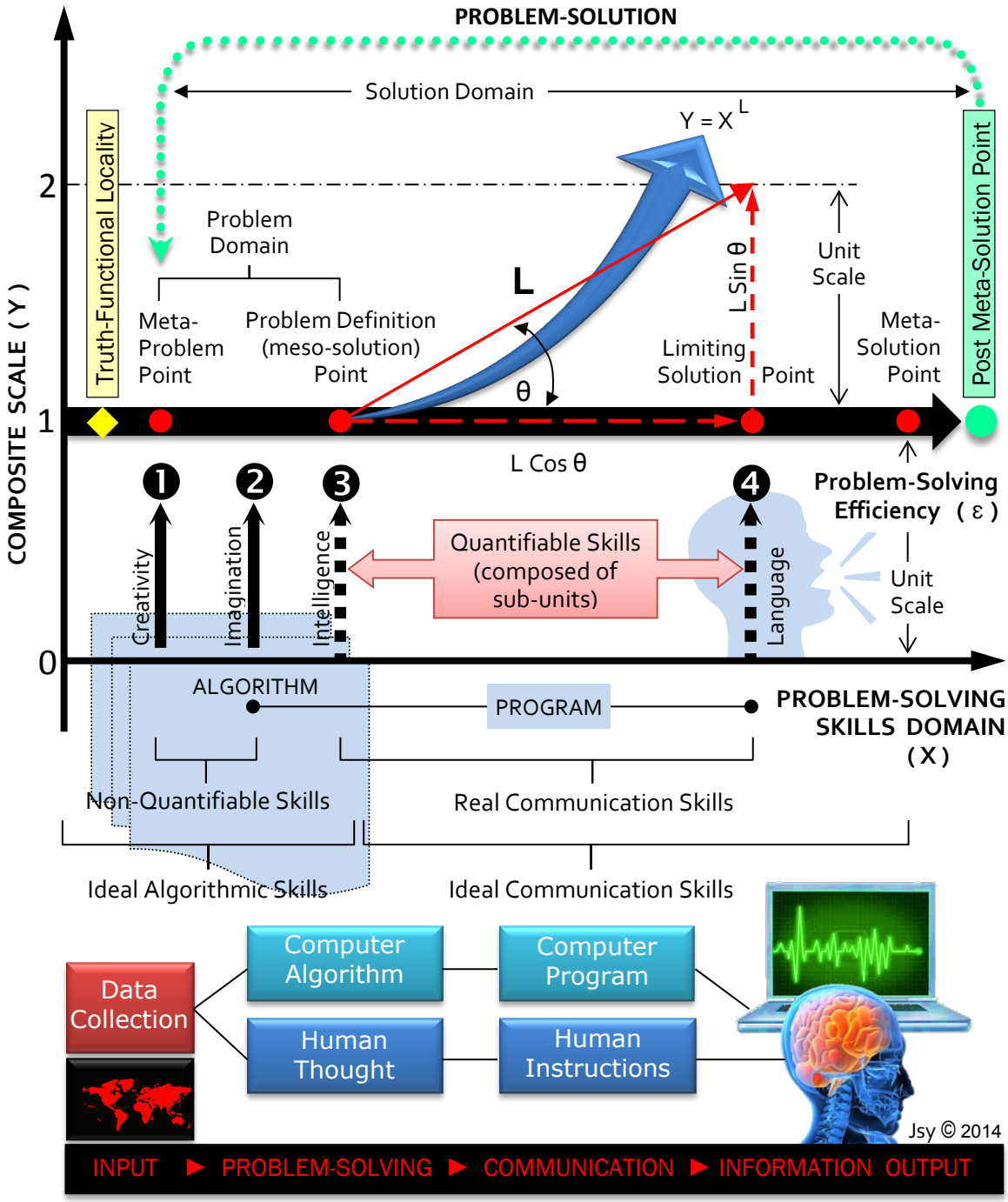

Figure 3. A graph representing a general analytic approach to the understanding of the dynamics involved in the efficiency determination of a problem-solving process.

This lack of truth-functionality renders contemporary trending in the introduction and acquisition of knowledge or part thereof in both new and existing programming languages, an inefficient process as depicted in the illustration in figure 3. Generally, it is reasonable to say that the usage of a language be it computer language, mathematical language or natural language as a means of computer, human or mathematical logic communication, respectively increases in efficiency when it is limited to a minimum that approaches one. This is the case with the pedagogical use of natural languages. In a school setting, only one language of instruction is used for the multiple subjects that would be studied by students. This approach efficiently yields excellent results. However in the computing scenario, the opposite is done and this affects the efficiency of solution processes. The dependency on multiple languages, naturally leads to lesser emphasis on the much needed computational and logic abilities (derivatives of intelligence) and creative skills for the creation of effective decision procedures to solve defined problems. The components of skills generally required in any problem-solving process, including scientific method which is a form of investigative algorithm, are creativity (phenomenon leading to the creation of something new and valuable), imagination (formation of new images and sensations not perceptible through normal senses) and intelligence (enables humans to experience and think) (Einstein & Infeld, 1938).

Intelligence, according to Merrian-Webster dictionary (merrian-webster, 2015) is: "the ability to learn or understand things or to deal with new or difficult situations." Thus, with intelligence, one pulls from a reserve of acquired knowledge (natural sciences, social sciences, technologies etc.) to understand things. However, since this capacity to learn is facilitated by communication tool, language is added as the fourth basic skill.

The appropriate data collected, as a meta-problem helps to define the problem and the resulting problem definition which serves as a solution to the meta-problem helps in the understanding of the procedure for data collection. Thus, there is a dichotomic relationship between meta-problem (resident phenomenon) and problem definition (presiding phenomenon) as shown in figure 2.

Interpretive Answer as Admissible Decision Rules

The rule for making a decision such that it is always "better" than any other rule is in statistical decision theory called admissible decision rule (Dodge, 2003). Under a problem-solution process, such admissible decision rule is formally determined as follows.

Let Θ, X, π and Δ represent sets defined as follows: Θ is the natural laws or principles governing the environment, X the possible observed phenomena, π the actions taken to define

problems and Δ the progressive changes or shifts in the understanding or interpretation of inexplicable environmental principles. Then the evidence of an unexplained environmental principle θ ∈ Θ through an observed phenomenon x ∈ X (resident phenomenon) forms a random distribution dubbed presiding enquiry phenomenon which is denoted as

$$F(x|\theta)$$

A decision rule which forms the problem continuum is defined as a function given by

$$\sigma : X \longrightarrow \pi$$

Based on a phenomenal observation x ∈ X, the decision rule leads to a problem definition action which is denoted as

$$\sigma(x) \in \pi$$

On the basis of a defined meta-problem p ∈ π honed by truer state of environmental principle θ ∈ Θ which is achieved by observed data x ∈ X, the general solution function Ψ representing the solution continuum is defined as

$$\Psi : \Theta \times \pi \longrightarrow \Delta$$

It must be noted here that the dichotomic relationship resulting from the Cartesian product Θ × π gives the set of all ordered pairs with the first element of each pair selected from Θ and the second element selected from π. On the other hand, Δ represents the gained interpretation of initial inexplicable environmental principle via meta-solution which constitutes a feedback to problem. This implies the culminating meta-solution function will be given by

$$\Psi\big(\theta, \sigma(x)\big)$$

By definition, the expected value E(X) of a random variable x repeated k number of times with corresponding probability P_k is given by the average of values obtained as

$$E[X] = \frac{x_1 p_1 + x_2 p_2 + \cdots + x_k p_k}{p_1 + p_2 + \cdots + p_k}$$

Consequently on the basis of expectation, the interpretation function which represents the post meta-solution can thus be defined as

$$\Delta(\theta, \sigma) = E_{F(x|\theta)}\big[\Psi\big(\theta, \sigma(x)\big)\big]$$

This implies the terminating phase of problem-solution cycle occur when

$$\Delta(\theta, \sigma) < \Delta(\theta, \sigma^*) \;\; for\ all\ \theta$$

where the post decision rule σ* based on the post meta-problem

action which is essentially the meta-solution given by $\sigma^*(x) \in \pi$ performs better or dominates that of the pre-decision rule σ which is based on the meta-problem and denoted as $\sigma(x) \in \pi$. The maximal elements of the above partial order of the decision rules form the admissible decision rules (not dominated by any other rule) called interpretative answer.

Skills Proportions Based on Language to Computational Skills Ratio

Given each skill has a unit value, the LTCSR ratio which is 1: X can be expressed as 1:3 with 3 representing the number of computational skills. Given an absolute state of efficiency, the following proportions can be derived.

The total number of skills units possible in the given system above is 4 (namely language, creativity, intelligence and imagination). Thus, the proportion of language unit is ¼ which gives 0.25 or 25%. That for the other complementing or multiple computational skills units for which the total count, X = 3 is given as ¾ = 0.75 or 75%. Without any additional or extra language unit skill, the vector L in figure 3 above will be given by

$$L = L\,cos\theta \;\; where \;\; \theta = 0°$$

However, as the multi-unit languages increases with time, effort in solution activity shifts. All of the fundamental skills are of a one or single unit. Only intelligence and language skills

can be sub-scaled into multiple sub-units, each lacking absolute truth-functionality but together absolute truth functionality is attained and as such can be compared in terms of a gain or loss of skill units. Thus, the skills unit transfer will be the difference between intelligence and language skills. In a scenario where language skill has more attention than the intelligence skill, there will be more gain for the language skill. To compute this change, an ideal condition will have to be considered first. Under this ideal condition, all skills have to be considered as equal and of magnitude 1. Here, the change in language sill vector and actual exponential growth can be denoted as

$$L\,cos\theta \;=\; Ln\,1 = 0$$

where 1 represents the count for language skill unit and Ln the natural logarithm. In the case where there is a gain in language skill magnitude by count and a corresponding decrease in intelligence skill magnitude, the LTCS ratio proportions changes to the following. X is now is given by the original value of 3 plus an extra unit gained by the language skill for its exponential growth. Thus, the new value of X is 5. Hence, the proportion for the language skills is now 2/5 = 0.4 or 40% and that for the multiple computational skills will be 3/5 = 0.6 or 60%. Let the equation of the exponential growth of multiple language usage be given by

$$y = X^{L}$$

where L is the ideal unit (IU) of language skill necessary to bring about an exponential change. Observe that if L = 1 then y = X which is the ideal unit of L. Also, note that y is the units scale. For an ideal unit of 1, which is the case when there is no exponential change δx_o, the closed system situation can be represented as

$$\delta x_o = L\, cos\theta \;=\; \ln 1 = 0$$

Any exponential change in the problem-solution process must be accompanied by a corresponding increase in X in a close system as shown in figure 4. Under a balanced logarithmic change condition, this implies a change δx that draws on X can be

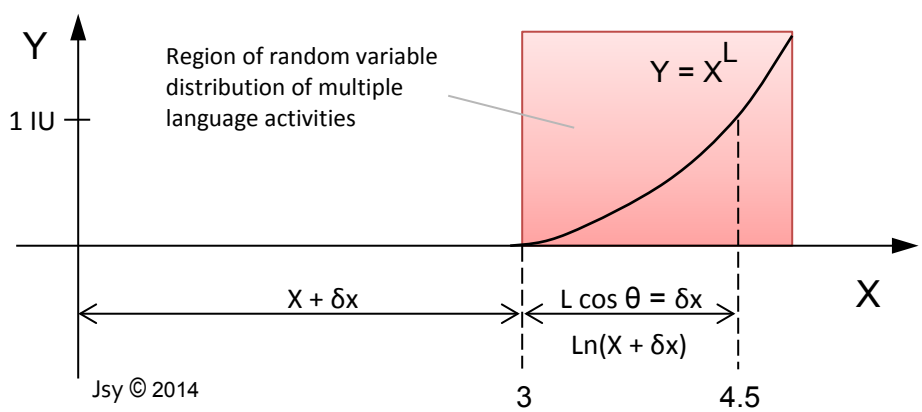

Figure 4. A balanced logarithmic change resulting from aggregated language skill within the close system of problem-solving process.

denoted as

$$\ln(X + \delta x) = \delta x \quad where \quad \delta x \;> 0$$

Ideally, if the original LTCS ratio of 1:3 is to be maintained in the close system of problem-solution process, then any addend language skill must also be of a 1 IU. In aggregation, this gives the exponential language skills a total of 2 IU. By proportion, if 1 IU of language skill interacts with 3 IU of multi-computational skills, then 2 IU of aggregated language skills will under a close system correspond to lesser units of multi-computational skills which can be expressed as (½)3 = 1.5 IU. Substituting the change value δx in the balance logarithmic change condition as 1.5 IU, the following is derived

$$\ln(X + \delta x) = 1.5$$

which implies

$$X + \delta x = e^{1.5} = 4.48 = 4.5 \quad Q.E.D$$

In general, let IU be an ideal unary unit and RU be a real unit such that

$$|IU| = 1 \quad and \quad |RU| \; is\ a\ real\ number$$

then

$$\lim_{|RU| \to |IU|} \frac{X}{|RU| + X} = \frac{X}{\ln(X + \delta x) + X} = \frac{X}{1.5 + X}$$

where X is the number of multi-computability skills. Thus, the proportion for aggregated language skills is 1.5/4.5 = 0.33 or 33.33%. On the other hand, the multi-computational skills give (3/4.5) = 0.6667 or 66.67%. The implication here is that under an aggregated language scenario (see figure 5 below) in a

problem-solution process, the resources of solution skills are drained towards language resources. This siphoning effect suffocates the process of solution creation due to lack of adequate essentials for solution creation. Thus, a random sampling of activity (see figure 4) under conditions of multiple languages is expected to mostly show a normal distribution as a result of the balanced logarithmic change condition and be bound mostly by 1 standard deviation (68%). This is largely due to the **latent language inefficiency** of 33.33% attributed to the sapping effect of multiple language condition on resources of multi-computational skills. According to Encyclopedia of Computer Languages, over the years 8500 programming languages have been created. Later, the above assertion will be definitively supported by empirical analysis.

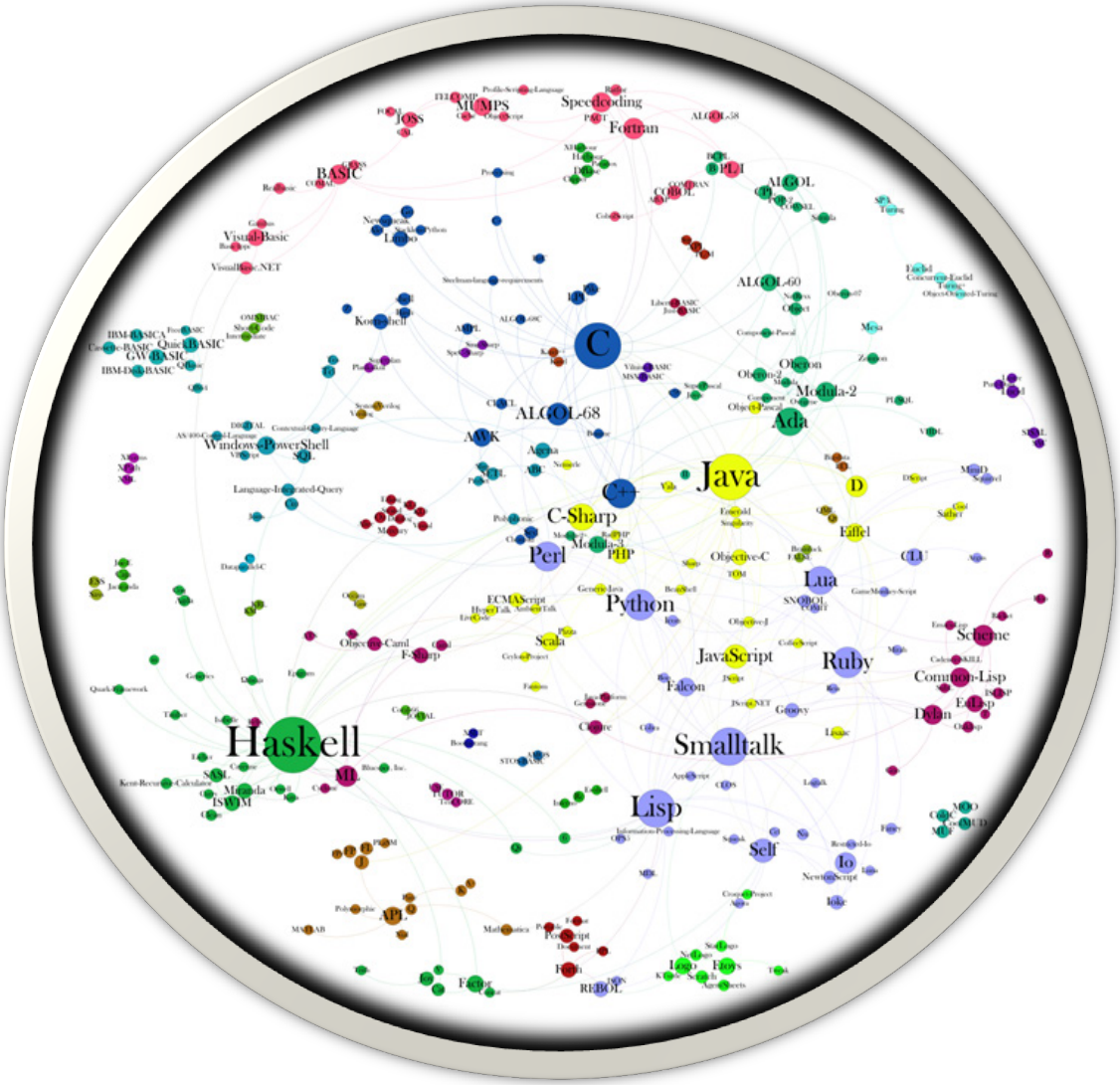

Figure 5. A chart showing cluster of computer programming languages. Adapted from *Graphs of Wikipedia: Programming Languages*, by Brendan Griffen, retrieved January 1, 2014, from http://brendangriffen.com/blog/gow-programming-languages/

CHAPTER 3

SPLICED DECISION SPERNER SYSTEM

In a general decision problem-solving activities, let the sample space $\mathcal{S}$ of n sets of outcomes be derived from n events each with k possible outcome types namely, success (S), failure (F) and mixed (M) outcomes. Then, the following generality can be put forth. Let the set of the output rates of a given general problem-solution process be

$$O = \{O_S, O_F, O_M\}$$

where

$$O_M = O_S \cap O_F$$

and O_S, O_F, O_M are sets representing success rates, failure rates and mixed rates respectively. This implies the decision set be given by $D = \{O_S, O_F\}$. Thus, the set of all the subsets of the set D (i.e. the elements of the set O) including the empty set and D itself represents the power set of the set D, denoted P(D). Also, let each output set be given as $O_S = \{O_{S1}, O_{S2}, O_{S3}, \ldots, O_{Sn}\}$, $O_F = \{O_{f1}, O_{f2}, O_{f3}, \ldots, O_{fn}\}$ and $O_M = \{O_{m1}, O_{m2}, O_{m3}, \ldots, O_{mn}\}$ as shown in table 1. Then, there exists a decision Sperner family $\mathcal{F}$ or decision Sperner system (DSS) over O such that

$$\mathcal{F} = \{F_1, F_2, F_3, \ldots, F_n\}$$

where the family of sets are $F_1 = \{O_{s1}, O_{f1}, O_{m1}\}$, $F_2 = \{O_{s2}, O_{f2}, O_{m2}\}$, $F_3 = \{O_{s3}, O_{f3}, O_{m3}\}$, and $F_n = \{O_{sn}, O_{fn}, O_{mn}\}$ and each n-element/member set of the family of sets ($\mathcal{F}$, O) has a *k*-element size and none of the sets is contained in another. See table 1 for a tabulation of these sets and their inter-relations. Below

Table 1

A Decision Sperner System Composed of n-Element Set and Corresponding k-Element Subsets

DECISION SPERNER SYSTEM							
	DECISION SET (D)	SAMPLE SPACE	DECISION SPERNER FAMILY	OUTCOME SET (O) Size = k			EVENTS
	$\{O_S, O_F\}$	($\mathcal{S}$)	$\mathcal{F}$ Size = n	O_S	O_F	O_M $O_S \cap O_F$	(E) Size = n
POWER SAMPLE SPACE	POWER SET OF DECISION P(D)	S_1	F_1	O_{11}	O_{12}	O_{13}	E_1
		S_2	F_2	O_{21}	O_{22}	O_{23}	E_2
		S_3	F_3	O_{31}	O_{32}	O_{33}	E_3
		.	.	.	.	.	.
		.	.	.	.	.	.
		.	.	.	.	.	.
		S_n	F_n	O_{n1}	O_{n2}	O_{n3}	E_n

in figure 6 is a hand template identifying set, subsets and elements of a decision Sperner system. The 4 subsets (represented by the index fingers) instead of the 6 maximum

subsets means that the hand template is a golden ratio (4:6) model decision Sperner system. It must be noted that DSS is an independent and randomized system or a clutter.

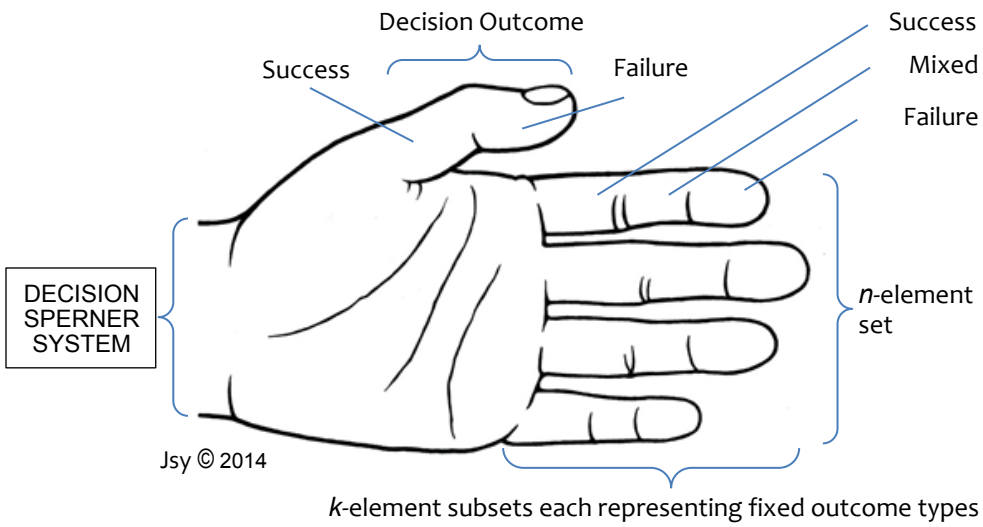

Figure 6. A human hand template for identifying the family of sets of a decision Sperner system. Image adapted from Daily Mail, *Fight or flight: Experts say human hands evolved for punching and not just dexterity*, by Mark Prigg, retrieved December 20, 2012, from http://www.dailymail.co.uk/sciencetech/article-2250720/Fight-flight-Experts-say-human-hands-evolved-punching-just-dexterity.html

In accordance with Sperner's theorem, the largest possible size of the family of sets of a Sperner family with k-element subsets and an n-element set occurs when

$$k = \frac{n}{2}$$

if n is even. But if n is odd, then the nearest integer thereof of k is taken. Formally stated, for every Sperner family $\mathcal{F}$ over an n-element set, its size is given by

$$|\mathbf{F}| \leq \binom{n}{\lfloor n/2 \rfloor}$$

where $\lfloor n/2 \rfloor$ of the combination at the right hand side of the inequality is the floor or the largest integer less than or equal to n/2. With each 3-element subset of the n-element set of the decision Sperner system (family of sets) of the decision analysis of a general problem-solution, the maximum size of the number of subsets is given as

$$Maximum\ number\ of\ sets = 2k = 6\ \ decision\ events$$

Thus, a maximum of 6 subsets are needed in the decision analysis of a general problem-solution. It gives the maximum size of the decision Sperner system as

$$|\mathbf{F}| \leq \binom{6}{3} = \frac{6!}{3!\,(6-3)!} = \frac{720}{6(6)} = \frac{720}{36} = 20$$

This implies the maximum number of outcome elements or events under the decision Sperner system is 20. Consequently, it is expected that for a 3-element outcome 6 events, there will be 18 outcome elements since an increase to a 3-element outcome 7 events will yield 21 outcome elements which is against the stipulated maximum of 20. Table 2 (below) shows the maximum outcomes of a spliced decision Sperner system which will be further explained later on.

Table 2

A Spliced Decision Sperner System Composed of 6-Element Set and Corresponding 3-Element Subsets in Accordance with Theoretical Proof

DECISION SET (D)	TIME FRAME	SAMPLE SPACE	DECISION SPERNER FAMILY	OUTCOME SET (O) Size = k			EVENTS
$\{O_S, O_F\}$	(T)	($\mathcal{S}$)	$\mathcal{F}$ Size = 6	O_S	O_F	O_M $O_S \cap O_F$	(E) Size = 6
POWER SET OF DECISION P(D)	0	S_1	F_1	O_{11}	O_{12}	O_{13}	E_1
	1	{ }	{ }	{ }	{ }	{ }	$E_{\emptyset 1}$
	2	S_2	F_2	O_{21}	O_{22}	O_{23}	E_2
	3	{ }	{ }	{ }	{ }	{ }	$E_{\emptyset 2}$
	4	S_3	F_3	O_{31}	O_{32}	O_{33}	E_3
	5	{ }	{ }	{ }	{ }	{ }	$E_{\emptyset 3}$
	6	S_4	F_4	O_{41}	O_{42}	O_{43}	E_4
	7	{ }	{ }	{ }	{ }	{ }	$E_{\emptyset 4}$
	8	S_5	F_5	O_{51}	O_{52}	O_{53}	E_5
	9	{ }	{ }	{ }	{ }	{ }	$E_{\emptyset 5}$
	10	S_6	F_6	O_{61}	O_{62}	O_{63}	E_6

Partitioning and Induction of Mixed Outcome Set

Consider a spliced mixed outcome set O of a decision Sperner system in which its *n* elemental subsets are interleaved with an empty set $\emptyset$. Then a right-open interval over a general spliced mixed outcome can therefore be expressed as

$$[O_{m1}, O_{mn}) = \{O_M \in O: O_{m1} \cup \emptyset_1 \cup O_{m2} \cup \emptyset_2 \cup O_{m3} \cup \emptyset_3 \cup \cdots \cup O_{mn} \cup \emptyset_n\}$$

where O is the set of output rates of a given general problem-solution process. Since every mixed outcome of the *n*-element subset is different, each empty set interleaving the elemental

mixed outcomes must be different from each other. This can be expressed mathematically as

$$\{O_M: O_{m1} \cap O_{m2} \cap O_{m3} \cdots \cap O_{mn}\} = \{\emptyset_1 \cap \emptyset_2 \cap \emptyset_3 \cdots \cap \emptyset_{n-1}\} = \emptyset \ \ or \{\ \}$$

This expression reads: the mixed outcome is such that its elemental intersections are equal to interleaving empty sets. The *n*-element mixed outcome and its intervening *n*-element empty sets form a mesh or lattice through signed connectivity. This lattice structure is facilitated by a partially induced decision partitioning of each of the *n* elements of the mixed outcome and a partially induced zero sign transformation of each of the intervening *n*-element empty sets.

Under a partially induced decision partitioning, the success and failure outcomes are respectively mapped to 1 and 0 on a probability scale. Thus, the mixed outcome which is neutral has a mean probability of 0.5. Since the mixed outcome is a composite of some degree of success and failure, its internal components after partitioning can be ordered generally as follows

$$P(O_{fx}) < P(O_{Sx})$$

where x = 1, 2, 3, …, n. On the other hand, the induced zero sign transformation of an empty set is derived from a positive or negative signed zero. While the number 0 is usually encoded as +0, it can however be represented as either positive zero (+0) or negative zero (-0). These signed zeroes are included in IEEE 754 (Kahan, 1987). They have applications in computing under

most floating-point number representations for integers, the sign and magnitude and ones' complement signed number representations for integers. Also, they have theoretical applications in disciplines such as statistical mechanics. Regarded as equal in numerical operations as the number 0, the signed zeroes have opposite sign behaviours just like positive integers $\mathbb{Z}^+$ and negative integers $\mathbb{Z}^-$ (both signed integers) (Kahan, 1987).

Let the partially induced partition (⊢) of a general mixed outcome, O_M be given as

$$\{O_{mx}^{+}\ ,\ O_{mx}^{-}\} \vdash O_M$$

Then each of the double elements of the partitioned set O_M is subject to an induced ordering that yields a double or 2-tuple expressed as

$$O_{mx}^{+} \vDash \langle O_{S1}, O_{f1} \rangle \quad and \quad O_{mx}^{-} \vDash \langle O_{S2}, O_{f2} \rangle$$

where x = 1, 2, 3, …, n and $O_{S1} < O_{f1}$ and $O_{S2} < O_{f2}$. The above mathematical expression reads: the partially induced positive partition entails (⊨) an induced upper pair of success and failure outcome and the partially induced negative partition entails an induced lower pair of success and failure outcome. In general, the implication is that each of the paired elements of the partitioned set O_M has a maximum and minimum element given by

$$\forall\, O_{mx}^{+} : O_{mx}^{+} \vee \bot = O_{S1} \ and\ \forall\, O_{mx}^{+} : O_{mx}^{+} \wedge \top = O_{f1}$$

$$\forall\, O_{\overline{m}x} : O_{\overline{m}x} \vee \bot = O_{S2} \;\; and \;\; \forall\, O_{\overline{m}x} : O_{\overline{m}x} \wedge \top = O_{f2}$$

which means for all positive O_M each corresponding paired tuple, in terms of a join (∨) with its top or largest element (⊤) of the order, has a maximum success outcome O_{S1} and in terms of a meet (∧) with its bottom or smallest element (⊥) of the order a minimum failure outcome O_{f1}. In similitude, for all negative O_M each corresponding paired tuple has a maximum success outcome O_{S2} and a minimum failure outcome O_{f2}.

Under Bayesian statistical inference, the principle of indifference or insufficient reason is a rule for assigning evidential probabilities based on n (greater than one) mutually exclusive and collectively exhaustive possibilities that except for their names are indistinguishable such that each elemental possibility is assigned a probability equal to the reciprocal of n. Though the partially induced success and failure outcomes of the mixed outcomes in a spliced DSS constitute uninformative or objective prior, the probabilities can be ascribed here is slightly different. In order for the assigned probabilities to fit equally within the probability range from 0 to 1, each elemental outcome is assigned a probability equal to the reciprocal of n + 1. By invocation of the principle of indifference, the ascribed probabilities will each be 1/5 = 0.2 apart. Thus, the double pair of tuples can be evenly ordered between the mappings of the success and failure outcomes as follows

$$\begin{array}{cccccc} O_F & O_{f2} & O_{S2} & O_{f1} & O_{S1} & O_S \\ \downarrow & \downarrow & \downarrow & \downarrow & \downarrow & \downarrow \\ 0 & 0.2 & 0.4 & 0.6 & 0.8 & 1 \end{array}$$

Also, let a partially induced zero sign transformation of an empty set be denoted as

$$\{+0, -0\} \vdash \emptyset$$

where the equivalent signed zero transformation of the empty set is given as

$$\emptyset^+ \equiv +0 \quad and \quad \emptyset^- \equiv -0$$

then the following expression

$$\emptyset_0^- \cup \{O_{m1}^+ \cup O_{m1}^-\} \cup \emptyset_1^+ \cup \{O_{m2}^- \cup O_{m2}^+\} \cup \emptyset_2^- \cup \{O_{m3}^+ \cup O_{m3}^-\} \cup \emptyset_3^+ \cup \cdots \cup \{O_{mn}^- \cup O_{mn}^+\} \cup \emptyset_n^-$$

is representative of the said induced lattice of spliced mixed outcome linked by sign connectivity. By definition, all intervening empty sets are automatically sensitized once two bordering subsets from an *n*-element subset are the subject of decision analysis.

Proof of Partitioning and Inductive Processes

The Lubell-Yamamoto-Meshalkin inequality (LYM inequality) which provides a bound on a Sperner family, stipulates that: if a_k denotes the number of sets of size k in a Sperner family over a set of n elements, then (Engel, 1997)

$$\sum_{k=0}^{n} \frac{a_k}{\binom{n}{k}} \leq 1$$

The proof of partitioning and induction processes applied on the mixed outcome subset lies in its testability with LYM theorem which is an inequality on the sizes of sets in a Sperner family. If emphatically correct, the value of computed LYM inequality for a spliced DSS must correspond to a 95% confidence interval which is the most used traditionally (Zar, 1984) and also seen as a realistic precision and sample size estimate (Altman, 2005). Under a spliced decision Sperner system (SDSS), the number of sets of size k in the family of subsets is best envisaged when the effect of both partially induced partitions of mixed outcomes is extended to the whole system as denoted below

$$\emptyset_0^- \cup \begin{Bmatrix} O_{S1} \cup O_{S1} \\ O_{m1}^+ \cup O_{m1}^- \\ O_{f1} \cup O_{f1} \end{Bmatrix} \cup \emptyset_1^+ \cup \begin{Bmatrix} O_{S2} \cup O_{S2} \\ O_{m2}^- \cup O_{m2}^+ \\ O_{f2} \cup O_{f2} \end{Bmatrix} \cup \emptyset_2^- \cup \begin{Bmatrix} O_{S3} \cup O_{S3} \\ O_{m3}^+ \cup O_{m3}^- \\ O_{f3} \cup O_{f3} \end{Bmatrix} \cup \emptyset_3^+ \cup \cdots$$

$$\cup \begin{Bmatrix} O_{Sn} \cup O_{Sn} \\ O_{mn}^- \cup O_{mn}^+ \\ O_{fn} \cup O_{fn} \end{Bmatrix} \cup \emptyset_n^-$$

with corresponding induced family of sets of the spliced decision Sperner system over the outcome or output rates O denoted as

$$\begin{array}{ccccccccccccccccccc} F: \{F_1^- & ,F_2^+ & F_3^- & ,F_4^+ & ,F_5^- & F_6^+ & ,F_7^- & ,F_8^+ & F_9^- & ,F_{10}^+ & ,\cdots & ,F_n^- & F_n^+ & ,F_n^-\} \\ & \Downarrow & & & & \Downarrow & & & \Downarrow & & & & \Downarrow & \\ & F_1 & & & & F_2 & & & F_3 & & & & F_n & \end{array}$$

It must, however, be noted that the extended success and failure outcomes due to the partially induced partitions of mixed outcomes are in effect redundant to the partial induction of sign

transformation of the mixed outcomes. This is because by idempotent law of sets, given a set A

$$A \cup A = A$$

Therefore, the extended success outcomes can be expressed as

$$\prod_{i=1}^{n}(O_{Si} \cup O_{Si}) = (O_{S1} \cup O_{S1}, O_{S2} \cup O_{S2}, O_{S3} \cup O_{S3}, \cdots, O_{Sn} \cup O_{Sn})$$

$$= (O_{S1}, O_{S2}, O_{S3}, \cdots, O_{Sn})$$

which means the set of all (n + 1)-tuples of union between two equal success outcomes. Similarly, the extended failure outcomes is denoted as

$$\prod_{i=1}^{n}\left(O_{fi} \cup O_{fi}\right) = \left(O_{f1} \cup O_{f1}, O_{f2} \cup O_{f2}, O_{f3} \cup O_{f3}, \cdots, O_{fn} \cup O_{fn}\right)$$

$$= \left(O_{f1}, O_{f2}, O_{f3}, \cdots, O_{fn}\right)$$

which interprets as the set of all (n + 1)-tuples of union between two equal failure outcomes. Consequently, the number of sets of size $k = 3$ in the family of subsets under a SDSS is given by the sum of the components of the partially induced decision partitioning and the sign-transformed empty sets that are connected by the sense of their signs. This can be expressed as

$$a_3 = \sum_{x=1}^{6}[|O_{mx}^{+}| + |O_{mx}^{-}|] + |\emptyset_0^{-}| + \sum_{x=1}^{3}|\emptyset_{2x-1}^{+}| + \sum_{x=1}^{3}|\emptyset_{2x}^{-}|$$

$$a_3 = (6 + 6) + 1 + 3 + 3 = 19$$

This means that the number of sets of size $k \geq 0$ and k > 3 in the family of subsets under a SDSS will all be given by

$$a_i = 0$$

where $i \geq 0$ and $i > 3$. It is important to note that the consideration of the sign-transformed empty sets under a three-type outcome (i.e. k equals to 3) is validated by the idempotent law as shown below

$$\prod_{i=0}^{n}\left(\emptyset_i^{\pm} \cup \emptyset_i^{\pm} \cup \emptyset_i^{\pm}\right) = \left(\emptyset_1^{\pm} \cup \emptyset_1^{\pm} \cup \emptyset_1^{\pm}, \emptyset_2^{\pm} \cup \emptyset_2^{\pm} \cup \emptyset_2^{\pm}, \emptyset_3^{\pm} \cup \emptyset_3^{\pm} \cup \emptyset_3^{\pm}, \cdots, \emptyset_n^{\pm} \cup \emptyset_n^{\pm} \cup \emptyset_n^{\pm}\right)$$

$$= \left(\emptyset_1^{\pm}, \emptyset_2^{\pm}, \emptyset_3^{\pm}, \cdots, \emptyset_n^{\pm}\right)$$

By definition of SDSS, the number of elements in its underlying set is given as n = 6. Also, the general values of k applicable in the spliced DSS are those for the n-element empty sets and those n-element subsets with 3 types of outcomes. Therefore by invocation of LYM inequality, the summation term for $k = 0$ (empty set case) and $k = 3$ (outcome types) under the SDSS is given as

$$\sum_{k=0}^{6} \frac{a_k}{\binom{6}{k}} = \frac{a_0}{\binom{6}{0}} + \frac{a_3}{\binom{6}{3}}$$

But

$$\binom{6}{0} = \frac{6!}{0!\,(6-0)!} = \frac{6!}{6!} = 1$$

and

$$\binom{6}{3} = \frac{6!}{3!\,(6-3)!} = \frac{6!}{3!\,3!} = \frac{720}{36} = 20$$

Therefore

$$\sum_{k=0}^{6} \frac{a_k}{\binom{6}{k}} = \frac{0}{1} + \frac{19}{20} = 0.95$$

Generally, the analysis of spliced DSS involves both Bayesian and frequentist statistics. In contrast to the interpretation of frequentist probability as a phenomenal likelihood, frequency or propensity, the Bayesian probability is a theoretically assigned quantity that represents a state of knowledge (Justice, 1986) as is the case of the induced success and failures of the mixed outcomes. The Bayesian statistical inference uses credible intervals for interval estimation (Edwards, Lindman & Savage, 1963). It incorporates, from prior probability distribution (priors), problem-specific contextual information as is the case of the partially induced mixed outcomes under the SDSS. The incorporated information includes

1. **Informative Prior Probability Distribution**: This is based on specific variable information not derived from the data. As an example, the inner upper and lower boundaries of a spliced DSS, according to LYM inequality is within 95% or 2 standard deviations of the collected data distribution.
2. **Uninformative Prior Probability Distributions (Objective Prior)**: This is based on a variable's objective general information such as its sign or limit to its magnitude. Examples include partially induced partition and sign transformation of mixed outcomes and the maximum number of event data (i.e. 6) in a spliced DSS.

The confidence interval used by frequentist statistics as interval estimation or to indicate the reliability of an estimate includes the true value of a fixed parameter on the basis of repeated large random samples. Due to its dependence on random samples, confidence interval tends to be random. By definition, confidence intervals are analogous to credible intervals (Lee, 1997). While confidence interval is not determined by data, it is however set by researchers. Typically, in applied practice and in literature, confidence intervals are stated at the 95% confidence level (Zar, 1984) which reflects a generally accepted significance level of 0.05 (Field, 2013). Consequently, the above theoretical result of 0.95 based on LYM inequality analysis of SDSS is a statement of statistical importance. Not only does it theoretically confirm the empirical significance of using a 95% confidence level but also confirms the sample size and the processes of partially induced partitions and sign transformations within a SDSS as realistic.

By definition, the Decision Sperner family or System is generally an antichain O_m (elements of mixed outcomes) in the inclusion lattice over the power set D. Thus by definition, the subset O_M of DSS has with no order relation between any two different elements in terms of success and failure. This mathematically means it forms no lattice which is a partially ordered set (poset) in which every two elements have a least upper bound or join (V) called supremum and also a greatest lower bound or meet (Λ) called an infirmum. The partially ordered set

(L, ≤) is called a lattice and the set L contains the lattice elements. Algebraically, the structure (L, V, Λ, 1, 0) defines a bounded lattice where (L, V, Λ) is the lattice, 0 the lattice's bottom and 1 the lattice's top.

The Lattice of Mixed Outcomes

The transformation of a mixed outcome into two pairs of polar outcomes composed of two pairs each made up of a success and failure elements, involves the partition of a mixed outcome set followed by their dissociation as discussed earlier on. Let P generally be the partitioned set which in DSS is the mixed outcome O_M. Then

$$P = \{P_1 + P_2\}$$

where P_1 and P_2 are a disjoint union of two polar outcome subsets (i.e. O_{mx}^{+} *and* O_{mx}^{-} in DSS) of a mixed outcome O_M. Then

1. Each polar subset does not contain an empty set. That is

$$\emptyset \in P$$

2. The polar subset P_1 is covered by the polar set P_2 (i.e. $P_1 <: P_2$) such that $P_1 \leq P_2$ and $P_1 \neq P_2$ which means no element fits between P_1 and P_2 and the partitioned set is given by

$$\bigcup_{P_x \in P} P_x = P = O_M \; where \; x = 1, 2.$$

3. The intersection of the two polar subsets is an empty element. This renders the combined induced elements of the

polar subsets a pairwise disjoint given as $(O_{S1}, O_{f1}, O_{S2}, O_{f2})$.

Thus, if P_1, $P_2 \in P$ and $P_1 \neq P_2$ then

$$P_1 \cap P_2 = \emptyset$$

where $\emptyset$ is the empty set.

Both P_1 and P_2 are generally the blocks or cells of the partitioned mixed outcome which when partially dissociated form the pair of polar outcomes. They are also jointly exhaustive which means

$$P_1 \cup P_2 = O_M$$

and are mutually exclusive.

Each subset of the polar outcome can be seen as a join (least upper bound) which forms a join-semilattice and a meet (greatest lower bound) which forms a meet-semilattice of a partially ordered set or poset given by $(O, \leq)$. Mathematically, the lattice of the mixed outcome $O_m^{\pm}$ can be represented as follows. Let the set of polar outcomes which are partially partitioned in accordance with the "law of Average" be given by

$$O_m^{\pm} = \{O_{S1}, O_{f1}, O_{S2}, O_{f2}\}$$

where O_{S1} and O_{S2} are partial success outcomes and O_{f1} and O_{f2} are partial failure outcomes of the polar outcome and the orders

$$O_{S1} \leq O_{S2} \; and \; O_{f1} \leq O_{f2}$$

implies that for

$$JOIN: O_{S1} \vee O_{f1} \leq O_{S2} \vee O_{f2} \; (greatest\ lower\ bound)$$

and

$$MEET: O_{S1} \wedge O_{f1} \leq O_{S2} \wedge O_{f2} \; (least\ upper\ bound)$$

If the decision characteristics of O_S and O_f are expressed as 1 and 0 which is equivalent to 100% completion of project on time and budget and 0% as incomplete project with budget overrun and lateness, then as a decision analysis the polar outcome which is the dissociated intersection of the elements of decision set D such that

$$D = \{O_S, O_f\}$$

is bounded by a greatest element O_S (with decision characteristic value 1) and a least element O_f with decision characteristic value 0). This means

$$0 \leq O_m^{\pm} \leq 1$$

Hence, the elements of an element of the decision Sperner family $\mathcal{F}$ are ordered as such

$$F_n = \{O_S, O_{S1}, O_{f1}, O_{S2}, O_{f2}, O_f\}$$

where the decision characteristic magnitudes of $F_n (i.e. = |F_n|_C)$ are given correspondingly as

$$|F_n|_C = [1, 0.8, 0.6, 0.4, 0.2, 0]$$

which represents the objective prior probability scale as shown in figure 7. Since the $O_{S1} \leq^* O_{f1}$ is also the case $O_{S2} \leq O_{f2}$, the partial order $\leq^*$ on the polar outcome set O_m^- is a linear extension (order) of the partial order $\leq$ on the polar outcome O_m^+ set. This is in support of the order-extension principle which

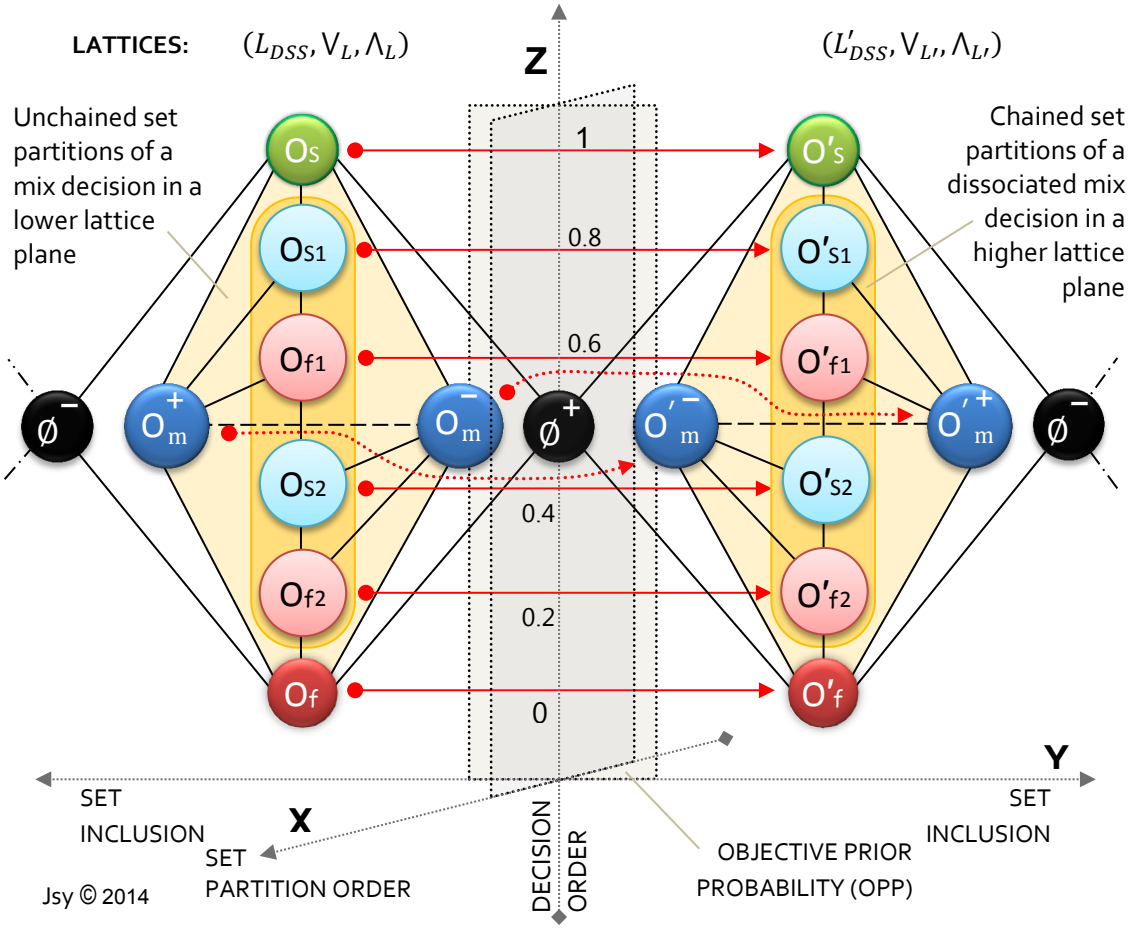

Figure 7. A Hasse diagram of bounded lattice homomorphism representation of a general quantum problem-solution processes within a decision Spercer system.

stipulates that every partial order can be extended to a total order (Thomas, 2008). The mappings between the partially ordered sets is shown by arrow lines (red) in figure 7 above which depicts a Hasse diagram of a bounded lattice homomorphism. Observe that the polar outcomes form an unchained (incomparable pair of elements) set partition in a lower lattice z-y plane. On

the other hand, the set partitions of the dissociated polar outcome is chained (comparable pair of elements) and in a higher lattice z-y plane. This order forms a bounded lattice $(L_{DSS}, \vee, \wedge, 1, 0)$ of the spliced DSS. By definition the morphism (structure-preserving mapping) between two partial lattices in a spliced DSS say $(L_{DSS}, \vee_L, \wedge_L)$ and $(L'_{DSS}, \vee_{L'}, \wedge_{L'})$ from sets F1 and F2, forms a lattice homomorphism from L to L′ given by the function f: L → L′ such that all

$$O_{S1}, O_{f1}, O_{S2}, O_{f2} \in L$$

F is a homomorphism of the following two underlying semilattices

$$f(O_{S1} \vee_L O_{f1}) = f(O_{S1}) \vee_{L'} f(O_{f1}) \text{ and } f(O_{S1} \wedge_L O_{f1}) = f(O_{S1}) \wedge_{L'} f(O_{f1})$$

$$f(O_{S2} \vee_L O_{f2}) = f(O_{S2}) \vee_{L'} f(O_{f2}) \text{ and } f(O_{S2} \wedge_L O_{f2}) = f(O_{S2}) \wedge_{L'} f(O_{f2})$$

The bounded-lattice homomorphism *f* which exists between two bounded lattices L and L′ (see figure 7) also obeys the following property

$$f(0_L) = 0_{L'} \text{ and } f(1_L) = 1_{L'}$$

which implies the homomorphism of lattices is a function preserving binary meets (∧) and joins (V).

DSS Mappings

Given these partially ordered sets (L, ≤), L′, ≤) and (L″, ≤), the following are the mappings existing between them in a spliced DSS.

1. **DSS Order-Preservation:** If for all O_{Sx} and O_{fx} in L

$$O_{Sx} \leq O_{fx} \;\; implies \;\; f(O_{Sx}) \leq f(O_{fx})$$

and alternatively, if for all O_m^- and O_m^+ in L

$$f(O_m^-) \leq f(O_m^+)$$

implies under reflexivity

$$O_m^- \leq O_m^+ \;\; \equiv \;\; O_m^{\pm} \leq O_m^{\mp}$$

then the function

$$f: L \longrightarrow L'$$

is a DSS order-preservation (monotone or isotone). See figure 7.

2. **DSS Order-Reflection:** If for all O_{Sx} and O_{fx} in L

$$f(O_{Sx}) \leq f(O_{fx}) \;\; implies \;\; O_{Sx} \leq O_{fx}$$

where x = 1, 2. Then

$$f: L \longrightarrow L'$$

is a DSS order-reflecting function.

3. **DSS Composition:** If both functions f : L → L′ and g: L′→ L″ are order-preserving, given that (L″, ≤) is an arbitrary partially ordered set in the spliced DSS, then their composition

$$(g \circ f): L \rightarrow L''$$

is order-preserving.

4. **DSS Order-Embedding:** Since the spliced DSS lattice is generally order-reflecting and order-preserving, it is by definition a DSS order-embedding

$$f: L \longrightarrow L'$$

of the poset (L, ≤) into the poset (L′, ≤) or simply put L is embedded into L′. This supports the induction of partially dissociated mixed outcome into signed polar outcomes as shown in the z-y plane in figure 7. Consequently, the joining of any two peripheral events in decision analysis is general established. This will be illustrated in an empirical analysis later.

5. **DSS Injection:** By definition, the implication of

$$f(O_{Sx}) = f\left(O_{fx}\right)$$

is that

$$O_{Sx} \leq O_{fx} \ and \ O_{fx} \leq O_{Sx}.$$

This means the function *f* is DSS injective or a one-to-one function which uniquely maps all elements in the domain to some codomain elements.

6. **DSS Order-Isomorphism:** If the order-embedding

$$f: L \longrightarrow L'$$

is bijective or a one-to-one correspondence where all elements in both domain and codomain are mapped to each other, then it is a DSS order isomorphism. Under this condition the posets (L, ≤) and (L′, ≤) are DSS isomorphic (structurally identical). Consequently, the DSS lattice is

structurally identical by order as depicted by the structural similarity in the Hasse diagram in figure 7.

7. **DSS Functional Identity**: If the functions

$$f: L \rightarrow L' \ \ and \ \ g: L' \rightarrow L''$$

are mapped by order-preservation such that $g \circ f$ and $f \circ g$ are each an identity function or map (returns argument value) on L and L′ respectively, then L and L′ are by definition DSS order-isomorphic (Davey & Priestley, 2002).

The study of morphism (structure-preserving mappings) between objects under category theory (objects that are linked by arrows) interprets structural understanding of said objects. In general, the formalization of any mathematical concept to satisfy basic conditions relating behaviour of objects and arrows (processes) validates the category. Consequently, a group homomorphism existing between any groups, though preserving the group structure, is a process involving a carrier of group structure information from one group to the next. This means, DSS lattice homomorphism represents a quantization of problem-solution process within a DSS. Bound or modulated by the success or failure outcomes within the DSS lattice homomorphism, the mixed outcome as partitioned blocks serves as modulated outcome consisting of quantized polar outcomes.

CHAPTER 4

THE QUANTUM PHENOMENON OF A GENERAL PROBLEM-SOLVING PROCESS

The mathematical principle which states a fundamental limit to the precision that pertains to complementary variables (pairs of physical quantities) of an object such as position (x) and momentum (p) is called the uncertainty principle in quantum mechanics. The Heisenberg's uncertainty principle is given as

$$\Delta p \cdot \Delta x \gtrsim h$$

where Δp and Δx represent uncertainty in momentum and uncertainty in position respectively and h the Planck constant which is equal to $6.62606957(29)\times10^{-34}$ J·s. Alternatively, Einstein's version (Gamow, 1988) of Heisenberg's uncertainty inequality in terms of uncertainty in energy ΔE and uncertainty in time Δt is given as

$$\Delta E \cdot \Delta t \gtrsim h$$

where h the Planck constant. On the other hand, the statistical treatment of the uncertainty principle (Kennard, 1927; Weyl, 1928) which relates the standard deviation of position σ_x and the standard deviation of momentum σ_p is also given as

$$\sigma_x \cdot \sigma_p \geq \frac{\hbar}{2}$$

where $\hbar$ the reduced Planck constant or Dirac constant is equal to

1.054571726(47) × 10^{-34} J·s (Mohr, Newell & Taylor, 2011) and can be expressed in terms of Planck constant *h* as

$$\hbar = \frac{h}{2\pi}$$

The above formal inequality derived by Earle Kennard and Herman Weyl, will be the basis for investigating the interplay between quantum uncertainty principle and a general problem-solving process. The theoretical construct for achieving this is as follows.

As an inherent property of all wave-like systems, the uncertainty principle is the result of matter wave nature of all quantum objects (Rozema et al., 2012). In equivalent manner, the quantized polar outcomes as algebraic objects must be susceptible to a flavour of the uncertainty principle in quantum mechanics.

General Similarities in Conceptual Interpretations of Uncertainty Principle

Quantum mechanics advances that the state of the wave function for a certain eigenvalue or measurement value is represented by an observable's eigenstate or characteristic state. This is precisely the case when the characteristic state of an observed environmental phenomenon is representative of the problem or solution state of the problem-solution cycle ideally governed by the environmental laws or principles pertaining to a measured characteristic value of its truth or success. In accordance to quantum mechanics, (Cohen-Tannoudji, Diu & Laloë,

1996) this implies that the measured characteristic of the observed environmental phenomenon puts the environmental system to a particular characteristic state Ψ relating said observed environmental phenomenon. If the characteristic state of the said environmental phenomenon is the same as another environmental phenomenon during the process of problem-solution cycle then the environmental system lacks a characteristic state of said observed environment. The reason, as stated earlier on, is that the solution phase of a problem-solution cycle is one of differential solutions forming a solution continuum which ends up in a post meta-solution. Thus, in accordance with de Broglie hypothesis in which case objects in the universe is a wave, the locality of an object (quantized polar outcomes) along the solution continuum of the problem-solution cycle can be describe by meta-solution function $\Psi(\theta, \sigma(x))$ in similitude to the position of a particle described by a wave function $\Psi(x, t)$ in quantum mechanics given x is the position and t the time.

In accordance with Born's rule, which determines the probability of a measurement on a quantum system yielding a given result, the time-independent of a single-moded plane wave have to be interpreted as a probability density function where the probability P of finding a particle's position X between points a and b is given by

$$P[a \leq X \leq b] = \int_a^b |\psi(x)|^2 dx$$

where $|\psi(x)|^2$ is the probability density function which represents the uniform distribution of the particle's uncertain position. The addition of multiple plane waves to the wave function, however, leads to an increased localization of the wave packet as shown in the figure 8 below. As the plane waves (red) are

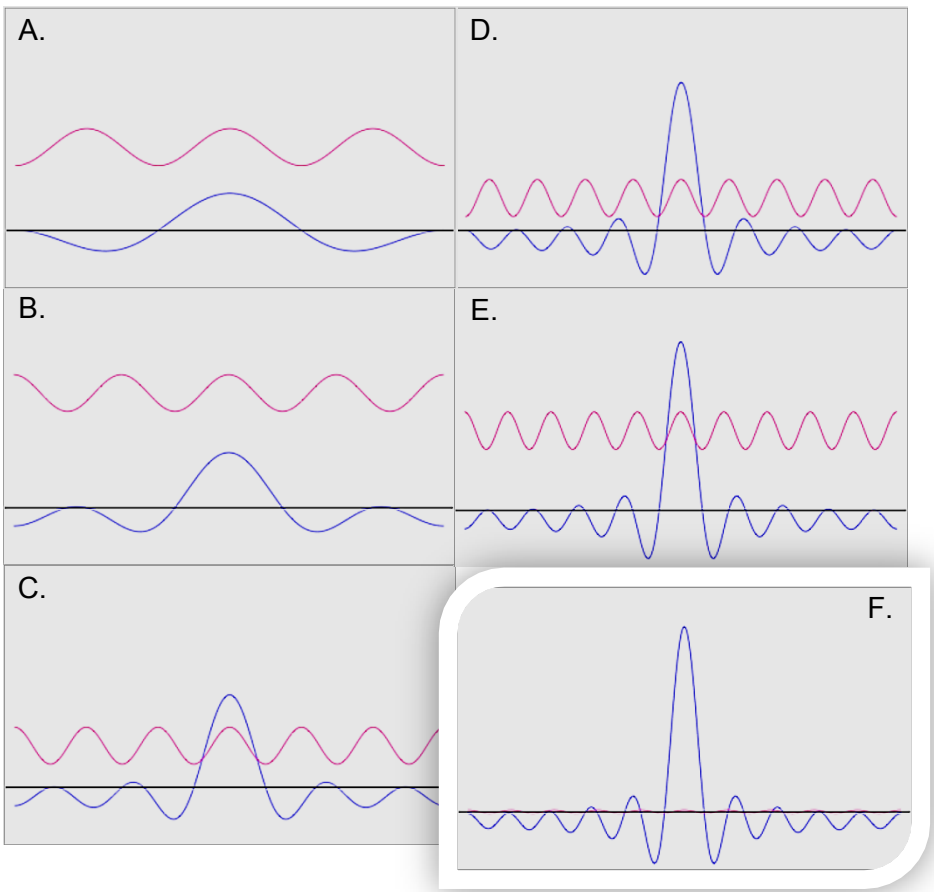

Figure 8. Illustration of superposition of many plane waves (red) to form an increasingly localized wave packet (blue) from A to F.

superposed with the wave function (blue) from A to E, the wave packet that eventually forms becomes localized as shown vividly in F. Also, figure 9 shows a depiction of propagation of de

Broglie waves. When the amplitude is greater than zero, it causes the wave to reverse sign and vice versa. The causes alternating amplitude wave to be formed. At a given point along the x-axis, the probability of locating the particle (shown as yellow colour opacity) is not definite but spread out like a waveform. Observe the blue and green curves representing the real part and the imaginary part of the complex amplitude. The blue curve represents the real part of the complex amplitude and the

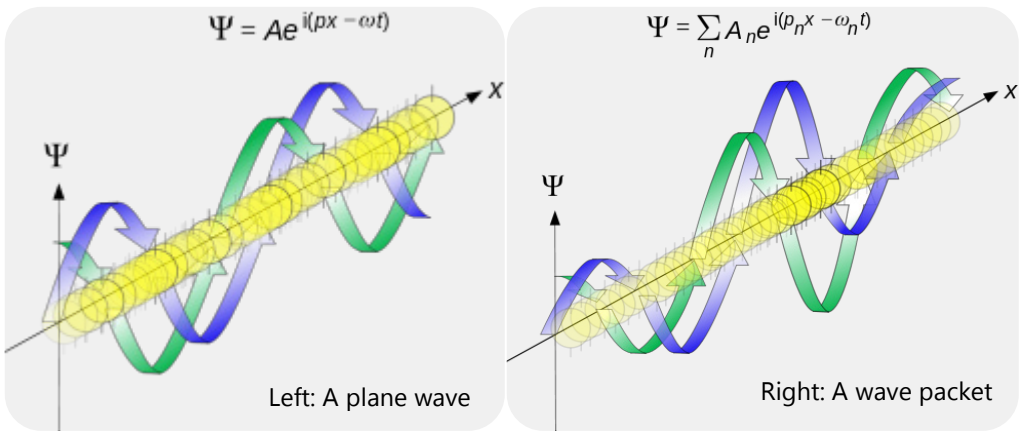

Figure 9. Depiction of propagation of de Broglie waves in 1d. The blue curve represents the real part of the complex amplitude and the corresponding imaginary part is the green curve. Source from Matter wave, in *Wikipedia, the free encyclopedia*, retrieved December, 2014, from https://en.wikipedia.org/wiki/Matter_wave

corresponding imaginary part is the green curve. These are analogous to the dotted arrow lines representing the functional mappings between O_m^- and O'^+_m and also O_m^+ and O'^-_m partially induced objects of the mixed outcomes in the bounded homomorphism lattice of spliced DSS shown in figure 7.

By considering all possible modes in the continuum limit, the wave function $\psi(x)$ is given as such

$$\psi(x) = \frac{1}{\sqrt{2\pi\hbar}} \int_{-\infty}^{\infty} \phi(p) \cdot e^{ipx/\hbar} dp$$

where i = √-1 is the imaginary number, x the position of the particle, p the momentum of the particle, ħ the reduced Planck constant, and the wave function in momentum space $\phi(p)$ is the amplitude of all the possible modes in the continuum limit. The mathematical operation called Fourier transform is used to separate a wave packet into individual plane waves. It therefore means that $\phi(p)$ is the Fourier transform of the wave function with x and p serving as the conjugate variables. The summation of the plane waves together leads to the rise and fall in the precision of the particle's position and momentum respectively and these are quantifiable via standard deviation σ. The increase in the precision of the particle's position (reduction in standard deviation, σ_x) is responsible for the localization of the wave packet. In similitude to the wave function in a momentum space $\phi(p)$, the problem-solution cycle is made up of a series of problem-solution modes whose general solution in the solution continuum (reminiscent to the superpositioning of multiple plane wave functions) is an interpretation function $\Delta(\theta,\sigma)$. By comparison, the interpretation function is an equivalent "Fourier transform" of the general solution function Ψ

of the solution continuum with each problem-solution pair serving as a conjugate variable pair within the problem-solution cycle. However in a multiplicity scenario of different problems definitions, a helical problem-solution cycle approach attributing a single cycle process per a defined problem, results to bring about respective interpretative answers.

Analysis under quantum Bayesianism, a subjective Bayesian account of quantum probability (Stairs, 2011), such as QBism rewrites quantum states as a set of probabilities defined over outcomes of a "Bureau of Standards" measurements (Schack, 2011; Appleby, Ericsson & Fuchs, 2011; Rosado, 2011). It uses what is called SIC-POVMs (symmetric, informationally-complete, positive operator-valued measures). This way, the translation of a density matrix (representing a mixed state quantum system) into a probability distribution over SIC-POVM experimental outcomes, enables the reproduction of all statistical predictions on the density matrix (normally computable via Born's rule) from the SIC-POVM probabilities. Similar to the technical approaches of quantum Bayesianism, the problem-solution cycle also uses symmetric, informationally-complete positive measures in its theoretic construct to expressed as success or failure rates or alternatively as 1 or 0, the outcome of a decision problem. By doing so, the quantum states of the problem-solution cycle performance is set forth as a set of standardized probabilities (0, 0.2, 0.4, 0.6, 0.8, and 1) over an objective prior

probability (OPP) scale. The translation of SDSS based on sampled performance rates of independent problem-solution cycles in a common distribution, consequently permits the reproduction of all the statistical predictions or inferences under a normal distribution on SDSS. Such a distributional inference would normally be computed on the basis of central limit theorem which stipulates that: the mean of several independently drawn variables from the same distribution is approximately normally distributed irrespective of the form of the original distribution.

Probability of Indecision Error Propagation

Each event in the statistical time frame of a SDSS is associated with the uncertainty of event success S and failure F. The outcomes of the events from the selected data set together form an outcome set. By definition, the data for each event must be randomly selected from a set of data pool. Let the data pool be represented by $\wp_1$, $\wp_2$, ... $\wp_{10}$ then the data set S for the statistical time frame is given by

$$S = \wp_1 \cap \wp_2 \cap \cdots \wp_{10} = D_1 \cup D_2 \cup \cdots \cup D_{10}$$

where D_1, D_2,... D_{10} represents selected data from the respective events E_1, E_2,..., E_{10} within the statistical time frame. Note that P represents failure outcome F and D represents object of mixed outcome O. Also, observe that both sets D and O are within

the intersection of the sets of data pools. Hence, since DE derives O transitively, the elements in both D and O can be considered to equivalently exist simultaneously. Therefore, the probability $\delta P_{dataset}$ of the rate uncertainty of sample space success and failure within the sample time frame is given by the temporal joint probability of all outcomes together and the probability of the rate uncertainty of event success and failure, within the statistical time framework. Therefore the probability $\delta P_{dataset}$ of the dataset associated errors of S and F of all the events (for example selected statistical data of software development projects) with the statistical time frame is

$$\delta P_{Data\ Set} = P\begin{pmatrix} Indecision\ Error \\ Propagation \end{pmatrix} = P\begin{pmatrix} Sample\ Space \\ Time\ Framework \end{pmatrix} \cdot P\begin{pmatrix} Decision\ Error \\ Propagation \end{pmatrix}$$

which can be expressed as

$$\delta P_{Data\ Set} = P\big(\delta(S \cap F)\big) = P\begin{pmatrix} Sample\ Space \\ Time\ Framework \end{pmatrix} \cdot P\big(\delta(S \cup F)\big)$$

In general,

$$\boxed{P\begin{pmatrix} Sample\ Space \\ Time\ Framework \end{pmatrix} = \left(P_{\substack{single \\ outcome}} \cdot P_{\substack{double \\ events}} \cdot P_{\substack{time \\ over\ run}} \cdot P_{\substack{temporal \\ non-outcome}} \right)^{N}}$$

and it is focused on the time of the overall sample space where

$P\begin{pmatrix} Sample\ Space \\ Time\ Framework \end{pmatrix}$: is the time frame probability of selecting all outcomes under all possible conditions in the overall sample space.

$P_{\substack{single \\ outcome}}$: is the probability of selecting a single outcome within the overall sample space.

$P_{\substack{double \\ events}}$: is the probability of selecting two events or sample spaces from the overall sample spaces.

$P_{\substack{time \\ over\ run}}$: is the probability of time over run between two events or the difference between time over run.

$P_{\substack{temporal \\ non-outcome}}$: is the temporal (time frame) probability of not selecting an outcome in the overall sample space.

N is the total number of outcomes in a general sample space.

It must be noted that the probability of the temporal non-outcome factor in an SDSS is a constant for any two event problem-solution processes. It is denoted by

$$P_{\substack{temporal \\ non-outcome}} = \left(\frac{1}{10}\right)^{30}$$

where 10 is the number of time frames and 30 is the number of possible outcomes given that each event has 3 possible outcomes of success, mixed and failure. The implication is that if the time span between the two events is less than 10 unit time measure, the mixed outcome is automatically sub-divided to give a total outcome count of 30 for the overall sample spaces. Also, generally

$$\boxed{P\begin{pmatrix} Decision\ Error \\ Propagation \end{pmatrix} = \left(P_{\substack{single\ triat \\ outcome}} \cdot P_{\substack{single\ definite \\ outcome}} \cdot P_{\substack{decisive \\ error}}\right)^{n}}$$

and is focused on the overall sample space or event outcomes where

$P\begin{pmatrix} Decision\ Error \\ Propagation \end{pmatrix}$: is the probability of selecting a success or failure outcome with its propagated error in the overall sample space.

$P_{\substack{single\ triat \\ outcome}}$: is the probability of selecting one of the three basic outcomes of an event.

$P_{\substack{single\ definite \\ outcome}}$: is the probability of selecting one outcome out of two possible decisive outcome.

$P_{\substack{decisive \\ error}}$: is the probability of success or failure error propagation.

Finally, n is the possible number of decisive outcomes (success and failure) of an event or sample space occurring simultaneously with respective propagated error.

In general, to convert the probability of the indecision error propagation of the data set to percentage, multiply it by 200% which is the total percentage of the joint event or sum of the individual events (success and failure) or number of sample spaces under analysis.

Probability of Normal Deviates with Outcome Characteristics

To validate the above principle, its application on empirical data spanning 12 years of cumulative research on 50,000 industry software development project over the period of 1994 to 2004 conducted by Standish Group will be scrutinized. The CHAOS research of Standish Group, done through focus groups, in-depth surveys and executive interviews and provide a global view of project statistics, with the aim of providing in-depth understanding:

1. The scope of application software development failures.
2. The major factor that cause these projects to fail.
3. The recognition of key ingredients that can reduce failures.

Below, in figures 10 and 11 are the survey results outlined in the CHAOS Report from Standish Group, a reputable research group (Galorath, 2012).

Under the results from CHAOS Report, the rate of projects completed on-time and within budget are labelled as Succeeded, those that are over time, budget and/or missing critical functionality are labelled as Challenged, and the rates of projects that are cancelled before completion are labelled as Failed. To facilitate an illustrative computation of the probability of the rate uncertainty of sample space success and

failure within the sample time frame, the data for 1994 and 2004 will be used. In table 3, observe that the events for 1994 to 2002 have been mindfully omitted. The labels of Succeeded, Failed and Challenged are relabeled as Success, Failure and Mixed. For any event of software development project, there are three Failure (F) and Mixed (M). Any developmental error δ within the data of rate outcomes can be propagated in this

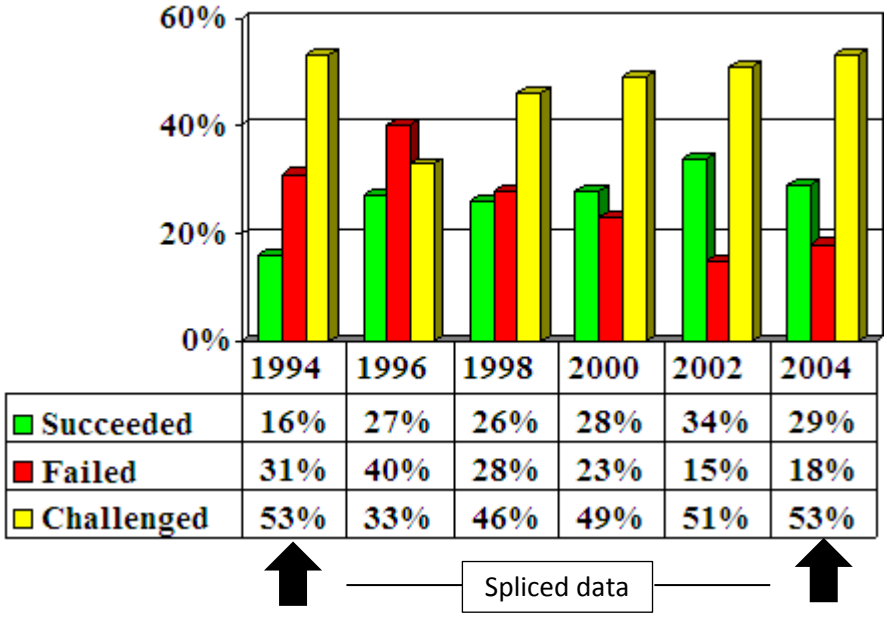

Figure 10. Resolution of software development projects from 1994 to 2004. Source from InfoQ, *Interview: Jim Johnson of the Standish Group*, by D. H. Preuss, retrieved February, 2014, from http://www.infoq.com/articles/Interview-Johnson-Standish-CHAOS

manner. An error in identifying M outcome can either be propagated to an S outcome or F outcome. This means that an

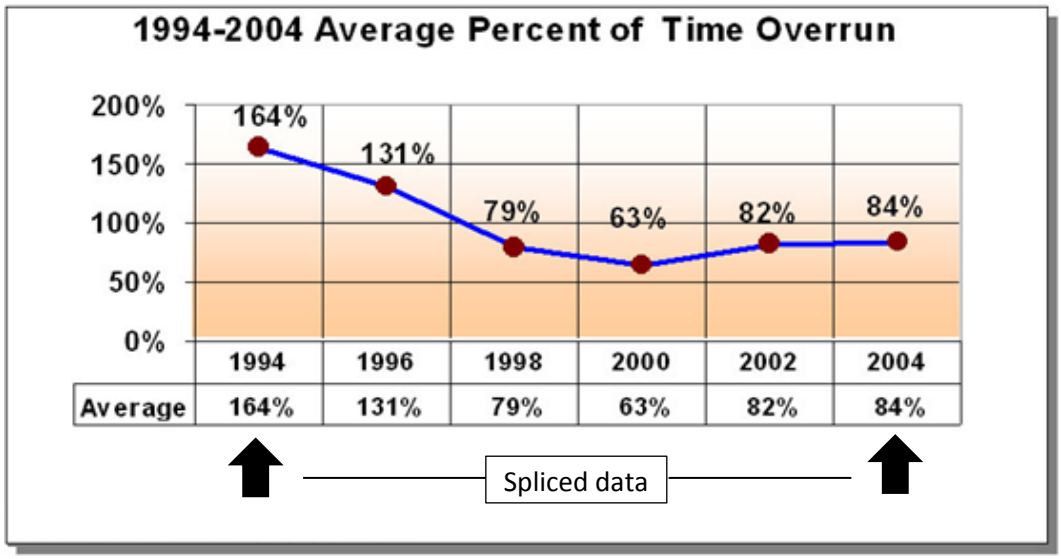

Figure 11. Average percent time above original time estimate of software development projects. Source from InfoQ, *Interview: Jim Johnson of the Standish Group*, by D. H. Preuss, retrieved February, 2014, from http://www.infoq.com/articles/Interview-Johnson-Standish-CHAOS

error in S or F outcomes would be propagated to M outcome. Thus, in table 3 the error propagation is directed towards M outcome. Since an event's error propagation can originate from S or F and there are two events under consideration, the error propagation contributed by either of S or F outcome in a single event is ½ δ(S U F). By definition, the M outcome rates contain net propagated error equal to δ. To determine δ, the joining of 1994 and 2004 events must be considered. Under this case, the summation of all the success and failure outcome rates, ∑(SUF) and those of all mixed outcome rates, ∑(M) can be expressed with respective propagated error term. This gives 94% + δ (SUF) and

Table 3

Analysis of 1994 and 2004 CHAOS Results Showing Propagation of Error from Success or Failure Outcomes to Corresponding Mixed Outcome and Its Computation

			RATE OUTCOMES				
SOFTWARE PROJECTS	TIME FRAME	SURVEY YEAR	SUCCESS (S)	FAILURE (F)	ERROR PROPAGATION	MIXED (M)	TOTAL (CERTAINTY)
EVENTS	0	1994	16%	31%	►½δ(SUF)	53%	100%
	1						
	2	1996					
	3						
	4	1998					
	5						
	6	2000					
	7						
	8	2002					
	9						
	10	2004	29%	18%	►½δ(SUF)	53%	100%
JOINT EVENT	0 AND 10	1994 AND 2004	∑(SUF)		± δ	∑(M)	**200%**
			94% + δ(SUF)			106% - δ(SUF)	
Rate Uncertainty of Sample Space Success OR Failure			δ(SUF)			6%	
Rate Uncertainty of Event's Outcome Success OR Failure			½δ(SUF)			3%	

106% - δ (SUF) respectively. Note that the grand total of all the rates under events and joint event will always be equal. In this analysis they are both equal to 200%. Since the rate of

certainty is 100%, by comparing the maximum joint event's summation to 100%, an event's single outcome's propagation error δ (SUF) can be computed as 106% - 100% to give 6%. This value represents the rate uncertainty of sample space success or failure, δ(S U F). On the other hand, the rate uncertainty of an event's outcome success or failure is given by ½ δ(S U F) since there are only two possible outcomes S and F) under consideration.

By application of the formula for determining P (δ(S U F)), the ensuing computation is done. From the Standish data the following probabilities are determined for the case of a two 10-year-interval event (1994 and 2004) analysis:

Using value for δ(SUF) in table 3, one gets

$$P_{\substack{decisive \\ error}} = 6\% \, per \, 100\,\%.$$

Also,

$$P_{\substack{single\ triat \\ outcome}} = 1 \, outcome \, per \, 3 \, possible \, outcomes$$

and

$$P_{\substack{single\ definite \\ outcome}} = 1 \, outcome \, per \, 2 \, outcomes.$$

Others are derived using data in figure 10 and figure 11 as follows:

$$P_{\substack{single \\ outcome}} = 1 \, event \, per \, 30 \, outcomes. \; P_{\substack{double \\ events}} = 2 \, events \, per \, 10 \, events.$$

$$P_{\substack{time \\ over\ run}} = 80\% \, time \, over \, run \, per \, 100\% \; and \; P_{\substack{temporal \\ non-outcome}} = 1 \, year \, in \, 10 \, years.$$

Therefore, the probability of decision error propagation is given by

$$P\big(\delta(S \cap F)\big) = \left(\left(\frac{1}{30}\right)\cdot\left(\frac{2}{10}\right)\cdot\left(\frac{80}{100}\right)\cdot\left(\frac{1}{10}\right)^{30}\right)\cdot\left(\frac{1}{3}\cdot\frac{1}{2}\cdot\left(\frac{6}{100}\right)\right)^{2}$$

$$= 0.533\overline{33} \times \left(\frac{1}{100}\right) \times 10^{-30} \times 1 \times 10^{-4}$$

$$= \frac{0.533\overline{33} \times 10^{-34}}{100} \times 100\%$$

$$= 0.533\overline{33} \times 10^{-34}\ \%$$

As a de facto probability, $P\big(\delta(S \cap F)\big)$ must be equal to the constant $\hbar/2$ of the formal inequality relating the standard deviation of position σ_x and the standard deviation of momentum σ_p of the statistical version of the uncertainty principle. But due to inherent system error ε_o the situation is rather given by

$$P\big(\delta(S \cap F)\big) - \varepsilon = \frac{\hbar}{2}$$

where ε is the total system composite error due to a single outcome and

$$\mathcal{E}_o = P\big(\delta(S \cap F)\big) - \frac{\hbar}{2}$$

where ε_o is the total system composite error due to S and F outcomes. Hence, to find the percentage of values (i.e. outcomes) drawn from a normally distributed gross sample space that has the probability of normal deviate ($n\sigma$) lying in the

range given by μ - nσ and μ + nσ where μ and σ are the mean and standard deviation of the normal distribution (gross sample space), and n a real number, one must compute the number of average reduce Planck's constant as following:

$$\boxed{Normal\ Deviate\ (n\sigma) = \frac{P\big(\delta(S \cap F)\big) - \varepsilon}{\frac{\hbar}{2}} \times 100\%}$$

The inherent system error (due to S and F outcome) is given by

$$\mathcal{E}_o = (0.533\overline{33} \times 10^{-34}) - \left(\frac{1.05457 \times 10^{-34}\, J.s}{2}\right)$$

$$= (0.533\overline{33} \times 10^{-34}) - (0.527285 \times 10^{-34})$$

$$= 0.006045 \times 10^{-34}$$

This error is the contribution from both S and F outcomes from the two events subjected to analysis. Thus, the error due to a single outcome will be

$$\mathcal{E}' = \frac{1}{2}(0.006045 \times 10^{-34}) = 0.003023 \times 10^{-34}$$

Since there are 3 possible outcomes in the system of problem-solution process, their error propagation effect must be determined. This is given by

$$\mathcal{E} = \mathcal{E}_o + \mathcal{E}' = (0.006045 \times 10^{-34}) + (0.003023 \times 10^{-34}) = 0.009068 \times 10^{-34}$$

Therefore, the normal deviate is given by

$$n\sigma = \frac{(0.533\overline{33} \times 10^{-34}) - (0.009068 \times 10^{-34})}{0.527285 \times 10^{-34}} \times 100\% = \mathbf{99.42669}\%$$

By the 68-95-99.7 (empirical) rule or what is known as 3 sigma rule under normal distributions, the result above means that:

1. About 99.7% of values lie within 3 standard deviations.
2. The values of the two 10-year-interval events (1994 and 2004) drawn from a normal distribution lie within 3 standard deviations.
3. The probability of the normal deviate for the two 10-year-interval events analyzed lies in the range μ - 3σ and μ + 3σ.

In the case of a two 6-year-interval event (1996 and 2002) analysis,

$$P(\delta(S \cap F)) = \left(\left(\frac{1}{18}\right) \cdot \left(\frac{2}{10}\right) \cdot \left(\frac{49}{100}\right) \cdot \left(\frac{1}{10}\right)^{30}\right) \cdot \left(\frac{1}{3} \cdot \frac{1}{2} \cdot \left(\frac{16}{100}\right)\right)^{2}$$

$$= 0.544\overline{44} \times \left(\frac{1}{100}\right) \times 10^{-30} \times 0.7.111\overline{11} \times 10^{-4}$$

$$= \frac{3.87157 \times 10^{-34}}{100}$$

which should be, by definition, equal to $\left(\frac{\hbar}{2}\right)\left(\frac{1}{100}\right)$. Therefore, to get the probability in percentage, one should simply multiply $P(\delta(S \cap F))$ by 100%. This gives

$$P\big(\delta(S \cap F)\big) = 3.87157 \times 10^{-34}\ \%$$

Therefore

$$\mathcal{E}_o = (3.87157 \times 10^{-34}) - (0.527285 \times 10^{-34}) = 3.34429 \times 10^{-34}$$

which is the inherent system error.

Mixed Outcome's Partial Dissociation

In order to facilitate the neutral condition of the mixed outcome as a state of decision outcome, it has to be subjected to 'partial outcome dissociation'. This results in a polar outcome with both partial success(es) and partial failure(s) which is needed decision analysis of a mixed outcome under normal distribution. A sub-division of the mixed outcome into 4 partial successes and failures results in a net of 6 decision outcomes. Included in said outcomes are the success and failure outcomes. The implication here is that the system error of a single outcome under a complete decision outcome of an event is given by:

$$\mathcal{E}' = \frac{1}{6}(3.34429 \times 10^{-34}) = 0.55738 \times 10^{-34}$$

Therefore, the total system composite error $\mathcal{E}$ is given by

$$\mathcal{E} = \mathcal{E}_o + \mathcal{E}' = (0.55738 \times 10^{-34}) + (3.34429 \times 10^{-34}) = 3.90167 \times 10^{-34}$$

The normal deviate is thus expressed as

$$n\sigma = \frac{(3.87157 \times 10^{-34}) - (3.90167 \times 10^{-34})}{0.527285 \times 10^{-34}} \times 100\% = -5.70849\%$$

The negative normal deviate is an event's mixed outcome's partial dissociation's problem-solution 'energy', that is required to bring about its polarization into two sets of polar outcomes each with a partial success and partial failure. This implies, of the total 100% rate of an event's three varied outcomes of S, M and F under the 1996-2002 data from CHAOS survey, 5.70849% is dissipated in the 'decisionization' of the full range of an event's possible outcomes. Hence, the 'decisionized' normal deviate ($n\sigma_{\pm}$) is expressible as

$$n\sigma_{\pm} = 100\% + n\sigma = 100\% - 5.70849\% = \mathbf{94.29151}\%$$

By the 3 sigma rule under normal distributions, about 95% of values lie within 2 standard deviations. The implication here is that:

1. The values of the two 6-year interval events (1996-2002) drawn from a normal distribution lie reasonably close to 2 standard deviations.
2. The probability of the normal deviate for the two 6-year-interval events analyzed lies in the range $\mu - 2\sigma_{\pm}$ and $\mu + 2\sigma_{\pm}$.

Observe that by the 3 sigma rule under a normal distribution, the difference between the second and first standard deviations of the spread of values is 27% and that between the third and second standard deviations is 4.7%. Therefore, it is more efficient to use the golden ratio model of the decision Sperner system (DSS) where only the second and fifth event outcome rates representing

95% of distribution are used for decision analysis. This is supported by the result of LYM inequality analysis of DSS which gave a 95% (2 s.d.) bound on the total size of data sets. In the case of a two 2-year interval events (1998-2000) analysis, one gets

$$P\big(\delta(S \cap F)\big) = \left(\left(\frac{1}{6}\right)\cdot\left(\frac{2}{10}\right)\cdot\left(\frac{16}{100}\right)\cdot\left(\frac{1}{10}\right)^{30}\right)\cdot\left(\frac{1}{3}\cdot\frac{1}{2}\cdot\left(\frac{5}{100}\right)\right)^{2}$$

$$= 0.533\overline{33} \times \left(\frac{1}{100}\right) \times 10^{-30} \times 0.694\overline{44} \times 10^{-4}$$

$$= \frac{0.3703 \times 10^{-34}}{100} \times 100\%$$

$$= 0.37037 \times 10^{-34}\ \%$$

The inherent system error is $\mathcal{E}_o = 0$, since

$$P\big(\delta(S \cap F)\big) = \frac{\hbar}{2}$$

Therefore, $\mathcal{E}' = 0$ and the total system composite error is given as

$$\mathcal{E} = \mathcal{E}_o + \mathcal{E}' = 0 + 0 = 0.$$

Hence, the normal deviate can be calculated as

$$n\sigma = \frac{3.37037 \times 10^{-34}}{0.527285 \times 10^{-34}} \times 100\% = \mathbf{70.24095}\%$$

By the 3 sigma rule under normal distribution, the result above means about 68% of values lie within one standard deviation. This implies the above result indicates that:

1. The values of the two 2-year-interval events (1998-2000) drawn from a normal distribution lie reasonably close to 1 standard deviation.

2. The probability of the normal deviate for the two 2-year-interval events analyzed lies in the range $\mu - 1\sigma$ and $\mu + 1\sigma$.

Table 4

Expected Values of Normal Deviates of 1994 to 2004 CHAOS Surveyed Projects' Outcomes Drawn From a Normal Distribution

PERIOD	OUTCOME	TIME UNITS	NORMAL DEVIATE
1994 -2004	Success	10	3σ
1996 - 2002	Mix	6	2σ
1998 - 2000	Failure	2	σ

The three outcomes namely success, mixed and failure each have values drawn from a normal distribution and specific periods shown in the table 4. The regions under a normal distribution are depicted in figure 12 below.

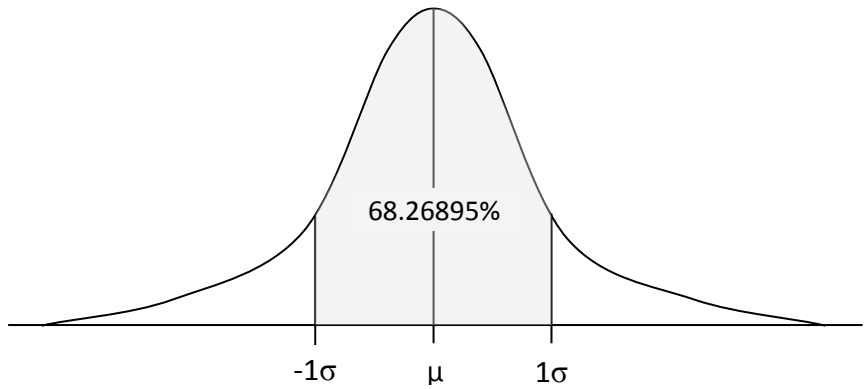

A. Spread of success values.

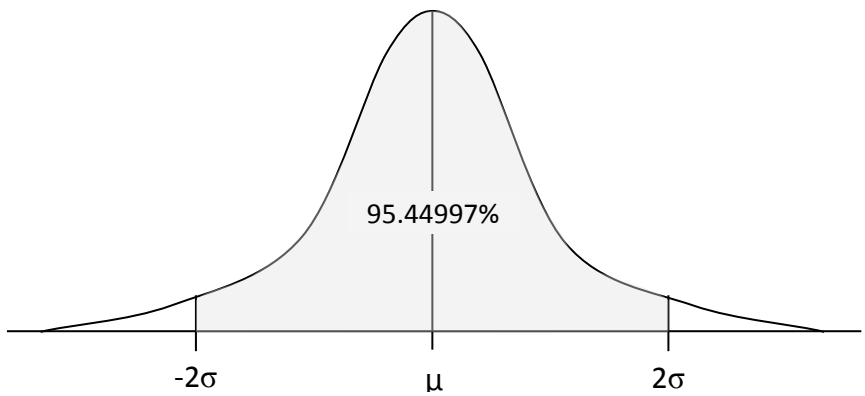

B. Spread of mix values.

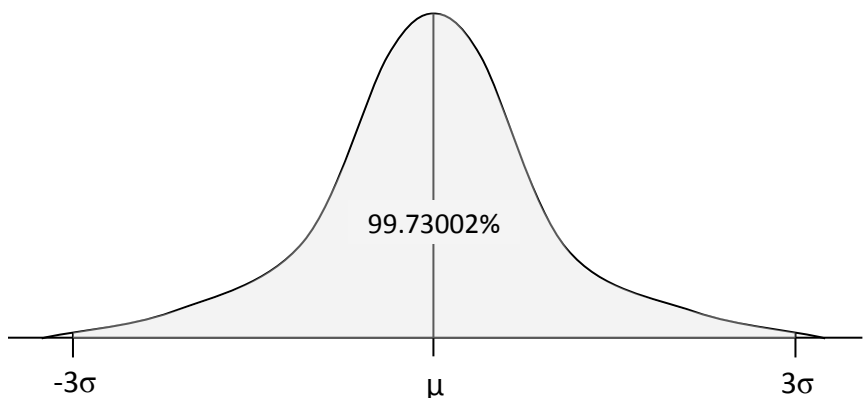

C. Spread of failure values.

Figure 12. The general spread of values of success, mix, and failure outcomes under a normal distribution.

CHAPTER 5

INTERPRETATION OF DECISION UNCERTAINTY

The indecision error of the event δ(S∩F) represents a decision uncertainty which can be stated as

$$\delta P_{Data\ Set} = \delta(S \cap F) = \delta S \cdot \delta F \geq \frac{\hbar}{2}$$

where δS and δF are the rate uncertainty of the sample space success or failure. This is an expression of the principle of uncertainty in a problem-solution process reminiscent to the Heisenberg's uncertainty principle. If δS is far larger, then it implies that δF is far smaller and vice versa. These extremities of δS and δF imply some task(s) or activities have been wrongly include in the schedule under scrutiny within a given project. It is their presence in a project scenario that brings about the propagated error in estimation of a project's progress by schedules. This assertion is held on the basis that other human error(s) are effectively absent. It must be borne in mind that excess task(s) which result in extreme error propagation is also the result of human error (i.e. improper scheduling of task(s). The key effective management of problem-solving processes is to maintain a balance in both δS and δF. Thus, a persistent extreme lopsidedness between δS and δF is sure to lead to project

failure. However, a persistent medium lopsidedness leads to a mixed project outcome while a persistent balance between δS and δF leads to a project success.

Dimensional Analysis of Decision Uncertainty

Data analysis of projects that engage in problem-solution processes are expressed in percentages (rates) for convenience sake. In order to interpret solutions based on decision uncertainty truthfully in order to bring forth the much needed understanding of a problem-solution process(es), the known value of δS and δF must be without unit or dimensionless. If it is expressed in percentage, it must be converted to a pure number which will lie between 0 and 1. This way, the unknown inexactitude will be in percentage which is easily integrable.

Application of Decision Uncertainty

Decision uncertainty though derived from statistical analysis of multiple projects outcomes, is particularly applicable to a single project or problem-solving scenario. Here, the success and failures can be monitored by schedule for adjustment(s).

Significance Level

With 99% standard deviation (s.d) coverage of the software project data normally distributed within 3 s.d, it means that

there is a permissible error of 1% attributed to the significance level of the normally distributed data. This means each tail of the normal distribution holds (1/100)/2 = 0.005 significance level α which is normally used in statistical analysis.

Interpretation

As was asserted under '*Skills Proportions Based on Language to Computational Skills Ratio (LTCSR)*', the production or development of software projects is normal distributed of which most activities fall under 1 standard deviation. Consequently, this reaffirms the assertion that a latent language inefficiency of 33.33% causing an inherent reduction in software production efficiency as a result of the multiple effects of programming languages naturally sets a 1 standard deviation boundary of efficiency. Any failure rate of software production greater than 33.33% has its excess due to other human error.

CHAPTER 6

EMPIRICAL EVIDENCE SUPPORTING RESULTS OF LTCSR ANALYSIS

In other to reduce inconsistencies, the data to be mostly used are those that are coming from surveys that explicitly measure success rates or failure rates and not the admixture of the two. The following are empirical data regarding software development project success and failure rates. They include:

1. McKinsey & Company in conjunction with the University of Oxford (2012) studied 5,400 largescale IT projects (projects with initial budgets greater than $15M) (Why Projects Fail, 2012).
2. PM Solutions (2011) report called Strategies for Project Recovery (PDF) study identifies top causes of IT failure covers 163 companies (Krigsman, 2011).
3. The 2010 IT Project Success Rates survey explore the success rates by paradigm of IT projects (successful, challenged, and failed) (2010 IT Project Success Rates, 2010; 2011 IT Project Success Rates, 2011).
4. Information Systems Audit and Control Association (ISACA) (2008) studied 400 respondents (Krigsman, 2011).

5. Survey conducted by Dr. Dobb's Journal's (DDJ) 2007 project success survey (successes or failures) using 586 respondents (2007 IT Project, 2007).
6. The European Services Strategy Unit (ESSU) Research Report No. 3 (2007) "Cost overruns, delays and terminations" on IT Projects Research report identifies 105 outsourced public sector ICT contracts in central government, NHS, local authorities, public bodies and agencies with significant cost overruns, delays and terminations. (Galorath, 2012)
7. Dynamic Markets Limited (2007) Study of 800 IT managers across eight countries. (Galorath, 2012)
8. KPMG – Global IT Project Management Survey (2005) studied 600 organizations globally (Global IT, 2005).
9. The Robbins-Gioia Survey (2001) study the perception by enterprises of their implementation of an ERP (Enterprise Resource Planning) package with 232 survey respondents spanning multiple industries including government, Information Technology, communications, financial, utilities, and healthcare. Note: While 51% viewed their ERP implementation as unsuccessful, 56% of survey respondents noted their organization has a program management office (PMO) in place (facilitates human error reduction), and of these respondents, only 36% felt their ERP implementation was unsuccessful (Failure Rate: Statistics over IT projects failure rate, 2014).

10. The Conference Board Survey (2001) survey interviewed executives at 117 companies that attempted ERP implementations (Failure Rate: Statistics over IT projects failure rate, 2014).
11. The Bull Survey, UK (1998) surveyed in the UK to identify the major causes of IT project failure in the finance sector by conducting a total of 203 telephone interviews with IT and project managers from the finance, utilities, manufacturing, business services, telecoms and IT services sectors in UK (Galorath, 2012).
12. The KPMG Canada Survey (1997) survey focused on IT project management issues to Canada's leading 1,450 public and private sector organizations to outline the reasons behind the failure of Information Technology projects (Failure Rate: Statistics over IT projects failure rate, 2014).
13. The Chaos report (succeeded, failed, challenged) of the Standish Group (1995) landmark study of IT project failure using sample size of 365 respondents (Galorath, 2012).

Of the success and failure rates, failure rates have been noted to be not only difficult to measure but also virtually impossible to compare. Below are tabulations (table 5 and 6) of the empirical data surveyed around the world which depicts the status of software production’s success and failure rates. The average failure rate of 33.94% is in very good agreement with the stipulated value of 33.33% for the latent language inefficiency.

On the other hand, the average success rate of 63.2% is also reasonably close to the 66.67% limit brought about by the multiplicity of programming languages.

Table 5

Project Failure Rates from Various Research Reports

SOFTWARE DEVELOPMENT PROJECT FAILURE RATINGS 1994-2009			
DATE	**SOURCE**		**RATE** *(%)*
2009	Standish Group Research Chaos Report (landmark study of IT project failure)	Failed	24
2004		Failed	18
2002		Failed	15
2000		Failed	23
1998		Failed	28
1996		Failed	40
1994		Failed	31
2012	McKinsey & Company /University of Oxford		17
2011	Strategies for Project Recovery (2011)		37
2008	Info. Systems Audit & Control Association (ISACA)		43
2007	Dynamic Markets Limited 2007		41
2007	Tata Consultancy		41
2007	European Services Strategy Unit Research Report 3		30
2005	KPMG – Global IT Project Management Survey		49
2001	Robbins-Gioia Survey		36
2001	Conference Board Survey		40
1998	Bull Survey, UK		37
1997	KPMG Canada Survey		61
		AVERAGE FAILURE RATE	**33.94**

While in general project failures attributed directly to poor requirements gathering, analysis, and management is between 60% and 80% (Meta Group), the fixing of self-inflicted problems

Table 6

Project Success Rates from Various Research Reports

SOFTWARE DEVELOPMENT PROJECT SUCCESS RATINGS 1998 - 2010					
DATE	**SOURCE**			**RATE (%)**	**GROUP AVERAGE**
2010	IT Project Success Survey	Ad-hoc Projects		49	54.25
		Iterative Projects		61	
		Agile Projects		60	
		Traditional Projects		47	
2009	Software Development Success Rates Survey (by paradigm and distribution)	Iterative	Average	71	71
			Co-located	80	
			Near Located	74	
			Far Located	59	
		Agile	Average	70	69.25
			Co-located	79	
			Near Located	73	
			Far Located	55	
		Traditional	Average	66	65.75
			Co-located	73	
			Near Located	69	
			Far Located	55	
		Ad Hoc	Average	62	61.75
			Co-located	72	
			Near Located	65	
			Far Located	48	
2007	DDJ's Project Success Survey	Agile		72	60.25
		Traditional		63	
		Data Warehouse		63	
		Offshoring		43	
1998	Bull Survey, UK			51	51
AVERAGE SUCCESS RATE				**63.2**	

is found to consume up to 80% of budgets (Dynamic Markets Limited 2007 Study). (Galorath, 2012) The 2008 and 2011 IT Project Success Survey (Ambler, 2009) and later that of 2011 (2011 IT Project Success Rates Survey, 2011) conducted by Scott W. Ambler

(Chief Methodologist for Agile and Lean for IBM Rational) and Dr. Dobb's with the goal of determining how project success was defined and the success of various approaches to software

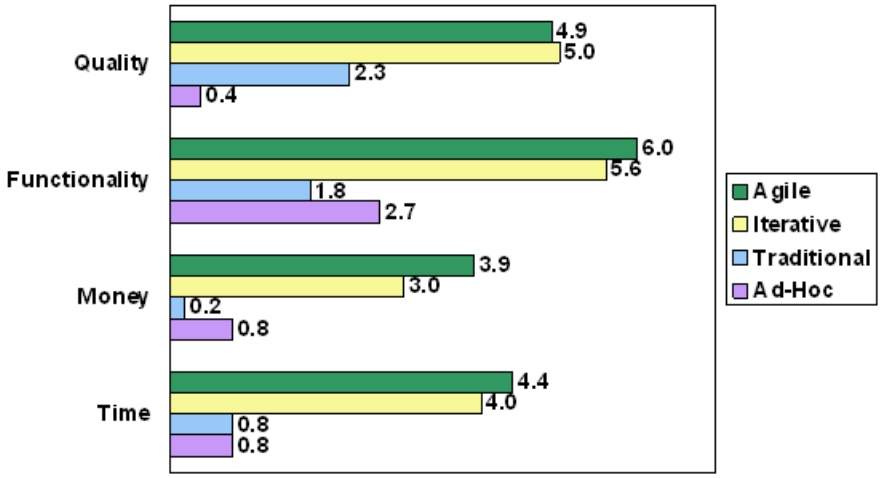

Figure 13. 2009 ratings of four success factors against four development paradigms showing effectiveness of software development paradigms. Source from Dr. Dobb's, *Software Development Success Rates*, by S. W. Ambler, retrieved November, 2013, from http://www.drdobbs.com/architecture-and-design/software-development-success-rates/216600177?pgno=3

development. The weightings were ranked as follows, 10 points for Very Effective, 5 points for Effective, 0 point for Neutral, - 5 points for Ineffective and - 10 points for Very Ineffective as shown in figures 13 and 14. Table 7 below shows pairings of

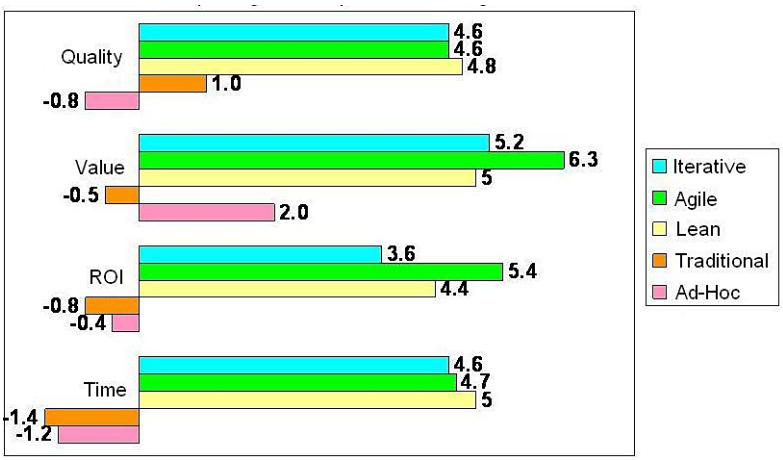

Figure 14. 2011 ratings of four success factors against four development paradigms showing effectiveness of software development paradigms. Source from Ambysoft, *2011 IT Project Success Rates Survey Results*, by Scott W. Ambler, retrieved November, 2013, from http://www.ambysoft.com/surveys/success2011.html

success factors namely quality-functionality and quality-value paradigms matched against agile, iterative and lean development paradigms.

Table 7

Highest Average Quality-Functionality and Quality-Value Success Factor Pairs for 2009 and 2011 Respectively

YEAR	DEVELOPMENT PARADIGM	SUCCESS FACTOR	EFFECTIVE SCORE	AVERAGE (%)
2009	Agile	Quality	4.9	55.0
		Functionality	6.0	
	Iterative	Quality	5.0	53.0
		Functionality	5.6	
2011	Agile	Quality	4.6	54.5
		Value	6.3	
	Iterative	Quality	4.6	49.0
		Value	5.2	
	Lean	Quality	4.8	49.0
		Value	5.0	

Evidently, these development paradigms have effectively brought about a software production success rate of 63% on the average. As such, they too are barely at the brink of their limit. Their limitation points to inadequacy of multi-computational resources which is caused by the latent language efficiency.

CHAPTER 7

THE CASE FOR A SILVER BULLET

Software development is riddled with problems of unreliability and low productivity that lead to many projects being cancelled without ever producing a working system. While some point to the lack of sound software construction methodology for managing high application complexity others blame a nonexistent discipline for the problem. On the other hand, the existence of hundreds of programming languages, operating systems and development tools have really brought about a kind of tower of Babel that can be called tower of programming languages where therein exists competition against each other. Such competitions lead to imperceptible inefficiency arising from latent language inefficiency. It therefore means that the presence of multiple languages invokes instantly a deficit efficiency or inefficiency of 33.33% even before a software project commences. This sets up an efficiency bound of 66.67% for which software production projects have approached to a level of 94.8% according to the following computation

$$\frac{Bound\ Efficiency}{Approch\ Level} = \frac{Average\ Success\ Rate}{Bound\ Efficiency} = \frac{63.2}{66.67} \times 100\% = 94.8\%.$$

Without addressing the real underlining problem as exemplified by the new Ur/Web compliable programming language which unifies web development technologies into a single and speedy technology with capability of streamlining web development, speeding up performance and providing better secure web sites (Jackson, 2014), any push in software production industry is merely to make up for the remaining 5.2% which is due to basic human errors. For sure, software crisis is something that no amount of quality assurance measure can ever cure. That is why there has been no major improvement for a very long time (more than 20 years).

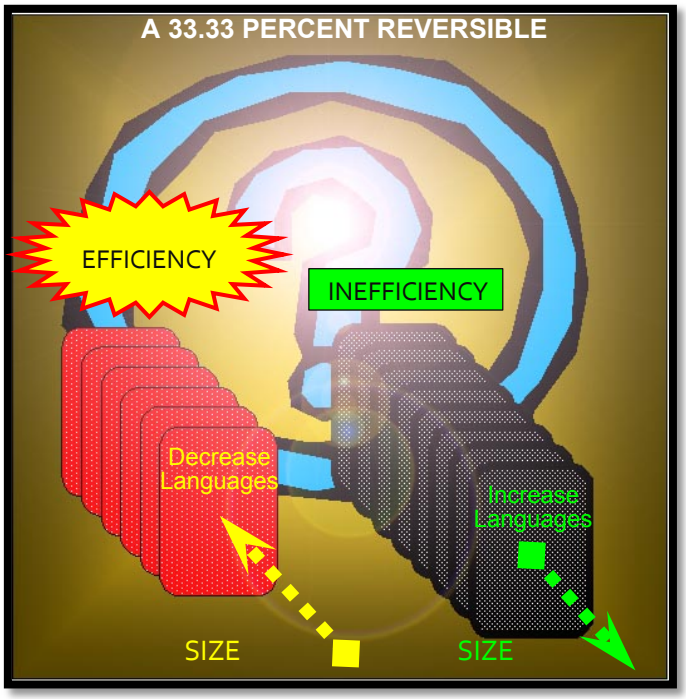

Figure 15. A depiction of rapid efficiency changes of the problem-solution cycle resulting from multiplicity of languages and its attendant reversibility.

The ensuing software crisis has led to calls for a silver bullet to provide a straightforward solution with extreme effectiveness. Though there is the thought that the diversity and complexity of software engineering is enormous to facilitate such solution approach, this is indeed a mistake. There is indeed a single cause identifiable as programming language multiplicity which is responsible for an upfront software construction inefficiency of 33.33%. So until a standard of very minimal programming languages (including supporting operating systems and development tools) is universally adopted, software construction will continue to achieve on the average below 66.67% efficiency (see figure 15).

CHAPTER 8

MEASURING MULTI-COMPUTATIONAL SKILLS

In statistical analysis, the importance of normal distributions in statistics cannot be overstated. A problem-solution cycle which involves the summation of many independent processes in the form of problem-solving skills is expected to have a distribution very close to the normal. Error propagation in a problem-solution cycle performance can thus be analytically derived once the problem-solving skills are normally distributed and subsequently, the performance rates are normally distributed. Consequently, its usage for real-valued random variables such as the problem-solving skills whose distributions are not yet known is a reasonable way to go.

Generally, the problem-solution continuum has been shown theoretically and empirically to be distributed normally. Consequently, the fundamental problem-solving skills used to achieve such outcome must take place in a normally distributed coordination in accordance with Cramér's decomposition theorem which state that: if X_1 and X_2 are independent random variables and their sum $X_1 + X_2$ has a normal distribution, then both X_1 and X_2 must be normal deviates (Galambos & Simonelli, 2004). This is equivalent to saying that the involvedness of two distributions

is normal if and only if both are normal. It is conversely derived from the property of infinite divisibility which states that: For any positive integer n, any normal distribution with mean μ and variance σ^2 is the distribution of the sum of n independent normal deviates, each with mean μ/n and variance σ^2/n (Patel & Read, 1996). Also, the problem-solving skills are independent. A proof to this assertion is given by invoking Bernstein's theorem. By definition, this theorem states that: If X and Y are independent and $X + Y$ and $X - Y$ are also independent, then both X and Y must necessarily have normal distributions (Lukacs & King, 1954; Quine, 1993). Subsequently, using the standard normal distribution (simplest case of a normal distribution) as a tool for analysis, the problem-solving skills can be formulated and measured. By definition, the standard normal distribution has a mean μ and standard deviation σ given by

$$\mu = 0 \ and \ \sigma = 1$$

as prescribed by the probability density function

$$\phi(x) = \frac{e^{-\frac{1}{2}x^2}}{\sqrt{2\pi}}$$

Also by definition, every normal distribution is the exponential of a quadratic function (Normal distribution, 2014) denoted as

$$f(x) = e^{ax^2+bx+c}$$

where the quadratic parameters a, b, and c are quadratic coefficient, the linear coefficient and the constant or free term respectively. The constant term, by definition, is denoted

$$c = \frac{-ln(-4a\pi)}{2}$$

while the mean which is expressed in terms of quadratic and linear coefficient is denoted as

$$\mu = -\frac{b}{a}$$

and the variance expressed in terms of the quadratic coefficient as

$$\sigma^2 = -\frac{1}{2a}$$

By definition, the quadratic and linear coefficients under the standard normal distribution is given by

$$a = -\frac{1}{2} \quad and \quad b = 0$$

In general, the quadratic skills function $f_s(x)$ can be given by

$$f_s(x) = e^{ax^2+bx+c}$$

While language is the means for inter-communication within the problem-solution cycle, it is as well used in intra-

communications between creativity, imagination and intelligence. Thus, language facilitates the interactions between the other problem-solving skills. Of the three problem-solving skills, namely creativity, imagination and intelligence, intelligence is the skill that is a constant per scenario. For example in a school setting, each level has a set knowledge to be acquired. Thus, intelligence can be represented by the constant term c of the quadratic skills function. However, both creativity and imagination need a variable x (i.e. subject to be tested) to function. While, of the said two skills, creativity incorporates imagination in its activities, the effect of imagination is lesser than that of creativity on the skills function of the problem-solution cycle. Thus, imagination is represented by bx while creativity is represented by ax^2. Since by definition, the value for a under a standard normal distribution is - 0.5, it implies from the value of variance given by

$$\sigma^2 = -1/(2a).$$

that σ is equal to 1. Therefore, by equating the problem-solving skills to possible modes in the problem-solution continuum limit of the problem-solution cycle, the following measure in quantum terms can be determined.

Distributive Interactions of Thought Process

In psychology, the super-factors of personalities that predict creativity are plasticity (involving openness to experience, extraversion, high energy and inspiration leading to high drive for exploration), convergence (high conscientiousness, precision, persistence and critical sense) and divergence (non-conformity, impulsivity, low agreeableness and low conscientiousness). While researches show there is a strong linkage between plasticity and creativity, on the other hand convergence is found to be strongly related to plasticity. (Kaufman, 2014) This means that there is association to being open to new experiences, inspiration, energetic and exploratory and that of having high levels of persistence and precision. However, depending on the phase of the creative process namely generation and selection phases, the three super-factors do differ. The generation phase constitutes the production of original ideas through silencing of inner critics and the imagination of many different possibilities. This phase is found to be strong in plasticity and divergence. On the other hand, the selection phase brings about new valuable ideas through criticism, evaluation, formalization, and elaboration of ideas. This process of constant checking is found to be strong in convergence. In general, the interaction of both generation and

selection phases leads to the achievement of intensified creative activities as found in human thought process.

Since the inadequacy of intelligence to explain inexplicable phenomenon leads the thought process through a problem-solution cycle, the embryonic intelligence during the problem-solution cycle is one that is not normalized. This implies the constant term *c* of the quadratic skills function which pertains to intelligence must be equal zero. Hence, the mean must be given as

$$\mu = -\frac{b}{a} = 0 \quad where \;\; b = 0$$

which is true. Given c = 0, the quadratic skills equation, the quadratic coefficient *a* can be derived from the variance equation as

$$a = -\frac{1}{2\sigma^2}$$

Substituting the above equation into the equation for the constant term of the quadratic skills equation and equating it to zero gives

$$c = \frac{-ln(-4a\pi)}{2} = \frac{-ln\left(\frac{2\pi}{\sigma^2}\right)}{2} = 0$$

Thus

$$\ln\left(\frac{2\pi}{\sigma^2}\right) = 0$$

$$\frac{2\pi}{\sigma^2} = e^0 = 1$$

which gives

$$\sigma^2 = 2\pi = 6.283185.$$

Generation Phase of Creativity

During the problem-solution cycle, the embryonic intelligence distribution, the other component distributions of the multi-computational skills namely creativity and imagination distributions (respectively green and blue curves in figure 16) and the resulting composition in the form of a standard normal deviate (red curve in figure 16) which constitutes a meta-solution distribution (interpretive answer) of the thought process must sum up to give a normalized intelligence distribution. This is in accordance with the infinite divisibility property (see infinite divisibility and Cramer's theorem) where the thought crucible filled with myriad interacting empiric distributions whose respective variable spreads eventually renormalizes the spread of the developing intelligence distribution which lacks adequate intelligence variables to comprehend ensuing phenomenon. Thus, to renormalization of the variance of the developing intelligence distribution during problem-solution cycle can be denoted as

$$\boxed{\tilde{\sigma}^2_{INT} + (-\sigma^2_{CRT}) + \sigma^2_{IMG} + (-\sigma^2_{ANS}) = \sigma^2_{INT}}$$

given that

$$\sigma^2_{ANS} = \sigma^2_{SND}$$

and $\tilde{\sigma}^2_{INT}$ is the developing intelligence variance, σ^2_{CRT} the normal creativity variance, σ^2_{IMG} the normal imagination variance, σ^2_{ANS} the variance of the interpretative answer which is equivalent to σ^2_{SND} the variance of the standard normal deviate and σ^2_{INT} the normal intelligence variance. Note that the in figure 16, the scale for $\varphi_{\mu,\sigma^2}(x)$ is the same as that for the objective prior probability (OPP) scale used for the representation of bounded lattice homomorphism in a Hasse diagram in figure 7.

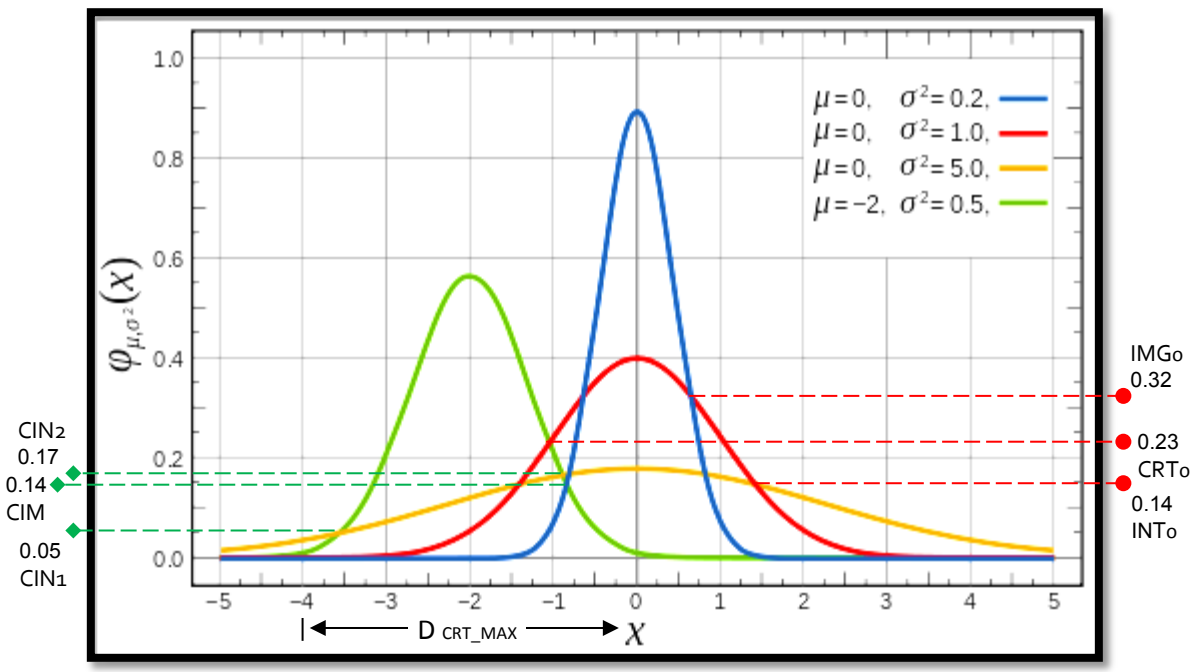

Figure 16. Graph showing normal probability density function for the normal distribution of creativity (green curve), imagination (blue curve), intelligence (yellow curve) and the standard normal deviate (red curve) which represents combined effect of creating an interpretive answer during problem-solution cycle. Adapted from Normal distribution, in *Wikipedia, the free encyclopedia*, retrieved June, 2014, from https://en.wikipedia.org/wiki/Normal_distribution

Also, the terms involving the variance of creativity and imagination distributions can be expressed as

$$\boxed{-\sigma_{CRT}^2 + \sigma_{IMG}^2 = -\{\sigma_{CRT}^2 - \sigma_{IMG}^2\}}$$

The variance of the solution distribution is negated due to the fact that it facilitates the extrusion of interpretative answer during problem-solution cycle to explain the inexplicable phenomenon. Also, the variance of creativity distribution is negated because it serves as a **thought catalyst** to speed up the development of a meta-solution without being consumed by the process. The action of the variance of imagination distribution on creativity distribution is also negated as shown from the right hand side of the above equation. This means the imagination distribution serves as a **thought promoter** (or co-catalyst) to improve the efficiency of creativity distribution in bringing about rapid solution. As a result of the coordinated efforts of creativity-imagination distributions, their special role in speeding up thought processes will be further investigated.

By definition, the variance of Stigler's normal distribution which represents imagination distribution is given by

$$\sigma^2 = \frac{1}{2\pi}$$

Therefore,

$$\sigma_{IMG}^2 = 0.16 = 0.2$$

Also, the variance of Gauss' normal distribution representing the creativity distribution is given by

$$\sigma^2 = \frac{1}{2}$$

which gives

$$\sigma_{CRT}^2 = 0.5$$

For the developing intelligence distribution, its variance is given by

$$\sigma^2 = 2\pi$$

This gives

$$\tilde{\sigma}_{INT}^2 = 6.28$$

Also, the variance for standard normal deviate or interpretative answer distribution is

$$\sigma_{SND}^2 = \sigma_{ANS}^2 = 1$$

Therefore the renormalization of the variance of the developing intelligence distribution to a normal intelligence distribution (see yellow curve in figure 16) which possess adequate intelligence variables to explain the inexplicable phenomenon via interpretative answer whose variance is equal to

$$\sigma_{INT}^2 = 5.0$$

is given by

$$\sigma_{INT}^2 = \tilde{\sigma}_{INT}^2 + (-\sigma_{CRT}^2) + \sigma_{IMG}^2 + (-\sigma_{ANS}^2) = 6.28 - 0.5 + 0.2 - 1 = 4.98 = \mathbf{5} \quad Q.E.D$$

The normal deviate is a symmetric function $\emptyset(x)$ at the mean value when x = 0 and μ = 0 attains its maximum value given by the simplest form of a standard normal distribution

$$\emptyset(x) = \frac{e^{-\frac{1}{2}x^2}}{\sqrt{2\pi}}$$

When x = 0,

$$\emptyset(x) = \frac{1}{\sqrt{2\pi}}$$

The mean value of the function $\emptyset(x)$ is the result of the mean interactions of creativity, imagination and intelligence via language. Therefore values of a, b and c can be inferred by equating the above equation to the quadratic skills function $f_s(x)$ when μ = 0 at x = 0. This gives $\emptyset(x) = f_s(x)$ at μ = 0 and σ = 1. With a = - ½ and b = 0 in the quadratic skills function, one gets

$$\frac{1}{\sqrt{2\pi}} = e^{\left(-\frac{1}{2}x^2 - \frac{\ln 2\pi}{2}\right)} = e^{-\frac{1}{2}(x^2 + \ln 2\pi)}$$

Taking natural logarithm of both sides gives

$$\ln\left(\frac{1}{\sqrt{2\pi}}\right) = -\frac{1}{2}(x^2 + \ln 2\pi)\ln e$$

$$\ln\left(\frac{1}{\sqrt{2\pi}}\right) = -\frac{1}{2}x^2 - \frac{1}{2}\ln(2\pi)$$

$$\ln\left(\frac{1}{\sqrt{2\pi}}\right) + \frac{1}{2}\ln(2\pi) = -\frac{1}{2}x^2$$

Multiplying through by 2

$$2\ln\left(\frac{1}{\sqrt{2\pi}}\right) + \ln(2\pi) = -x^2$$

Substituting appropriate values gives

$$\ln(0.15915494) + \frac{1}{2}\ln(6.2831853) = -x^2$$

$$-1.83787709 + 0.918938535 = -x^2$$

$$x^2 = 0.91893856$$

which gives

$$x = \sqrt{0.91893856} = 0.95861283$$

Therefore, the average value for normalized multi-computational skills $\bar{x}_{skills}$ is

$$\boxed{\bar{x}_{skills} = 0.95861283}$$

To find the average value $\bar{x}_{IMG}$ for normalized imagination (blue curve in figure 16), Stigler's normal distribution equation is equated with the quadratic skills function to give

$$\emptyset(x) = e^{-\pi x^2} = e^{\left(-\frac{1}{2}x^2 - \frac{\ln 2\pi}{2}\right)} = e^{-\frac{1}{2}(x^2 + \ln 2\pi)}$$

Taking the natural logarithm of both sides gives

$$-\pi x^2 \ln e = -\frac{1}{2}(x^2 + \ln 2\pi) \ln e$$

$$-\pi x^2 = -\frac{1}{2}x^2 - \frac{1}{2}\ln(2\pi)$$

$$-\pi x^2 + \frac{1}{2}x^2 = -\frac{1}{2}\ln(2\pi)$$

Multiplying through by 2

$$-2\pi x^2 + x^2 = -\ln(2\pi)$$

$$(1 - 2\pi)x^2 = -\ln(2\pi)$$

This gives

$$x^2 = \frac{-\ln(2\pi)}{(1 - 2\pi)}$$

$$x = \sqrt{\frac{-\ln(2\pi)}{(1 - 2\pi)}} = \sqrt{\frac{\ln(2\pi)}{(2\pi + 1)}} = \sqrt{\frac{1.837877}{7.2831853}} = \sqrt{0.25234522} = 0.50233975$$

Therefore, the average value for normalized imagination is

$$\boxed{\bar{x}_{IMG} = 0.502340}$$

To find the average value $\bar{x}_{CRT}$ for normalized creativity (green curve in figure 16), Gauss' normal distribution equation

is equated with the quadratic skills function to give

Using Gauss standard normal distribution equation gives

$$\emptyset(x) = \frac{e^{-x^2}}{\sqrt{\pi}} = e^{\left(-\frac{1}{2}x^2 - \frac{\ln 2\pi}{2}\right)} = e^{-\frac{1}{2}(x^2 + \ln 2\pi)}$$

Taking the natural logarithm of both sides gives

$$\ln e^{-x^2} - \ln\left(\sqrt{\pi}\right) = -\frac{1}{2}(x^2 + \ln 2\pi)\ln e$$

$$-x^2 - \ln\left(\sqrt{\pi}\right) = -\frac{1}{2}x^2 - \frac{1}{2}\ln(2\pi)$$

$$\frac{1}{2}x^2 - x^2 = \ln\left(\sqrt{\pi}\right) - \frac{1}{2}\ln(2\pi)$$

$$-\frac{1}{2}x^2 = \ln\left(\sqrt{\pi}\right) - \ln\left(\sqrt{2\pi}\right)$$

Applying laws of logarithm

$$-\frac{1}{2}x^2 = \ln\left(\frac{\sqrt{\pi}}{\sqrt{2\pi}}\right) = \ln\left(\frac{1}{\sqrt{2}}\right)$$

This gives

$$x^2 = -2\ \ln\left(\frac{1}{\sqrt{2}}\right) = \ln\left(\frac{1}{\sqrt{2}}\right)^{-2} = \ln\left(\frac{1}{2^{\frac{1}{2}}}\right)^{-2} = \ln\frac{1}{2^{\frac{1}{2}(-2)}} = \ln 2$$

Therefore

$$x = \sqrt{\ln 2} = \sqrt{0.69314718} = 0.83255461$$

Hence, the average value for normalized creativity is

$$\boxed{\bar{x}_{CRT} = 0.832555}$$

From the variance of Stigler's normal distribution, the standard deviation is

$$\sigma = \sqrt{\frac{1}{2\pi}} = 0.399$$

Also, from the variance of Gauss' normal distribution, the standard deviation of

$$\sigma = \sqrt{\frac{1}{2}} = 0.707$$

By comparing the creativity spread given by the standard deviation for Gauss' normal distribution to the imagination spread given by the standard deviation for Stigler's normal distribution, it can be said that imagination needs more of its values within a smaller region (minimum divergence effect) around its mean in order to form mental images. On the other hand, creativity needs widely spread values (maximum divergence effect) around its mean value. This obviously facilitates its task to create new things. Thus, creativity not only needs to be very distributed but also it needs to be "focused".

Selection Phase of Creativity

Observe that the cumulative distributive function for creativity shown in green in figure 17 is isolated at the 50th percentile

while the others intersect to form a common point. Thus, creativity is more sparsely distributed than the other problem-solving skills. This implies that in general, creativity is always uncommon on the average (50 percent or middle point). However, the commonality of creativity and intelligence at point CI in figure 17 is generally always 10%. Also, the commonality of creativity, imagination and intelligence is generally 0%. This is true for all three problem-solving skills are independent and cannot occur at the same time in a real system. However in an ideal or perfect system, the occurrence of all three problem-solving skills is certain (100%). Also, from the graph in figure 16 showing the normal probability density functions for creativity (green curve), imagination (blue curve), intelligence (yellow curve) and their combined effect which is the standard normal deviate, it can be shown that the sum of the value of normal probability function $\phi(x)$ for each intersection point between creativity, imagination, intelligence and their standard normal deviate (except for the interaction between creativity and intelligence whose greater value is taken by reason of maximizing effect) add up to 1. Equivalently, this set of fundamental skills intersections represents the general solution function Ψ of the **solution continuum** which was earlier defined as

$$\Psi : \Theta \times \pi \longrightarrow \Delta$$

where Θ represents natural laws or principles governing the environment, π the actions taken to define problems and Δ the

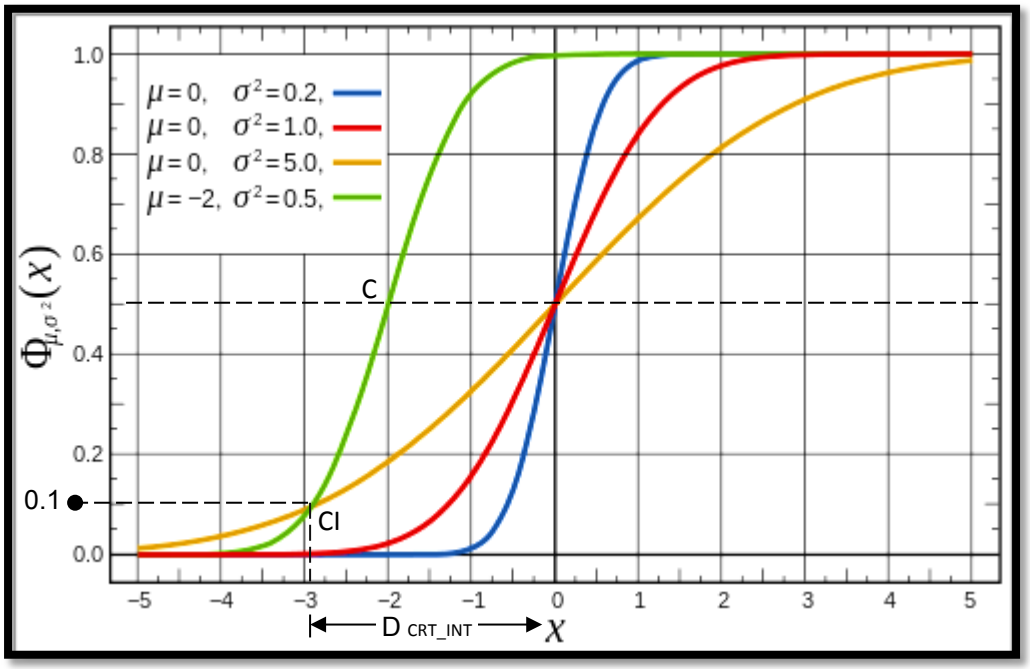

Figure 17. Graph showing cumulative distributive function for the standard normal distributions of imagination (blue curve), creativity (green curve), intelligence (yellow curve) and their combined effect (red curve). Adapted from Normal distribution, in *Wikipedia, the free encyclopedia*, retrieved June, 2014, from https://en.wikipedia.org/wiki/Normal_distribution

progressive changes or shifts in understanding inexplicable environmental principles. The ensuing set of problem-solving skills interactions is generally equivalent to the Cartesian product Θ × π which yields the set of all ordered pairs with the first element of each pair selected from Θ and the second element selected from π. Said set of interactions is equivalent to human brain interhemispheric connectivity which is essential for information integration and the expansion of creative thought.

By definition, creativity yields a new product represented by standard normal deviate through its interaction with

intelligence and imagination. Therefore pertaining to a problem-solution cycle (PSC), one can respectively denote PSC's back end phase $\mathfrak{B}$ and PSC's front end phase $\mathfrak{F}$ as

$$\mathfrak{B}_i = \{CRT, INT, IMG\} \quad and \quad \mathfrak{F}_i = \{INT, IMG, SND\}$$

The linkage between creativity and the front end phase of PSC and that of standard normal deviate and the back end phase of PSC can be represented by the following joined cross products

$$\left(CRT \times \bigcup_{i \in I} \mathfrak{F}_i\right) \cup \left(SND \times \bigcup_{i \in I} \mathfrak{B}_i\right)$$

$$= (\mathrm{CRT} \times (\mathrm{INT} \cup \mathrm{IMG} \cup \mathrm{SND})) \cup \mathrm{SND} \times (\mathrm{CRT} \cup \mathrm{INT} \cup \mathrm{IMG}))$$

where I is the set of integers. However, the embryonic transformational interactions which are facilitated by existing linkages will generally yield the solution function Ψ of the **solution continuum** of PSC. Mathematically, the above backbone interaction of a problem-solution cycle can be expressed as

$$\Psi(PSC) = \left(CRT \cap \bigcup_{i \in I} \mathfrak{F}_i\right) \cup \left(SND \cap \bigcup_{i \in I} \mathfrak{B}_i\right)$$

which gives

$$\Psi(PSC) = \big(\mathrm{CRT} \cap (\mathrm{INT} \cup \mathrm{IMG} \cup \mathrm{SND})\big) \cup \big(\mathrm{SND} \cap (\mathrm{CRT} \cup \mathrm{INT} \cup \mathrm{IMG})\big)$$

$$= ((\mathrm{CRT} \cap \mathrm{INT}) \cup (\mathrm{CRT} \cap \mathrm{IMG}) \cup (\mathrm{CRT} \cap \mathrm{SND})) \cup ((\mathrm{SND} \cap \mathrm{CRT}) \cup (\mathrm{SND} \cap \mathrm{INT}) \cup (\mathrm{SND} \cap \mathrm{IMG}))$$

$$= (\mathrm{CRT} \cap \mathrm{INT}) \cup (\mathrm{CRT} \cap \mathrm{IMG}) \cup (\mathrm{CRT} \cap \mathrm{SND}) \cup (\mathrm{SND} \cap \mathrm{INT}) \cup (\mathrm{SND} \cap \mathrm{IMG})$$

Substituting respective intersections with corresponding values of normal probability function $\phi(x)$ (see figure 16), the following is obtained.

$$\Psi(PSC) = CIN_2 + CIM + CRT_O + INT_O + IMG_O = 0.17 + 0.14 + O.23 + 0.14 + 0.32$$
$$= 1. \quad Q.E.D$$

In the case of the intersection between creativity and intelligence ($\mathrm{CRT} \cap \mathrm{INT}$), there exists two values notably CIN_1 which has a value of 0.05 and CIN_2 whose value is 0.17. It can therefore be deduced from set-theoretic rule that

$$A \subseteq B \quad if\ and\ only\ if \quad A \cup B = B.$$

Therefore, since

$$\mathrm{CIN}_1 \subseteq \mathrm{CIN}_2 \in CIN$$

and

$$\mathrm{CIN}_1, \mathrm{CIN}_2 \in CIN$$

one can write

$$CIN_1 \cup CIN_2 = CIN_2$$

which explains why CIN_2 was selected over CIN_1 in the computation of Ψ(PSC). As a matter of consequence, it can be concluded that: *The sum of all effective pdf values corresponding to points of intersections between the standard normal deviate and all its normal variations is equal to the sum of the area under the standard normal deviate which is a probability of 1.*

Consequently, when problem-solving skills intersect normally, they create joint entropies whose combined sum $fx(\mu)$ is equal to 1. Such group of **random pure state ensemble (RPSE)** must be of special interest in quantum information theory.

The Skills Formulation

Let the following (x1, x2, …, xn) be a stratified random sampling of performance over a period of time from a normal N(μ, σ^2) population where μ is the population mean and σ^2 is the population variance. Since the population μ and σ are not known because one cannot get every performance data of problem-solving activities of a subject for the stipulated period of time, the approximated values of μ and σ parameters are used. For a standard approach, the maximum likelihood method is applied. By definition, the maximum likelihood estimates are:

$$\hat{\mu} = \bar{x} \equiv \frac{1}{n}\sum_{i=1}^{n} x_i$$

and

$$\hat{\sigma}^2 = \frac{1}{n}\sum_{i=1}^{n}(x_i - \bar{x})^2$$

where the estimator $\hat{\mu}$ is the sample mean which is the arithmetic mean of all sample observations and $\hat{\sigma}^2$ is the sample variance.

According to Lehman-Scheffe' theorem, the uniformly minimum variance and unbiased estimator is $\hat{\mu}$ due to the completeness and sufficiency of $\bar{x}$ for μ (Krishnamoorthy, 2006). So, with $\hat{\mu}$ and $\hat{\sigma}^2$ determined, the following computes the measures of the problem-solving skills:

1. **Creativity Measure:** From the quadratic skills function, the creative term is ax^2. Using the corresponding variance given by $\sigma^2 = \frac{-1}{2a}$ one gets $a = \frac{-1}{2\sigma^2}$. Also, the mean creative value is given by $x_{CRT} = 0.833$. Hence, the creativity quotient CRT is denoted by

$$\boxed{CRTQ = ax^2 = -\frac{\bar{x}_{CRT}^2}{2\hat{\sigma}^2} \quad where\ \hat{\sigma} \neq 0}$$

where the estimator $\hat{\sigma}^2$ is the sample variance.

2. **Imagination Measure:** The imagination term from the quadratic skills function is bx. Using the corresponding mean value μ for the exponential of the quadratic skills function given by $\mu = \frac{-b}{a}$ and substituting for *a* using $\sigma^2 = \frac{-1}{2a}$ one gets $\mu = 2\sigma^2 b$ which implies $b = \frac{\mu}{2\sigma^2}$. Therefore the imagination quotient IMGQ is given by

$$\boxed{IMGQ = bx = \frac{\hat{\mu}\bar{x}_{IMG}}{2\hat{\sigma}^2} \quad where\ \hat{\sigma} \neq 0}$$

where $\hat{\mu}$ is the mean estimator of sample and $\bar{x}_{IMG}$ is the mean imagination value which is equal to 0.502.

3. **Intelligence Measure:** This is represented by the constant term of the quadratic skills function which is by definition given by

$$c = \frac{-\ln(-4a\pi)}{2}$$

Since $a = \frac{-1}{2\sigma^2}$ one gets $c = -\ln\left(\frac{2\pi}{\sigma^2}\right)/2$. Hence, the intelligent quotient INTQ is given as

$$\boxed{INTQ = c = \frac{-\ln\left(\frac{2\pi}{\sigma^2}\right)}{2} \quad where\ \hat{\sigma} \neq 0}$$

Generally, a smaller $\hat{\sigma}^2$ leads to greater skills quotients. This implies that more concentrated the facts are, the better it is for the problem-solving process.

By convention, if imagination which is an abstract activity is assigned a negative measure while creativity and intelligence are attributed positive sign, then the outcome of the problem-solving skills quotient can be aligned with the above convention by multiplying each quotient measure by -1. This gives the following:

$$CRTQ = (-1)ax^2 = \frac{\bar{x}_{CRT}^2}{2\sigma^2}$$

$$IMGQ = -bx = \frac{-\hat{\mu}\bar{x}_{IMG}}{2\hat{\sigma}^2}$$

and

$$INTQ = -c = \frac{\ln\left(\frac{2\pi}{\sigma^2}\right)}{2}$$

In general, under the initial condition of a problem-solution cycle, the relationship between the modulus of the multi-computational skills can be expressed as

$$\left|\frac{\hat{\mu}\bar{x}_{IMG}}{2\hat{\sigma}^2}\right| > \left|-\frac{\bar{x}_{CRT}^2}{2\hat{\sigma}^2}\right| > \left|-\frac{\ln\left(\frac{2\pi}{\hat{\sigma}^2}\right)}{2}\right|$$

That is, the initial condition of multi-computational skill magnitudes is such that

$$|IMGQ|_o > |CRTQ|_o > |INTQ|_o$$

It is understandable that INTQ is the least of all fundamental problem-solving skills. Since it is the lack of intelligence needed to understand observed environmental phenomenon that initiates a problem. For if one had adequate intelligence to understand the observed phenomenon, there would not have been the need to define a problem. In general, the measurer of creativity quotient (CRTQ), imagination quotient (IMGQ) and intelligence quotient (INTQ) must perform inferential statistical test(s) on the examined subject in order to determine the variance needed to compute a valid and universally standardized problem solving skills abilities. As such, these skills quotients will be computed and analyzed using two difference empirical data, namely CHAOS data and GCI data.

Prior Statistical Inference of Problem-Solving Skills

The formulation for CRTQ shows that as $\hat{\sigma}$ approaches zero CRTQ approaches zero. The former limit approach implies that as more information is concentrated around the mean (i.e. densely

distributed) the more creative skill is available and when information is rather scattered in a broader region (sparsely distributed) about the mean, the lesser creative skill is available. For IMGQ, it shows that the situation is the same as that for CRTQ as $\hat{\sigma}$ approaches zero or infinity. However, when the mean estimator $\hat{\mu}$ of the sample data is zero, IMGQ will be equal to zero. The implication here is simple. While imagination is needed in the process of solving a problem, its usage is diminished towards/to zero as a solution is approached. For INTQ, the only reasonable way for it to be zero is when its numerator is zero. This means that $\frac{2\pi}{\hat{\sigma}^2}$ will approach zero when $\hat{\sigma}$ approaches infinity. That is

$$\lim_{\hat{\sigma} \to \infty} \frac{2\pi}{\hat{\sigma}^2} = 0$$

However, this means that

$$\lim_{\hat{\sigma} \to \infty} \ln\left(\frac{2\pi}{\hat{\sigma}^2}\right) = \ln(0)$$

which is undefined. On the other hand, if the limit approach is zero, the result is as such given by

$$\lim_{\hat{\sigma} \to 0} \ln\left(\frac{2\pi}{\hat{\sigma}^2}\right) = \ln(\infty) = \infty$$

Hence, while a broader or sparse spread of information distribution leads to a decrease and in the worst case an undefined intelligence (which means it is in embryonic state), a

sparsely information distribution leads to an increase intelligence. This in turn leads to an infinite intelligence continuum.

As measured standard scores, INTQ, IMGQ and CRTQ are technically forms of "deviation measurements" rather than "ratio measurements" of brain traits.

CHAPTER 9

EMPIRICAL DETERMINATION OF FUNDAMENTAL PROBLEM-SOLVING SKILLS

Here use is made of the data from CHAOS research from Standish Group involving 12 years of cumulative research on 50,000 industry software development projects over a period of 10 years shown in the table 8 below.

Table 8

10-Year-Data of Software Development Projects Around the World from CHAOS Research of Standish Group (1994-2004)

CHAOS DATA: SOFTWARE DEVELOPMENT PROJECT SUCCESS RATE						
YEAR	1994	1996	1998	2000	2002	2004
SUCCESS RATE (%)	16	27	26	28	34	29

Since the process involves problem-solving, only a solved problem is required. A problem partially solved is therefore no solution. This is the why the data needed came from those who succeeded in completing their projects.

CHAOS Computations

The mean of CHAOS sample CHAOS X_{AVG} of size n equal to 6 is given by

$$CHAOS\ X_{AVG} = \bar{X} = \frac{1}{n}\sum_{i=1}^{n} x_i = \frac{16+27+26+28+34+29}{6} = \frac{160}{6} = 26.666667$$

Also, the CHAOS sample variance σ^2 is computed as

$$CHAOS\ \sigma^2 = \frac{1}{n}\sum_{i=1}^{n}(x_i - \bar{x})^2 = 35.066667\ (from\ excel\ var.s\ function)$$

Using earlier computed average values of normalized creativity $\bar{x}_{CRT}$ (0.832555) and normalized imagination $\bar{x}_{IMG}$ (0.502339), the multi-computational skills quotients are computed as follows.

$$CHAOS\ \ CRTQ = \left|-\frac{\bar{x}_{CRT}^2}{2\hat{\sigma}^2}\right| = \frac{0.832555^2}{2 \times 35.066667} = 0.009883 = \mathbf{0.99}\%$$

$$CHAOS\ \ IMGQ = \left|\frac{\hat{\mu}\bar{x}_{IMG}}{2\hat{\sigma}^2}\right| = \frac{26.666667 \times 0.502340}{2 \times 35.066667} = 0.191004 = \mathbf{19.10}\%$$

$$CHAOS\ \ INTQ = \left|-\frac{\ln\left(\frac{2\pi}{\hat{\sigma}^2}\right)}{2}\right| = \frac{\ln\left(\frac{2\pi}{35.066667}\right)}{2} = 0.859687 = \mathbf{85.97}\%$$

Also the average of CHAOS IMGQ and INTQ is given by

$$Average\ IMGQ\ \&\ INTQ = \frac{0.1910003 + 0.859687}{2} = 0.525344 = \mathbf{52.53}\%$$

The respective results are tabulated in table 9 below.

Table 9

Statistics Derived from the Computation of Creative, Imagination and Intelligence Quotient Based on CHAOS 10-Year-Data (1994-2004) of Software Development Projects Successes Around the World

CHAOS RESEARCH DATA (1994 - 2004): DESCRIPTIVE STATISTICS OF SUCCESS SAMPLE OF SOFTWARE PRODUCTION				
Mean X_{CRT}	0.832555		Sample Size (n)	6
Mean X_{IMG}	0.502340			
Sample Mean (X_{AVG})	26.666667	Measured Quotient Score		
Sample Variance (σ^2)	35.066667			
CRTQ ►	0.009883	0.99%		
IMGQ ►	0.191004	19.10%		
INTQ ►	0.859687	85.97%		
Average of IMGQ & INTQ	0.525344	52.53%		

Note: 1. The average of IMGQ and INTQ is approximately 50th percentile as expected from the inference of the cumulative distribution of problem-solving skills. 2. Success sample by definition is normally distributed.

On the other hand, computations related to the intersection or joint reaction of creativity and intelligence under cumulative distribution function (see figure 17) can be given as follows. From figure 17, the deviation $D_{CRT\&INT}$ of the point of intersection CI of creativity and intelligence from the mean X is equal to ± 2.87 and from figure 16, the maximum deviation of creativity

D_{CRT_MAX} is equal to − 4. Therefore, under cumulative density function (CDF) the deviated mean X_{CRT} is given by

$$\underset{(positive\ sign)}{CHAOS}: Deviated\ \bar{X}_{CRT} = \bar{X}_{CRT} - D_{CRT\ \&\ INT} = 0.832555 - 2.87 = \mathbf{-2.037445}$$

$$\underset{(negative\ sign)}{CHAOS}: Deviated\ \bar{X}_{CRT} = \bar{X}_{CRT} - D_{CRT\ \&\ INT} = 0.832555 - (-2.87) = \mathbf{3.702555}$$

and under probability density function (PDF)

$$CHAOS: Deviated\ \bar{X}_{CRT} = \bar{X}_{CRT} - D_{CRT\ MAX} = 0.832555 - (-4) = \mathbf{4.832555}$$

The translated CRTQ due to the translation of cumulative creativity under CDF (see green curve in figure 17) can be computed as

$$\underset{(positive\ sign)}{CHAOS}: Translated\ CRTQ = \left| -\frac{\bar{x}_{CRT}^2}{2\hat{\sigma}^2} \right| = \frac{(-2.037445)^2}{2 \times 35.066667} = \mathbf{0.059190}$$

$$\underset{(negative\ sign)}{CHAOS}: Translated\ CRTQ = \left| -\frac{\bar{x}_{CRT}^2}{2\hat{\sigma}^2} \right| = \frac{(3.702555)^2}{2 \times 35.066667} = \mathbf{0.195469}$$

and the translation of creativity distribution under PDF (see green curve in figure 16) can also be computed as

$$CHAOS: Translated\ CRTQ = \left| -\frac{\bar{x}_{CRT}^2}{2\hat{\sigma}^2} \right| = \frac{(4.832555)^2}{2 \times 35.066667} = \mathbf{0.332988}$$

The probability of translated CDF creativity interacting with intelligence is given by

$$\underset{(positive\ sign)}{CHAOS}: P(Trans\_CRTQ_{CDF}) \cdot P(INTQ) = 0.059190 \times 0.859687 = \mathbf{0.050885}$$

$$\underset{(negative\ sign)}{CHAOS}: P(Trans\_CRTQ_{CDF}) \cdot P(INTQ) = 0.195469 \times 0.859687 = \mathbf{0.168042}$$

and therefore the average of the probability of translated CDF creativity and intelligence is a

$$\underset{(positive\ sign)}{CHAOS}: Average\ Translated\ \ CRTQ_{CDF}\ \&\ INTQ = \frac{0.059190\ +\ 0.859687}{2}$$

$$= \mathbf{0.459438}$$

$$\underset{(negative\ sign)}{CHAOS}: Average\ Translated\ \ CRTQ_{CDF}\ \&\ INTQ = \frac{0.195469\ +\ 0.859687}{2}$$

$$= \mathbf{0.527578}$$

This gives an overall average of translated average CDF creativity and intelligence as

$$CHAOS: \underset{Translated\ Average}{Overall\ Average\ of}\ \ CRTQ_{CDF}\ \&\ INTQ = \frac{0.459438\ +\ 0.527578}{2} = \mathbf{0.493508}$$

By definition, the CHAOS creativity-imagination free entropy (CIFE) can be computed as

$$CHAOS: CIFE = P(Trans\_CRTQ_{PDF}) \cdot P(IMGQ) = 0.332988 \times 0.191004 = \mathbf{0.063602}$$

Finally, the average of the averages of both positive and negative cases of the probability of translated CDF creativity interacting with intelligence is given by

$$CHAOS: Average\ of\ P(Trans\_CRTQ_{CDF} \cdot P(INTQ) = \frac{0.050885\ +\ 0.168042}{2} = 0.109464$$

$$= \mathbf{10.95}\%$$

The respective results are tabulated in table 10 below.

Table 10

10-Year-Data of Software Development Projects from Around the World

CHAOS DATA: Cumulative Distributive Function (CDF) Analysis of Creativity & Intelligence			Creativity's Maximum Probability Density Function (PDF) Deviation D_{CRT_Max}
Deviation of Creativity & Intelligence Intersection	Positive	Negative	
$D_{CRT\ \&\ INT}$	2.87	- 2.87	- 4
Deviated Mean X_{CRT}	- 2.037445	3.702555	4.832555
Translated CRTQ ►	0.059190	0.195469	0.332988
P(Trans_$CRTQ_{CDF}$) * P(INTQ)	0.050885	0.168042	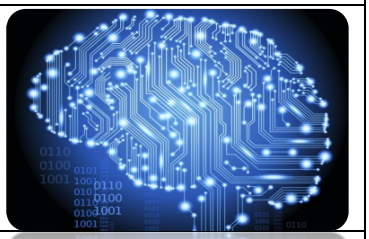
Average of Translated $CRTQ_{CDF}$ & INTQ	0.459438	0.527578	
Overall Average of Translated Average of $CRTQ_{CDF}$ & INTQ	0.493508		
P(Trans_$CRTQ_{PDF}$) * P(IMGQ) [Creativity-Imagination Free Entropy]	0.063602		
Average of P(Trans_$CRTQ_{CDF}$) * P(INTQ)	0.109464	10.95%	◄ INTELLI-CREATIVITY CUMULATIVE CONSTANT

The Global Creativity Index (GCI) data covers 82 nations spanning 2000-2009. Its technology index involves 3 variables namely R&D (research and development) investment, global research, and global innovation. The talent index uses human capital and creative class population and finally tolerance index uses tolerance towards ethnic and racial minorities and sexual orientation via Gallup Organization's World Poll. These three indices form the 3Ts of economic development. Figure 18 shows maps indicating scope of technology, talent and tolerance around

the world. The GCI score is determined by dividing the average score of 3Ts by the number of overall observations. The role of 3Ts in economic growth and development is underpinned by human creativity on which future progress and prosperity depends on. The overall Global Creativity Index ranking is shown in Appendix A. In order to facilitate data from GCI index in problem-solving skills analysis, it has to be converted into a sample of means using values of the 3Ts. The newly formed sample of means (see Appendix A and table 11 below) is approximately normal distributed in accordance with the central limit theorem (Rice, 1995).

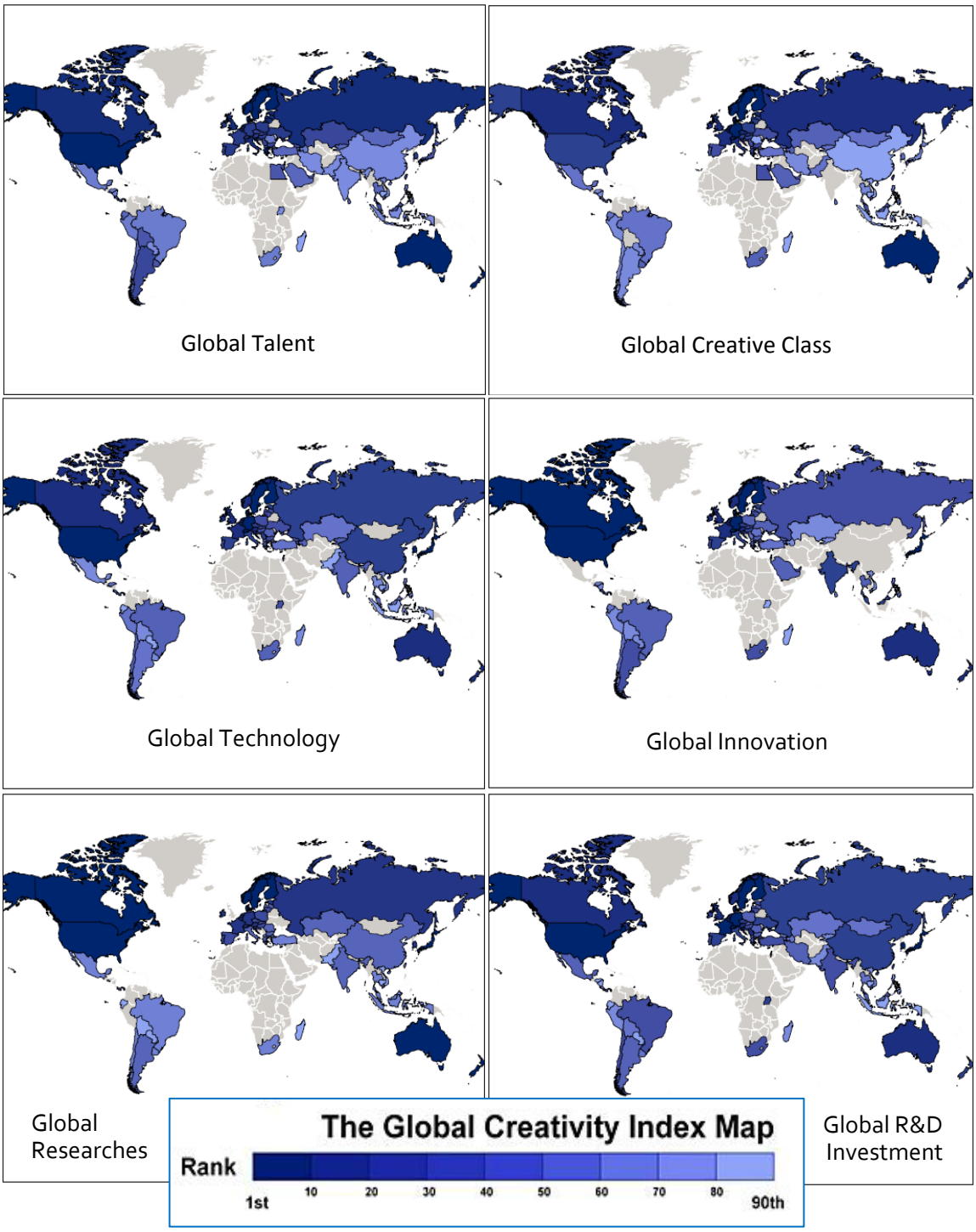

Figure 18. Global maps depicting factors involved in technology, talent and tolerance (3Ts) of economic development. Adapted from Martin Prosperity Institute, *Creativity and Prosperity: The Global Creativity Index*, by Zara Matheson, retrieved June, 2014, from http://martinprosperity.org/media/GCI%20Report%20Sep%202011.pdf

GCI Computations

Using 3T stratified sampled means data in table 11, the mean of GCI stratified random sampling of 3T means GCI X_{AVG} of size N equal to 12 is given by

$$GCI\ X_{AVG} = \bar{X} = \frac{1}{N}\sum_{i=1}^{N} \bar{x_i}$$

$$= \frac{7 + 9.67 + 16 + 30 + 33 + 37 + 40.67 + 44.33 + 52.67 + 54.33 + 58 + 63.67}{12}$$

$$= \frac{160}{12}$$

$$= 37.194444$$

Table 11

Data Showing Random Sampled Means Based on Technology, Talent and Tolerance Data from Global Creativity Index (GCI)

SAMPLED 3T (TECHNOLOGY, TALENT & TOLERANCE) MEANS GCI DATA - 2011												
Stratified Countries	1	2	3	4	5	6	7	8	9	10	11	12
Stratified Random Sampling of 3T Means	7.00	9.67	16.00	30.00	33.00	37.00	40.67	44.33	52.67	54.33	58.00	63.67

martinprosperity.org © 2010

Also, the GCI sample variance σ^2 is computed as

$$GCI\ \sigma^2 = \frac{1}{N}\sum_{i=1}^{N} (\bar{x}_i - \bar{\bar{x}})^2 = 356.170875\ \ (from\ excel\ var.s\ function)$$

This gives the standard deviation σ of the GCI 3T mean distribution as

$$GCI\ \sigma = \sqrt{\frac{1}{N}\sum_{i=1}^{N}(\bar{x}_i - \bar{\bar{x}})^2} = \sqrt{356.170875} = 18.872490$$

Therefore, the GCI 3T mean distribution's standard deviation σ_M is given by

$$GCI\ \sigma_M = \frac{\sigma}{\sqrt{N}} = \frac{18.872490}{\sqrt{12}} = 5.448019$$

which gives the variance ${\sigma_M}^2$ of the GCI 3T mean distribution as

$$GCI\ {\sigma_M}^2 = (GCI\ \sigma_M)^2 = (5.448019)^2 = 29.680906$$

Using earlier computed average values of normalized creativity $\bar{x}_{CRT}$ (0.832555) and normalized imagination $\bar{x}_{IMG}$ (0.502340), the multi-computational skills quotients are computed as follows.

$$GCI\ \ CRTQ = \left|-\frac{\bar{x}_{CRT}^2}{2\hat{\sigma}^2}\right| = \frac{0.832555^2}{2 \times 29.680906} = 0.011677 = \mathbf{1.17}\%$$

where $\hat{\sigma}^2$ is equal to σ_M^2.

$$GCI\ \ IMGQ = \left|\frac{\hat{\mu}\bar{x}_{IMG}}{2\hat{\sigma}^2}\right| = \frac{37.194444 \times 0.502340}{2 \times 29.680906} = 0.314752 = \mathbf{31.48}\%$$

where $\hat{\mu}$ is equal to X_{AVG}.

$$GCI\ \ INTQ = \left|-\frac{\ln\left(\frac{2\pi}{\hat{\sigma}^2}\right)}{2}\right| = \frac{\ln\left(\frac{2\pi}{29.680906}\right)}{2} = 0.776313 = \mathbf{77.63}\%$$

Also the average of GCI IMGQ and INTQ is given by

$$IMGQ\ \&\ INTQ\ Average = \frac{0.314752 + 0.776313}{2} = 0.545532 = \mathbf{54.55}\%$$

The respective results are tabulated in table 12 below.

Table 12

Statistics Derived from the Computation of Creative, Imagination and Intelligence Quotient Based on 3Ts (Technology, Talent and Tolerance) Global Creativity Index (GCI) 2010 Data of Economic Activities of the World

GCI DATA (2010) ANALYSIS: DESCRIPTIVE STATISTICS OF RANDOM SAMPLING OF 3T MEANS				
Mean X_{CRT}	0.832555		Means Sample Size N	12
Mean X_{IMG}	0.502340			
Sample Mean (X_{AVG})	37.194444			
Sample Variance (σ^2)	356.170875			
Distribution Standard Deviation (σ)	18.872490			
Mean Distribution Standard Deviation (σ_M)	5.448019	$\sigma_{mean} = \frac{\sigma}{\sqrt{N}}$	N is the number of mean observations in the means sample used to estimate sample mean.	
Variance of Mean Distribution (σ_M^2)	29.680906	Measured Quotient Score		
CRTQ ►	0.011677	1.17%		
IMGQ ►	0.314752	31.48%		
INTQ ►	0.776313	77.63%		
IMGQ & INTQ Average	0.545532	54.55%		

Note: 1. The average of IMGQ and INTQ is approximately 50th percentile as expected from the inference of the cumulative distribution of problem-solving skills. 2. The sample of means is normally distributed in accordance with the central limit theorem.

On the other hand, computations related to the intersection or joint reaction of creativity and intelligence under cumulative distribution function (see figure 17) can be given as follows. From figure 17, the deviation $D_{CRT\&INT}$ of the point of intersection CI of creativity and intelligence from the mean X is equal to ± 2.87 and from figure 16, the maximum deviation of creativity

D_{CRT_MAX} is equal to - 4. Therefore, under cumulative density function (CDF) the deviated mean X_{CRT} is given by

$$\underset{(positive\ sign)}{GDI}: Deviated\ \bar{X}_{CRT} = \bar{X}_{CRT} - D_{CRT\ \&\ INT} = 0.832555 - 2.87 = \mathbf{-2.037445}$$

$$\underset{(negative\ sign)}{GDI}: Deviated\ \bar{X}_{CRT} = \bar{X}_{CRT} - D_{CRT\ \&\ INT} = 0.832555 - (-2.87) = \mathbf{3.702555}$$

and under probability density function (PDF)

$$GCI: Deviated\ \bar{X}_{CRT} = \bar{X}_{CRT} - D_{CRT\ MAX} = 0.832555 - (-4) = \mathbf{4.832555}$$

The translated CRTQ due to the translation of cumulative creativity under CDF (see green curve in figure 17) can be computed as

$$\underset{(positive\ sign)}{GCI}: Translated\ CRTQ = \left| -\frac{\bar{x}_{CRT}^2}{2\hat{\sigma}^2} \right| = \frac{(-2.037445)^2}{2 \times 29.680906} = \mathbf{0.069930}$$

$$\underset{(negative\ sign)}{GCI}: Translated\ CRTQ = \left| -\frac{\bar{x}_{CRT}^2}{2\hat{\sigma}^2} \right| = \frac{(3.702555)^2}{2 \times 29.680906} = \mathbf{0.179280}$$

and the translation of creativity distribution under PDF (see green curve in figure 16) can also be computed as

$$GCI: Translated\ CRTQ = \left| -\frac{\bar{x}_{CRT}^2}{2\hat{\sigma}^2} \right| = \frac{(4.832555)^2}{2 \times 29.680906} = \mathbf{0.393411}$$

The probability of translated CDF creativity interacting with intelligence is given by

$$\underset{(positive\ sign)}{GCI}: P(Trans\_CRTQ_{CDF}) \cdot P(INTQ) = 0.069930 \times 0.776313 = \mathbf{0.054288}$$

$$\underset{(negative\ sign)}{GCI}: P(Trans\_CRTQ_{CDF}) \cdot P(INTQ) = 0.230938 \times 0.776313 = \mathbf{0.179280}$$

and therefore the average of the probability of translated CDF creativity and intelligence is a

$$\underset{(positive\ sign)}{GCI}: Average\ Translated\ \ CRTQ_{CDF}\ \&\ INTQ = \frac{0.069930\ +\ 0.776313}{2}$$

$$= \mathbf{0.423122}$$

$$\underset{(negative\ sign)}{GCI}: Average\ Translated\ \ CRTQ_{CDF}\ \&\ INTQ = \frac{0.230938\ +\ 0.776313}{2}$$

$$= \mathbf{0.503626}$$

This gives an overall average of translated average CDF creativity and intelligence as

$$GCI: \begin{matrix} Overall\ Average\ of \\ Translated\ Average \end{matrix}\ \ CRTQ_{CDF}\ \&\ INTQ = \frac{0.423122\ \ +\ 0.503626}{2} = \mathbf{0.463374}$$

By definition, the GCI creativity-imagination free entropy (CIFE) can be computed as

$$GCI:\ CIFE = P(Trans\_CRTQ_{PDF}) \cdot P(IMGQ) = \ 0.393411 \times 0.314752 = \mathbf{0.123827}$$

Finally, the average of the averages of both positive and negative cases of the probability of translated CDF creativity interacting with intelligence is given by

$$GCI:\ Average\ of\ P(Trans\_CRTQ_{CDF} \cdot P(INTQ) = \frac{0.054288\ +\ 0.179280}{2} = 0.116784$$

$$= \mathbf{11.68}\%$$

The respective results are tabulated in table 13 below.

Table 13

Data Analysis of Inhibiting Interaction Between Intelligence and Creativity Based on Cumulative Distributive and Probability Density Functions of 2010 Global Creativity Index Data

GCI DATA: Cumulative Distributive Function (CDF) Analysis of Creativity & Intelligence			Creativity's Maximum Probability Density Function (PDF) Deviation D_{CRT_Max}
Deviation of Creativity & Intelligence Intersection $D_{CRT\ \&\ INT}$	Positive	Negative	
	2.87	- 2.87	- 4
Deviated Mean X_{CRT}	- 2.037445	3.702555	4.832555
Translated CRTQ ►	0.069930	0.230938	0.393411
$P(Trans\_CRTQ_{CDF})$ * P(INTQ)	0.054288	0.179280	
Average of Translated $CRTQ_{CDF}$ & INTQ	0.423122	0.503626	
Overall Average of Translated $CRTQ_{CDF}$ & INTQ Average	0.463374		
$P(Trans\_CRTQ_{PDF})$ * P(IMGQ) [CIFE]	0.123827		
Average of $P(Trans\_CRTQ_{CDF})$ * P(INTQ)	0.116784	11.68%	◄ INTELLI-CREATIVITY COMMULATIVE CONSTANT

Interpretations of Empirical Analysis Outcome

Attempts made to develop creativity quotient of an individual in similitude to that for intelligence quotient (IQ), has been seemingly futile (Craft, 2005). Within the circles of cognition pedagogies, creativity skill or "divergent thinking" is very pivotal in the activities of exceptional prodigy. It also involves intelligence skill which is "convergent thinking" with

abilities such as reasoning, computational, and symbolic manipulation. Thus, the display of exceptional divergent and convergent thinking is considered a genius trait. In accordance with Stanford-Binet scale, a normal intelligence quotient (IQ) ranges from 85 to 115. Other designations on the IQ scale are:

- 115 - 124: Above average
- 125 - 134: Gifted
- 135 - 144: Very gifted
- 145 - 164: Genius
- 165 - 179: High genius
- 180 - 200: Highest genius

By conventional estimation, approximately 1% of the people in the world have IQ over 135. They are thus considered to be within the genius or near-genius IQ level (140 – 145) (What Goes into the Making of a Genius, 2014; Estimated IQ's of Famous Geniuses, 2014). In the analysis for CHAOS and GCI data, the determined CRTQ values are consistently about 1% (CHAOS: 0.99% and GCI: 1.17%) and thus in agreement with conventional thought. Though the genius IQ concept presumes a steady state of intelligence, there exists periods (as discussed in the next topic below) when one’s thought function is at an exceptionally sparked levels (genius IQ spikes) where it capitalizes on developing ideas and solutions related to defined problem(s).

The consistently near 1 percent CRTQ score may seem ridiculous at a glance. However, without an interpretative answer to link back to the root of the initial problem, no solution is complete. Since all activities of humans and as such all living things are processes of problem-solving, the effect of creativity must culminate in global effects such as the economy

via GDP or software production success outcomes. Thus, in a general or group sense, the problem-solving skills measured are not per individual but per average. To personalize such global or general scores, one would have to consider that a person is either creative or not on the average. This way, the 1 percent CRTQ score means that of the entire human race only 1 percent are exceptionally creative with 95 ± 5% normal population distribution (i.e. within 2 standard deviations) on the average. Based on Differentiated Model of Giftedness and Talent (DMGT) (Colangelo & Davis, 2003), this micro-percentage of population creativity is the culmination of intellectual giftedness into a talent domain of dominant creativity. According to Joseph Renzulli's frequently cited concept of intellectual giftedness (Renzulli, 1978), the 3 basic behavioral traits of giftedness are above average ability, high levels of task commitment, and high levels of creativity. With IQ more than 130, the domain of giftedness (very advanced level of giftedness) on the average forms the top 2% of the human population (Intellectual giftedness, 2015). Thus, the global population's **uncreative giftedness** (lacking originality) is computable as

$$\boxed{Uncreative\ Giftedness\ = Average\ Giftedness - Average\ Creativity}$$

This gives a world population uncreative giftedness of 2% – 1.08% (average of CHAOS and GCI creativity) which is 0.92%.

As expected, the average of both IMGQ and INTQ (CHAOS: 52.53% and GCI: 54.55%) reasonably approximate the 50th percentile of the cumulative distribution of problem-solving

skills (see figure 17). However, the overall average for the skewed creativity distribution and the normal distribution of intelligence is the probability of an occurrence at the 50th percentile of creativity's cumulative distribution (see point c of figure 17) for which the value of a variable x equals to -0.2. This value represents the mean for the normal pdf distribution of creativity.

On the other hand, the **Intelli-creativity cumulative constant (ICCC)** shows that the chances of creativity and intelligence working together as joint problem-solving skills is consistently approximating 10% (CHAOS: 10.95%, GCI: 11.68% and average is 11.32%) of the time during problem-solution cycle. This is consistent with the commonality of creativity and intelligence (see point CI in figure 17) which generally is always 10%. Perhaps, the misnomer that 10% of human brain is only used can find solace here. Since the lack of requisite intelligence for understanding a phenomenon brings about a problem, the initial normal distribution of intelligence is comparatively of the lowest mean probability. Thus, intelligence becomes the backbone of the problem-solution cycle. In general, the final condition of multi-computational skill magnitudes is such that

$$|INTQ| > |IMGQ| > |CRTQ|$$

Observe that the summation of the multi-computational skills respectively under CHAOS and GCI is in each case greater than 1. The extra probability value is due to the additional effect

produced by the interaction between creativity and imagination as free entropy to facilitate the rate of thought processes. The removal of said effect gives the following results:

Under CHAOS:

Total probability = 0.009883 + 0.191003 + 0.859687 − 0.063602

= **0.996972**

Under GCI:

Total probability = 0.011677 + 0.314752 + 0.776313 − 0.123827

= **0.978915**

More details of such activities will be given in the next discussion.

In order to detect genes responsible for heritability of intelligence, a quantitative genetic study conducted in King's College London (Spain et al., 2015) focused on the positive end of intelligence distribution by comparing genotyping data involving single nucleotide polymorphisms (SNPs) from a sample of 3,000 people in the general population. By definition, SNPs represent differences in each single nucleotide base pair. The case-control association analysis based on 1409 individuals (from the Duke University Talent Identification Program)with IQ greater than 170 constituting top 0.03% of the population distribution of intelligence and 3253 unselected population-based controls, found no significant associations of any functional SNPs (protein-altering variants). This reasonably indicates that of the inherited differences between people, functional SNPs are not merely intelligence determinants but composite of intelligence

and other brain traits namely imagination and creativity. According to consistent indications from extensive quantitative genetic research on intelligence (Deary, Johnson, & Houlihan, 2009; Plomin et al., 2013) around half of the differences between people can be explained by genetic factors. Interestingly, for both CHAOS and GCI cumulative distributive function analysis of creativity and intelligence interaction, the respective average of translated CRTQ and INTQ due to negative deviation was 52.7578% and 50.3626% (see tables 10 and 13). Also, the average interaction of imagination and intelligence under both CHAOS and GCI data analyses (see tables 9 and 12) were 52.53% and 54.55% respectively. These generally compute to 52.49% overall average interaction for imagination, creativity and intelligence interaction. On the other hand, of the differences between people in intelligence, the genetic study found that 17.4% (with 1.7% standard error) was explained by functional SNPs. This is emulated by both CHAOS and GCI cumulative distributive function analysis of creativity and intelligence interaction due to negative deviation. Here, the interaction resulting from translated CRTQ and INTQ due to negative deviation was 16.80% and 17.93% respectively. Overall, this averages to 17.37%. Generally, the above near-consistent statistical emulation of functional SNPs within the purview of brain traits interactions is a reasonable basis for affirming the existence of a genetic architecture linking human thought process as facilitated through problem-solution cycle.

CHAPTER 10

THE CATALYTIC EFFECT OF CREATIVITY

Creativity acts as a catalyst in a thought process thereby speeding or increasing its rate of entropic interaction. The effect of **thought catalyst** (creativity) can be altered as a result of interaction with **thought inhibitor** (intelligence) or **thought promoter** (imagination) to respectively cause a decrease or increase in thought catalytic activities.

In general, the interaction between imagination (thought promoter) and other fundamental brain skills leads spontaneously to creativity (thought catalyst) in order to bring about quick solution. As a result, thought catalysis causes glutamate neurons in the brain to activate dopamine-containing neurons in the brain's reward circuit (dopamine reward system) (Jia Qi et al., 2014). This leads to sudden excitement as was the case of the famous euphoric eureka story of the discovery of Archimedes' principle. Note that as neurotransmitters, dopamine is known to regulate movements, emotion, motivation and feelings of pleasure while glutamate is known for communication, memory formation and learning. The depiction in figure 19 below generically shows

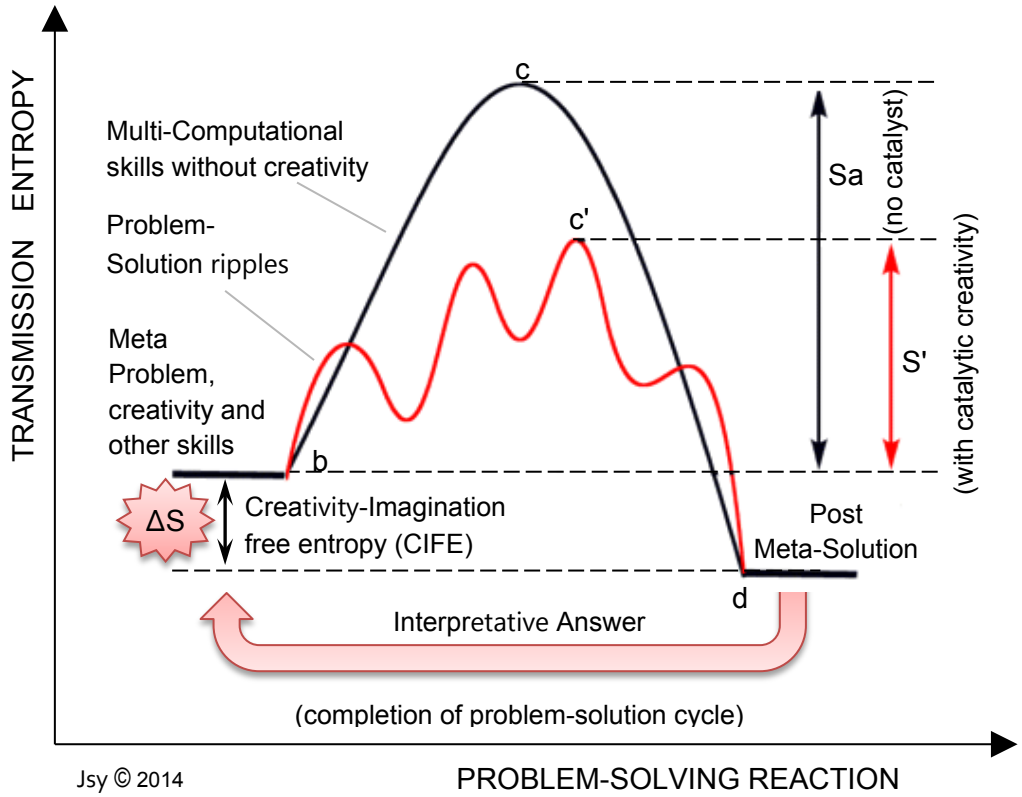

Figure 19. A general entropy diagram showing the effect of catalytic creativity in a hypothetical problem-solution cycle reaction involving meta problem and imagination to produce interpretive answer (post meta-solution).

entropic pathways bcd with entropic energy S_A as a result of the activity of creativity in a thought process. From the interaction involving meta-problem and creativity which produces interpretive answer (post meta-solution), notice how the involvement of catalytic imagination opens a different reaction pathway (shown in red bc′d) consisting of an avalanche of differential problem-solutions that leads to a lower activation entropy S′a. The final result (interpretive answer) of the

creative dynamics and that of the overall problem-solution cycle are however equivalent. Due to the catalytic effect of imagination on creativity, little amount of creative probability (which in general is 1%) is needed during a problem-solution cycle. The reduced entropy (degree of disorderliness) leads to a more orderly process which eventually culminates into an interpretative answer for the misunderstood environmental phenomenon.

The **creativity-imagination free entropy (CIFE)** measures the effective process-initiating entropy obtainable from the dynamic entropic information system that is not available to do work. Though its presence as mutual entropy (or constant potential entropy) has no effect on the entropic difference between meta-problem and creativity as reactants and also on the produced post meta-solution or the available entropy provided by the environment as information, it however necessitates spontaneous problem-solution cycle. By describing the productivity of catalytic creativity in terms of **turn over number (TON)**, the catalytic activity of creativity with imagination as a thought promoter can be described by the **turn over frequency (TOF)** measurable in terms of TON per unit time. This measurement is easily convertible to frequency probability.

The uncertainty in a random variable is, by definition, information theory entropy (Ihara, 1993). It is one of the few processes that are not time-reversible. The arrow of time, in

accordance with statistical idea of incremental entropy, comes with a decrease of in free energy (Tuisku, Pernu, & Annila, 2009). Interestingly, this phenomenon is observed in the empirical analysis of CHAOS and GCI data where the creativity-imagination free entropy (CIFE) decrease form the sampled thought activity (software construction) of the world population to the total thought activity of the world population where there is a decrease from 0.063602 to 0.123827 below initial probability (see tables 10 and 13). Consequently, imagination creates an increase rate of thought process by lowering the activation entropy of the thought reaction. Just as b-ary entropy of a source $\mathcal{S}$= (S, P) with source alphabet $S = \{a_1, ..., a_n\}$ and discrete probability distribution $P = \{p_1, ..., p_n\}$ where p_i is the probability of a_i (say $p_i = p(a_i)$) is defined by:

$$H_b(S) = -\sum_{i=1}^{n} p_i \log_b p_i$$

in human thought processes the d in its attributed "denary entropy" represents the different thought symbols namely creativity, imagination, intelligence and of course language of an **ideal thought alphabet** which serve as standard thought process yardstick for measuring brain alphabets (source).

As a heterogeneous catalyst, creativity acts in a different phase (primary) than the phase (secondary) involving the other reacting multi-computational skills' distributions namely

imagination and intelligence skills. This is evinced by the fact that the creativity distribution curve (see figures 16 and 17) is translated away from the rest of the multi-computational skills. Consequently, creativity is "supported" in a form of cooperative thought catalysis by imagination serving as a thought promoter (co-catalyst) in order to improve its effectiveness. Depending on the phase orientation, there is residual creativity-imagination free entropy (CIFE) effect present in the net probability of all multi-computational skills as a secondary process. The excess probability represents **thought flow noise**. Since the primary goal of CIFE is to increase the rate of thought flow along problem-solution cycle without being directly involved, the net effect of CIFE on the thought flow is the sum of that which is caused by itself in the primary phase as it speeds up thought processes and that due to its residual present in the net probability of the multi-computational skills in the secondary phase. By definition, the multi-computational skills are normally distributed which means the optimal probability distribution given by their point of interactions is 1. However, with a given empiric probability distribution (such as CHAOS and GCI data) relating multi-computational skills in a thought process, the distribution tends to be non-uniformly distributed. This is as a result of the deficiency in entropy (CIFE plus thought noise) caused by the cooperative thought catalysis which essentially should not be consumed by the other interactions of

the thought process. As a result, the deficiency in entropy due to CIFE (since it is not consumed by the problem-solution cycle process) which quantifies the effective use of communication channel of the thought process via language skill, is a measure of **thought flow language inefficiency** η'(τ) in accordance with information theory's definition for information efficiency. This is denoted as

$$\boxed{\eta'(\tau) = \left(-\sum_{i=1}^{n} \frac{P(\tau_i)\ln\big(P(\tau_i)\big)}{\ln n}\right) \cdot n_{CI}}$$

where n is the number of events in the problem-solution cycle and n_{CI} is the number of events in the cooperative thought catalysis. The inefficiency is multiplied by 2 since each of the two events in the cooperative thought catalysis that creates CIFE via interactions between creativity and imagination skills contribute equally. Thus, an inefficient communication in any problem-solution cycle process must cause a loss of efficiency in the thought process by a magnitude equal to η'(τ) as is the case for latent language inefficiency.

While the number of possible outcome events n for CHAOS is 3 namely success, failure and mixed events, those for GCI includes: 3 events under Technology Index namely R&D (research and development) investment, global research, and global innovation, 2 events under Talent Index namely human capital and creative class population and 3 events under Tolerance Index

namely ethnic and racial minorities and sexual orientation. This gives a total of 7 events for the 3Ts of GCI. Table 14 below gives values of the respective transmission of multi-computational skills during problem-solution processes under CHAOS and GCI data distributions.

Table 14

Comparison of Thought Flow Between CHAOS and GCI Data Distributions and Their Associated Thought Noises During Respective Problem-Solving Processes

Transmission of Networked Multi-Computational Skills During Problem-Solution Cycle				
Thought Process	CHAOS (1994-2004)	GCI (2010)	CHAOS Event Size	GCI Event Size
Probability of Real Thought $P(\tau)$	0.996972	0.978915	3	7
Probability of Thought Noise $P(\eta)$	0.003028	0.021085	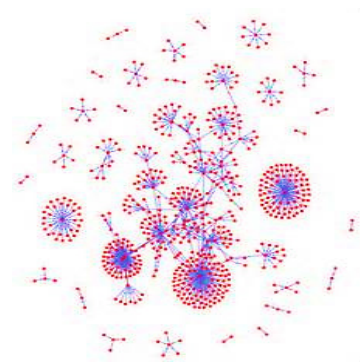	
Real Thought Flow Entropy, H (bit)	0.003024	0.020861		
Thought Noise Entropy, $H\eta$ (bit)	0.017563	0.081371		
CIFE Entropy H_{CIFE} (bit)	0.175231	0.258659		
CIFE Net Entropy Net_H_{CIFE} (bit)	0.192794	0.340030		
Thought Flow Language Inefficiency, $\eta'(\tau)$ (%)	35.0977	34.9482		

Jsy © 2014

The determination of **real thought flow entropy** and **thought noise entropy** during problem-solution cycle in CHAOS data distribution is given as

$$CHAOS:\ H = -P(\tau)\ln P(\tau) = -0.996972\ln 0.996972 = \mathbf{0.003024}\ \boldsymbol{bit}$$

$$CHAOS: H_{\eta} = -P(\eta)\ln P(\eta) = -0.003028\ln 0.003028 = \mathbf{0.017563}\ \boldsymbol{bit}$$

Also, the determination of real thought flow entropy and thought noise entropy during problem-solution cycle in GCI data distribution is given as

$$GCI:\ H = -P(\tau)\ln P(\tau) = -0.978915\ln 0.978915 = \mathbf{0.020861}\ \boldsymbol{bit}$$

$$GCI: H_{\eta} = -P(\eta)\ln P(\eta) = -0.021085\ln 0.021085 = \mathbf{0.081371}\ \boldsymbol{bit}$$

Notice that the computed entropies for CHAOS data distribution are lesser that that of GCI data distributions. This is however expected since software development is only one of the major industries in the world's economy. Given that the CIFE values for CHAOS and GCI are 0.063602 and 0.123827 respectively, the entropies due to CIFE can be expressed as

$$CHAOS:\ H_{CIFE} = -P(\tau)\ln P(\tau) = -0.063602\ \ln 0.063602\ = \mathbf{0.175231}\ \boldsymbol{bit}$$

$$GCI:\ H_{CIFE} = -P(\tau)\ln P(\tau) = -0.123827\ \ln 0.123827\ = \mathbf{0.258659}\ \boldsymbol{bit}$$

The, total entropy of CIFE in the thought process is given as

$$CHAOS:\ Net\_H_{CIFE} = H_{\eta} + H_{CIFE} = 0.017563 + 0.175231 = \mathbf{0.192794}\ \mathbf{bit}$$

$$GCI: Net\_H_{CIFE} = H_{\eta} + H_{CIFE} = 0.081371 + 0.258659 = \mathbf{0.340030}\ \mathbf{bit}$$

Finally, the thought flow language inefficiency η'(τ) is

computed as

$$CHAOS\text{: } \eta'(\tau) = \left(\frac{0.192794}{\ln 3}\right) \cdot 2 \times 100\% = \mathbf{35.1}\%$$

$$GCI\text{: } \eta'(\tau) = \left(\frac{0.340030}{\ln 7}\right) \cdot 2 \times 100\% = \mathbf{35.0}\%$$

By respective comparison of both empirically determined average failure rate of software production of 33.94% (mainly due to multiplicity of programming languages) and the theoretically determined latent language inefficiency of 33.33%, there exists a remarkable accuracy in the computed thought flow language inefficiency. There also exists remarkably high precision in the computed thought flow language inefficiencies for both CHAOS and GCI data distributions (CHAOS: 35.1% and GCI: 35.0%). These optimal measuring qualities of accuracy and precision are indicative of the sober fact that thought catalysis actually takes place in a thought process during problem-solution cycle.

An equivalent equation for **information entropy** which is directly comparable to the statistical thermodynamic entropy equation expressible as Gibbs entropy by

$$S = -k_B \sum p_i \ln p_i$$

where k_B a physical constant called Boltzmann constant relates energy at the individual particle (microstate) level with

temperature given by

$$k_B = \frac{R}{N_A}$$

where R is the gas constant and N_A the Avogadro constant, and p_i is the probability of a microstate, can be derived. This can be done in accordance with Shannon's information theory where the average number of bits per symbol needed to encode it is representative of the entropy rate of a data source. As required by the probabilistic model of information entropy, the probability of each random variable must be equal. To obtain a representational and equal probability for a given discrete random variable outcome, the mean of the probability mass function $f_X(x)$ must be used. Thus, the normalization of the probability distribution of a discrete random variable (to that of a continuous random variables) is by definition given by the mean probability mass function $f_X(\mu)$ which is expressed as

$$f_X(\mu) = \overline{P(X)} = \frac{1}{n}\sum_{i=1}^{n} P(x_i)$$

where $\overline{P(X)}$ is the mean of the discrete probabilities $p(x_i)$ = { $p(x_1)$, $p(x_2)$, ..., $p(x_n)$} of the distribution of a discrete random variable X with possible values {x_1, ..., x_n}. This central tendency (mean) of the probabilities of a discrete random variable mimics the common probability approach of a continuous

distribution (given by the area under the curve) such as the normal probability density function (pdf) of creativity, imagination and intelligence (Massey, 1994; Malone & Sullivan, 2005). Thus, the averaged informational entropy $\bar{H}$ is defined as

$$\boxed{\bar{H} = -\mathrm{K}_{\varphi} f_X(\mu) \log\big(f_X(\mu)\big) = -\mathrm{K}_{\varphi} \overline{P(X)} \log\big(\overline{P(X)}\big)}$$

where Kφ is designated the **continuity entropic constant.** Also, the differential entropy of a normal distribution is by definition given by (Norwich, 2003)

$$H = \frac{1}{2}\ln(2\pi e\sigma^2)$$

where π is the constant pi, e Euler's number and σ the sample standard deviation. Since both differential entropy of a normal pdf distribution (continuous) and averaged information entropy of a discrete random distribution have a common probability representation, one can equate them to solve for the unknown constant k if and only if the discrete random distribution is normally distributed as is the case for software development success rates sampled by CHAOS research of Standish Group (1994 – 2004). Under said normalized and randomized discrete distribution as is the case of multi-computational skills (creativity, imagination and intelligence), one can write

$$\frac{1}{2}\ln(2\pi e\sigma^2) = -\mathrm{K}_{\varphi} \overline{P(X)} \log\big(\overline{P(X)}\big)$$

which gives

$$\boxed{\mathrm{K}_{\varphi} = -\frac{\ln(2\pi e\sigma^2)}{2\overline{P(X)}\log\left(\overline{P(X)}\right)}}$$

where for consistency, the base of log is e.

In psychology, the theory of cognitive dissonance deals with the contention for internal consistency. Thus, by definition cognitive dissonance is a measure of inconsistency in a thought process. Its avoidance is therefore based on compartmentalization. Due to the consonant relationship between H and $\overline{\mathrm{H}}$ (consistency with one another in terms of the search for interpretive answer), one could measure the number of **thought compartmentalization.** This is given by the ratio of H in bit logarithmic unit (base 2) of information (representing entropy via normally distributed multi-computational skills in bits) to $\overline{\mathrm{H}}$ in nat logarithmic unit (base 10) of information (representing entropy via random variables in a non-binary scenario) and denoted as

$$\boxed{\frac{\mathrm{H}}{\overline{\mathrm{H}}} = K_{\mu}}$$

where K_{μ} is the mean continuity entropic constant in bits per nats representing the number of basic thought generally compartmentalizing a thought process. Analysis of the

continuity entropic constant using success rate data from CHAOS research and sampled 3T means from GCI data 2011 gives the following.

CHAOS Data Computations

The net CHAOS percent success rate expressed as a decimal is given by

$$\begin{matrix} Net\ CHAOS \\ Success\ Rate \end{matrix} = \frac{Sum\ of\ Percent\ Success\ Rate}{100} = \frac{16+27+26+28+34+29}{100} = 1.60$$

With CHAOS sample size n of 6, the mean CHAOS probability mass function CHAOS $f_X(\mu)$ which is given by the maximum likelihood mean estimate is

$$CHAOS\ f_X(\mu) = \bar{x} = \frac{1}{n}\sum_{i=1}^{n} x_i = \frac{Net\ CHAOS\ Success\ Rate}{Sample\ Size} = \frac{1.60}{6} = 0.266667$$

Also, from the CHAOS table 9 or table 15 below, the sample variance σ^2 is equal to 35.06666667. Therefore, the CHAOS continuity entropic constant CHAOS_Kφ based on bits information state (ST 2) can be computed as (excel calculation)

$$Binary\ \text{CHAOS\_K}_{\varphi} = -\frac{\ln(2\pi e \times 35.06666667)}{2 \times 0.266667 \times \ln 0.266667} = \mathbf{9.071921}$$

Also, on the basis of nats information state (ST 10) it is computed as (excel calculation)

$$\text{Denary CHAOS\_K}_{\varphi} = -\frac{\ln(2\pi e \times 35.06666667)}{2 \times 0.266667 \times \log_{10} 0.266667} = \mathbf{20.88886}\ \boldsymbol{bits\ per\ nats}.$$

GCI Data Computations

The net GCI percent success rate is given by

$$\begin{matrix} Net\ GCI \\ 3T\ Success\ Rate \end{matrix} = Sum\ of\ Percent\ 3T\ Success\ Rate$$

$$= 7.00 + 9.67 + 16.00 + 30.00 + 33.00 + 37.00 + 40.67$$

$$+ 44.33 + 52.67 + 54.33 + 58.00 + 63.67$$

$$= 446.34$$

But the GCI data has a sample space size N of 74 and the 3T subgroup has a subsample size n of 3 elements namely technology, talent and tolerance used to determining the 3T mean. Hence, the mean GCI probability mass function GCI $f_X(\mu)$ which is given by the mean of the maximum likelihood mean estimate is expressed as

$$GDI\ f_X(\mu) = \bar{\bar{x}} = \frac{1}{N}\left(\frac{1}{n}\sum_{i=1}^{n} x_i\right) = \frac{Net\ GDI\ 3T\ Success\ Rate}{3T\ SubSample\ Size\ \times\ Sample\ Space\ Size} = \frac{446.34}{12 \times 74}$$

$$= 0.502635$$

Also, from GCI table 12 or table 15, the variance of mean distribution σ_M^2 is equal to 29.68090629. Therefore, the GCI continuity entropic constant GCI_Kφ based on bits information

Table 15

Computation of Continuity Entropic Constant Using Both CHAOS and GCI Datasets and the Determination of Compartmentalized Units of the Human Brain via Figure-8 Knot

CHAOS & GCI DATA: Determination of Continuity Entropic Constant Under Normal Distributions					
Mean CHAOS Probability Mass Function $_{CHAOS}f_X(\mu)$		0.266667	Net CHAOS Success Rate	1.60	
CHAOS Continuity Entropic Constant CHAOS_Kφ	ST 10	20.88886	CHAOS Sample Size	6	
	ST 2	9.071921			
Mean GCI Probability Mass Function $_{GCI}f_X(\mu)$		0.502635	Net GCI 3T Means	446.33	
GCI Continuity Entropic Constant GCI_Kφ	ST 10	20.739033	GCI Means Sample Size	12	
	ST 2	9.006848			
Mean Continuity Entropic Constant Kμ	ST 10 ▶	20.813945	GCI Sample Size	74	
Figure-8 Knot Hyperbolic Volume V_8	■	2.029883	CHAOS Sample Variance	35.066667	
Volume of Figure-8 Knot's 10 Surgical Manifolds $10V_8$		20.298832	GCI Variance of Mean Distribution	29.680906	

NOTE. 1. ST 2 represents the Binary CHAOS Continuity Entropic Constant under a binary average information state.
2. ST 10 represents the Denary CHAOS Continuity Entropic Constant under a denary average information state.
3. Mean Continuity Entropic Constant Kμ measures the unitary compartments within a centralized thought command centre (human brain).

state (ST 2) can be computed as (excel calculation)

$$Binary\ GCI\_K_{\varphi} = -\frac{\ln(2\pi e \times 29.68090629)}{2 \times 0.502635 \times \ln 0.502635} = \mathbf{9.006848}$$

Also, that due to nats information state (ST 10) is computed as (excel calculation)

$$Denary\ GCI_{K_\varphi} = -\frac{\ln(2\pi e \times 29.68090629)}{2 \times 0.502635 \times \log_{10} 0.502635} = \mathbf{20.739033\ bits\ per\ nats}$$

In general, the average value of continuity entropic constant Kφ based on denary average information state is denoted by

$$\frac{\mathrm{H}}{\overline{\mathrm{H}}} = K_\mu = \frac{Denary\ CHAOS\_\mathrm{K}_\varphi + Denary\ GCI\_\mathrm{K}_\varphi}{2} = \frac{20.88886 + 20.73903}{2} = \mathbf{20.813945}$$

This determines the number of units of centralized thought compartments in the human brain via association with figure-8 knot whose constant volume of 2.029883 forms a 10 unit volume of 20.298832 which is equivalently equal to that of K_μ.

Experimental Evidences Supporting Thought Catalysis, Inhibitor and Promoter

Each side of the brain has a hippocampus. It is located under the cerebral cortex in human (see left of figure 20) and in the medial temporal lobe (underneath cortical surface) in primates. Its important functions are spatial navigation and the consolidation of information from short to long-term memories. It is the centre of thought processing (brainstorming) of a brain.

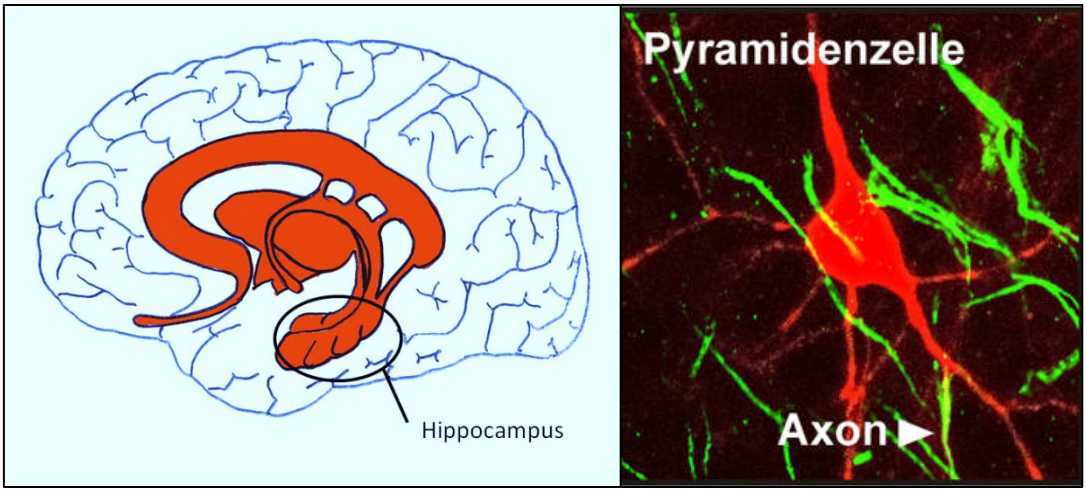

Figure 20. Strange new brain cell. Left: Lateral view of the human brain with occipital lobe at right and the frontal lobe at left. Right: A neuron (pyramidal brain cells) dyed with fluorescent red protein that stuck to the origin of each axon protruding from a cell showing a newly found axon protruding directly from a dendrite rather than from the cell body. Source from Axon-Carrying Dendrites Convey Privileged Synaptic Input in Hippocampal Neurons, by Christian Thome et al., *Neuron*, 2014; 83(6).

In general, mice have similar brain structure and hippocampus as humans.

A strange new brain cell (more than 50%) in the hippocampus of mice identified by researchers (Thorme et al., 2014) on the contrary bypasses its cell body (normally responsible for processing received signals) to directly transmit signals along an axon projecting from lower dendrites (branchlike nerve cell structures capable of receiving signals from other nerve cells). Due to its unique figure (see right of figure 20), it gives stronger signals and is less prone to signal inhibition. Thus, its transmitted information is more influential compared to

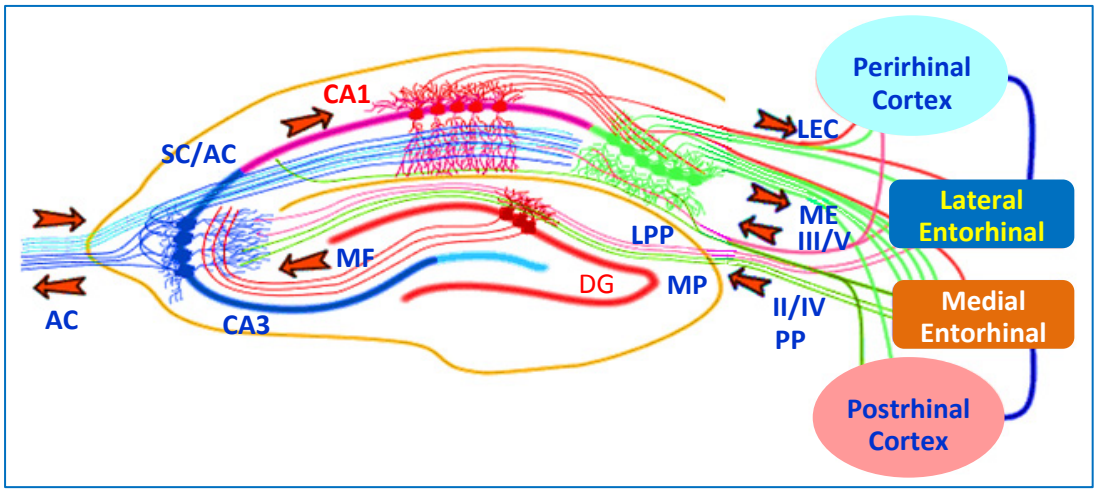

Figure 21. A principal uni-directional hippocampal network within the brain which forms a loop with input from the entorhinal cortex (EC) and an eventual main hippocampal output back to EC. DG is dentate gyrus, PP the performant path, MF the mossy fibres, SC the schaffer collateral pathway, AC the associational commissural, Sb the subiculum, II/IV the layers II and IV, III/V the layers III and V, LPP the lateral pathway and MPP the medial pathway. Source from Centre for Synaptic Plasticity, University of Bristol, *Neural pathways*, by Zara Matheson, retrieved September, 2014, from http://www.bris.ac.uk/synaptic/pathways/

inputs from any other traditionally operating dendrite. The unanswered pertinent question it immediately presents is this: which signals use the so-called "privileged" channel and why? The answer is simple. The newly identified nerve cell is direct physical evidence for the existence of creativity's transient solution path which is caused by the catalytic effect of imagination on intelligence (a process dubbed thought catalysis) during PSC (problem-solution cycle). Thus, this new brain cells (dendrite-originating axon neurons) directly supports all catalyzed creative transformation processes in the brain thereby

creating a **neuro-quantum tunneling (NQT) effect.** The nature of the hippocampal network in the brain is shown in figure 21. Worthy of note is the function of the perirhinal and postrhinal **c**ortices. They closely function as interpreters of novelty and familiarity which are significant characteristics in creative processes.

As the centre for problem-solution cycle (PSC) activities, the network of the four areas of the hippocampus must directly interrelate the fundamental characteristics of PSC namely, language, intelligence, imagination and creativity. According to the research findings (Thorme et al., 2014), the larger CA1 region

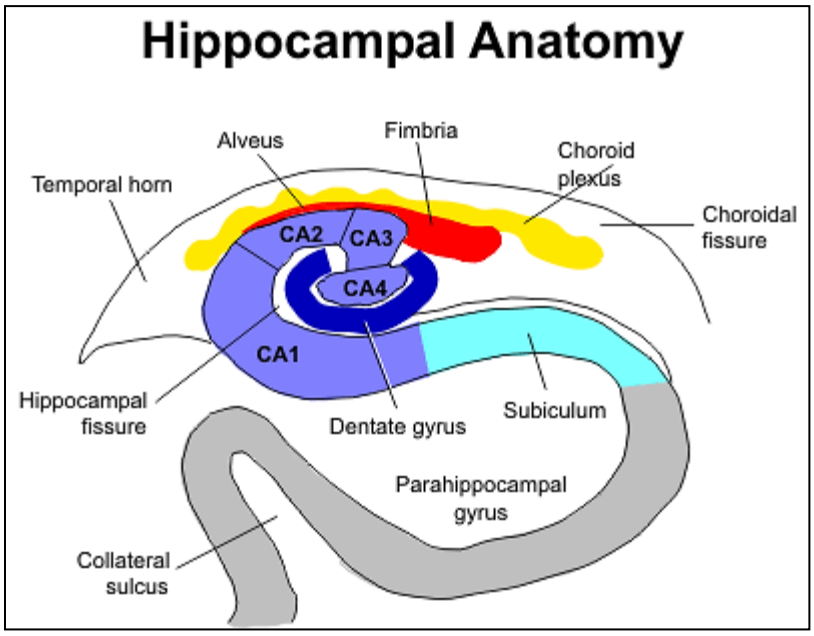

Figure 22. The base of hippocampus showing it four areas labeled as CA1, CA2, CA3 and CA4. Source from Spinwarp, *The temporal lobe & limbic system*, by John R. Hesselink, retrieved September, 2014, from http://spinwarp.ucsd.edu/NeuroWeb/Text/br-800epi.htm

(see figure 22) was composed of about 50 percent of cells with dendrite-originating axons. This was differentially reduced to about 28% of cells in region CA3. The lack of oxygen (source of energy) which is needed for the proper functioning of the activities of CA1 to CA4 regions of hippocampus leads to its damage. In a reverse sense, it is reasonable to propound that the a higher usage of said regions of hippocampus due to problem-solution cycle activities demanding higher creative works will lead to higher energy demand. Such a high demand can be satisfied primarily through the conversion of stored glycogen from the liver to produce blood glucose to fuel the excess energy need by the hyperactive hippocampus. Thus, people with higher energy intensive hippocampus creative activities may be prone to slightly higher than normal blood sugar level. If true, it is reasonable to see this as normal. On the other hand, cognitive signal together with motor and sensory signals are known to emanate from the cortex of the brain to the basal ganglia and then out through the thalamus to the cortex. However, recent research findings (Saunders et al., 2015) indicate that newly found globus pallidus neurons projecting from the core of the basal ganglia directly connect to the frontal cortex. The shortcut neurons, directly involved in the basal ganglia-to-cortex pathway, consist of two forms namely ChAT- and ChAT+. ChAT+ consists of both GABA (cell inhibiting neurotransmitter) in similitude with thought inhibitor and acetylcholine (cell

exciting neurotransmitter) in similitude with thought promoter. The current quest for how precisely ChAT+/- neurons interact together and use the shortcut inputs from the globus pallidus lies in the aforementioned mechanism underlying the human thought catalytic process(es).

Data from a novel study (Saggar et al., 2015) suggest, on the basis of functional evidence (cerebral-cerebellar interaction) that the cerebellum is associated with high creative activities and acts as an executive-control center of the brain on the basis that it may be able to model behavioural types for which the frontal lobe acquire. Hitherto, the cerebellum is known to play an important role in motor control (coordination of movement) and also may be involved in some cognitive function namely attention and language among others (Wolf, Rapoport, & Schweizer, 2009). This suggestive assertion is in support of the theoretical views of human thought process (HTP) in which case the cerebellum is fully tasked with control balance and general coordination (like a master of ceremony, MC) such as motor coordination. More specifically, the cerebellum helps in the coordination of thinking processes which is the backbone of every single human endeavour. As the centre for brain coordination, the cerebellum receives inputs from different parts of the brain and through language it integrates intelligence and imagination (received inputs) in an iterative and subconscious manner to via new modelling achieve creativity. This leads to a sudden realization of new knowledge which is acquired in the frontal

lobe of the brain. Thus, imagination is the feature of the brain through which the cerebellum creates its planning (modeling) to facilitate coordination of effective thinking processes.

Identification of Thought Process Features Using Figure-Eight Knot

In knot theory, the figure-eight knot or listing's knot is a hyperbolic knot with hyperbolic complement (see figure 23 below) whose knot complement's hyperbolic volume is the smallest possible hyperbolic volume given by 2.0298832 (Bailey et al. 2007). With its proof based on geometrization conjecture and computer assistance, the Lackenby (Lackenby, 2000) and Meyerhoff theorem stipulates that 10 is the largest possible number of

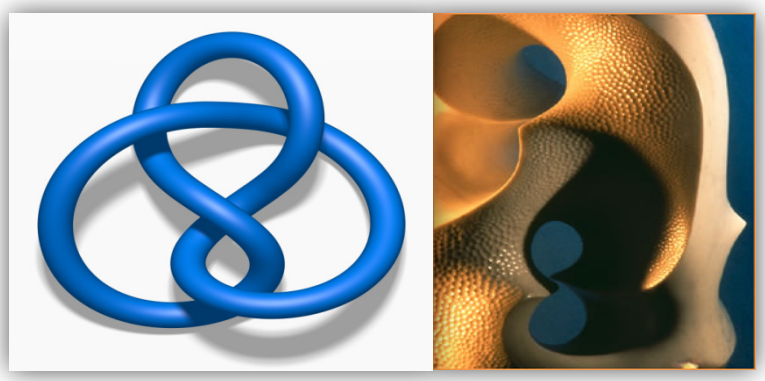

Figure 23. Figure eight knot. Left: The hyperbolic volume of figure eight knot. Right: Helaman Ferguson's sculpture "Figure-Eight Complement II" illustrates the knot complement of the figure eight knot. Source from Hyperbolic volume, in *Wikipedia, the free encyclopedia*, retrieved July, 2014, from https://en.wikipedia.org/wiki/Hyperbolic_volume. Source from Helaman Ferguson's sculpture, *Visualization of Figure Eight Knot Complement*, retrieved July, 2014, from http://www2.lbl.gov/Science-Articles/Archive/assets/images/2003/Nov-03-003/figure_eight_knot.jpg

exceptional surgeries (finitely many exceptions) of any hyperbolic knot. Dehn surgery is an operation that creates a new 3–manifold from a given cusped 3–manifold or a given knot. It involves the operation of drilling out a neighbourhood of the link and filling back in. Note that a 3-manifold is a space that looks like Euclidean 3-dimensional space to a small observer. Comparatively, as a sphere looks like a plane to a small enough localized observer so does a 3-manifolds look like our universe to a small enough localized observer. On the other hand, the operation of a hyperbolic Dehn surgery which exists only in three dimensional space, involves the creation of more hyperbolic 3-manifolds from a given cusped (a point where two arcs or branches of a curve intersect) hyperbolic 3-manifold. It actually involves only filling. Currently, figure-eight knot is the only hyperbolic knot that achieves the bound of 10 (by admitting 10 surgeries which produces 10 non-hyperbolic manifolds).

In left of figure 24 is a normal human brain function depicting a figure-eight structure. Similarly, in right of figure 24 above shows striking structural equivalence between the neural signal route within the human brain which is identifiable in a lateral view of a human brain imaged by a functional magnetic resonance imaging and the figure-eight knot shape. Thus, representational of an equivalent 3-manifold figure-8 hyperbolic knot, the human brain equivalently under the "operations" of 10 bound Dehn surgeries produces 10 non-

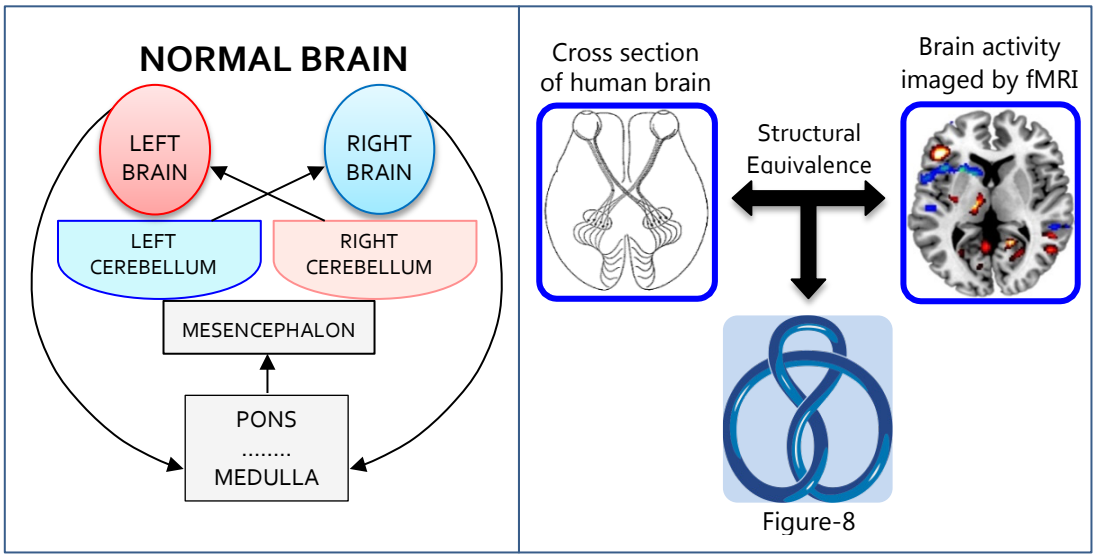

Figure 24. Structural equivalence between brain and figure 8. Left: A depiction of the functional loop of a normal human brain. Right: A depiction of routing of neural signals from the two eyes to the brain and the lateral view of a human brain activity imaged using functional magnetic resonance imaging (fMRI) in comparison to an equivalent figure-8 knot structure. Adapted from USC News, *USC study charts exercise for stroke patients' brains*, by Robert Perkins, retrieved July, 2014, from https://news.usc.edu/52202/usc-study-charts-exercise-for-stroke-patients-brains/

hyperbolic manifolds evident as the cerebellum and the lobes of cerebrum (5 identical sections on both sides of the hemispherical left and right brain) as shown in figure 25 below.

Research work in cognitive neuroscience (Bae et al., 2014), has shown that a specific gene (a mutation affecting GPR56) controls the number of gyri formation in the cerebral cortex region including the major language area (Broca's area) (Bae et al., 2014). Equivalently, this is indicative of the operational role of Dehn surgery in creating new 3-manifolds. While the cerebrum or cortex (see figure 26) is associated with higher

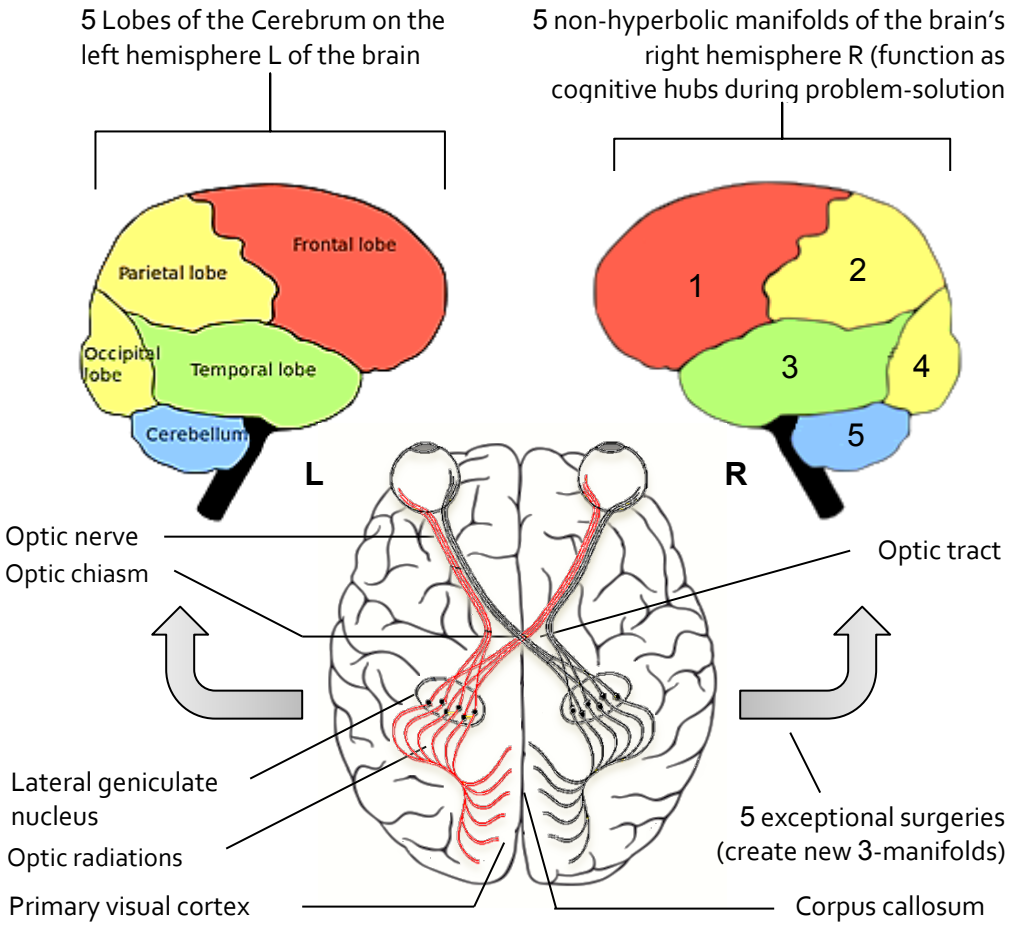

Figure 25. Human brain as equivalent 3-manifold hyperbolic knot. This produces 10 non-hyperbolic manifolds (five on each of the left (L) and right (R) brain hemispheres under operations of Dehn surgeries. Adapted from *Brain diagram with eyes*, by Akita, retrieved July, 2014, from http://www.akitarescueoftulsa.com/brain-diagram-with-eyes/ . Adapted from *List of regions in the human brain*, in *Wikipedia, the free encyclopedia*, retrieved July, 2014, from http://www.cognopedia.com/wiki/List_of_regions_in_the_human_brain

brain function such as thought and action, the cerebellum is the source of all answers. Of the left and right hemisphere of the human brain, the varied important functions that facilitate the process of problem-solution cycle are depicted in figure 27.

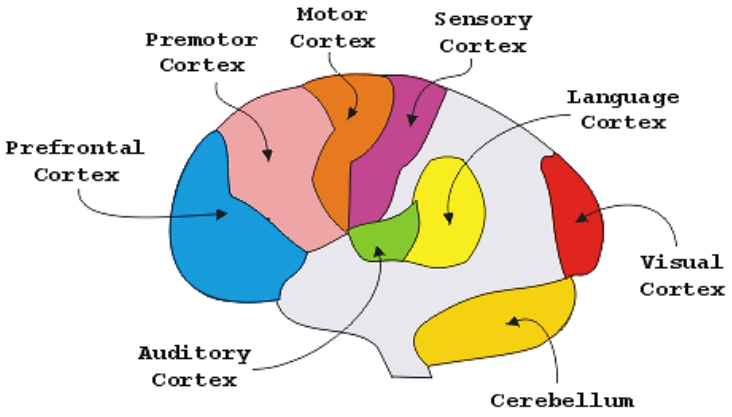

Figure 26. Human brain showing various sections of the cerebral cortex which forms the outermost layered structure of neural tissue of the cerebrum. Source from Dan's Website, Neural Networks in Nature, by Akita, retrieved July, 2014, from http://logicalgenetics.com/neural-networks-in-nature/

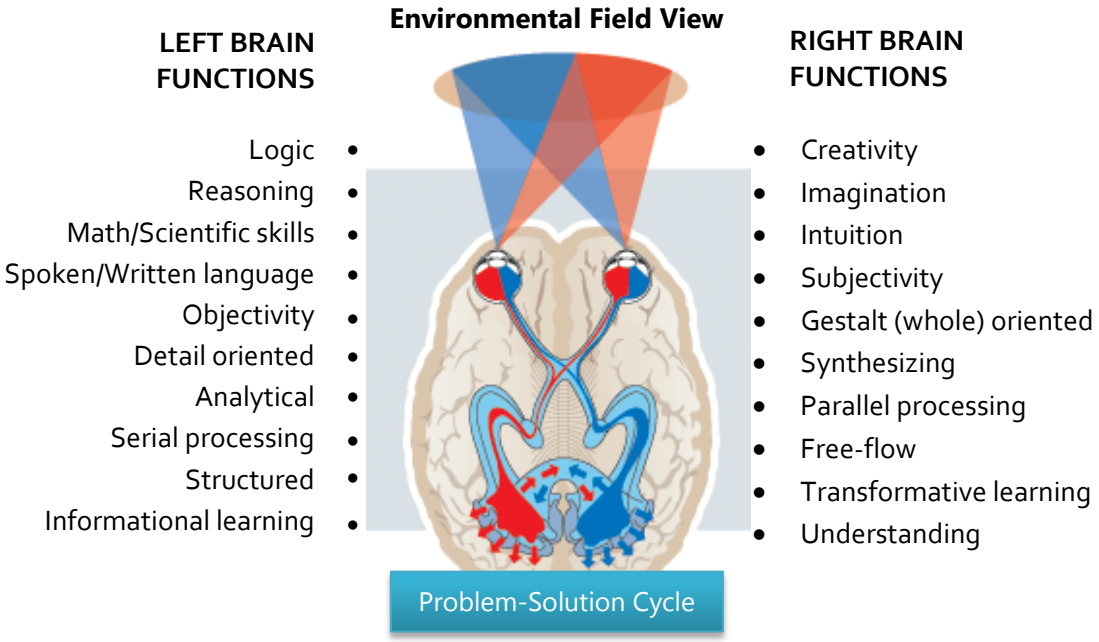

Figure 27. Essential functions of the left and right human brain during problem-solution cycle. Adapted from Wiring the Brain, *Do you see what I see?*, by Kevin Mitchell, retrieved December, 2012, from http://www.wiringthebrain.com/2012/12/do-you-see-what-i-see.html

The integration of information and the expansion of creative thought facilitated essentially by interhemispheric connectivity are empirically supported by the positive correlation between FA and the corpus callosum (Carlsson et al., 1994; Atchley, Keeney & Burgess, 1999). Such is the case for interactions between the multi-computational skills namely creativity, imagination and intelligence facilitated by language as communication link. By far, empirical study (Buckner et al, 2009) shows that the localization of creative processes within the human brain apparently not only functions like hubs but form "networks" (Buckner et al., 2009). These correspond to stimulus independent thought (i.e. default mode network (DMN)), stimulus-dependent thought (i.e. cognitive control network (CCN)), and switching of attention between salient environmental stimuli (salience network) (Bressler & Menon, 2010). Under various types of information processing such as auditory-temporal and visual-occipital, the human brain is known to be organized in order to achieve optimization with heteromodal association cortices (Mesulam, 1998). Such cortices bind together by joining sensory information emerging from multiple sources in similitude with the theoretically asserted activities of multi-computational skills. Using resting-state functional magnetic resonance imaging and a creativity test of divergent thinking (DT), researchers (Takeuchi et al., 2012) have found association between higher creativity (via DT) and rFC between the key nodes of default mode network (DMN). Also, another research work (Jung et al., 2010) indicates

that the development of creative ideation and achievement may be essential for the information flow network between many different areas of the human brain. As supported by several electroencephalographic (EEG) studies (Fink & Benedek, 2012), there exists "disinhibition" of cognitive control mechanisms or decrease in cortical arousal which is associated with increased creative cognition (Fink & Benedek, 2012). For example, a recent research (Jung et al., 2009, 2010) found that some normal brains with normal creativity performance tend to be not only more "disinhibited" in their organization with anterior cingulate biochemistry tending to "gate" frontal information flow but also show lower cortical volume in certain regions of the brain (Jung et al., 2009, 2010). Also a study conducted on full-time musicians' overlearned or improvised performances of piano pieces using functional Magnetic Resonance Imaging (fMRI) found an association between spontaneous improvisation and widespread deactivation of the lateral prefrontal cortex along with simultaneous activation of medial frontal cortex (Limb & Braun, 2008). This is indicative of the action of imagination as a thought promoter on creativity (a thought catalyst). The decrease in cortical arousal can be associated with the lowering of activation entropy of thought reaction as a result imagination (thought promoter) reacting with creativity (thought catalyst). It also supports the notion of a minimal volume given by the knot compliment of figure eight knot. One must note that the brain's frontal lobe functions associated with creativity which are

necessary for the development of new patterns of thinking include working memory, sustained attention, idea generation and cognitive flexibility. Further functional studies with the rap musicians revealed dissociation of brain regional activities involving simultaneous increased and decreases activation within mPFC (medial prefrontal cortex) and dorsolateral prefrontal cortex respectively (Liu et al., 2012). The mPFC activation correlated with activations across a broad network (amygdala, inferior frontal gyrus, and inferior parietal gyrus, etc.). These decreases within the dorsolateral prefrontal cortex are reminiscent of the decrease in entropic activity cause by the interaction between creativity and imagination. As shown by the study with improvisation (creating rap on the fly), the back and forth between large brain networks leads to increased activation of the DMN and decreased activation within CCN (Liu et al., 2012). This scenario is reasonably comparable to the increase activation entropy of imagination or intelligence and the decrease activation entropy of creativity respectively. The salience networks (anterior cingulate, insula, etc.) were also found to modulate the interplay between the said two basic networks. It was therefore hypothesized that the vacillation between the two networks serving as a default cognitive control, likely corresponds to creative cognition's BVSR (blind variation and selective retention) components (Liu et al., 2012). The decrease in cognitive activity within a discrete network of the

brain regions and the numerous studies pointing to reduction in cortical thickness/volume or white matter integrity in association with increased human cognitive ability are "problems" to cognitive neuroscience of creativity (Raichle & Snyder, 2007).

Creative cognition as a production of something both new and useful is like other types of cognition (thoughts such as imagination and intelligence) except for its specialized focus which is domain (field) specific and type of adaptive problem solving which is often abductive reasoning than deductive reasoning. In Dietrich's statement (Dietrich, 2004), creativity is made up of multiple cognitive processes which among others between the ranges of BVSR include defocused attention, mental flexibility and cognitive control (Dietrich, 2004). As a consequence of empirical evidences indicating the existence of a dynamic interplay between inhibitory (reminiscent to creativity and intelligence interactions) and excitatory networks (reminiscent to creativity and imagination interactions) are seen as likely corresponding to BVSR components and creative cognition respectively.

CHAPTER 11

MAPPING PROBLEM-SOLUTION CYCLE (PSC) WITH HUMAN BRAIN

To date, there exists a lack of generally agreed comprehensive explanation as to how the brain works. The brain is basically divided into two parts which are both used equally in the management of both ordinary and more complex tasks of daily life. The left hemisphere is responsible for language production and so linked to the language trait or communication in problem-solution cycle activities. It is also responsible for counting and memory recall (logical activities) which are both linked to intelligence. On the other hand, the right hemisphere is responsible for spatial reasoning and estimation which is akin to imagination when done beyond reality. It is deals with creative activities and so it is also linked with creativity. The characteristic centres of fundamental brain activities as shown in figure 28 are those of intelligent (yellow circle), language (red circle), imagination (blue circle) and creativity (green circle). Their inter-connectedness forms the general pathway of fundamental characteristic interactions of human thought process which constitutes the problem-solution cycle

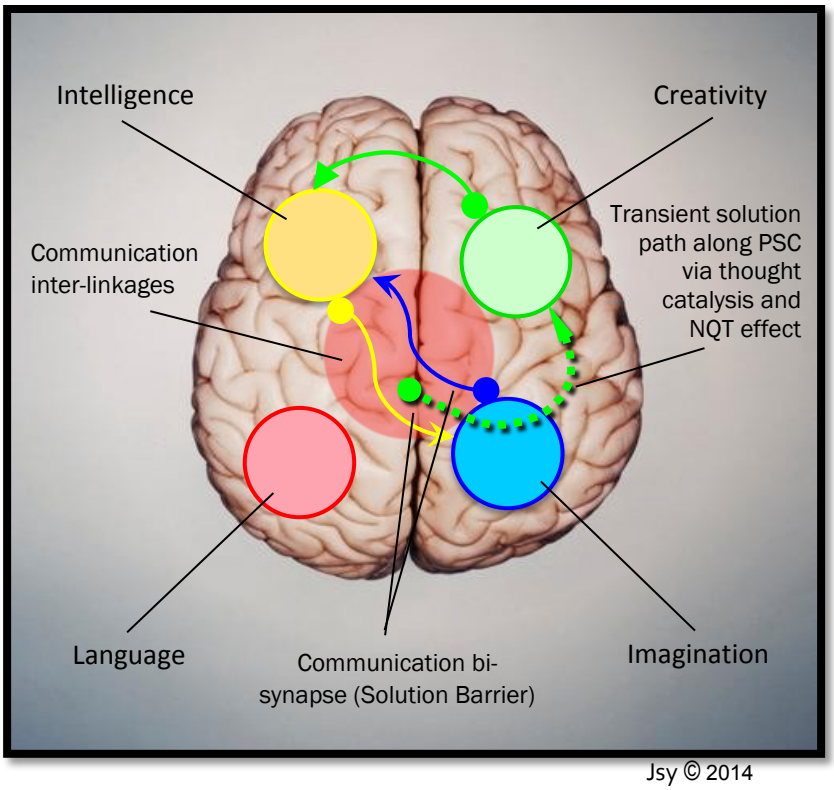

Figure 28. General mapping of the fundamental characteristic interactions of human thought process showing the problem-solution cycle (PSC). The centres of intelligent activities (yellow circle), language activities (red circle), imagination activities (blue circle) and creative activities (green circle) are shown interconnected by a central language inter-communication linkage (transparent light red region). Adapted photo from Getty Images, *Model of a human brain*, by PM Images, retrieved July, 2014, from http://www.gettyimages.com/photos/brain?excludenudity=true&family=creative&page=2&phrase=brain&sort=best

(PSC). They are interconnected by a central language inter-communication linkage shown as a transparent light red circular region. Also, the thought catalytic reaction involving communication linkage shown as a transparent light red circular region. Also, the thought catalytic reaction involving intelligence and imagination centres are shown by yellow and blue

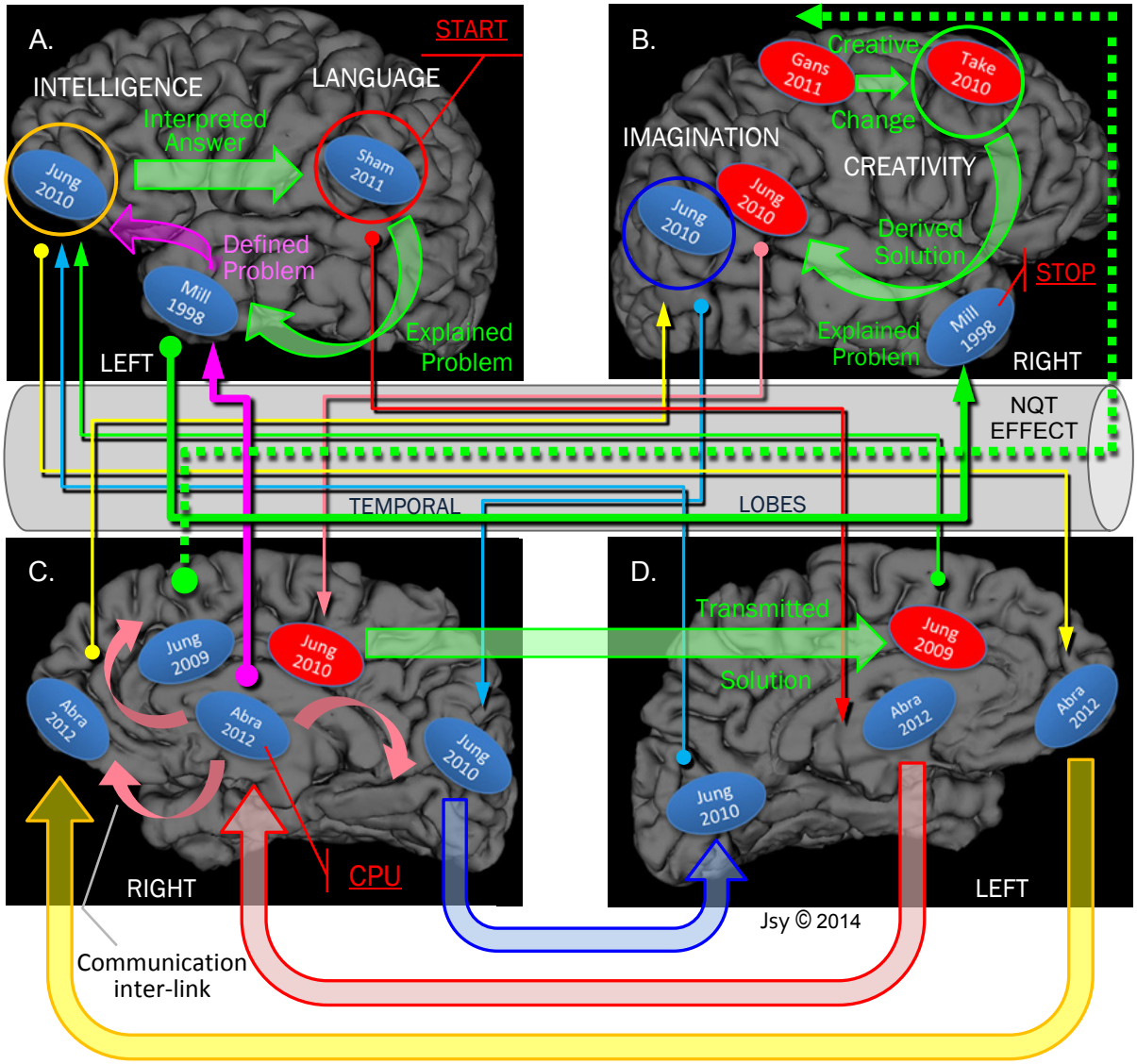

Figure 29. Problem-solution cycle (PSC) in stereotyped left (L) and right (R) hemispheres of the human brain. The core areas of higher creativity measures are associated with lower brain integrity measures (blue regions) and higher brain integrity measures (red regions) respectively. Outer Slides: (A) left lateral hemisphere and (B) right lateral hemisphere. Inner Slides: (C) right medial hemisphere and (D) left medial hemisphere. Adapted photo from Frontiers in Human Neuroscience, *The structure of creative cognition in the human brain*, by Rex E. Jung et al., retrieved July, 2014, from http://journal.frontiersin.org/article/10.3389/fnhum.2013.00330/full

curved arrow connectors while the catalyzed creative transformation via neuro-quantum tunneling (NQT) effect is depicted with a green square dotted curved arrow connector. The NQT effect spontaneously provides an effective transient solution path (green square dot line) in furtherance of a solution search beyond solution barrier (communication bi-synapse) in the PSC as a result of the tinkering of human intelligence together with human imagination as its catalyst. This is supported by the newly found brain cells (dendrite-originating axon neurons) in the hippocampus (Thorme et al, 2014). Lastly, the derived solution and its interpretive answer to the defined problem are indicated by a green curved arrow connector in the pathway of PSC. The core areas of higher creativity measures by experimentation are associated with lower brain integrity measures (blue regions) and higher brain integrity measures (red regions) as indicated in figure 29. These areas of higher creativity measures are appropriately interconnected in figure 29 to simulate the activities of problem-solution cycle (PSC). Observe that the both left and right lateral brains are connected to the right and left medial brain by a common region in the temporal lobe known to be responsible for memory, understanding language, facial recognition, hearing, vision, speech, and emotion. By reason of processes under PSC, said common region is associated with neuro-quantum tunnel (NQT) effect. In generally, the interactions between the higher creativity core areas in line with the basic

processes of PSC have an associated focal point of activities at the lower brain integrity measure (Abra 2012 in section C of figure 29) dubbed as the central processing unit (CPU) of the brain. It also fans-out inter-communication links (three curved rose coloured arrows) to three other lower brain integrity measures namely Jung 2009, Jung 2010 and Abra 2012 which lead to the gathering of intelligence, imagination and creativity respectively.

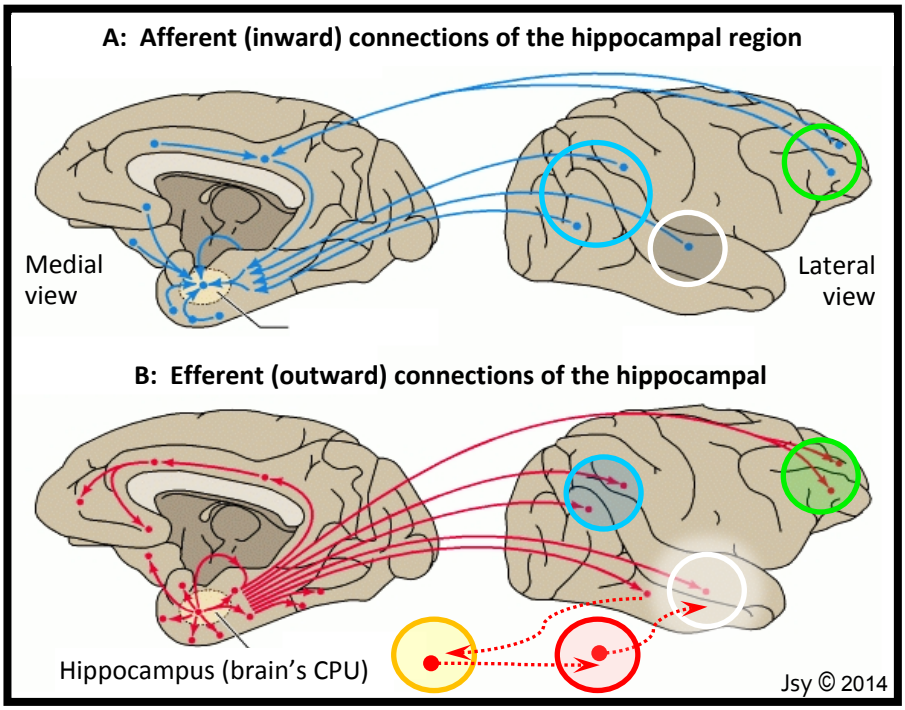

Figure 30. Mapping densely interconnections between hippocampus and major areas of the brain namely imagination (blue circle), creativity (green circle), problem definition (dark white circled area), explained problem (white circled area with glow), intelligence (yellow circle), and language (red circle). Adapted photo from Mnemonic Techniques, by Dr. Jack Lewis, retrieved July, 2014, from http://www.drjack.co.uk/mnemonic-techniques-a-k-a-memory-tricks-by-dr-jack-lewis/

By comparison, there exist similarities between known interconnections of hippocampus (a region of highly interconnected network of brain cells residing deep within the temporal lobes) and other major brain areas as mapped out in figure 30 and that shown in figure 29. In A of figure 30, the inward bound hippocampus connections from the medial right brain hemisphere are identify with areas of imagination (blue circle), creativity (green circle) and problem definition (white circled light black area) of the right lateral brain. Similarly, in B of figure 30, the right lateral brain areas for imagination (blue circle), creativity (green circle) and explained problem white circle) are linked with the outward bound hippocampus connections from the medial right hemisphere of the brain. There is however

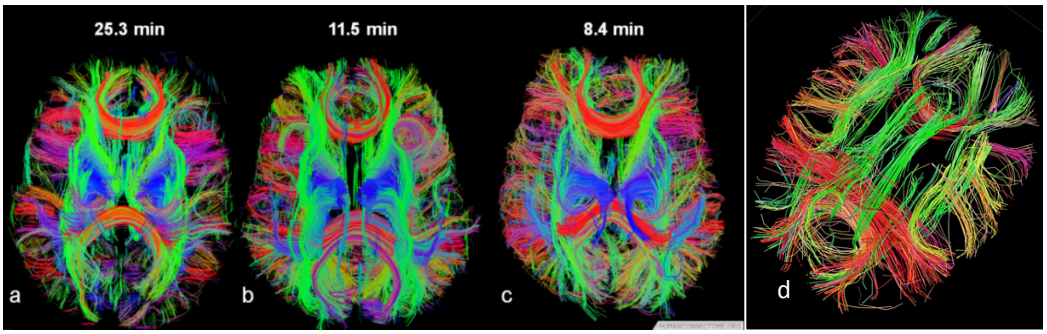

Figure 31. Multiple images refocused simultaneously in each Echo Planar Imaging (EPI) pulse sequence to effectively reduce scan time of HARDI fiber tractography (Diffusion Spectral Imaging, DSI). It is constructed from (a) regular EPI (b) two images per EPI readout and (c) three images per readout for 3x acceleration. In (d) is measured white-matter connectivity of human brain showing fiber architecture (neural circuits) based on diffusion imaging techniques such as diffusion tensor imaging (DTI) and diffusion spectrum imaging (DSI). Source from Frontiers in Human Connectome Project, *Faster Whole Brain coverage for fMRI and Diffusion Imaging*, retrieved July, 2014, from http://www.humanconnectome.org/about /project/pulse-sequences.html & http://www.massgeneral.org/ psychiatry/assets/images/Connectome_MGH.jpg

an exceptional location which links externally (left lateral brain not shown) the area of intelligence (yellow circle) with the area of language (red circle) before linking back to the area of explained problem in the right lateral brain where PSC activities stop. The simple neural architecture shown in figure 29 reasonably represents the complex changes in communications among human brain neurons (see figure 31) over the course of their development as mapped out under Human connectome project (Mapping structural and functional connections in the human brain , 2014).

Conclusively, the lower brain integrity measure area (see Abra 2012 in C of figure 29) with fan-out inter-communication links to fundamental brain process characteristics (language, intelligence, imagination and creativity), by identical inter-connectedness, originates from the hippocampus which serves as the brain's CPU used in PSC activities.

The Saddle of Problem-Solution Cycle

In a problem-solving scenario, the defined problem as an inquisition for unknown truth must be based on truth. If it is based on falsehood then its answer must always be invalid. That is why every defined problem must have a valid answer. The anatomy of problem-solving process includes a back-end problem and a front-end solution which together form the saddle of PSC.

Since a problem is the reverse of a solution and vice versa, the PSC saddle is a problem-solving conjugate pair. Figure 32 below, shows position of both back-end problem and a front-end solution in the problem-solving process.

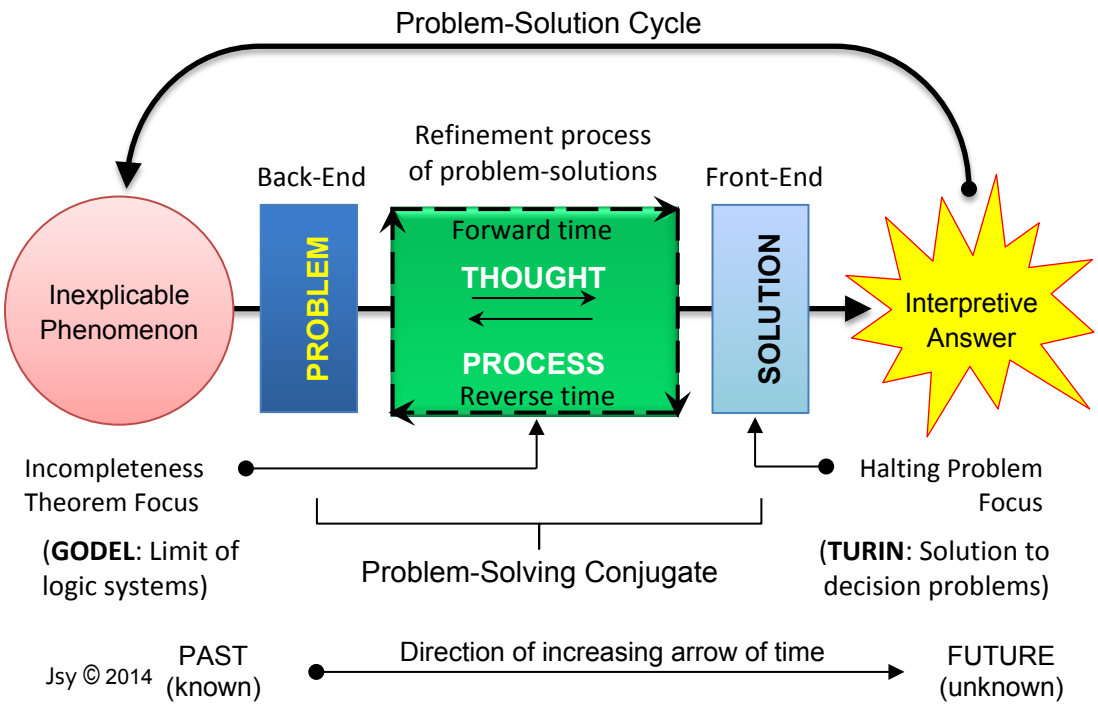

Figure 32. A general problem-solving process depicting its back-end and front-end as a defined problem and its solution (conjugate pairs).

As shown in figure 32, while the halting problem focuses on solution, the incompleteness theorem which is in the saddle of PSC focuses generally on implementing fundamental rules for thinking through problems.

CHAPTER 12

DESCRIPTIVE COMPLEXITY

One can correlate the increase in both quantum and thermodynamic entropies with the passage of time (see Appendix B: Linking Quantum and Thermodynamics Arrow of Time). In general, particles of an isolated system are initially uncorrelated but their final conditions are correlated due to interactions between themselves which cause their characteristics (such as locations and speed) to be dependent on each other.

The contrast between statistical nature of entropy and the deterministic nature underlying its physical processes is emphasized by Maxwell's thought experiment. In Maxwell's demon experiment, a trapdoor between two containers filled with gases at equal temperatures is controlled by a hypothetical "demon". The "demon's" purpose is to defy the second law of thermodynamics – a good law of nature that operates well. This is done by allowing the exchanges of molecules such that fast molecules move in only one direction while slow molecules move in the opposite direction. In so doing the temperature of the container with fast molecules will be raised while that with the slow molecules will be lowered. But for the demon's entropy due its tracking of information on the system's particles in order to perform its job

reliably, the above temperature difference between the two containers would have violated the second law of thermodynamics. This information on fast and slow particles of an isolated system is a form of entropy referred to as information entropy (Kolmogorov complexity). Even as the gas loses entropy, the information entropy increases. Consequently, the "demon" is considered a macroscopic system with non-vanishing entropy. In the case of thought process, the human brain experiences thought entropy through the interactions of its microstate activities namely creativity, imagination and intelligence even as interactive answer is approached. The chain of information processed on the microstate activities of problem-solving skills is what constitutes a form of entropy called **thought entropy**. To perform reliably, the brain's memory stores microscopic information resulting from problem-solving skills interactions between creativity, imagination and intelligence via the use of human language. Thus, as a quantum process, the human thought process also undergoes thermodynamic energy transfer or energy change with time. This is evinced by the fact that the human brain consumes up to 20% of the energy of the human body (Swaminathan, 2008). For any isolated system of particles with uncorrelated initial conditions, the second law of thermodynamics is provable if all microscopic physical processes are reversible. Under this condition, the measured entropy of a system such as volume and temperature differs from the system's information entropy (Halliwell et al., 1994). While measured entropy is

independent of system's particle correlations but dependent only on its macrostate, the information entropy rather depends on particle correlations. This is because the randomness of the system is lowered by particle correlations thereby lowering the amount of information needed for its description (Halliwell et al., 1994). Generally, the information entropy is less than the measured entropy but both are equal if correlation is lacking.

According to Liouville's theorem, an isolated system's information-theoretic joint entropy which refers to the needed amount of information to describe its exact microstate is an implication of time-reversal of all microscopic processes and is constant in time. By definition, joint entropy is the sum of marginal entropy (based on no particle correlations) and mutual entropy (based on particle correlations or negative mutual information). Therefore the lack of particle correlation in a system's initial state by assumption means that joint entropy becomes marginal entropy. However, if initial correlations between particles really exist then their formation must occur with time. The implication here is that correlations between particles generally increase with time. As a result, mutual entropy increases with time while mutual information decreases with time and vice versa. On the other hand, thermodynamics is constrained to indistinguishable microstates in which case only marginal entropy (proportional to thermodynamic entropy) can be measured and it also increases with time (Gull, 1989). The general characteristics relating various entropies in relation to

both microstate and macrostate are shown in table 16. The general trend of correlations between particles, increasing

Table 16

Generalized Entropic Correlations of an Isolated System's Microscopic and Macroscopic States

ISOLATED SYSTEM			
		QUANTUM ENTROPY	THERMODYNAMIC ENTROPY
Dependence		Microstate	Macrostate
Physical Process	Microscopic	Distinguished	Not distinguished
	Macroscopic	Distinguished	Independent of particle correlation
Time Forwarding (Arrow of Time)		Yes	Yes
State	Initial	Uncorrelated (random)	Uncorrelated
	Final	Correlated (particle dependence via interactions)	Correlated
Entropy	Marginal	Decreases with time	Decreases with time
	Mutual	Increases with time	Increases with time
	Joint [via Liouville Theorem]	Constant	Constant
	Information/Thought	Decreases with time (reverse time arrow)	Decreases with time
Time-Reversibility (Reverse Arrow of Time) [via 2nd Law of Thermodynamics]		Yes	Yes

only with time, is a recipe for entropic cross over from marginal entropy to mutual entropy with time as shown in figure 33. Marginal entropy which occurs with greater randomized system particles in the initial state is ascribed a bit value of "0" for lack of correlation. However, mutual entropy which occurs with

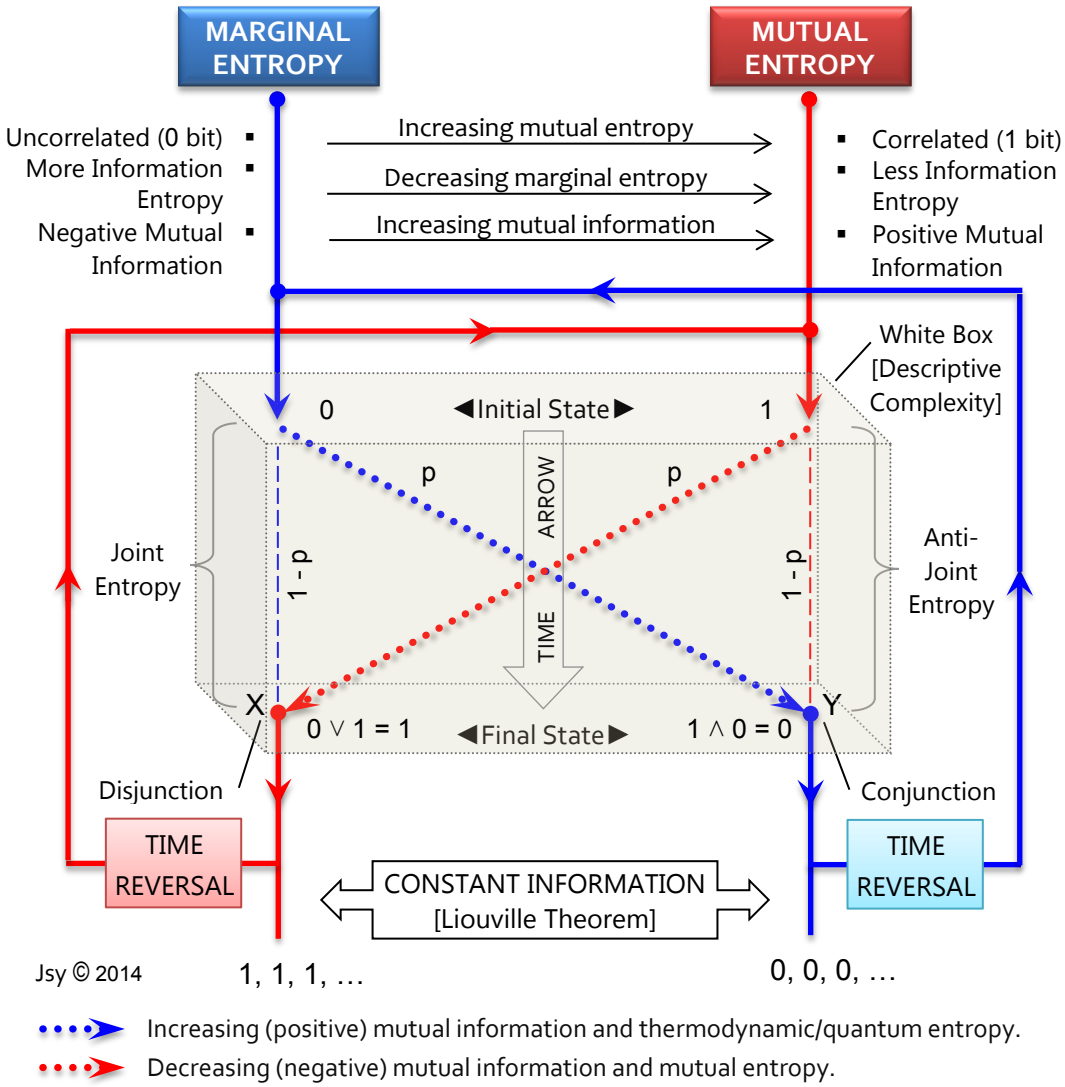

Figure 33. A depiction of the joint and information entropic interrelationships between particles of an isolated system's within the purview of time-reversal.

lesser randomized system particles in the initial state is ascribed a bit value of "1" due to the presence of correlation between particles. Observe in figure 33 that the entropic cross over situation between both initial marginal entropy and mutual entropy from the initial state, leads to a disjunction at point X

and a conjunction at point Y. At point X the decreasing mutual entropy (information) unionizes with the phase of marginal entropy to form Joint entropy at the final state. This is the result of a logical disjunction at X whose statement is given as $0 \vee 1 = 1$. Thus, the information output exiting point X is bit 1 or "true". On the other hand, at point Y the increasing mutual entropy (information) or decreasing marginal entropy as a result of increasing thermodynamic (or quantum) entropy intersects with the phase of mutual entropy at the final state to form anti-joint entropy. The logical statement for the latter situation at Y is given as $1 \wedge 0 = 0$. Therefore, the information output existing point Y is bit 0 or "false". The cross over thus formed and shown in the white box represents a thermodynamic system's descriptive complexity along a time arrow. The reversal of the final states of the microscopic processes back to their initial states means that the bit information must describe the isolated system' microstate when reversed. This repeats the entire thermodynamic procedure thereby leading to a consistent information output as shown in figure 33 above. It must be noted that time-reversibility means two things here. These are as follows:

1. There must be a reverse of correlation in time.
2. The information bit reversed must end up exactly in its original or initial conditions in accordance with Liouville theorem.

Failure to adhere to this rule will lead to a contradiction in the isolated system's particles initial conditions. Consequently, such disparity between the reversed and original initial conditions of an isolated system's particles violates Liouville theorem of constant information.

White Box Interpretations

The region encompassing the crossover of mutual entropy and information entropy forms a white box with pair of output strings referred to as descriptive or Kolmogorov complexity box of an isolated thermodynamic system. Kolmogorov complexity (algorithmic entropy) in algorithmic information theory, measures computability resources needed to specify a mathematical object (example string of characters). By definition, a formal language L (set of sequences of symbols) is defined as L = (A, F) where the set A is the alphabet made up of symbols of the language and the set F is a strings of symbols or sequence of elements from which a well-formed formulas wff (or simply formulas or words) can be derived. Subsequently in mathematical logic, theorems which are proven statements based on previously established statements (example if X, then Y where the hypothesis is X and the conclusion without assertion or affirmation is Y) can be derived from a set of well-formed formulas.

Generally, complexity characterizes the multiplicity of interacting parts of a system. However, this can be seen as an

algorithmic problem involving difficulty in solving defined problems as measured by time. Thus, by definition, the complexity of a string (as a mathematical any object) in a fixed universal description language is the problem involved in defining its shortest possible description (via string length). This means complexity is nonexistent if Kolmogorov complexity is relatively smaller than the string's length. If an arbitrary description d capable of producing a string s be defined as d(s), then the length of the minimal description of d(s) defines Kolmogorov complexity K(s) of the string which is expressed as

$$K(s) = |d(s)|$$

The problem-solution cycle of a thought process can be viewed as a general **thought program** of the human brain. Since the ability to solve a problem in an effective manner refers to computability and a problems' computability is closely linked to the existence of an algorithm to solve the problem, the representation of a problem-solution cycle is given by the following thought program equivalence

$$Thought\ Program \equiv Computability \equiv Algorithm$$

Thus, a general **thought program** $\mathbb{P}$ will be equivalent to the general solution function Ψ representing the **solution continuum** of a problem-solution cycle. This means

$$\mathbb{p} \equiv \Psi$$

Since the thought program outputs the post meta-solution or interpretation Δ of the solution continuum during a problem-solving scenario, it represents its description. This implies the description D of the thought program can be mathematically stated as

$$D(\mathbb{P}) = \Delta$$

where Δ is the gained interpretation/understanding of inexplicable environmental phenomenon. Consequently, the **thought complexity** T(Δ) which represents the minimum length of the minimal **description of interpretation** D(Δ) is given by

$$T(\Delta) = |D(\Delta)|$$

It must be noted that the minimum length required of the general description of the interpretive answer of the solution which is given by the thought complexity is necessitated by the catalytic action of imagination on creativity during synthesis of intelligence. This thought catalysis helps the human brain to operate efficiently by utilizing the minimum required resources during the problem-solution cycle.

In a problem-solving scenario, the computability of a problem and its minimum resource requirement are paramount for the production of a solution which can be interpreted to answer the problem. The resource requirement for a thought program can generally be seen as equivalent to that of a computer program. Support for such equivalent resource association is generally drawn from the following empirical evidences:

1. The increase in grey matter volume (structural neuroplasticity) in the structure of an adult human brain when a new cognitive/motor skill or vocabulary is learned (Lee et al., 2007).
2. The correlations of around 0.3 to 0.4 in majority of MRI studies between brain volume and intelligence predicting larger brains predict higher intelligence (McDaniel, 2005; Luders et al., 2008). It was however noted that other factors are also involved (Luders et al., 2008; Hoppe & Stojanovic, 2008).

The linkage of computability resource measure with computability measure can be expressed as follows. If the human brain HB as a natural processor is functionally encoded as <HB>, then on input with a given problem definition σ to output interpretative answer Δ, the composition given by <HB> σ which defines the description of Δ can be expressed as

$$< HB > \sigma = \mathbb{P}\sigma$$

An efficient computability of the problem definition generally can take place only when given its minimum resource requirements. This implies the human thought complexity T(Δ) is such that

$$\mathrm{T}(\Delta) \geq |\mathbb{P}\sigma| = |D(\Delta)|$$

In accordance with the invariance theorem, the description language is:

1. Dependent upon by the shortest description.

2. Bound or limited by its variations.

If one considers the human language L_H with a thought complexity function T and a computer language L_C with a Kolmogorov complexity function K, then in accordance with the invariance theorem there exists a constant c dependent only of said two languages such that

$$\forall s,\Delta: -c < T(s,\Delta) - K(s) < c$$

where T(s, Δ) is the thought complexity of the interpretative answer (post meta-solution) given the meta solution and K(s) the Kolmogorov complexity of the meta solution. But irrespective of the language used, the meta-solution outputs from the defined problem as input into appropriate programs must be the same. Therefore, it can be stated that

$$T(s) = K(s)$$

Hence in accordance with the chain rule for Kolmogorov complexity, the thought complexity of the interpretative answer given the occurrence of meta solution can be expressed as

$$T(s,\Delta) = T(s) + T(\Delta|s) + O(\log T(s,\Delta))$$

Substituting for T(s) gives

$$\boxed{T(s,\Delta) = K(s) + T(\Delta|s) + O(\log T(s,\Delta))}$$

The left hand term $T(s,\Delta)$ represents the application of human thought process via the shortest thought program (provided by the catalytic effect of imagination on creativity) to yield *s* and Δ. On the other hand, the right hand term represents the combination of mixed applications namely

1. A computer process via the shortest program $K(s)$ to yield *s*.
2. A human thought process via the shortest thought program $T(\Delta|s)$ to yield Δ given that s is recursive input.
3. The order of function (big O notation) or responds to changes in a human thought process based on processing time or working space requirements. This provides an upper bound on the growth rate of the function of human thought process.

The reasonability of the above equation lies in its practicality. As an undeniable truth in a problem-solving process using the aid of a computer to get an outcome which is then interpreted using the human thought process (human brain) for understanding is faster than using human thought process alone to fathom the entire problem-solving process. A case in point is found in weather analysis where supercomputers are used to churn mounds of data to yield outcomes for meteorologists to conveniently interpret in their weather forecasts. Due to its lack of expediency, such vital weather analysis would mostly have ended up disastrous if only human brain was entirely applied.

Subsequently, the invariance theorem can be restated by substituting for T(s, Δ) as follows

$$\forall s,\Delta: -c < K(s) + T(\Delta|s) + O(\log T(s,\Delta)) - K(s) < c$$

which boils down to

$$\boxed{\forall s,\Delta: -c < T(\Delta|s) + O(\log T(s,\Delta)) < c}$$

By definition, an interpretive answer is attainable or occurs at a specific spontaneous phase of the thought process as a result of the action of imagination on creativity. However, in order to reach this **spontaneous creativity phase (SCP)**, other **auxiliary mixed-skills phases (AMP)** have to be transcended. While SCP represents T(Δ|s), on the other hand AMP represents O(logT(s, Δ)). Thus, on the basis of needed **human thought procedural phases (HTPP)**

$$T(\Delta|s) \equiv 1$$

and that of the big O term can be deduced as follows. The AMP represents the internal phases of the problem-solution cycle each of which culminates with its own solution. Such micro problem-solution cycles can be represented as a function composition involving the functional application of meso-solution s_o (i.e. f_1: X→ Y) to that of meta-solution s (i.e. f_2: Y → Z) to produce post meta-solution Δ which is the interpretive answer. The composition of f_1 and f_2 is shown in figure 34 below. Given

functional spaces Y^{So} and Z^{S} the following elements can be constructed from functional space Z^{So} which represents the solution continuum. From figure 34, $s = f_1(s_o)$ and $\Delta = f_2(s)$. Therefore,

$$(f_2 f_1)(s_0) = f_2\big(f_1(s_0)\big) = \Delta$$

For the functional space X^{Po} which represents the problem continuum and the functional space Z^{So}, the functional composition

$$f_2{}^{\circ}(f_1{}^{\circ}f_0)(P_0) = f_2\Big(f_1\big(f_0(P_0)\big)\Big) = \Delta$$

where P_0 is the meta-problem of the resident phenomenon, represents the function composition of the problem-solution cycle of the human thought process which yields an interpretative answer.

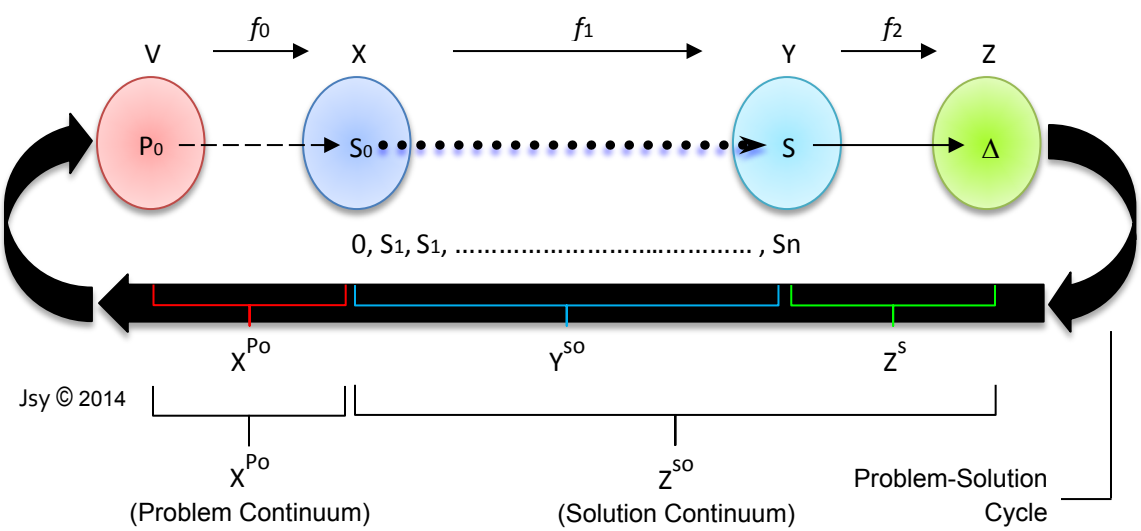

Figure 34. Functional application of solution continuum functions.

Consequently, the big O term from the restated invariance theorem can be represented as a function composition by the following

$$O(\log T(s,\Delta)) \equiv O\left(\log T\left(f_2\left(f_1(s_0)\right)\right)\right)$$

Let the big O term which determines the upper bound on the growth rate of the function of human thought process on the basis of HTPP be defined as

$$f_{htpp}(s_0) = O\left(\log T\left(f_n\left(f_{n-1}\left(\cdots\left(f_3\left(f_2\left(f_1(s_0)\right)\right)\right)\right)\right)\right)\right)$$

$$as\ s_0 \to \infty\ taking\ values\ s_1, s_2, s_3, \cdots, s_n\ \ and\ where\ s_n = s.$$

If and only if there exists a positive real number M and a real number s_1, then by definition of big O notation

$$\left|f_{htpp}(s_0)\right| \leq M\left|\log T\left(f_n\left(f_{n-1}\left(\cdots\left(f_3\left(f_2\left(f_1(s_0)\right)\right)\right)\right)\right)\right)\right|\ \ for\ all\ s_0 > s_1.$$

On the other hand,

$$f_{htpp}(s_0) = O\left(\log T\left(f_n\left(f_{n-1}\left(\cdots\left(f_3\left(f_2\left(f_1(s_0)\right)\right)\right)\right)\right)\right)\right)\ as\ s_0 \to 0$$

$$where\ 0 < s_1 < s_2 < s_3 < \cdots < s_n\ \ given\ that\ s_n = s$$

if and only if there exists positive number δ and M such that

$$\left|f_{htpp}(s_0)\right| \leq M\left|\log T\left(f_n\left(f_{n-1}\left(\cdots\left(f_3\left(f_2\left(f_1(s_0)\right)\right)\right)\right)\right)\right)\right|\ \ for\ |s_0 - 0| < \delta.$$

and in terms of a limit superior, if and only if

$$\limsup_{s_0 \to 0} \left| \frac{f_{htpp}(s_0)}{\log T\left(f_n\left(f_{n-1}\left(\cdots\left(f_3\left(f_2\left(f_1(s_0)\right)\right)\right)\right)\right)\right)} \right| < \infty.$$

The general implication here is that the number of HTPP units that is needed to arrive at an interpretive answer of a defined problem must lie between zero and infinity. The bound is expressible as

$$\boxed{0 < \sum_{i=1}^{n} i(HTPP\ units) \leq 1 + M}$$

where the term 1 is the HTPP unit for the spontaneous creativity phase which occurs when the shortest thought program T(Δ|s) is fed with recursive input s to eventually output an interpretative answer Δ. Thus, in generally the number of cycles in human thought procedural phases or number of loops in a computer program needed to achieve an answer to a given problem is bound by a fixed integer number. This integer bound would be determined under the Halting Problem analysis.

CHAPTER 13

A GENERAL INFORMATION WAVEFORM

The central challenge in network science, involves predicting and controlling of the dynamics of complex networks. However, results from conducted computer simulation (Krioukov et al., 2015; 2012) suggests that a single fundamental law may govern the temporal growth of brain networks, social networks, the internet , biological networks and the expansion of the physical universe. As the study showed, there exists functional similarity or equivalence between the growth of the physical universe and aforementioned complex networks.

By Liouville's theorem, the amount of information that exactly describes the microstate of a system is constant in time. Therefore the mechanical entropy of an isolated particle or system of particles must constitute a constant energy transfer by means of work interactions as shown in figure 35. As a particle appears in space-time at the zeroth point time, its pure state information is given by the total quantum mechanical entropy which is the net sum of invariant zeroth potential entropy S_{zp}, the potential entropy S_p and the kinetic entropy S_k (see figure 35). As the particle's total quantum mechanical energy of its

pure state begins to lose entropy via decreasing kinetic entropy, its information begins to dissipate. At the same time, the particle gains more potential entropy which ensures that its

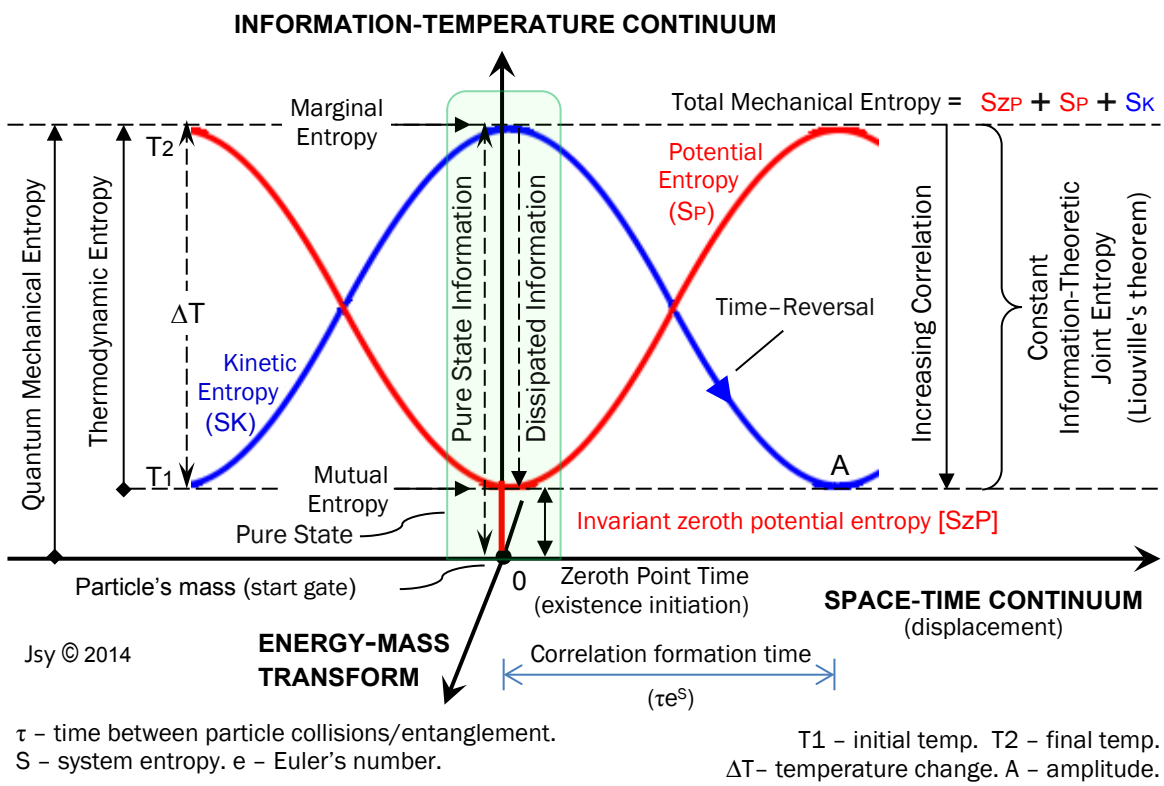

Figure 35. Graph showing variation of potential and kinetic entropies and information dissipated by a particle at its point of existence along a wave path in space-time continuum.

total mechanical entropy which is equal to the joint entropy is a constant in accordance with Liouville's theorem. Observe that for the particle to get back to its initial pure state conditions, it must undergo a time-reversal which is estimated to take a value given by τe^S where τ is the time between particle

collision during entanglement, e Euler's number and S the entropy, as depicted in figure 35 (Krioukov et al., 2012). The assertion made here is that a **universal quantization of dimensional (UNIQOD) framework** is associated with each particle, object or system. UNIQOD framework is a multiple dimensioned three-dimensional system where each axis is represented by a paired dimension. Thus, in general, all UNIQOD frameworks work together through quantum entanglement to represent the physical universe. In this sense, UNIQOD frameworks can be seen as quantized or packets of physical dimensions within the physical universe. The concept of UNIQOD is equivalent to the subdividing of early universe into tiniest possible units smaller than subatomic particles prior to the computer simulation of the growth of the physical universe as a complex network. These cell units of the universe were called **quanta of space-time** (Krioukov et al., 2012). The pertinent question to be asked here, however, is: what happens to the lost information as a result of quantum entanglement? This question can be answered by illustration using a hypothetical system with three particles A, B and C. In such a tripartite system, the information lost by particle A is gained by the rest of the particles in the environment namely particles B and C. That lost by particle B is also gained by both particles A and C and finally that lost by particle C is gained by both particles A and B. This forms a system of shared or exchanged information network. Thus, the dissipation of

quantized information entropy in space-time creates **inforentropic waves (IEW)** within and between micro and macro systems (see figure 36). The analogy of concentric circular water waves used under floating ping pong balls analogy reminiscent of an average dissipated information entropy scenario. Like Bohr's circular electronic orbits, the actual information entropy dissipated can be represented by a more accurate wave description similar to that of Schrödinger's wave equation for probabilistic electronic orbits.

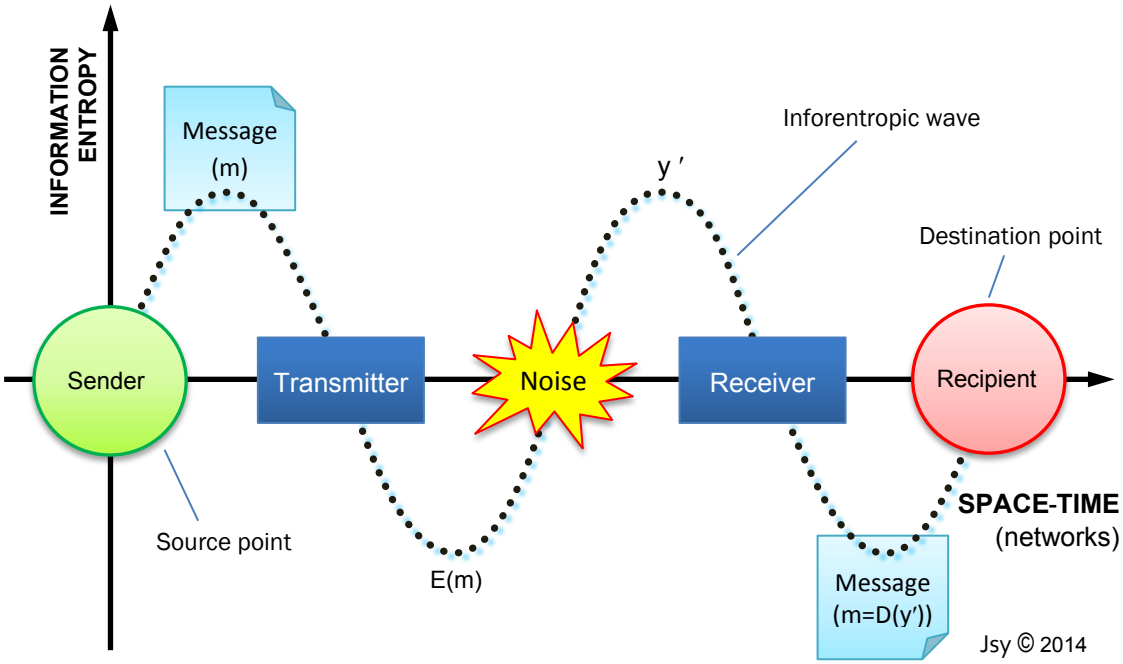

Figure 36. Information transmission over a noisy communication channel within a network system in space-time showing sequence basic communication elements.

Essentially, the white box encountered earlier on is a communication channel model referred to as binary asymmetric channel (BAC). During transmission of a message, due to transmission noise, the bits (one and zero) that are transmitted get flipped with a crossover probability of error p (see figure 33). In coding theory and information theory, the assumption is that $0 \leq p \leq 0.5$. Thus, an output bit received is swapped when p is greater than 0.5. In other words, a message m from a sender at a source point transmitted over a noisy communication channel in a network gets to a receiver as a distorted signal y′ which is then decoded D(y′) as an output message to the recipient at the destination point will have a crossover probability of error greater than 0.5 (see figure 36). This means an equivalent transmission channel crossover probability 1 − p for a BAC_p will be less than or equal to 0.5.

The Trichotomic Effect

The physical universe as a huge complex network system is estimated to be equal to or greater than 10^{250} atoms of space and time in comparison to 4.4×10^{46} water molecules in all the oceans in the world (Universe, human brain and Internet have similar structures, 2015).

With the aid of complex supercomputer simulations of the universe, researchers (Krioukov, Zuev, Boguñá, & Biancon, 2015) have been able to proven the causal network representing the

large-scale structure of spacetime the physical universe shows remarkable similarity to many complex networks such as the Internet, social, or even biological networks (see figure 37). This means that the laws that govern the growth of the structure of the universe are similar to that of the human brain and other complex networks (internet/social network of trust relationship between humans). The nature and common origin of such said law however remains elusive. To date, the prediction and control of the dynamics of complex networks still remains a central challenge in network science (Human brain, Internet, and cosmology, 2012).

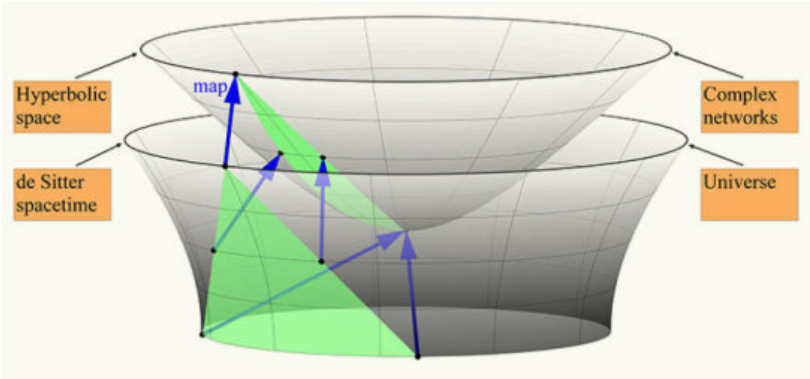

Figure 37. Simple mapping between the two surfaces representing the geometries of the universe and complex networks proves that their large-scale growth dynamics and structures are similar. Source from UC San Diego News Center, *Human Brain, Internet, and Cosmology: Similar Laws at Work?*, by Jan Zverina, retrieved July, 2015, from http://ucsdnews.ucsd.edu/pressrelease/human_brain_internet_and _cosmology_similar_laws_at_work

The constant interactions with human brain networks and the internet constitute a tripartite system of hyper-complex networks (Peckham, 2012). In figure 38, the points A, B and C

respectively represent the core activities of human brain networks, the universe and the internet. Through human thought process (HTP), humans interact with the environments of the physical universe in a quest to understand inexplicable phenomena. Also, through social networks, humans interact with each other thereby forming the global network called the internet via thought processes. These thought interactions resulting from

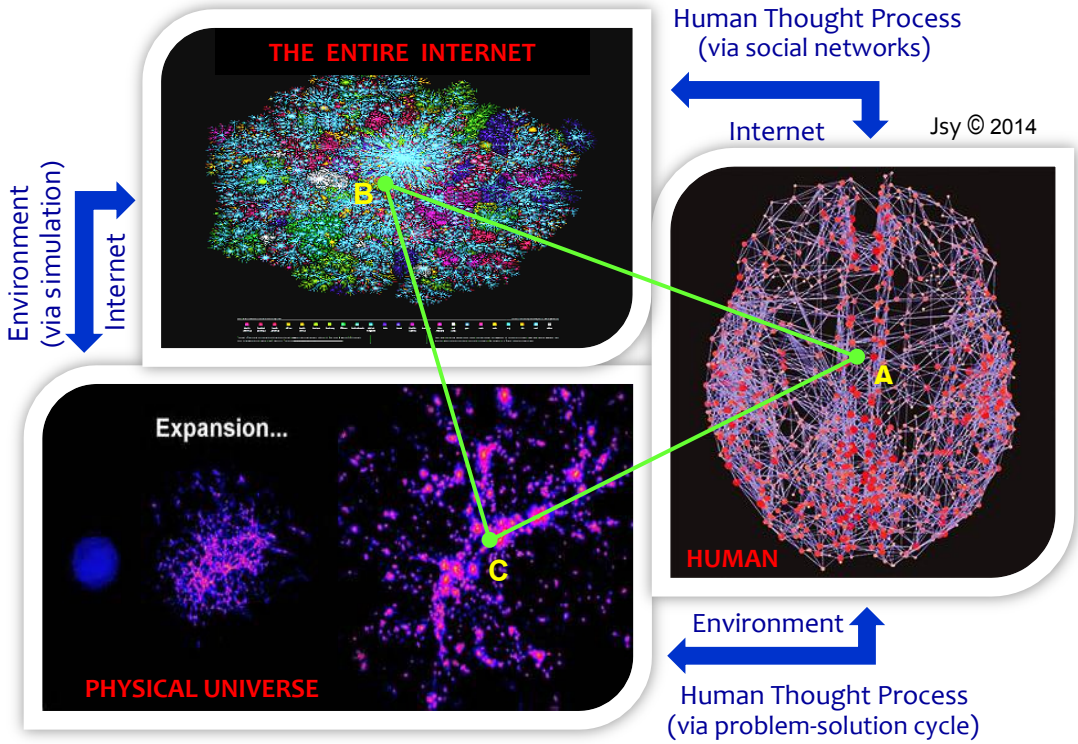

Figure 38. Similarities between brain network, social network (the internet) and the growth of the universe. Top Left: The mappings of all network backbones and servers of the Internet. Bottom Left: A simulation of the expansion of the universe. Centre Right: Neural networks of the human brain showing connections between brain "hub" and a central "core" during relays of commands for thoughts and behaviours. Sources from *History of the internet*, retrieved August, 2014, from http://www.unc.edu/~unclng/Internet_ History.htm & *What's new? Connectivity and a superhighway of the human brain*, retrieved August, 2014, from http://college.indiana.edu/magazine/summer2013/spotlight.shtml

HTP between the physical universe (including biological networks) and the internet sets up a triangle of thought interaction. This constitutes a complex information network on the large-scale. The triangulation of thought interactions (see green triangle in figure 38) according to the results from the computer simulation conducted by Krioukov's team of researchers (Universe, human brain and Internet have similar structures, 2015), by virtue of their functional similarity in structure and the laws that govern their growth can be considered as existing in a state of "equilibrium". This is in accord with the zeroth law of thermodynamics, which states:

> If two systems are separately in equilibrium with a third system, then they must also be in equilibrium with each other.

Thus, the structural and dynamical similarities that exist between the different tripartite complex networks should operate under a common universal law(s). Therefore, the latter should govern **infodynamic equilibrium** via information exchanges facilitated by HTP.

Informatics Wave Equation

Within the physical universe, the atomic system represents a fundamental network of subatomic particles. The energy and probability of location of an electron within an atomic system is perfectly described by Schrödinger's wave equation. Every location visited by an electron carries with it a specific energy

described by its probability distribution of different energies. As said earlier, the physical law governing complex information network such as the internet, by virtue of the similarity between the physical universe and the internet, can be represented by an informatics wave equation similar to the Schrödinger's wave equation. Unlike the electrons which function as probabilistic carriers of energy within the network of electronic orbitals within an atomic system, the nodes or computers in an information network can be static such as office computers connected to a LAN (local area network) or a home desktop computer connected to the internet. On the other hand, the nodes or computers in an information network can be dynamic as is the case of mobile devices connected to the internet. In general, the messages that are exchanged within the nodes of the information system of networks such as the internet equivalently serve as the probabilistic carriers of information entropy. Consequently, the law that governs the complex atomic orbital energy network must be fundamentally identical to that which governs complex entropic information network.

The time-dependent Schrödinger's wave equation (of a single non-relativistic particle) which was derived by treating an electron a wave Ψ(x, t) moving in a potential well V to explain spectral energy series is given by

$$\boxed{i\hbar\frac{\partial}{\partial t}\psi(r,t) = \left[\frac{-\hbar^2}{2m}\nabla^2 + V(r,t)\right]\psi(r,t)}$$

where i is the imaginary unit, $\hbar$ is reduced Planck's constant, $\partial/\partial t$ the partial derivative with respect to time t, ψ the wave function of the quantum system, r is the position vector, m the mass, ∇^2 is the Laplacian and V the potential energy. There are two foundations for Schrödinger's equation namely

1. Energy of the system and
2. Wave function ψ which is the description of all the system's information (Atkins, 1977). This is seen as the probability amplitude of the system. Its absolute square represents the probability density (Moore, 1992).

The wave equation needed to describe the dynamics of complex networks can be derived by determining the potential, kinetic and total mechanical entropy equivalent in information theory terms.

On the basis of quantum entropy, a particle at its point of existence along a wave path in space-time continuum has a total mechanical entropy (see figure 35) given as

$$Total\ Mechanical\ Entropy = S_{zp} + S_p + S_k$$

where S_{ZP} is the invariant zeroth potential entropy, S_P the potential entropy and S_K the kinetic entropy. This can however be expressed in terms of information entropy of a single node in an information network as follows

$$\begin{array}{c} Pure\ State \\ Information \\ Entropy \end{array} = \begin{array}{c} Invariant\ Potential \\ Information \\ Entropy \end{array} + \begin{array}{c} Dissipated \\ Information \\ Entropy \end{array}$$

$$= \begin{array}{c} Invariant\ Potential \\ Information\ Entropy \end{array} + Joint\ Entropy$$

This can further be expressed as

$$\begin{matrix} Pure\ State \\ Information \\ Entropy \end{matrix} = \begin{matrix} Invariant\ Potential \\ Information\ Entropy \end{matrix} + Mutual\ Entropy + Marginal\ Entropy$$

where mutual entropy is the gained potential entropy and the marginal entropy the gained kinetic entropy. By definition, information entropy is the amount of information in a source representing the fewest number of bits able to represent the source in a message. Thus, given a random variable, entropy as defined in information theory is a measure of uncertainty (Ihara, 1993). Thus, the expected value of a message's information can be quantified by entropy (Shannon) which is measured in bits, nats or dits for the base of its logarithm equal to 2, e (Euler's number) and 10 respectively. The average unpredictability in a random variable which represents Shannon entropy is equivalent to its information content. Let the uncertainty (Shannon entropy) of the distribution of an event or message variable X with possible values given by $\{x_1, ..., x_n\}$ from a node A in a network be given by

$$H(X) = E[I(X)] = -\sum_i P(x_i) \log_b P(x_i)$$

given that $I(x_i) = -\log_b P(x_i)$. Then $P(x_i)$ is the probability mass function (or relative frequency) which defines a discrete probability distribution based on the discrete random variable and I is the information content of X which is the unit of self-

information (Borda, 2011). For distribution between two events X and Y, I is given as

$$I(X;Y) = H(X) - H(X|Y) = H(Y) - H(Y|X)$$

Since a random event's information entropy is the expected value of its self-information, the chance of an event which has not yet taken place, will have information content only when it actually occurs.

By definition, when particle(s) in a quantum system engages in quantum entanglement the resulting equilibrium state is balanced. This means that a particle's marginal entropy in a lesser correlated state gets reduced to mutual entropy in a more correlated state. Thus, marginal entropy vanishes to zero with time. This scenario of entangled information entropy is illustrated in figure 39 where A and B represents two nodes in a network system with node A as the nuclear node. Observed that the region of balanced information entropic equilibrium (blue) is represented by the transmission or mutual information T(X, Y) between node A and node B which is defined as

$$\boxed{T(X,Y) = H(X) - H(X|Y)}$$

where the H(X|Y) is the conditional entropy of the two messaging events X and Y which respectively take values of x_i and y_j.

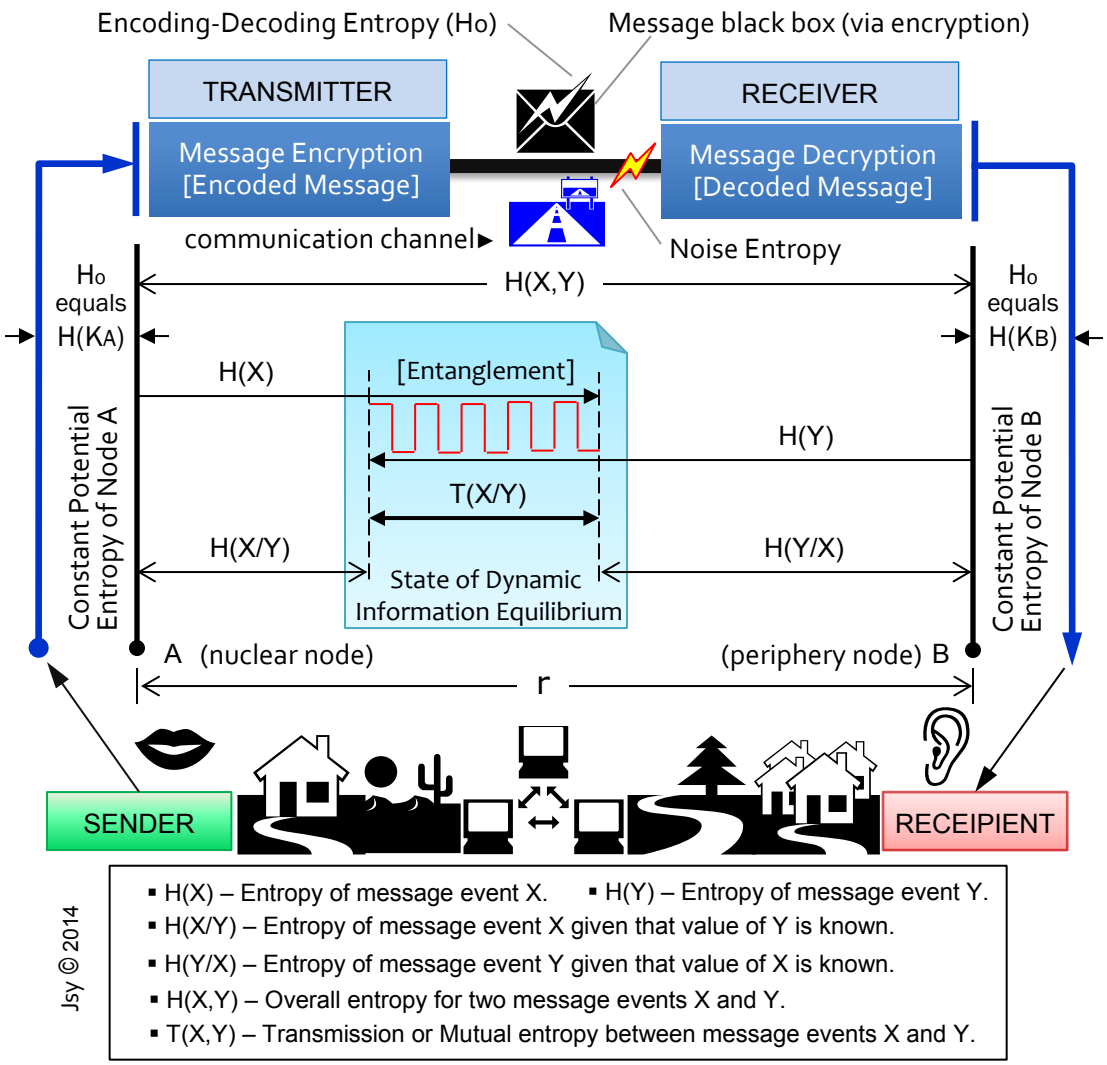

Figure 39. Quantum entanglement relations of expected information contents, mutual and conditional information entropies between two nodes in a network system.

It is defined as

$$H(X|Y) = \sum_{i,j} P(x_i, y_j) \log \frac{P(y_j)}{P(x_i, y_j)}$$

where the amount of randomness in the random variable X given that the value of Y is known is represented by $p(x_i, y_j)$ is the probability that $X = x_i$ and $Y = y_j$. The transmission information represents the uncertainty relating the prediction of X given knowledge about the distribution of Y. On the other hand, the overall entropy H(x, y) for X and Y discrete random variables is given by

$$\boxed{H(x,y) = H(y) + H(x|y) = H(x) + H(y|x)}$$

The set illustration below (figure 40) shows how the various types of information entropies are related.

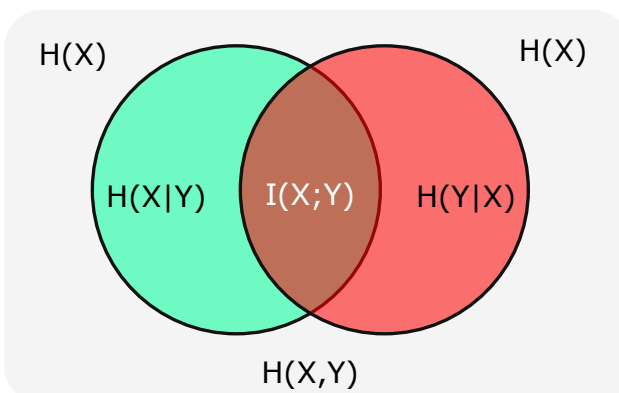

Figure 40. A set illustration generally depicting individual (H(X), H(Y)), joint (H(X,Y)), and conditional H(X|Y),H(Y|X)) entropies for a pair of correlated subsystems X,Y with mutual information I(X; Y).

By characterizing Shannon entropy H using the additivity criteria, which stipulates that entropy should be independent of the characterization of the entropy of a system with sub-systems,

the following information partitioning can take place. By definition, an ensemble of n uniformly distributed elements can be divided into sub-systems of k boxes each with b_1, b_2,..., b_k elements. Then with each box weighted with a probability, the entropy of the whole ensemble is equal to the total of the entropy of the system of boxes and that of the individual entropies of respective boxes. Thus, given positive integers b_i where $b_1 + \ldots + b_k = n$, the entropy of the whole ensemble is given by

$$H_n\left(\frac{1}{n},\cdots,\frac{1}{n}\right) = H_k\left(\frac{b_1}{n},\cdots,\frac{b_k}{n}\right) + \sum_{i=1}^{k}\frac{b_i}{n}H_{b_i}\left(\frac{1}{b_i},\cdots,\frac{1}{b_i}\right).$$

Alternatively, the decomposition of H of a system into g groups can be expressed as

$$\boxed{H = H_0 + \sum_g P_g * H_g}$$

given that the uncertainty among the groups or the specificity of the distribution of relevant variables within groups is Ho (see figure 39). Observe that the total entropy of the individual entropies of respective boxes (see second term in the equation above) is alternatively is equal to the overall entropy. This can be expressed as

$$\boxed{H(x,y) = \sum_g P_g * H_g}$$

It is interesting to note that under earlier quantum entropy analysis, a particle possessed invariant potential entropy by virtue of its existing mass, in addition to its prevailing mechanical entropy. This, under information theory, is equivalent to the concept of a box potentially having its own entropy (i.e. potential entropy). Thus, Ho at node A is equivalent to H_{KX} (see figure 39) which is the invariant potential entropy or uncertainty among groups within which the nuclear node belongs. In reality Ho belongs to the mode of transmission of a message across a communication channel. It represents the entropy of encoding of a message before it is sent over a communication channel which is equal to that due to decoding of message and so can be called encryption-decryption error entropy. The encoded message represents a message in sub-black boxes. Hence, the ensuing composed message black box (see figure 39 above) possesses an invariant potential entropy Ho due to the encryption-decryption error entropy which represents uncertainty among the groups or the specificity of the distribution of relevant variables within groups. Note that at node B, the uncertainty of the decoding of the message received is denoted by H_{KY}.

Under what can be called **infodynamics** which concerns dynamics of information, the gross information entropy of a network system is conserved. That is:

The total mechanical entropy associated with encoded message at the transmitter must be equal to that of its decoded message at the receiver of the same network system.

This principle is an adaptation of the first law of thermodynamics which stipulates that energy is conserved. In the atomic scenario, the electron(s) which carry energy do not possess any error in energy. They are consistent in their characteristic or eigenbehaviour. However within a network system, transmission of message(s) is not perfect due to the existence of noise in the transmission channel(s). Invariably, this leads to a wrong bit being received by a receiver resulting in an error in the information transmitted. This error in message transmission certainly affects the change in mechanical entropy. Hence, by definition of entropy conservation

$$\boxed{Total\ Mechanical\ Entropy = Total\ Information\ Entropy + Error\ Entropy}$$

Using a binary symmetric channel BSC_P with crossover probability p as a basic standard network error calibration due to its simplistic nature in terms of noisy channel analysis, the transmission error entropy of random variable X from a node A and the receiving of random variable Y from a node B leads to the following conditional probabilities

- $P(Y=0|\ X=0) = 1 - p$
- $P(Y=0|\ X=1) = p$
- $P(Y=1|\ X=0) = p$
- $P(Y=1|\ X=1) = 1 - p$

These conditional probabilities are equivalent to H(X|Y) and as such can be used to determine the exact given data. This leads to an accepted assumption that p lies between 0 and 0.5. If p > 0.5, then an error occurs in a transmitted bit. Hence, the calibrated error entropy for the determination of a switch bit during transmission is

$$\boxed{Calibrated\ Error\ Entropy = 0.5}$$

Using conditional entropy between two messaging events X and Y and the calibrated error entropy, the **information noise error entropy** over the communication channel can be computed as

$$H(X|Y) = \sum_{i,j} P(x_i, y_j) \log \frac{P(y_j)}{P(x_i, y_j)} \ = 0.5$$

For a single intersection of message events between X and Y,

$$P(x, y) \log \frac{P(y)}{P(x, y)} = 0.5$$

Using the product law of logarithm to expand gives

$$P(x, y)(\log(y) - \ \log P(x, y)) = 0.5$$

which expands into

$$P(x, y)^2 - \ \log(y) P(x, y) + 0.5 = 0$$

This is a quadratic equation in $P(x, y)$ which can be solved by

applying the quadratic formula as follows. Given

$$ax^2 + bx + c = 0$$

Let x = P(x, y), a = 1, b = log(y) and c = 0.5. Then using

$$x = -\frac{b \pm \sqrt{b^2 - 4ac}}{2a}$$

gives

$$\boxed{P(x,y) = -\frac{\pm \log y \sqrt{\log(y)^2 - 2}}{2}}$$

where log(y) is a known value. Hence, the **information noise error entropy** H_η is given as

$$\boxed{H_\eta = -P(x,y) \log P(x,y)}$$

Determination of Gross Information Entropy

A complete framework for the development of an informatics wave equation lies in the determination of the gross information entropy in a given network system. This can be achieved by tracking entropy activities as a message is exchange between a source and destination in a network.

Messages exchanged within the space-time continuum of an isolated network system possess entropy which is conserved. On

the basis of a syntactic interpretation of information entropy (based on probability rules) and the conservation rule, the total information entropy existing at the transmitter point and at the receiver point in a given network system is equal. That is

$$\boxed{Total\ Entropy\ at\ Transmitter = Total\ Entropy\ at\ Receiver}$$

This can be expressed mathematically (see figure 39) as

$$H_{K_X} + H(x,y) = H_{K_Y} + H(x,y)$$

given that

$$H_{K_X} = H_{K_Y} = H_o$$

where $H(x,y)$ is the overall entropy of the network system's purview, H_{K_X} is the constant potential entropy at source (node A), H_{K_Y} the constant potential entropy at the destination (node B) and H_o **encryption-decryption entropy** which is also called the invariant potential entropy. By definition, the net information entropy $\mathbb{E}_N$ is given by

$$\mathbb{E}_N = H_0 + H(x,y)$$

Note that the conservation of information entropy is an expected value (transmission not yet occurred) of the message's self-information at the transmission and receiver points within the network system. It only transforms into information content when transmission of the message actually takes place along the communication link. During this transmission phase, the sent

message not only has gained potential entropy in addition to encryption-decryption entropy but also acquired kinetic entropy and noise error entropy. Thus, the transmission phase of a network system is not entropy conserved because it is not isolated due to the effect of noise. In the sense of gained mechanical entropy, as a message leaves its transmission point, its gained information potential entropy is mostly transformed into gained information kinetic entropy. In return as message approaches the receiver point its kinetic information entropy gets quickly reduced to gained information potential entropy. This means that though

$$H(x, y) = Gained\ Potential\ Entropy$$

at the source (node A), a message's gained kinetic information entropy is zero. However, on the basis of a semantic interpretation of information entropy (different words or symbols meaning) the gross information entropy which exists along the communication link between transmitter and receiver due to a sent message represents all the information entropy within the source node, the transmitter, communication link, the receiver and the destination or sink node. Due to the lack of isolatedness of a network system, unlike an atomic system, there exist possibilities of external interferences on a transmitted encoded message along a communication link. Additional entropies that come to play due to communication link effect under such

circumstances are **gained information kinetic entropy** and **information noise error entropy** along the communication link. Thus, the gross information entropy $\mathbb{E}_G$ can be expressed as

$$\mathbb{E}_G = \begin{matrix} Contant \\ Potential \\ Entropy \end{matrix} + \begin{matrix} Gained \\ Potential \\ Entropy \end{matrix} + \begin{matrix} Gained \\ Kinetic \\ Entropy \end{matrix} + \begin{matrix} Noise \\ Error \\ Entropy \end{matrix}$$

This can be expressed mathematically as

$$\boxed{\mathbb{E}_G = H_0 + H(x,y) + H_{EK}(x,y) + H_\eta}$$

where $H_{EK}(x,y)$ is the gained information kinetic energy as a result of the transmission of encrypted massage along communication link. Also, the **total information potential entropy** H_{EP} is given by

$$H_{EP} = H_0 + H(x,y)$$

Generally given a message at a source node in a network system, its gross information entropy $\mathbb{E}_G$ in travelling through a communication link to a destination node within the space-time of a network system can be expressed as

$$\mathbb{E}_G = \mathbb{H}$$

where $\mathbb{H}$ the Hamiltonian. This can be expressed as

$$\boxed{\mathbb{E}_G = H_0 + T(x,y) + H_{EK}(x,y) + H_\eta = \mathbb{H}}$$

where $T(x,y)$ is the transmission or mutual information entropy which is also equal to the gained information potential entropy when the entangling network interaction between variables X and Y from source and destination points are at entropic equilibrium with each other. In the atomic system, the electron which is dynamic possesses energy and mass. In similitude, the message in a network system is not only dynamic but possesses entropy and **information "mass"** I_m. The information mass can be defined as the number of characters or symbols in a message event X and expressed as

$$\boxed{I_m = \sum_{i=1}^{N} n\{X_i\}}$$

where n is the number of characters in a message set X*i* and N the number of message sets in a set of message event X. If one imagines a hypothetical case where bits of a message are string end-to-end between a sending node and a receiving node at a distance r, then the time *t* it takes the last bit to get to the receiving node form the initial time of transmission can be used to determine the average velocity (rate of change of distance) experienced by each bit which is: $v_{AVG} = r/t$. Alternatively, the average velocity of the bits can be defined by the entropy rate or source information rate of the data source which is defined as the average number of bits per symbol needed to encode it.

Consequently, the **information "momentum"** I_P can be defined as

$$\boxed{I_P = I_M H(X) \quad or \quad I_P = I_M H'(X)}$$

where $H(X)$ and $H'(X)$ are the entropy rate of a stochastic process given by the limit of the joint entropy of n members of a process X_K as it approaches infinity which is defined as

$$H(X) = \lim_{n \to \infty} \frac{1}{n} H(X_1, X_2, \cdots, X_n)$$

or

$$H'(X) = \lim_{n \to \infty} \frac{1}{n} H(X_n | X_{n-1}, X_{n-2}, \cdots, X_1)$$

By definition, in the case of a strong stationary stochastic processes,

$$H(X) = H'(X)$$

By virtue of existing functional similarity or equilibrium among the physical universe, the internet and human thought process as a complex network systems, the invocation of a similar plane wave equation such as the simplest wave function ψ governing electrons in an atomic system is appropriate for the wave analysis of all general complex network via communication (language). By definition

$$\psi = Ae^{i(k.r - \omega t)}$$

where A is the amplitude, ω the angular frequency of the plane wave, i the imaginary unit, r the single direction position of network messaging node from its recipient node, t the time and **k** the wavenumber which is expressed as k = 2π/ λ. Using the natural system of units where the reduced Planck's constant is given by $\hbar$ = 1, the follow results

$$\psi = Ae^{i(\boldsymbol{p}.r\ -Et)/\hbar}$$

since the momentum vector **p** of the dynamic event in the network system (message) and its wavevector **k** have the following relation

$$\boldsymbol{p} = \hbar\boldsymbol{k} = \boldsymbol{k}\ \ and\ |\boldsymbol{k}| = \frac{2\pi}{\lambda}$$

given that $\hbar$ = 1. By existing functional similarity between the atomic system and complex information network system, the momentum vector is equivalent to the **information momentum** Ip and the equivalent of energy E in terms of information entropy is equivalently determined by using the basic definition of entropy form the thermodynamics perspective. By definition, the energy in a thermodynamic microscopic system is given as

$$Energy = Entropy \times Temperature$$

While in the case of thermodynamics, heat capacity of a substance (say water) measures its value of heat energy reservoir, in the case of the infodynamics (dynamics of information) the information entropy capacity existing within a given

communication channel or medium between a transmitter and a receiver measures the value of entropy reservoir. This equivalence as

$$\begin{matrix} Thermodynamic \\ Heat\ Capacity \end{matrix} \equiv \begin{matrix} Infodynamics \\ Entropy\ Capacity \end{matrix}$$

can be expressed mathematically

$$\boxed{mc\theta \equiv I_m\, I_c\, \vartheta}$$

where m is the mass of a substance or medium, c is the specific heat capacity, θ the change in temperature, I_m the information mass, I_c represents the specific entropy capacity of a channel, and ϑ the change in transmission signal temperature accompanying the sending of message over the channel.

In accordance with information theory, the information channel capacity defines the maximum mutual information with reference to the input distribution (say node A) between input and output (say node B) of a channel (Cover & Thomas, 2006). By definition, the capacity of a communication channel C of a binary symmetric channel (BSCp) with crossover probability p is given by

$$C = 1 - H_b(p)$$

where $H_b(p)$ is the binary entropy function which involves the entropy of a Bernoulli process with probability of success p.

Given a random variable X with binary values 0 and 1 then with P(X=1) = p and P(X=0) = 1 − p the entropy of X is by definition expressed as

$$H_b(p) = -p\log_2 p - (1-p)\log_2(1-p)$$

where $0\log_2 0$ is taken as 0. It must be noted that while the entropy function H(X) takes random variables (distribution) as a parameter the binary function $H_b(p)$ takes as parameter a single real number. Note that the calibrated error entropy given as p = 0.5 will cause the binary entropy function to attain a maximum value. It represents an unbiased bit and is information entropy's most common unit.

With the equivalent relation between the amount of energy reservoir and the amount of information entropy reservoir (i.e. the gross information entropy) given as $E \equiv \mathbb{E}_G$, it implies that the information wavefunction can be expressed as

$$\psi = Ae^{i(I_p.\boldsymbol{r} - \mathbb{E}_G t)/\hbar}$$

where $\boldsymbol{r}$ the position vector of messaging node in 3-dimensinal space relative to recipient node(s) in a complex network system and I_p the information momentum. Differentiating with respect to space of the message within the complex network, the first order partial derivatives gives

$$\nabla\psi = \frac{\partial}{\partial \boldsymbol{r}}\left(\frac{iI_p\boldsymbol{r}}{\hbar}\right)\cdot Ae^{i(I_p.\boldsymbol{r}\,-\,\mathbb{E}_G t)/\hbar} = \frac{i}{\hbar}I_p Ae^{i(I_p.\boldsymbol{r}\,-\,\mathbb{E}_G t)/\hbar} = \frac{i}{\hbar}I_p\psi$$

Also, the partial derivatives with respect to time of messaging in a complex network is given by

$$\frac{\partial\psi}{\partial t} = \frac{\partial}{\partial \boldsymbol{r}}\left(\frac{-i\,\mathbb{E}_G t}{\hbar}\right)\cdot Ae^{i(I_p.\boldsymbol{r}\,-\,\mathbb{E}_G t)/\hbar} = -\frac{i\,\mathbb{E}_G}{\hbar}Ae^{\frac{i(I_p.\boldsymbol{r}\,-\,\mathbb{E}_G t)}{\hbar}} = \frac{i\,\mathbb{E}_G}{\hbar}\psi$$

Using both gross information entropy operator $\widehat{\mathbb{E}_G}$ and information momentum operator $\hat{\mathrm{I}}_p$ to redefine the above partial derivatives one gets

$$\widehat{\mathbb{E}_G}\psi = i\hbar\frac{\partial}{\partial t}\psi = \mathbb{E}_G\psi$$

where $\mathbb{E}_G$ here represents the eigenvalues or characteristic values of the message event, and

$$\hat{\mathrm{I}}_p\psi = -i\hbar\nabla\psi = I_p\psi$$

where I_p here represents a vector of the **information momentum eigenvalues** or characteristics.

An action of the gross information entropy operator on the information wavefunction ψ will result in the following. The space-time continuum of message transmission within a complex network system from a single one dimensional transmission of message events X and Y respectively from say node A (transmitter) to node B (receiver) has a gross information entropy given by

$$\mathbb{E}_G = H_0 + T(x,y) + H_{EK}(x,y) + H_\eta$$

where H_0 is the constant potential entropy, $T(x,y)$ the transmission or mutual information entropy, $H_{EK}(x,y)$ the gained information kinetic energy and H_η the noise error entropy of the communication channel. It must be noted that changes in the spatial configuration of nodes in a network can affect the gained information potential entropy in time. Hence, the gained information potential entropy functions in relation to all associated recipient nodes (betweenness centrality- see next sub-topic) under consideration within space-time continuum of a complex network system. Thus, a multiple one dimensional transmission of message is represented by

$$\mathbb{E}_G = H_0 + T(x_1, x_2 \cdots x_N,\ y_1, y_2 \cdots y_N) + H_{EK}(x_1, x_2 \cdots x_N,\ y_1, y_2 \cdots y_N) + \sum_{i=1}^{N} H_{\eta_i}$$

where N is the maximum number of message transmission. The substitution of both gross information entropy and information momentum operators into the gross information entropy equation gives

$$\mathbb{E}_G = H_0 + T(x,y) + \frac{I_p \cdot I_p}{2I_m} + H_\eta \rightarrow \hat{\mathbb{E}}_G = H_0 + T(x,y) + \frac{I_p \cdot I_p}{2I_m} + H_\eta$$

where I_m is the information mass.

Since a messaging event that has not yet taken place has an expected value of its self-information (equal to information entropy) representing its gained potential entropy, the act of actually transmitting the message across a communication link

gives the messaging event an information content which represents its gained kinetic entropy. By definition, the gained kinetic entropy is given by

$$\boxed{H_{EK}(x,y) = I(\omega_n) = -\log(P(\omega_n))}$$

where $I(\omega_n)$ is the information content or self-information associated with outcome ω_n whose probability is $P(\omega_n)$. Alternatively, the corresponding prior probabilities P_i of a given system of mutually exclusive events is transformed into posterior probabilities q_i by the expected information content I of the message. This by definition I is given by

$$I = \sum_i q_i \log\left(\frac{q_i}{p_i}\right)$$

In the case of the difference between two random values X and Y forming a matrix of variables, the total information content is given by

$$\boxed{I = \sum_i \sum_j (f_{ij}/N) * \log\left\{\frac{(f_{ij}/N)}{(f_{ji}/N)}\right\}}$$

where *i* represents x_1, x_2, … x_n and *j* represents y_1, y_2, … y_n and N the Grand sum of the matrix data.

Substituting for the operators using derivatives with respect to space and time in the equation for the gross information entropy operator equation and acting the resulting operator on the wavefunction gives the following

$$i\hbar\frac{\partial\psi}{\partial t} = -\frac{\hbar^2}{2I_m}\nabla^2\psi + [H_0 + T(x,y)]\psi + H\eta\,\psi$$

In general, for a single message in three dimensions, the time-dependent informatics wave equation is given by

$$\boxed{i\hbar\frac{\partial}{\partial t}\psi(\boldsymbol{r},t) = -\frac{\hbar^2}{2I_m}\nabla^2\psi(\boldsymbol{r},t) + [H_0 + T(x,y)]\psi(\boldsymbol{r},t) + H\eta\,\psi(\boldsymbol{r},t)}$$

where r is the distance between the source and the destination nodes and t the time. Alternatively, the above can be written as

$$\boxed{i\hbar\frac{\partial}{\partial t}\psi(\boldsymbol{r},t) = -H_{EK}(x,y)\psi(\boldsymbol{r},t) + [H_0 + T(x,y)]\psi(\boldsymbol{r},t) + H\eta\,\psi(\boldsymbol{r},t)}$$

For multiple messages in three dimensions, the inputs of ψ of the time-dependent informatics wave equation will be equal to $(r_1, r_2, \cdots r_N, t)$. ψ represents the probability of measuring a message at a position x at a time t.

The above wave function for information entropy provides a framework in which a holistic analysis of a complex network system can be achieved. Its application to complex networks facilitates the functional similarity of the subatomic world of the physical universe in light of quantum analysis of the microcosm to be rendered on the complex networks of the macrocosm. As illustrated in figure 41 below, the solutions of the functional similarity of the subatomic particle wavefunction to that of the message wavefunction allows for a fuller description of messaging or any form of exchanges within a complex network system. Observe in figure 41 that the message density and probability distributions in relation to complex network analysis are the result of said corresponding functional similarity with the atomic system. Correspondingly, the distributions at C and D shows graphical representations of the density distribution and the probability function in relation to the distance from the centre of an atomic system.

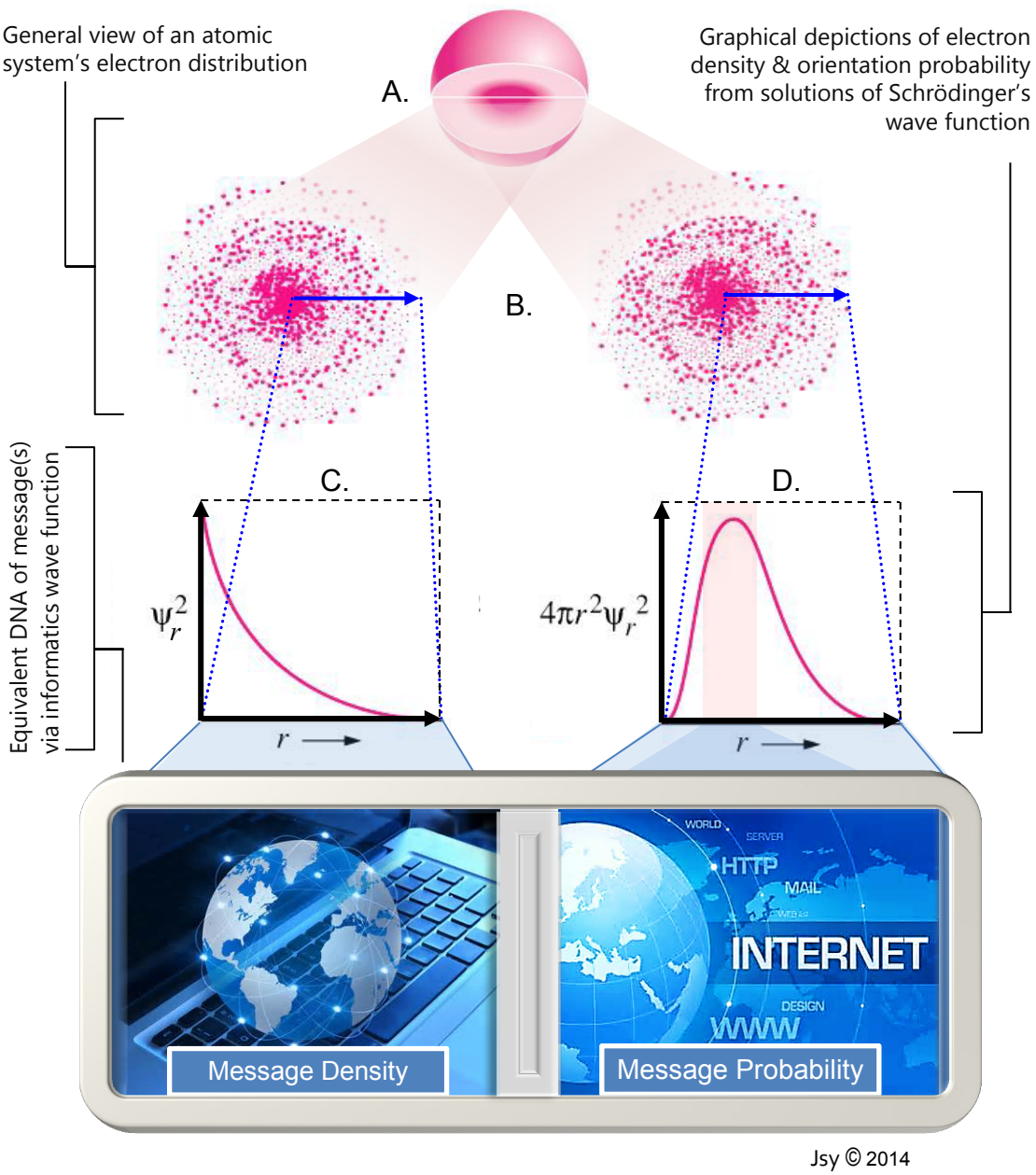

Figure 41. The illustration of mathematical descriptions for electrons, messages or network nodes (EMNN) based on wave function solutions from a time-dependent Schrödinger equation and informatics equation. A: Sphere region of an atom system in which is found atomic electrons or equivalently network nodes. B: Density map showing locations of EMNN. C: Graphical representation of an EMNN density as a function of distance r (focal node) such as from atomic nucleus. D: Plot of total probability of locating an EMNN as a function of distance from atomic nucleus (focal node). Adapted image from TechHive, *U.S. states' attorneys general to take aim at Internet 'safe harbor' law*, by Elizabeth Heichler, retrieved August, 2014, from http://www.techhive.com/article/2042351/us-states-attorneys-general-to-take-aim-at-internet-safe-harbor-law.html

It is worthy of note that in the microcosm, the atomic system explicitly shows its energy conservation but conceals its invariant potential energy in its wave function. However, in the macrocosm a network system only implicitly evince entropy conservation at its transmission and receiver points but explicitly shows its constant potential entropy and non-isolated gross entropy along its communication link in its wave function.

Statistical Analysis of Dynamic Network Analysis Data

As an embryonic field of scientific study, dynamic network analysis (DNA) involves the traditional social network analysis (SNA), link analysis (LA) and multi-agent systems (MAS) within the purview of network science and network theory. It involves statistical analysis of DNA data and the use of computer simulation in addressing network dynamics issues. Unlike the static traditional SNA model, SNA model is capable of learning which means

1. Its properties change over time.
2. Its nodes can propagate changes.
3. Its nodes can undergo adaption.
4. Its consideration of the probability of a change leading to network evolution.

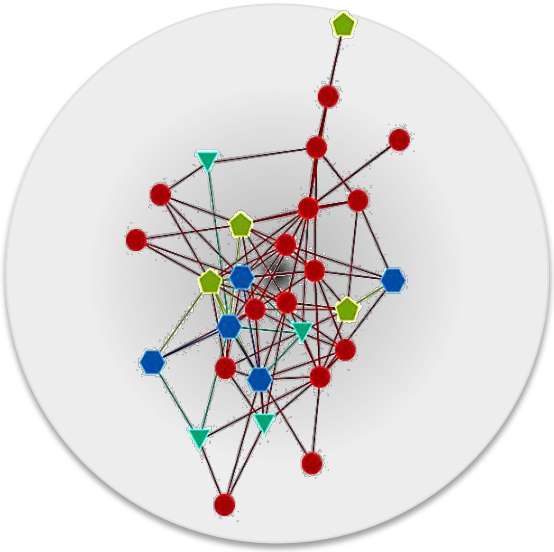

Figure 42. A multi-entity, multi-network and dynamic network depicted as an atomic system. Each node represents an electron. Adapted from Dynamic network analysis, *in Wikipedia, the free encyclopedia*, retrieved August, 2014, from https://en.wikipedia.org/wiki/Dynamic_network_analysis

Three main features to dynamic network analysis distinguishing it from standard social network analysis are:

1. It focuses on meta-networks. This involves multi-mode (people and locations), multi-link (friendship and advice), multi-level network (some nodes may be composed of others as in people and organizations nodes).
2. It uses simulations in understanding network evolvement, adaptation and impact of network interventions.
3. Its links are generally represented as probability of a link existing or as varying levels of uncertainty.

The computer simulation aspect of DNA envisages nodes as atoms in quantum theory and as such they are subjected to probabilistic

treatment. On the contrary, nodes in complex network system are like electrons in an atomic system as depicted in figure 42. As it was said earlier on, such nodes though generally not dynamic, can undergo **node surrogacy** where the messages that are received from or sent to them represent their hypothetical dynamics within the complex networks.

The general objective of network analysis is to determine the type of centrality measure to be used. To be able to target a node in a complex network system, centrality measurements which give information about the relative importance of nodes are used. This way, an intervention on a complex network system in order to control holistic message dissemination or curtailment can be effectively manage. The formally established measures of centrality are eigenvector centrality, degree centrality, betweenness centrality, Katz centrality and closeness centrality. The following outline shows a new atomic conceptual view of measures of centrality:

1. Eigenvector centrality (quality and number of incident link on node) should facilitate a new measurement concept of **network node characteristic** which is to determine the probabilistic stability of a node's traffic flow in a network. This measurement mimics the admissible energy and number of electrons in an electronic stationary orbit. It is also reminiscent to the energy eigenvectors used to determine electronic energy levels in an atomic system.

This means both electronic orbit and energy level and its corresponding energy is known. Using adjacency matrix of the network, the quality factor is determinable.

2. Degree centrality (number of links or vertices incident on the node) should facilitates a new measurement concept of **network node valency** which determines node's ability to combine with others.
3. Betweenness centrality (relative importance of a node) should facilitate a new measurement concept of **network node message affinity** which is to determine the amount of traffic flow existing between a node and others in the network. This measurement mimics electronic energy level series such as the Balmer, Paschen and Lyman series.
4. Katz centrality (summation of all geodesic or shortest weighted paths between a node and all other reachable nodes) should facilitate a new measurement concept of **network node ionization energy**. This is to determine the ease of detachment of a node from the network. Note that immediate neighbouring nodes have higher weights than those farther away.
5. Closeness centrality (closeness of node to others) should facilitate a new measurement concept of **network node bond length** which is to determine the strength of the link between a node and all other nodes in the network.

Of these, eigenvector centrality is the most appropriate to use in the informatics wave analysis of complex networks based on its energy and probabilistic description of all network system's information. Though DNA is tied to temporal analysis, the reverse is not necessarily true due to possible external factors which can cause changes in the network.

CHAPTER 14

DNA DATA COLLATION AND ANALYSIS

Data from a random stochastic space involving citing and cited journals from major chemistry journals will be analyzed both dynamically and statically for its information entropy. The list of randomly selected journals is shown in table 17 below.

Table 17

13 Randomly Selected Major Chemistry Journals from Which Data Was Collected

13 Major Chemistry Journals	
Journal Title	**Variable Name**
Chemical Physics	ChemPhys
Chemical Physics Letters	ChemPhLt
Inorganic Chemistry	InorgCh
J. of the American Chemical Society	JACS
J. of Chemical Physics	JChemPh
J. of Chemical Society - Dalton T	JChemSc
J. of Organic Chemistry	JOrgChem
J. of Organametallic Chemistry	JOrgmetC
J. of Physical Chemistry	JPhChUS
Molecular Physics	MolPhys
Physical Review A	PhysRevA
Tetrahedron	Tetrahe
Tetrahedron Letters	TrahLt

The multivariate and time-series asymmetric data randomly selected from the social networks of chemistry publications is shown in table 18. Observe that it includes missing data. These missing data however are not due to mistakes in data gathering. As such they are considered a non-procedural source of noise. In Loet Leydesdorff's work (Leydesdorff, 1991), the missing data in the data matrix was rectified by across the board replacement of 5 (shown in red in table 18) since the cut-off level of the printed edition of the Journal Citation Reports from which data was collected is 5. This was to minimize the effect of the missing data on the amount of expected information content to be derived from analysis (Leydesdorff, 1991). In the table provided in table 18, each cell a_{ij} contains the number of citations journal i gives to journal j and vice versa. Applying information theory to the data matrix, comparison between two distributions (via a_{ij} as priori values and a_{ji} as a posteriori or vice versa) as dynamic analysis and relation between the citing and cited journals as static analysis can be done. The static analysis generally gives insight into the relation between citing and cited while the dynamic analysis gives a direct interpretability of its decomposition into each of the selected journals. Also, $\Sigma\Delta I$ for each subset is a direct measure of relative source (e.g. transmitter) or relative sink (e.g. receiver). Notice in table 19 that $\Sigma\Delta I \geq 0$ for each corresponding row and column.

Table 18

Data Matrix Analyzed by Loet Lesderdoff with Red Numbers Indicating Rectification of Missing Data by Assigning 5 to Each Cell

Original Data Matrix for (1984) With Replacements for Missing Data: Aggregated Journal - Journal Citations Among 13 Major Chemistry Journals

CITED (*i*)		CITING (j)													Row Total
Variable Name	Sequence Number	1	2	3	4	5	6	7	8	9	10	11	12	13	
ChemPhys	1	984	724	51	189	1136	5	5	5	459	142	74	5	5	3784
ChemPhLt	2	963	2387	206	810	2816	31	40	5	1660	331	250	53	5	9557
InorgCh	3	35	157	5480	1912	138	1242	111	1228	319	14	5	28	29	10698
JACS	4	344	1102	4873	15521	1185	1214	6952	2448	3240	126	5	3045	3694	43749
JChemPh	5	2732	4622	715	2240	15069	166	157	163	5199	1575	1134	117	30	33919
JChemSc	6	5	5	946	452	5	1443	28	830	52	5	5	5	26	3807
JOrgChem	7	5	29	157	2264	5	62	5024	484	74	5	5	1617	2259	11990
JOrgmetC	8	5	32	713	958	5	641	307	3765	5	5	5	106	211	6758
JPhChUS	9	257	845	511	1208	1538	87	191	45	4315	122	41	51	56	9267
MolPhys	10	330	455	84	220	1195	5	5	5	395	1082	113	26	5	3920
PhysRevA	11	162	327	5	5	1115	5	5	5	170	183	3977	5	5	5969
Tetrahe	12	13	29	49	831	5	24	891	131	49	5	5	806	724	3562
TrahLt	13	5	32	84	1918	5	37	2802	548	61	5	5	1819	3385	10706
Column Total		5840	10746	13874	28528	24217	4962	16518	9662	15998	3600	5624	7683	10434	**157686**

Note: Missing cells replaced with a value of 5 (in red). **Reason**: Cut-off level of printed edition of the Journal Citation Reports from which the data were obtained.

Table 19

Marginal Changes in Information Content for Data Matrix with Fixed Adjustment of 5 for Every Missing Data

DYNAMIC ANALYSIS: CHANGES IN INFORMATION CONTENTS (ΔI) FOR FIXED ADJUSTED AGGREGATED JOURNAL - JOURNAL CITATIONS DATA (1984)

CITED: Change in I, ΔI (j)	Sequence No.	CITING : Change in Information Content, ΔI (i)													Self-Info. Row	
Variable Name		**1**	**2**	**3**	**4**	**5**	**6**	**7**	**8**	**9**	**10**	**11**	**12**	**13**	**(ΔI)**	
ChemPhys	1	0	-0.0019	0.0002	-0.0010	-0.0091	0	0	0	0.0024	-0.0011	-0.0005	0.0000	0	-0.0111	CITING:CITED
ChemPhLt	2	0.0025	0	0.0005	-0.0023	-0.0128	0.0005	0.0001	-0.0001	0.0103	-0.001	-0.0006	0.0003	-0.0001	-0.0026	
InorgCh	3	-0.0001	-0.0004	0	-0.0164	-0.0021	0.0031	-0.0004	0.0061	-0.0014	-0.0002	0	-0.0001	-0.0003	-0.0121	
JACS	4	0.0019	0.0031	0.0417	0	-0.0069	0.0110	0.0714	0.0210	0.0292	-0.0006	0	0.0362	0.0222	0.2301	
JChemPh	5	0.0219	0.0210	0.0108	0.0130	0	0.0053	0.0050	0.0052	0.0579	0.0040	0.0002	0.0034	0.0005	0.1481	
JChemSc	6	0	-0.0001	-0.0024	-0.0041	-0.0002	0	-0.0002	0.0020	-0.0002	0	0	-0.0001	-0.0001	-0.0053	
JOrgChem	7	0	-0.0001	0.0005	-0.0232	-0.0002	0.0005	0	0.0020	-0.0006	0	0	0.0088	-0.0045	-0.0168	
JOrgmetC	8	0	0.0005	-0.0035	-0.0082	-0.0002	-0.0015	-0.0013	0	-0.0001	0	0	-0.0002	-0.0018	-0.0163	
JPhChUS	9	-0.0014	-0.0052	0.0022	-0.0109	-0.0171	0.0004	0.0017	0.0009	0	-0.0013	-0.0005	0.0000	0.0000	-0.0313	
MolPhys	10	0.0025	0.0013	0.0014	0.0011	-0.0030	0	0	0	0.0042	0	-0.0005	0.0004	0	0.0075	
PhysRevA	11	0.0012	0.0008	0	0	-0.0002	0	0	0	0.0022	0.0008	0	0	0	0.0048	
Tetrahe	12	0.0001	-0.0002	0.0003	-0.0099	-0.0001	0.0003	-0.0049	0.0003	0.0000	-0.0001	0	0	-0.0061	-0.0203	
TrahLt	13	0	0.0005	0.0008	-0.0115	-0.0001	0.0001	0.0055	0.0048	0.0000	0	0	0.0153	0	0.0156	
Self-Info. Column (ΔI)		0.0287	0.0194	0.0524	-0.0733	-0.0519	0.0197	0.0769	0.0422	0.1040	0.0005	-0.0020	0.0639	0.0098	**0.2902**	I
		CITED:CITING													↑ I	

The following, table 20, shows results obtained from Lesderdoff's work on the 1984 journal-journal data matrix (Leydesdorff, 1991) and current analysis of same data.

Table 20

Comparison of Results of Both Analyzed Data Matrix with Same Level Adjustments and Relative Level Adjustments of Missing Data

METHODOLOGY		STATUS QUO	HUMAN THOUGH PROCESS
ANALYSIS TYPE	**RESULTS STATISTICS**	**CUT-OFF LEVEL ADJUSTMENT (bits)**	**ERROR-BASED NOISE ADJUSTMENT (bits)**
Dynamic	I	0.290	0.2902
Static	Imatrix (column groups)	-	2.2621
	Imatrix (row & col groups)	-	4.6872
	H(citing, cited)	5.667	5.6704
	H(citing)	3.457	3.4574
	H(cited)	3.173	3.1374
	H(citing | cited)	2.493	2.5330
	H(cited | citing)	2.209	2.2130
	T(citing, cited)	**0.964**	**0.9244**
	Ho	2.1352	2.5330
	U(citing | cited)	27.9%	26.74%
	U(cited | citing)	30.4%	29.46%
	R	**0.1454**	**0.1402**

■ I – information content. ■ Imatrix – information content of error-based noise corrected data matrix.
■ H(citing, cited) – overall entropy or joint entropy of journal-journal citations.
■ H(citing) – information entropy, expected information content or uncertainty of citing journals.
■ H(cited) – information entropy, expected information content or uncertainty of cited journals.
■ H(citing | cited) – amount of uncertainty of citing journals given the uncertainty in cited journals.
■ H(cited | citing) – amount of uncertainty of cited journal given the uncertainty in citing journal.
■ T(citing, cited) – mutual transmission or mutual entropy between citing and cited journals.
■ Ho – "in-between group uncertainty" (JACS in Inorg. Chem. Group) or constant potential entropy.
■ U(citing | cited) – uncertainty coefficient indicating fraction of citing bits predictable given cited.
■ U(cited | citing) – uncertainty coefficient indicating fraction of cited bits predictable given citing.
■ R – redundancy measure indicates variable independence when zero.

According to Leydesdorff's (Leydesdorff, 1991) conclusion, with remarkably low mutual information, the citing pattern is 10 percent ($[U_{cited} - U_{citing}]/U_{cited}$) better predictor of the cited pattern but not the other way around. The mutual information (transmission entropy) is identified to be 30 percent mutual reduction of the uncertainty in the prediction (via uncertainty coefficient). That is, 30 percent of the cited pattern is predictable given citing information and thus not information or cannot inform (see U(cited | citing) in table 20). On inferring the grouping of journals using statistical decomposition analysis, the exact number of clusters is determinable if there exists a maximum value of "in-between group uncertainty" H_o.

Noise Error Optimization Process

Due to the lack of prudence in the rectification of missing data, a more scientific way is introduced to help alleviate any possible noise error that these omissions will bring to the results. Analysis of the same data in light of a better estimation of missing data can only be achieved through proper estimation procedure that is bound by would-be actual data. As an instance of a Boolean constraint satisfaction problem, the missing data in the data matrix are considered as m eliminating Boolean constraints of "0"s applied through random interaction (or intersection) with n Boolean variables of "1"s which represent randomly sampled data matrix as shown in table 21. The goal here is to find an optimization procedure based on entropic

noise error that will maximize the estimation of all missing cell data comparably to that which would have been the case if data was given at all cost. To suppose that data was not sent by said journals due to lack of interest or other mitigating factors would mean that even if the issuing of journals was mandatory, the journals involved would have performed abysmally. Such performance would have reasonably bordered the minimum cut-off level. The pertinent question here is: what happens if data is not sent for whatever reason by journals? The answer lies in the information entropy or mutual entropy of said journals (less random environment) from which the missing data should have been sent. It will be greater compared to the scenario where data is sent (more random environment). Hence, the yardstick for comparison of the two methods of estimating values for missing data will be based on the computed information entropy for both optimizing methods on the data matrix. The better estimation optimizer of missing data should therefore have lesser information entropy.

From table 21, the relative frequency of missed data (i.e. "0"s) in the bit matrix is given as

$$Relative\ Frequency\ of\ Missed\ Data = \frac{Number\ of\ Missed\ Data}{Data\ Size} = \frac{42}{169} = 0.3307.$$

But by definition, the crossover probability error p limit that should cause data erasure is $0 \leq p \leq 0.5$. Therefore, the implication here is that the outputting of journal indeed did not take place. The meaning is that rectification of the missing data in the data matrix is very essential to reducing any noise

effect in the analysis to be done. This can be achieved by first determining both column and row marginal estimation of the missing data (see table 22). The computation of these missing data estimations is based on the portion of the total column or row frequency F_{total} of which the probability of a cell being void of data P_{miss} and a member of a column or row missing cells P_{rc} and a member of false bits P_F all occur. Thus, the estimated value of a missing cell is given as

$$Estimated\ Cell\ Frequency = P_{miss} \cdot P_{rc} \cdot P_F \cdot F_{total} \qquad where \quad P_{rc} = \frac{ic}{n} + \frac{jc}{n}$$

where ic and jc are respectively the number of row cells and column cells with missing data and n the total number of missing data. By assigning corresponding column estimation of missing cell frequency in table 22 to each corresponding missing cell member of the same column in table 23, the corresponding margin totals for columns n_p and rows n_q are computed. The noise error optimization process can be approached in twofold. Firstly, an asymmetric estimation of the missing data is done using subgroupings based on column shown in table 23 where each missing cell data of the same column in the data matrix receives the same column estimation value from the raw data matrix (table 22). Secondly, a symmetric estimation is done using both row and column subgrouping estimates in which case a missing cell data is given an estimate based on the average estimation of row and column estimated frequencies (see tables 22 and 23) corresponding to the missing cell value.

Table 21

Bit Matrix of Boolean Constraint Satisfaction Problem Representing Data Matrix for Noise Error Optimization Process

Bit matrix for 1984. Aggregated Journal-Journal Citations Among 13 Major Chemistry Journals

Sequence Number	CITED (j) Variable Name	C I T I N G: Data & Missing Data Represented by Bits 1 and 0 Respectively (i)													Row Total
		1	2	3	4	5	6	7	8	9	10	11	12	13	
1	ChemPhys	1	1	1	1	1	0	0	0	1	1	1	0	0	8
2	ChemPhLt	1	1	1	1	1	1	1	0	1	1	1	1	0	11
3	InorgCh	1	1	1	1	1	1	1	1	1	1	0	1	1	12
4	JACS	1	1	1	1	1	1	1	1	1	1	0	1	1	12
5	JChemPh	1	1	1	1	1	1	1	1	1	1	1	1	1	13
6	JChemSc	0	0	1	1	0	1	1	1	1	0	0	0	1	7
7	JOrgChem	0	1	1	1	0	1	1	1	1	0	0	1	1	9
8	JOrgmetC	0	1	1	1	0	1	1	1	0	0	0	1	1	8
9	JPhChUS	1	1	1	1	1	1	1	1	1	1	1	1	1	13
10	MolPhys	1	1	1	1	1	0	0	0	1	1	1	1	0	9
11	PhysRevA	1	1	0	0	1	0	0	0	1	1	1	0	0	6
12	Tetrahe	1	1	1	1	0	1	1	1	1	0	0	1	1	10
13	TrahLt	0	1	1	1	0	1	1	1	1	0	0	1	1	9
Column Total		9	12	12	12	8	10	10	9	12	8	6	10	9	**127**
													Bits Grand Total ▲		
Data Size		169	**Number of Missed Data**				42		**Relative Frequency of Missed Data**						0.3307

NOTE: Since the probability of missed data is less than 0.5 (within the limit for crossover probability error, $0 \leq p \leq 0.5$), it implies the output of journal to recipient did not take place. Hence, the missing data when not rectified will create noise in the analysis.

In table 24, the updated empty cells are based on average estimations of respective row and column frequencies determined in table 22 as a way to normalize the optimized estimation process since journals interact with each other. Based on the overall matrix, the expected information content is computed using the following

$$I_{matrix} = \sum_i \sum_j \left(\frac{f_{ij}}{N}\right) * \log \frac{(f_{ij}/N)}{(f_{ji}/N)}$$

where f_{ij} and f_{ij} are the a prior frequencies and a posterior frequencies of the data matrix and N the grand total of all frequencies in the data matrix. On the other hand, the information content contributed by each cell data is computed by

$$\Delta I = (f_{ij}/N) * \log(f_{ij}/f_{ji}) = (f_q/N) * \log(f_q/f_p)$$

In the case of applying the technique of multiplying both a priori *q* and a posteriori *p* relative frequencies (in terms of grand total of matrix frequencies) by N/nq and N/np respectively to achieve normalization relative to the margin totals as suggested by Leydesdorff (Leydesdorff, 1991) the following equation is used (see Appendix C for details)

$$I_{journal} = \sum \frac{f_q}{n_q} \log\left(\frac{f_q}{f_p}\right) = \sum \frac{f_{ij}}{n_{ij}} \log\left(\frac{f_{ij}}{f_{ji}}\right)$$

where

$$q = \frac{f_q}{N} = \frac{f_{ij}}{N} \quad and \quad p = \frac{f_p}{N} = \frac{f_{ji}}{N}$$

Results for I_{matrix} and $I_{journal}$ are shown in table 24. From the data in table 27, H(citing, cited) which is the grand total from

individual cells in the matrix is equal to **5.6704 bits.** Using values of the prior probabilities P and posteriori probabilities Q from table 24 and the equation for information expectation content, the following is derived

$$H(citing) = -\sum P \log P = 3.4574\ bits$$

and

$$H(cited) = -\sum Q \log Q = 3.1374\ bits$$

The following computations yield other joint and conditional expected information entropies of for the 1984 journal-journal citation data matrix. By definition, the expected joint information entropy between citing and cited is expressed as

$$H(citing, cited) = H(citing) + H(cited \mid citing)$$

This gives the following expected conditional information entropy

$$H(cited \mid citing) = H(citing, cited) - H(citing)$$

$$= 5.6704 - 3.4574 = \mathbf{2.2130\ \boldsymbol{bits}}.$$

Alternatively, by definition, the expected joint information entropy between citing and cited can be expressed as

$$H(citing, cited) = H(cited) + H(citing \mid cited)$$

which gives the following expected conditional information entropy

$$H(citing \mid cited) = H(citing, cited) - H(cited)$$

$$= 5.6704 - 3.1374 = \mathbf{2.5330\ \boldsymbol{bits}}.$$

To compute the transmission entropy T, the following equation is

applied

$$T(citing, cited) = H(cited) - H(cited \mid citing)$$

$$= 3.1374 - 2.2130 = \mathbf{0.9244}\ \boldsymbol{bit}.$$

Thus

$$\boxed{T(citing, cited) = 0.9244\ bit}$$

The above results obtained from the static analysis (see table 27) of the data matrix using optimized estimation process is shown in table 20. A comparison of the transmission entropy between the cut-off level adjustment method and error-based noise adjustment method shows that while cut-off level adjustment method yielded a higher value of 0.964 bit that of the error-based noise adjustment method yielded a lower value of 0.9244 bit. Hence, in accordance with the yardstick defined to determine the better approach to maximization in optimizing the estimation of the missing data in the 1984 journal-journal data matrix, the **synchronized noise error optimization process** is certainly a much better **missed data estimation optimizer method (MiDEOM)** to use.

Table 22

Estimations of Missing Cell Data Using Rows and Columns Subgroupings in Accordance With Probability Theory

Estimated Values of Missing Data: Original Data Matrix (1984) Aggregated Journal - Journal Citations Among 13 Major Chemistry Journals

CITED (j) Variable Name	Sequence Number	CITING (i) 1	2	3	4	5	6	7	8	9	10	11	12	13	Row Total	Estimation of Row Cell Freq.
ChemPhys	1	984	724	51	189	1136				459	142	74			3759	3.52
ChemPhLt	2	963	2387	206	810	2816	31	40		1660	331	250	53		9547	3.58
InorgCh	3	35	157	5480	1912	138	1242	111	1228	319	14		28	29	10693	2.00
JACS	4	344	1102	4873	15521	1185	1214	6952	2448	3240	126		3045	3694	43744	8.20
JChemPh	5	2732	4622	715	2240	15069	166	157	163	5199	1575	1134	117	30	33919	0
JChemSc	6			946	452		1443	28	830	52				26	3777	4.25
JOrgChem	7		29	157	2264		62	5024	484	74			1617	2259	11970	8.98
JOrgmetC	8		32	713	958		641	307	3765				106	211	6733	6.31
JPhChUS	9	257	845	511	1208	1538	87	191	45	4315	122	41	51	56	9267	0
MolPhys	10	330	455	84	220	1195				395	1082	113	26		3900	0.30
PhysRevA	11	162	327			1115				170	183	3977			5934	7.98
Tetrahe	12	13	29	49	831		24	891	131	49			806	724	3547	1.99
TrahLt	13		32	84	1918		37	2802	548	61			1819	3385	10686	8.01
Column Total		5820	10741	13869	28523	24192	4947	16503	9642	15993	3575	5589	7668	10414	**157476**	
Estimation of Col. Cell Freq.		4.36	2.01	2.60	5.35	22.68	2.78	9.28	7.23	3.00	3.35	7.33	4.31	7.81	▲**Grand Total**	
												Number of Missing Data (n)				42

NOTE: The determined value for a missing data (orange cells) is based on column subgroupings. It is given by the probability of a missing cell P_{miss} being a member of column or row missing cells P_{rc} and a member of the false bits PF out of the total column or row frequency F_{total}.
Estimated Cell Frequency = $P_{miss} \cdot P_{rc} \cdot P_F \cdot F_{total}$ where $P_{rc} = (ic / n) + (jc / n)$ where ic and jc are respectively the number of row cells and column cells with missing data and n is the total number of missing data.

Table 23

Assignment of Corresponding Column Estimates of Missing Cell Frequencies to All Cells within Each Column Respective

Missing Data Estimation Via Column Groupings: Original Data Matrix (1984) Aggregated Journal - Journal Citations Among 13 Major Chemistry Journals

CITED (j): Freq., fq	**Sequence Number**	**C I T I N G** (i): Frequencies, fp													**Row Total** (n_q)
Variable Name		**1**	**2**	**3**	**4**	**5**	**6**	**7**	**8**	**9**	**10**	**11**	**12**	**13**	
ChemPhys	1	984	724	51	189	1136	3	9	7	459	142	74	4	8	3790
ChemPhLt	2	963	2387	206	810	2816	31	40	7	1660	331	250	53	8	9562
InorgCh	3	35	157	5480	1912	138	1242	111	1228	319	14	7	28	29	10700
JACS	4	344	1102	4873	15521	1185	1214	6952	2448	3240	126	7	3045	3694	43751
JChemPh	5	2732	4622	715	2240	15069	166	157	163	5199	1575	1134	117	30	33919
JChemSc	6	4	2	946	452	23	1443	28	830	52	3	7	4	26	3820
JOrgChem	7	4	29	157	2264	23	62	5024	484	74	3	7	1617	2259	12007
JOrgmetC	8	4	32	713	958	23	641	307	3765	3	3	7	106	211	6773
JPhChUS	9	257	845	511	1208	1538	87	191	45	4315	122	41	51	56	9267
MolPhys	10	330	455	84	220	1195	3	9	7	395	1082	113	26	8	3927
PhysRevA	11	162	327	3	5	1115	3	9	7	170	183	3977	4	8	5973
Tetrahe	12	13	29	49	831	23	24	891	131	49	3	7	806	724	3580
TrahLt	13	4	32	84	1918	23	37	2802	548	61	3	7	1819	3385	10723
Column Total (n_p)		5836	10743	13872	28528	24307	4956	16530	9670	15996	3590	5638	7680	10446	**157792**
NOTE: These updated missing data will lead to anomalies in the assertion that the sum of the aggregated ΔIs for corresponding rows and columns must be equal or greater than zero.														**Grand Total ▲**	

Table 24

Assignment of Missing Cells Data Based on Average Estimations of Respective Corresponding Column and Row Frequencies in Table 22

CITED (j) Frequency fq	Normalized Values of Missing Data: Original Data Matrix (1984) Aggregated Journal - Journal Citations Among 13 Major Chemistry Journals													Row Total n_q	Post-erior Prob. Q	ΔIq	NORM. ΔIq
	CITING (i): Frequencies, fp																
Var. Name	1	2	3	4	5	6	7	8	9	10	11	12	13				
1.ChemPhys	984	724	51	189	1136	3	6	5	459	142	74	4	6	3783	0.0240	-0.0150	-1.6E-16
2. ChemPhLt	963	2387	206	810	2816	31	40	5	1660	331	250	53	6	9558	0.0606	-0.0102	0.0E+00
3. InorgCh	35	157	5480	1912	138	1242	111	1228	319	14	5	28	29	10698	0.0678	-0.0254	0.0E+00
4. JACS	344	1102	4873	15521	1185	1214	6952	2448	3240	126	8	3045	3694	33919	0.2150	0.0537	-3.2E-16
5. JChemPh	2732	4622	715	2240	15069	166	157	163	5199	1575	1134	117	30	33919	0.2150	0.1039	0.0E+00
6. JChemSc	4	3	946	452	13	1443	28	830	52	4	6	4	26	3811	0.0242	-0.0092	0.0E+00
7. JOrgChem	7	29	157	2264	16	62	5024	484	74	6	8	1617	2259	12007	0.0761	-0.0351	0.0E+00
8. JOrgmetC	5	32	713	958	14	641	307	3765	5	5	7	106	211	6769	0.0429	-0.0220	0.0E+00
9. JPhChUS	257	845	511	1208	1538	87	191	45	4315	122	41	51	56	9267	0.0587	-0.0463	0.0E+00
10. MolPhys	330	455	84	220	1195	5	5	4	395	1082	113	26	4	3918	0.0248	0.0030	0.0E+00
11. PhysRevA	162	327	5	7	1115	9	9	8	170	183	3977	6	8	5986	0.0379	0.0033	0.0E+00
12. Tetrahe	13	29	49	831	12	24	891	131	49	3	5	806	724	3567	0.0226	-0.0250	0.0E+00
13. TrahLt	6	32	84	1918	15	37	2802	548	61	6	8	1819	3385	10721	0.0680	0.0026	0.0E+00
Col. Total, n_p	5842	10744	13874	28530	24262	4964	16523	9664	15998	3599	5636	7682	10438	**157756**		**-0.0217**	**-4.8E-16**
Prior Prob. P	0.0370	0.0681	0.0879	0.1808	0.1538	0.0315	0.1047	0.0613	0.1014	0.0228	0.0357	0.0487	0.0662	**▲Grand Total**		▲	▲
ΔIp	0.0232	0.0115	0.033	-0.045	-0.074	0.0120	0.0482	0.0315	0.0799	-0.0028	-0.0031	0.0539	-0.0026	**0.1652**		◄ I journal	▲
Norm. ΔIp	00E+00	0.0E+00	0.0E+00	3.2E-16	0.0E+00	0.0E+00	0.0E+00	0.0E+00	0.0E+00	0.0E+00	0.0E+00	0.0E+00	0.0E+00	**3.2E-16**		◄ Norm. I journal	

NOTE: **1**. Each red number or black number in an orange cell represents a normalized missing data estimate. They are based on an average determination using corresponding row and column estimated cell values associated with each blank cell's corresponding row and column. **2**. The sum of corresponding row and column ΔIs is greater than or equal to zero. **3**. The ΣΔI for rows and columns in aqua and light green show significant difference at 16 decimal places attributable to noise error.

Using the value for I(citing, cited) from the harmonized noise error optimization process (see table J) and the information content equation

$$I(citing, cited) = -\log_b P(citing, cited)$$

one can write

$$\log_2 P(citing, cited) = -4.6872$$

which gives

$$P(citing, cited) = 2^{-4.6872} = 0.0388.$$

From the above results, the information noise error entropy H_η which is given by

$$H_\eta = -P(citing, cited) \log P(citing, cited) = -0.0388 \times (-4.6872)$$

can be computed as

$$\boxed{H_\eta = 0.1819 \text{ bit}}$$

Also, using the following equation for the decomposition of H(citing) of a system into g groups can be expressed as

$$H(citing) = H_0 + \sum_g P_g * H_g$$

given that the total entropy of the individual entropies of respective cells forming a group (data matrix) is equal to the

overall entropy or joint entropy which is expressed as

$$H(citing, cited) = \sum_g P_g * H_g$$

the constant potential entropy is computed as

$$3.4574 = H_0 + 0.9244$$

which yields

$$\boxed{H_0 = 2.5330\ bits}$$

From previous definition, the gained kinetic entropy H_{EK} is equal to I(citing, cited), therefore it can be stated that

$$\boxed{H_{EK}(citing, cited) = 4.6872\ bits}$$

In order to further ascertain how well the error-based noise adjustment method (synchronized noise error optimization process) is over the cut-off level adjustment method, the normalized variants of mutual information (transmission entropy) namely uncertainty coefficient U(X|Y) which is equivalent to coefficients of constraint C_{XY} or proficiency is used (William et al., 1992; Coombs, Dawes, & Tversky, 1970; White, Steingold, & Fournelle, 2004). By definition, the uncertainty coefficient which tells which fraction of the bits of X containing "true" values can be predicted given Y is expressed as

$$U(X|Y)=\frac{I(X;Y)}{H(X)}=\frac{H(X)-H(X|Y)}{H(X)}$$

Therefore, under the synchronized noise error optimization process

$$U(\text{citing}|\text{cited})=\frac{H(\text{citing})-H(\text{citing}|\text{cited})}{H(\text{citing})}$$

$$=\frac{3.4574-2.5330}{3.4574}=26.74\ \%$$

Also,

$$U(\text{cited}|\text{citing})=\frac{H(\text{cited})-H(\text{cited}|\text{citing})}{H(\text{cited})}$$

$$=\frac{3.1374-2.2130}{3.1374}=29.46\ \%$$

In order to ascertain the effect of both estimation methods on the independence of the random variables cited and citing, the redundancy measure R is used. If the variables involved are independent, R attains a value of zero. By definition

$$R=\frac{I(X;Y)}{H(X)+H(Y)}=\frac{H(X)-H(X|Y)}{H(X)+H(Y)}$$

Thus, for the cut-off level adjustment method (COAM)

$$R_{COAM}=\frac{H(\text{citing})-H(\text{citing}|\text{cited})}{H(\text{citing})+H(\text{cited})}$$

$$= \frac{3.457\text{-}2.493}{3.457+3.173} = 0.1454$$

and for synchronized noise error optimization process (SNEOP)

$$R_{SNEOP} = \frac{3.4574\text{-}2.5330}{3.4574+3.1374} = 0.1402$$

By comparison, unlike the synchronized noise error optimization process, the cut-off level adjustment method introduces 0.005 more dependency into the 1984 journal-journal data matrix. Therefore the synchronized noise error optimization process is a better way to estimate missing data.

Under the assertion that $\Delta I \geq 0$ always, the sum of corresponding ΔIp and ΔIq is always equal to zero. However, for the normalized ΔI, the summation of corresponding normalized ΔIp and normalized ΔIq is not always equal to zero. In table 24, the sky blue and rose red cells of corresponding rows and columns shows that at the microscopic level of 16 decimal places whereas all else is absolutely zero, there apparently exist some discrepancies in the foregone assertion of a must positive $\Sigma\Delta I$. Could the seemingly difference in $\Sigma\Delta I$ be attributable to numerical accuracy error in Excel 2010 functions or could it be something else which is subtly at play here? To unravel this pertinent case, there is the need to look further into ΔI summations in light of column in a bigger scale. This is the case when ΔI determinations are based on corresponding column

estimates as in table 23 or on both corresponding row and column as in table 24.

The effect of normalizing the optimized estimation process can be clearly seen if contrasted with its skewed case where cell estimation is based only on estimates from column cell frequencies (see tables 25 and 26). Based on the computed ΔIs shown in tables 25 and 26 respectively, it can be seen that while the skewed estimation method via corresponding column estimates showed uneven noise discrepancies (see sky blue rows and columns in table 25), that of the balanced estimation method via corresponding average row and column estimates showed even noise discrepancies (see sky blue rows and columns in table 26). From these noise discrepancies, it is however evident that the seemingly single noise discrepancy under the microscopic scale of table 24 (shown as sky blue row and column) multiplies under the macroscopic scales of tables 25 and 26 (shown as sky blue rows and columns). This potential for heavily dependence on initial noise condition is a case of **information butterfly effect** where a microscopic noise discrepancy in an initial information content of a given information network scenario multiplies at the macroscopic noise discrepancy level during maximized noise optimization. It is reminiscent to chaos theory's butterfly effect where a small change in initial the sensitive conditions at one place in a deterministic nonlinear system later results in large differences.

While the level of sensitivity of information system to small changes in initial noise condition (missing data) given optimization process is an important empirical evidence, there is also the need to ascertain why the assertion that the summation of marginal ΔIs for each corresponding rows and columns of a cell in the data matrix (i.e. row and column summations of ΔIs of cells) must be greater than or equal to zero seem to dither. The proof of this assertion can be found in Appendix C. However, to investigate the cause of this noise anomaly, scenario in random variable distributions will be considered.

Table 25

A Residual Asymmetric Noise Effect (Sky Blue Cells) Resulting from Skewed Noise Error Optimization Process on Original 1984 Data Matrix of Journal-Journal Citations

STATIC ANALYSIS: CHANGES IN INFORMATION CONTENTS (ΔI) FOR COMPUTATIONALLY ADJUSTED AGGREGATED JOURNAL - JOURNAL CITATIONS DATA (1984) BASED ON COLUMN GROUPINGS

CITED (j): Change in I, ΔI		**C I T I N G** (i): Change in Information Content, ΔI													**Self-Info. Row**	
Variable Name	**Sequence Number**	**1**	**2**	**3**	**4**	**5**	**6**	**7**	**8**	**9**	**10**	**11**	**12**	**13**		
ChemPhys	1	0.1617	0.0404	0.0157	-0.0120	-0.1928	0.0002	0.0043	0.0026	0.1768	-0.0222	-0.0099	-0.0011	0.0034	0.1669	**C I T I N G : C I T E D**
ChemPhLt	2	0.0584	0.0419	0.0121	-0.0234	-0.1610	0.0134	0.0026	-0.0015	0.1983	-0.0101	-0.0057	0.0058	-0.0015	0.1292	
InorgCh	3	-0.0006	-0.0003	0.1918	-0.1743	-0.0258	0.0891	-0.0013	0.1330	-0.0091	-0.0029	0.001	-0.0011	-0.0031	0.1965	
JACS	4	0.0019	-0.0044	0.0816	-0.2189	-0.0416	0.0224	0.1592	0.0412	0.0597	-0.0041	0.0000	0.0875	0.0277	0.2124	
JChemPh	5	0.0632	0.0319	0.0399	0.0289	-0.2136	0.0116	0.0106	0.0113	0.1957	-0.0038	-0.0153	0.0064	-0.0001	0.1668	
JChemSc	6	0.0008	-0.0019	-0.0042	-0.1242	-0.0149	0.1419	-0.0057	0.1626	-0.0050	0.0003	0.0029	-0.0023	-0.0009	0.1494	
JOrgChem	7	-0.0002	0.0000	0.0126	-0.2182	-0.0044	0.0083	0.1930	0.0451	-0.0056	-0.0003	0.0001	0.1779	0.0283	0.2364	
JOrgmetC	8	-0.0002	0.0128	-0.0285	-0.1188	-0.0078	0.0133	-0.0065	0.2856	-0.0015	-0.0003	0.0005	0.0033	-0.0269	0.1250	
JPhChUS	9	-0.0014	-0.0170	0.0809	-0.0829	-0.1609	0.0144	0.0444	0.0228	0.3667	-0.0119	-0.0056	0.0047	0.0040	0.2581	
MolPhys	10	0.0914	0.0382	0.0525	0.0378	-0.1606	-0.0001	0.0033	0.0019	0.1575	-0.0357	-0.0237	0.0198	0.0026	0.1849	
PhysRevA	11	0.0284	0.0166	-0.0007	-0.0005	-0.0201	-0.0007	0.0004	-0.0001	0.0560	0.0188	-0.0554	-0.0006	0.0001	0.0424	
Tetrahe	12	0.0102	0.0019	0.0261	-0.1793	-0.0080	0.0247	0.0601	0.0515	0.0143	-0.0017	0.0037	0.2479	-0.0461	0.2053	
TrahLt	13	-0.0004	0.0059	0.0117	-0.1759	-0.0009	0.0016	0.0713	0.0684	0.0005	-0.0004	-0.0002	0.2191	-0.0119	0.1889	
Self-Information Column		0.4133	0.1660	0.4916	-1.2616	-1.0125	0.3401	0.5358	0.8244	1.2042	-0.0744	-0.1076	0.7670	-0.0243	**2.2621**	**I** MATRIX
		C I T E D : C I T I N G													↑ **I MATRIX**	

NOTE: Sky blue cells indicate noise cells of data matrix with cross probability error of 0.3307. **I**matrix ≥ 0, with the number of ΣΔIs ≤ 0 (sky blue cells) unbalanced.

Table 26

Residual Symmetric Noise Effect (Sky Blue Cells) Resulting From Harmonized Noise Error Optimization Process on the Original 1984 Data Matrix of Journal-Journal Citations

STATIC ANALYSIS: CHANGES IN INFORMATION CONTENTS (ΔI) FOR COMPUTATIONALLY ADJUSTED AGGREGATED JOURNAL - JOURNAL CITATIONS DATA (1984) BASED ON NORMARLIZATION OF ROWS & COLUMNS GROUPINGS

CITED (j): Change in I ΔI		**C I T I N G** (i): Change in Information Content, ΔI													**Self-Info. Row**	
Variable Name	**Sequence Number**	**1**	**2**	**3**	**4**	**5**	**6**	**7**	**8**	**9**	**10**	**11**	**12**	**13**		
ChemPhys	1	0.1631	0.0412	0.0158	-0.0118	-0.1919	-0.0005	0.0006	0.0008	0.1776	-0.0221	-0.0098	-0.0011	0.0010	0.1628	**C I T I N G : C I T E D**
ChemPhLt	2	0.0585	0.0421	0.0121	-0.0233	-0.1609	0.0009	0.0026	-0.0013	0.1985	-0.0101	-0.0057	0.0058	-0.0014	0.1177	
InorgCh	3	-0.0005	-0.0002	0.1921	-0.1742	-0.0258	0.3900	-0.0013	0.1331	-0.0091	-0.0029	0.0002	-0.0011	-0.0031	0.4970	
JACS	4	0.0062	0.0063	0.1580	-0.1142	-0.0408	-0.0411	0.2806	0.0797	0.1121	-0.0039	0.0000	0.1458	0.0758	0.6645	
JChemPh	5	0.0630	0.0315	0.0398	0.0287	-0.2148	0.0142	0.0130	0.0147	0.1952	-0.0039	-0.0153	0.0097	0.0005	0.1763	
JChemSc	6	0.0008	-0.0024	-0.0028	-0.1238	-0.0112	1.8637	-0.0056	0.1642	-0.0049	0.0001	-0.0003	-0.0023	-0.0009	1.8745	
JOrgChem	7	0.0004	0.0000	0.0126	-0.2183	-0.0038	-0.0304	0.1927	0.0450	-0.0056	0.0004	0.0002	0.1778	0.0282	0.1992	
JOrgmetC	8	0.0004	0.0151	-0.0285	-0.1189	-0.0063	0.0870	-0.0065	0.2857	-0.0020	0.0006	0.0003	0.0033	-0.0269	0.2034	
JPhChUS	9	-0.0014	-0.0170	0.0809	-0.0829	-0.1609	0.0096	0.0444	0.0192	0.3668	-0.0119	-0.0056	0.0047	0.0040	0.2500	
MolPhys	10	0.0919	0.0391	0.0528	0.0383	-0.1589	-0.0005	-0.0005	-0.0005	0.1585	-0.0338	-0.0236	0.0199	-0.0007	0.1820	
PhysRevA	11	0.0282	0.0164	-0.0001	-0.0003	-0.0207	0.0001	0.0001	0.0001	0.0558	0.0186	-0.0577	0.0002	-0.0001	0.0406	
Tetrahe	12	0.0102	0.0019	0.0263	-0.1786	-0.0073	-0.0334	0.0617	0.0519	0.0144	-0.0017	0.0012	0.2501	-0.0451	0.1515	
TrahLt	13	0.0000	0.0071	0.0117	-0.1761	-0.0015	-0.0206	0.0711	0.0684	0.0005	0.0003	0.0000	0.2190	-0.0122	0.1677	
Self-Information Column		0.4208	0.1812	0.5707	-1.1555	-1.0047	2.2389	0.6531	0.8611	1.2579	-0.0705	-0.1163	0.8314	0.0190	**4.6872**	I_{MATRIX}
		C I T E D : C I T I N G													$\uparrow I_{MATRIX}$	

NOTE: Sky blue cells indicate noise cells of data matrix with cross probability error equal to 0.3307. More balanced ΣΔIs ≤ 0 in data matrix and Imatrix ≥ 0.

Table 27

Expected Information Contents for 1984 Journal-Journal Citation Data Matrix Computed From Synchronized Noise Error Optimization Process

Results for Static Analysis: Original Data Matrix (1984) Aggregated Journal - Journal Citations Among 13 Major Chemistry Journals

CITED (j)	Seq. Number	CITING (i): Joint Entropies, H(i, j)													Column Total H(i, j)	INFORMATION ENTROPY DATA
Var. Name		1	2	3	4	5	6	7	8	9	10	11	12	13		
ChemPhys	1	0.0457	0.0356	0.0037	0.0116	0.0513	0.0003	0.0006	0.0005	0.0245	0.0091	0.0052	0.0004	0.0006	0.1890	
ChemPhLt	2	0.0449	0.0915	0.0125	0.0391	0.1037	0.0024	0.0030	0.0005	0.0691	0.0187	0.0147	0.0039	0.0006	0.4045	
InorgCh	3	0.0027	0.0099	0.1684	0.0772	0.0089	0.0550	0.0074	0.0545	0.0181	0.0012	0.0005	0.0022	0.0023	0.4082	
JACS	4	0.0193	0.0500	0.1550	0.3291	0.0530	0.0540	0.1985	0.0933	0.1151	0.0082	0.0007	0.1099	0.1268	1.3130	
JChemPh	5	0.1013	0.1492	0.0353	0.0872	0.3236	0.0104	0.0099	0.0102	0.1623	0.0664	0.0512	0.0077	0.0024	1.0171	
JChemSc	6	0.0004	0.0003	0.0443	0.0242	0.0011	0.0619	0.0022	0.0398	0.0038	0.0004	0.0006	0.0004	0.0021	0.1815	
JOrgChem	7	0.0006	0.0023	0.0099	0.0879	0.0013	0.0044	0.1584	0.0256	0.0052	0.0006	0.0007	0.0677	0.0877	0.4524	
JOrgmetC	8	0.0005	0.0025	0.0352	0.0447	0.0012	0.0323	0.0175	0.1286	0.0005	0.0005	0.0006	0.0071	0.0128	0.2839	
JPhChUS	9	0.0151	0.0404	0.0268	0.0538	0.0651	0.0060	0.0117	0.0034	0.1420	0.0080	0.0031	0.0037	0.0041	0.3832	
MolPhys	10	0.0186	0.0243	0.0058	0.0132	0.0534	0.0005	0.0005	0.0004	0.0216	0.0493	0.0075	0.0021	0.0004	0.1975	
PhysRevA	11	0.0102	0.0185	0.0005	0.0006	0.0505	0.0008	0.0008	0.0007	0.0106	0.0113	0.1339	0.0006	0.0007	0.2397	
Tetrahe	12	0.0011	0.0023	0.0036	0.0399	0.0010	0.0019	0.0422	0.0085	0.0036	0.0003	0.0005	0.0389	0.0356	0.1795	
TrahLt	13	0.0006	0.0025	0.0058	0.0773	0.0013	0.0028	0.1033	0.0284	0.0044	0.0006	0.0007	0.0742	0.1189	0.4208	
Column Total H(i, j)		0.2610	0.4294	0.5068	0.8858	0.7154	0.2329	0.5559	0.3944	0.5809	0.1744	0.2199	0.3188	0.3949	**5.6704**	◄ **H(citing, cited)**
Marginal Entropy (column)		0.1761	0.2640	0.3084	0.4462	0.4154	0.1570	0.3409	0.2468	0.3348	0.1244	0.1717	0.2123	0.2592	**3.4574**	◄ **H(citing)**
Marginal Entropy (row)		0.1291	0.2451	0.2633	0.4768	0.4768	0.1298	0.2828	0.1949	0.2402	0.1324	0.1791	0.1236	0.2636	**3.1374**	◄ **H(cited)**
H (citing|cited)		**2.5330**			**H (cited|citing)**			**2.2130**			**T (citing|cited)**				**0.9244**	◄ **H(citing | cited)**

NOTE: Each red number represents a normalized non-noise missing data. It is based on an average determination using corresponding row and column estimated cell values associated with each blank cell's corresponding row and column.

Proving Non-Universality of Zero Factor Based-Rules

Random variable distributions are statistical distributions whose curves generally according to central limit theorem approach normal distribution. Consequently, so is the distribution of ΔIs or the sum of two ΔIs for row an column for each element k of a square matrix which is asserted to be larger than or equal to zero always (Leydesdorff, 1991, pp. 312).

Generally, in a quadratic equation there are two basic ways of finding the solution(s) to an equation namely factorization method and completing the square method. For example, a quadratic equation $ax^2 + bx + c = 0$ can be expressed as a product $(px + q)(gx + h) = 0$. This way, the zero factor property implies that the quadratic equation is satisfied if $px + q = 0$ or $gx + h = 0$. Thus, the roots of the quadratic equation is given by the solution of the above two linear equations. On the other hand, the use of completing the square method on a quadratic equation leads to the derivation of the quadratic formula

$$x = \frac{-\mathrm{b} \pm \sqrt{\mathrm{b}^2 - 4\mathrm{ac}}}{2\mathrm{a}}$$

which can be used for the determination of solutions to the roots of a quadratic equation (Rich & Schmidt, 2004). While the method involving factorization of equation reliably depends on only

rational roots of the equation, that of the method of completing the square is reliably dependent on rational, irrational and complex roots. Also, the method of completing the square necessitates the verification of solutions since not all of its solutions are necessarily true. In general, the quadratic equation can be expressed as a factor involving the quadratic formula given a quadratic equation $ax^2 + bx + c = 0$ as follows

$$ax^2+bx+c=a\left(x - \frac{-b+\sqrt{b^2-4ac}}{2a}\right)\left(x - \frac{-b-\sqrt{b^2-4ac}}{2a}\right)$$

This implies that in general depending on the distribution of variables, there can be undesired solutions or noise to the equation of the distribution due to the equivalence of the factorability of quadratic formula to the basic factors. Therefore the assertion that

$$\Delta I_{row} + \Delta I_{column} \geq 0$$

cannot be entirely true for every random situation. By definition, if X is a set and Σ a σ-algebra over X, then the function μ from Σ to an extended real number line becomes a measure on the basis that

1. **Non-Negativity:** For all E in Σ the measure of E is equal to or greater than zero. That is

$$\forall\, E \in \sum : \mu(E) \geq 0$$

2. **Null Empty Set:** The measure of an empty set $\mu(\emptyset)$ is equal to zero.
3. **Countable Additivity:** The measure of the union of all countably disjoint sets of E is equal to the sum of all measures of each subset. That is, with at least one finite measure of set E

$$\mu\left(\bigcup_{i \in N} E_i\right) = \sum_{i \in N} \mu(E_i)$$

This implies the null set is a measure of zero since $\mu(E) = \mu(E \cup \emptyset) = \mu(E) + \mu(\emptyset)$ and therefore $\mu(\emptyset) = \mu(E) - \mu(E) = 0$.

Let the measure (systematic assignment of numbers to suitable subsets) on the set of rational roots solutions from factorization method and that for the set of rational, irrational and complex roots solutions from quadratic formula be given by μ. Then let X_F and X_Q respectively represent measurable sets (see figure 43) of the solutions to the roots of quadratic equation obtained via factorization and quadratic formula and also let φ be the set representing the non-solution set of the quadratic equation. Again, let the pairs of field of sets (X_F, Σ), (XQ, Σ) and (φ, Σ) be the two respective measurable spaces of the solutions to the roots of quadratic equations and the non-solution space of the quadratic equation given that Σ is a σ-algebra over X_F and X_Q. The σ-algebra is a collection of subsets

of a set closed (operations on members of set yields a member of the same set) under countably infinite set operations.

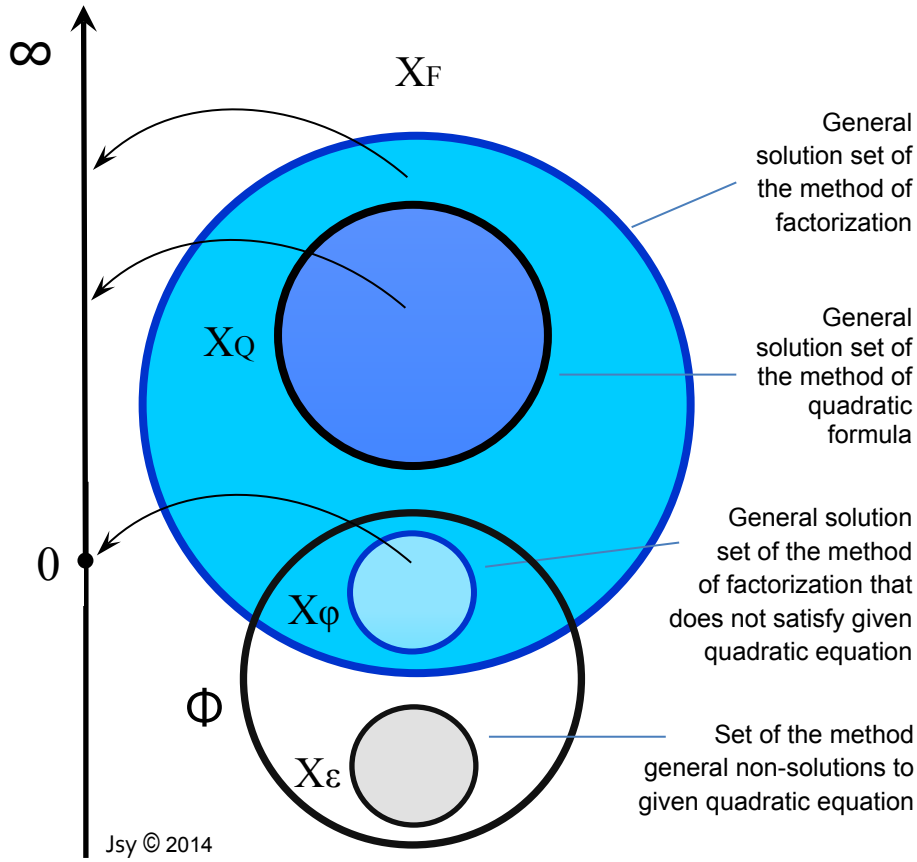

Figure 43. A representation showing the monotone property of measure based on solution sets of the roots of a quadratic equation under factorization and quadratic formula.

The set of root solutions X_φ from X_Q which do not satisfy given quadratic equation intersects with the non-solution set φ and forms a negligible set φ (see figure 43). The measure of X_φ in terms of satisfying the roots of the quadratic equation is zero and is expressed mathematically as $\mu(X_\varphi) = 0$. Let the complement of X_φ be the negligible set X_ε. Then X_ε represents all

the members of the non-solution set of the quadratic equation. However in terms of satisfying the roots of the quadratic equation, X_ε is not measurable. As such, $\mu(X_\varepsilon) \neq 0 = \epsilon$ where means or represents nothing. Alternatively if $\mu(X_\varphi)$ is denoted as equal to +0 (positive zero) then $\mu(X_\varepsilon)$ can be denoted as -0 (negative zero) since they are compliment of each other. Then, by the countably additivity (σ-additivity) property, it can be expressed that

$$\mu(\emptyset) = \mu(X_\phi \cup X_\varepsilon) = \mu(X_\phi) + \mu(X_\varepsilon) = 0 + \epsilon = (+0) + (-0) = 0.$$

This result implies that the null set φ automatically has measure zero (neutral) within the measurable space (φ, Σ). Since by definition every measurable negligible set is automatically a null set, the negligible set X_φ is therefore automatically a null set. Contrary to this, the negligible set X_ε by definition, need not be measurable and is not measurable relative to a satisfactory quadratic equation roots solution as the unit of measure. In support of the fact that by definition: a measure is called complete if every negligible set is measurable, the null set φ is therefore not complete. Consequently, the set φ is incomplete since it intersects the set X_Q. However, the set X_F is complete since it is disjointed with the null set φ. By definition, to extend the measure of the set X_F to the complete measure of the null set φ, the consideration of the σ-algebra of subsets X_F which differ in terms of a satisfactory quadratic

equation roots solution by a negligible set X_φ from a measurable set X_Q must be invoked. Thus, by definition, the symmetric difference (union of sets without the intersection) of the set X_Q and subsets X_F must be contained in a null set which is φ. This can be expressed as

$$X_Q \vartriangle X_F = X_Q \oplus X_F = X_Q \ominus X_F = \emptyset$$

Therefore from the mathematical analysis, it can be conclusively stated that within the measure space (X_Q, Σ, μ), the completeness of $\mu(X_F)$ is equal to that of $\mu(X_Q)$. From the general equality between the factors from factorization method and the factors involving the quadratic formula given a quadratic equation viewpoint, it therefore means that while there is equivalence between both methods of determining the root solutions of quadratic equations, there exists no equivalence between them in terms of completeness. As a result, no generalization can be made on the equivalence between both methods of finding root solutions to quadratic equations. In effect, by the **principle of non-universality of zero factor property-based statements or rules**:

> Assertions made based on implication(s) from the zero factor property are not true for all the instances of the situation or all the time and as such cannot be generalized.

It must be observed that in terms of a probability space, the $P(\mu(X_Q)) = P(\mu(X_F)) = 1$ and $P(\mu(X_\varphi)) = 0$ but $P(\mu(X_\varepsilon))$is undefined. Q.E.D.

Information Transmission Principle for
Differential Equation Analysis

As a principle, the transmission entropy which is equal to the amount of information sent (negative kinetic entropy) and the information received and the constant potential entropy (net positive potential entropy) plus the information error (noise entropy) in transmitting or sending must be equal to zero if entropy of information exchange is conserved.

Using respective values of information entropies attributed to the journal-journal case stud

y: $H_{EK} = 4.6872$, $H_0 = 2.5330$, $T(citing, cited) = 0.9244$ and $H_\eta = 0.1819$, the following is calculated.

$$E\psi = -4.6872\psi + (2.5330 + 0.9244)\psi + 0.1819\psi$$

$$= -4.6872\psi + 3.6393\psi$$

which gives

$$E\psi = -1.0479\psi$$

Note that the wave function ψ measures the quantum-mechanical entropy of information transfer. Thus, based on the following atomic units: $h/2\pi = m_e = e = 1$, it can be reasonably inferred from the result for Eψ that the implication of the above principle is that: if the absolute total entropy E of information exchange in a network system is less than or greater than zero then the information undergoes a net effective exchange else it

is holistically non-effective. On the other hand, if the absolute total entropy E is equal to zero, the implication is that the information exchange in the network system is non-existent. Thus, in general, if the net energy of any activity or object is absolutely zero, then it does not exist. Under stationary states (eigenlevels or characteristics levels) n, the probability density $|\psi(x)|^2$ is not time dependent and so represents states of definite total energy. Using the initial message wave function $\psi(x)$, the dynamics of the message event is derived by solving the informatics wave equation for when E = 0 and when E > 0 given the atomic units substitutions:

$$\hbar = h/2\pi = m_e = e = 1$$

For a valid statistical interpretation, the wave function must be normalized. This according to Born's statistical interpretation of wave function occurs when the probability of finding a **messaging waveform** within the entire network system equal to 1. By definition, a normalized wave function occurs when

$$\int_{-\infty}^{\infty} |\psi(x,t)|^2 dx = 1$$

This situation is shown in F of figure 44. In the absence of normalization, the axis of the messaging wave function $\psi(x)$ is substituted by a potential energy V(x) or PE(x) axis when the m is positive and a kinetic energy KE(x) axis when m is negative.

CHAPTER 15

LANGUAGE ANALYSIS OF THOUGHT PROCESS

The erstwhile analysis dealt with the functions of intelligence (prior knowledge), imagination (strategic and tactical planning/coordination) and creativity (engine for acquired new knowledge). However, without a language function (a basic brain characteristic), the other 3 basic brain features would be functionally incapacitated and no thought process would take place. The fundamental importance of language in human thought process as a basic communication framework in any information exchange system will be analyzed through IWEA.

Results of Graphical Analysis of Journal-Journal Case Study Using IWEA

Using time-dependent informatics wave equation quantified earlier on, the conveyance of a single message along a communication link of length x from a sender (at point *a*) to a receiver (at point *b*) can be expressed as

$$i\hbar\frac{\partial}{\partial t}\psi(X,t) = -\frac{\hbar^2}{2I_m}\nabla^2\psi(X,t) + [H_0 + T(a,b)]\psi(X,t) + H\eta\,\psi(X,t)$$

Alternatively

$$\boxed{i\hbar\frac{\partial}{\partial t}\psi(\boldsymbol{r},t) = -\frac{\hbar^2}{2I_m}\nabla^2\psi(\boldsymbol{r},t) + [H_0 + T(x,y)]\psi(\boldsymbol{r},t) + H\eta\,\psi(\boldsymbol{r},t)}$$

or

$$\boxed{i\hbar\frac{\partial}{\partial t}\psi(\boldsymbol{r},t) = -H_{EK}(x,y)\psi(\boldsymbol{r},t) + [H_0 + T(x,y)]\psi(\boldsymbol{r},t) + H\eta\,\psi(\boldsymbol{r},t)}$$

where r is the distance between the source and the destination nodes and t the time. For multiple messages in three dimensions, the inputs of ψ relating the time-dependent informatics wave equation will be equal to $(r_1, r_2, \cdots r_N, t)$. As done in the analysis of Schrodinger equation, in IWEA the atomic units: $h/2\pi = m_e = e = 1$ are used.

With the following input parameters derived from the journal-journal case study earlier on,

Integration limits: x max = 5.

Effective Mass: μ = 1. (natural system of units)

Gained kinetic entropy: $H_{EK} = 4.6872.$

Information noise error entropy: $H_\eta = 0.1819.$

Constant potential entropy: $H_0 = 2.5330.$

Transmission entropy: $T(citing, cited) = 0.9244.$

and using Maple 18 software (from Maplesoft) to numerically solve informatics wave equation thereof, graphical outputs depicting messaging space dubbed **messaging phase space** in which all possible states of a messaging system are present are generated as shown (selected few) in figures 43 and 44.

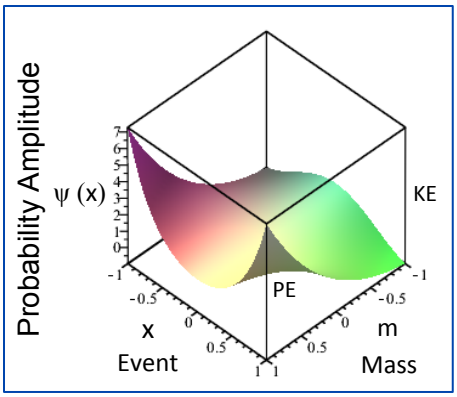

A. Message Orbitals' KE, PE and probability amplitude at m = ±1.

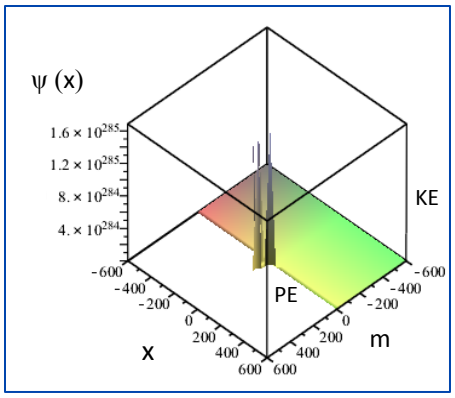

B. Entangled Message pair (potential spikes) at m = ± 600.

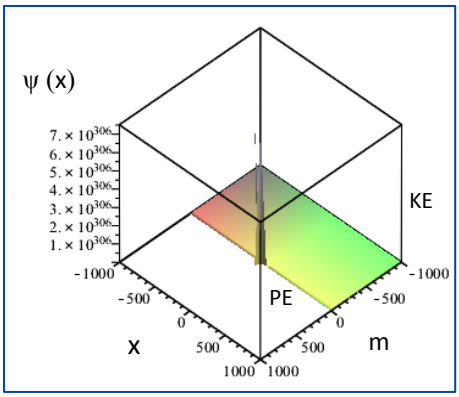

C. Message Superposition (PE spike interference) at m = ±1000.

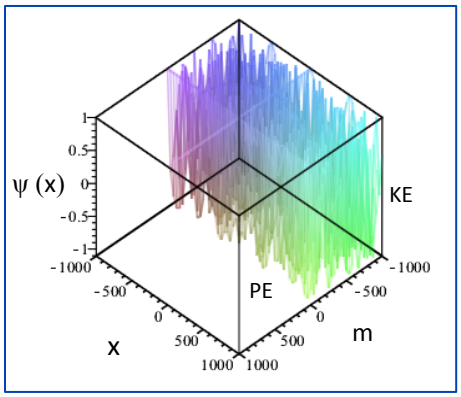

D. Harmonic Messaging oscillations (normalization) at m = ±1003.

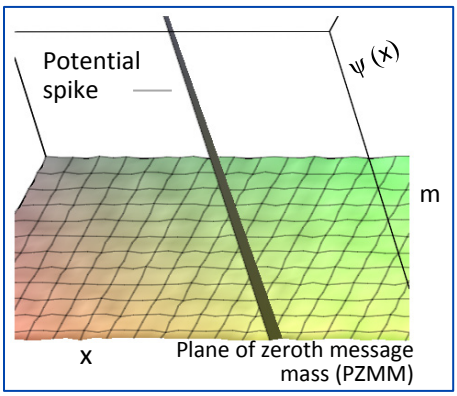

E. Surface Ripples of messaging event horizon at m = ±10 E16.

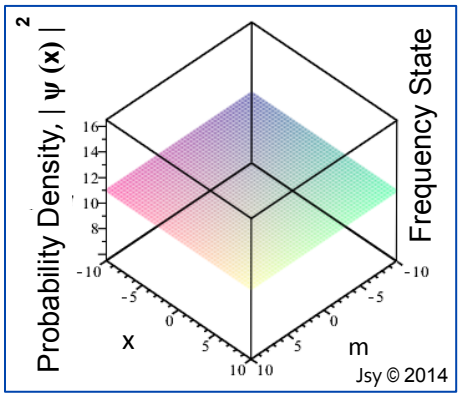

F. Frequency State of messaging network system at m ≥ ±1.

Figure 44. Message phase spaces based on 1984 journal-journal citation data (13 random-selected major chemistry journals).

THERMOGRAMS

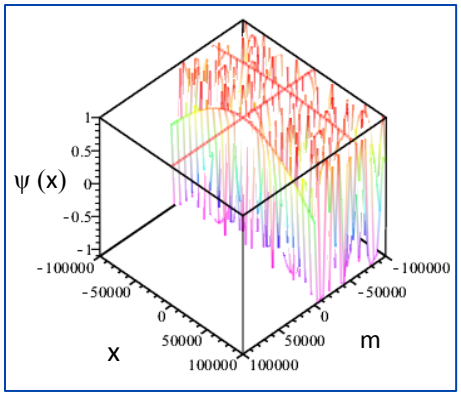

A1. Message Phase TGM at m = ± 100K + 1.

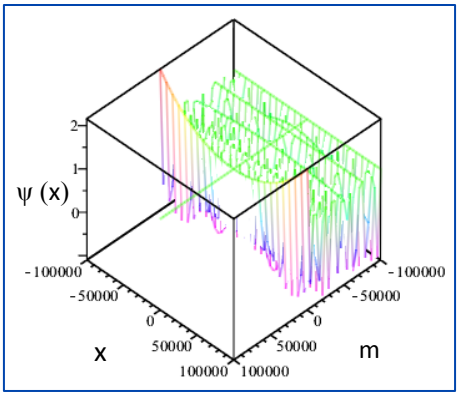

B1. Message Phase TGM at m = ± 100K + 9.

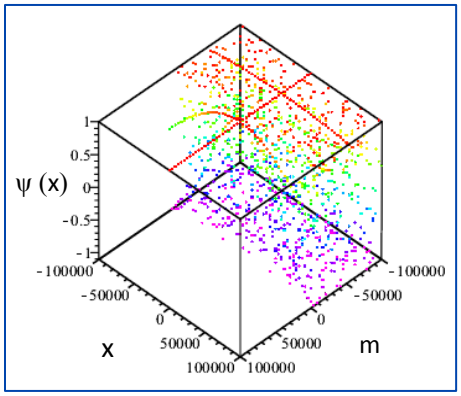

A2. Passive Message Phase TGM at m = ±100K+1 (Red Elv Prob:1).

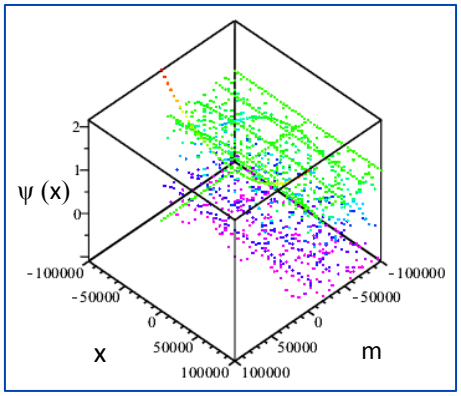

B2. Passive Message Phase TGM at m = ±100K+9 (Green Elv Prob:0.5).

CHROMATOGRAMS

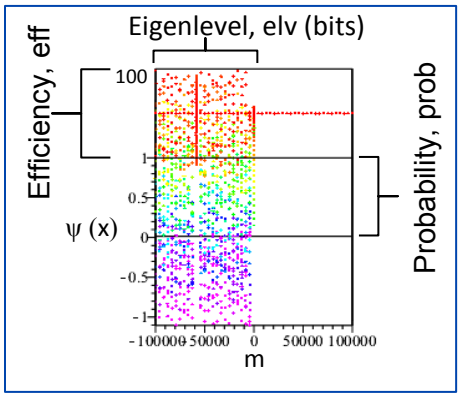

A3. Message Phase CGM at m = ±100K+1: 60Kb elv: approx. 100% eff.

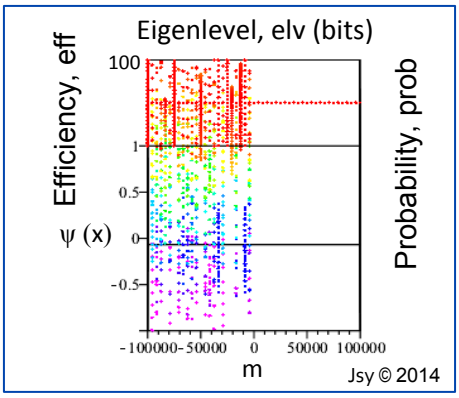

B3. Message Phase CGM at m = ±100K+9: 100, 80, ∂ 50, 10Kb elv: 100, 100, 85 and 98% eff.

Figure 45. Message phase spaces showing thermograms (TGM) and chromatograms (CGM) simulations based on 1984 journal-journal citation data (13 random-selected major chemistry journals).

A complex entropic information network is generated by the information interchanges within a messaging system. The information entropy provides an entropic framework for achieving holistic analysis of a complex network system's messaging or communication. The informatics wave analysis equation (IWAE), as a quantum mechanically modelling information wavefunction equation, is efficient in determining underlying structures that give rise to consistent and replicable patterns. Thus, IWAE processes data derived from a network into visual information with characteristic structures and properties that can be analyzed for the system's operational efficiency or effectiveness level(s) in terms of probabilities for system optimization. The quantum analysis eigen-processes involved render two eigen-distributions. These are

1. **Eigen-Thermography**: This process illustrates probable energy patterns in a complex system in the form of a **thermogram** as shown in A1, A2, B1 and B2 of figure 45.
2. **Eigen-Chromatography**: This process isolates characteristics of a complex system via sizes of messaging events and their corresponding probabilities in its **chromatogram** output as shown in A3 and B3 of figure 45.

They provide fuller description of messaging via message wavefunctions of existing information entropy of analyzed system. Message entanglement results due to uncertain (entropy)

messaging. As an arrow of time, it becomes the arrow of increasing correlations or perfecting associations which leads to perfect coincidence of message pair or two entangled potential spikes (see B and C of figure 44) dubbed **message coincidence correlation**. Eventually through measurement(s) via data collection by the outside world of the messaging system, **message decoherence** occurs. The destruction of perfectly correlated quantum states of the pair of potential spikes that ensues eventually leads to information transfer in the form of normalized and harmonized oscillations as shown in D of figure 44. As depicted in A3 and B3 of figure 45, the **messaging line spectra** in messaging systems represent stationary energy states or levels of message eigenstates within messaging wave function distribution.

Formalism of IWEA Interpretation

The complete behavioral simulation of a networks system's messaging activities, such as the simulation graphs depicting differential analysis of journal-journal case study, the variable x represents **message event** or message orbital/eigenstate. When x is in an unknown or unpredictable state, it represents information (new knowledge). But when it is in a predictable (known) state, it represents no information (old knowledge). The variable m along the horizontal y-axis of the graphs represents the information or **message mass**. It generally identifies the number of characters or symbols in a message event x.

The messaging wave function distribution, is the distribution of a message (event) variable x which is transmitted with possible values given by x_1, x_2,..., x_n from a source node A in a network (equivalent to the distance r between source and destination nodes). In the analysis of a general messaging system, the target objective is to determine its wave function $\psi(x)$ which signifies existing unpredictability (Shannon entropy) of measuring a message at a position (state) x, say source node, in a given time t. Alternatively, the wave function represents the probability amplitude of the eigenstate of a message. On the other hand, the message probability density $\psi(x)^2$ of a messaging distribution is the probability that a message event x lies between points *a* and *b* in a messaging space-time which defines a discrete probability distribution on the message event. Thus, the discrete probability amplitude defines the probability of being in a message state x as a fundamental frequency in the probability frequency domain. The phase space plots of $|\psi(x)|^2$ in F of figure 44 has an invariant value of 11 which represents the fundamental frequency of messaging states. In the messaging analysis by Leydesdorff, the cut-off level of 5 printed editions of the Journal Citation Reports (source of data) was used to substitute missing values (Leydesdorff, 1991, p. 6). However, from optimization processes in table 23 and table 24, by counting the most frequent updated missing data one gets 11 (from updated value of 7) and 10 (from updated value of 5) respectively. This reasonably shows that both missing data estimation and its

normalized version (tables G and H) are basically in agreement with the fundamental frequency of 11 from the phase space analysis using IWAE.

While positive values of m exclusively have potential energies, negative values of m rather have exclusive kinetic energies as shown in figure 44. This scenario is reminiscent to the respective energy of a relatively stationary nucleus and that of its dynamic electron(s) in an atom. When x and m are consistently increased, the messaging wave function approaches normalization. At normalization (as shown in D of figure 44, the wave function lies between ±1 and a messaging wave packet consisting of characteristic message or **eigenmessage waveforms** with messaging phase energy occurs when m is exclusively negative. The eigenmessage waveforms are borne out of the localization of the summation of all the kinetically energized sinusoids of the network system's messaging via messaging

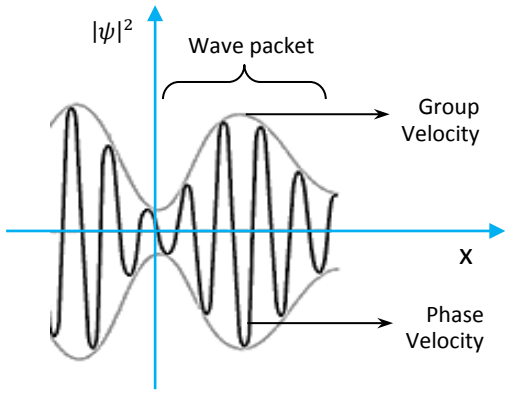

Figure 46. A wave packet of modulated messaging "carrier" waves in a messaging network system.

interference pattern. Alternatively, it can be described as a messaging "carrier" waves enclosed or "envelope" by the modulating effect of the messaging network system as illustrated in figure 46. The statistical information about transformation of messaging event's potential energy (PE) to kinetic energy (KE) under energy conservation can be shown to be equivalent to the scenario in quantum mechanics where the same possible results of a first and a quick second measurement of a particle's position is done. According to quantum mechanics, the conserved measurements that result is due to the "collapse" of wavefunction of the particle caused by the first measurement which in turn caused the formation of a probability spike at the particle's position (see figure 47) where it was quickly measured by the second measurement.

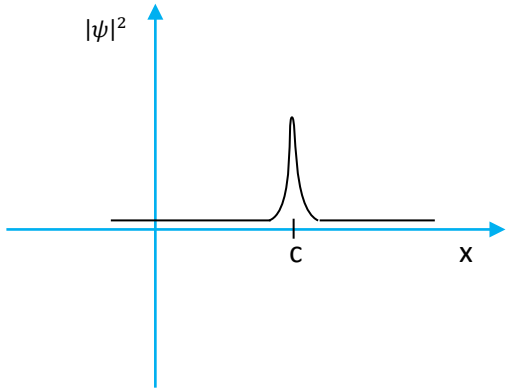

Figure 47. Probability distribution of a particle's position C after measurement (from a first and quick second).

In accordance with Schrodinger equation, the formation of probability spike is followed by the spreading of the wavefunction (see figure 47). The spreading of wavefunction is consistent with messaging activities in a network system as shown in C and E figure 44 where the dispersion of message events occurs in the formation of message waveform. The superposition of potential spikes enables message transfer (quantum teleportation) via quantum computations to be carried out by nodes in a messaging system. Message entanglement occurs via physical interaction between two entangled emergent potential spikes considered as a whole in a common quantum state (see C of figure 44) and derived from the split of an emergent potential spike (see B of figure 44). The outlining principle of **data-information driven message transmission (DIDMT)** to be used to comprehensively classify a network system on the basis of data erasure and information erasure, is as follows. During message transmission from sender to receiver:

1. Data erasure occurs when there is a change in the data of the received message. This constitutes a noise error in the transmitted message.
2. Information erasure occurs when there is no change in the information of the received message. This constitutes a recurrent error in the transmitted message.

Generally, noise error creates imprecise data messaging while recurrent error creates redundant information messaging. In

principle, both imprecise data and redundant information messaging are technically equivalent to a non-informative transmission of a message.

By definition, raw facts are data which when processed into meaning form become information. Information should bring forth meaning, understanding, knowledge, revealed pattern, entropy (a measure of unpredictability) and communication among many others when it is not predictable. In mainstream information theory, the idea of information is however perceived as the message while its transmission is seen as the content of a message (Floridi, 2010). Both data and information have contents (data and processed data). Therefore, if information is perceived as message and its transmission as content of a message (processed data via encryption and decryption) so should data be seen as message and its transmission as content of a message (data). Also, information is alternatively regarded as sequentially derived symbols from an alphabet such as inputted at source and destination of a communication link. Thus, information processing is perceived to consist of an input source sequence of symbols functionally mapped unto an output destination sequence of symbols (Wicker & Kim, 2003). If the technical notion of information as data processed into a meaningful form should be strictly upheld, then the label 'information processing' is a wrong name for a real process.

In reality, a company's advertisement represents sender's seed in the form of a source message. When transmitted to

recipients (as seed growth), further dissemination of the advertisement in the form of perpetuated message (seed dispersal) can occur as a result of interest borne out of a meaningful processing of the source message into information (harvested fruit). This causes a chain reaction of emergent information transmissions in a networking manner. The measurement of the amount of sprawling emergent information attained by said advertisement is one of the fundamental descriptions that can be derived from a network system using IWEA. In general, a network system of emergent information is generated as sprawling destination messaging (citing | cited) out of a source data messaging (cited | citing). Invariably, both non-informative message and informative message transmissions form the standard indices for measuring message transmission of any network system due to the universal role of problem-solution cycle as a means of providing solution. In a referenced-oriented application of DIDMT to the journal-to-journal case study, it is incumbent for one to ascertain the bottom-line effect of the usage of existing references (cited) as quotations in newly research papers (citing) which is conditioned as citing | cited and/or new research papers (citing) having references (cited) as a condition of cited | citing on the network system. On the other hand, in a system of advertising network, a referred advertisement (cited) by referrers who have become potential purchasing-oriented people (citing) as a condition of citing | cited and/or targeting people (citing) as referees to whom a

referable advertisement (cited) is issued as a condition of cited | citing. Due to the commonality of creativity and intelligence as captured in **intelli-creativity cumulative constant (ICCC)** which generally forms 10% of a standard normal distribution (see the common point CI of creativity and intelligence in figure 17), the limit of an **intelli-creative crossover probability error** P_{ICCC} that should cause data erasure as a result of combined creativity and intelligence activities must be one-tenth of the limits of the crossover probability error $0 \leq p \leq 0.5$. This results in an intelligence-creative crossover probability error range of $0 \leq P_{ICCC} \leq 0.05$. Note that 0.05 is the normal level of significance used in statistical analysis.

From the respective redundancy measures R (an indicator for random variable independence such as cited and citing) determined earlier on for both estimation methods namely the cut-off level adjustment method (COAM) and the synchronized noise error optimization process (SNEOP), the limits of crossover probability error can be monitored. In principle, a zero redundancy measure is equivalent to a condition of data erasure where the involved variables (cited and citing for example) are independent and/or have no information flow existing between them as a result of duplication of information. The difference between the values of R (see table 20) for both COAM (conventional analysis) and SNEOP (proposed efficient analysis) is given by 0.1454 - 0.1402 which results in a redundancy differential equal to 0.005. In one decimal place, it is equal to 0. By lying within the range of

crossover probability error, the interaction of cited and citing variables not only experienced data erasure which renders them independent but also no information flow exists between them. Rather than using the conventional COAM, the better accuracy-driven IWEA comparatively lowers computed values of analyzed information interchanges within a general network system. As such, the cited predictability differential indicates that the IWEA approach gives an accurate measure than that of COAM without any loss of information. On the other hand, the citing predictability differential indicates that though IWEA approach gives an accurate measure than that of COAM, it does so with a degree of information (new knowledge) loss.

From informatics wave analysis plots in figure 48, the number of message units ΔX (shown in red braces) that span along the **constant information-theoretic (CIT)** joint entropy (via Liouville's theorem) in spacetime is given by twice the ratio ΔX:X. The reason is that twice ΔX is always equal to the total message unit X. Thus, the message ratio can be expressed as

$$2\left(\frac{\Delta x}{x}\right) = 1\ amu$$

The message ratio is invariantly equal to 1 atomic message unit (amu). Thus, in general, the continuum of any messaging event(s) is tailed by a **constant message span (CMS)** of 1 atomic message unit. To express CMS in terms of predictable units of joint

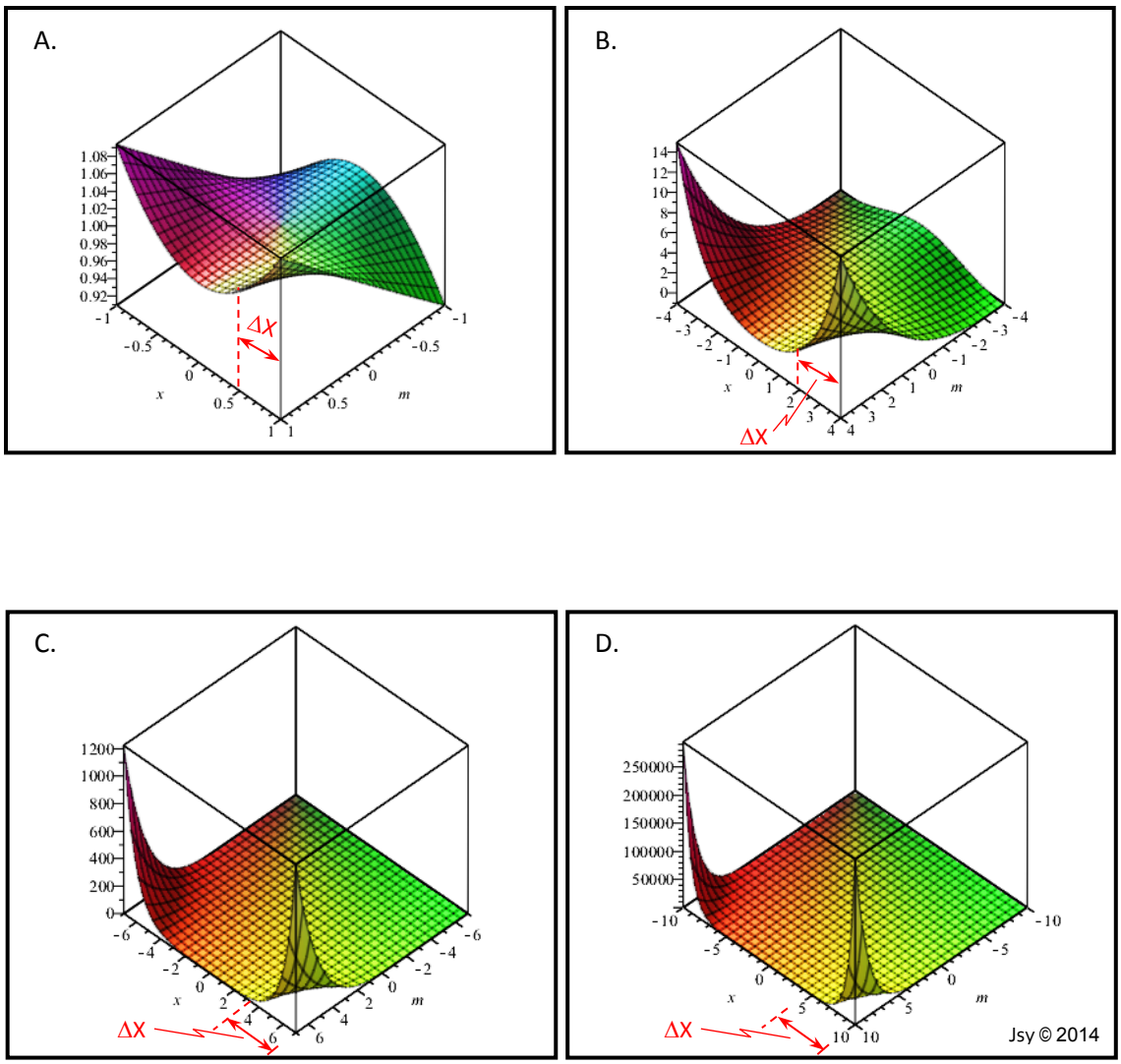

Figure 48. Plots of IWEA for journal-journal case study showing probability spikes: A. m = x = ±1, B. m = x = ±5, C. m = x = ±7 and D. m = x = ±10.

intelligence-creativity of problem-solution cycle, it must be multiply by the units of ICCC in the error range of crossover probability. By virtue of the fundamental basis of problem-solution cycle (PSC), the IWEA's creative phase is its sole

differential when compared to COAM. The joint action of intelligence and creativity in PSC is pivotal to emergent solution phase which predictably provides new knowledge or information. Consequently, the crossover probability error which measures units of noise error during messaging must be calibrated to measure units of **recurrent error** (due to lack of emergent information) as a result of the predictable nature of the solution path. By definition, the **standard index of recurrent error (SIRE)** is quantified as

$$SIRE = \frac{Crossover\ Probability\ Error}{Intelli\_Creative\ Cumulative\ Constant} = \frac{0.5 \times 100}{10} = 5$$

As a result, the invariant message predictability that span along the CIT joint entropy for any messaging event, is therefore quantified as

$$\begin{matrix} Constant\ Message \\ Predictability \end{matrix} = \begin{matrix} Constant\ Message \\ Span \end{matrix} \times SIRE = 1 \times 5 = 5$$

By definition, the ratio of the transmission entropy between two transmission variables (cited and citing) to the constant message predictability is equal to the predictable information (cited given citing or vice versa) whose standard recurrent error corresponds to its span of data erasure. This can be expressed as

$$\begin{matrix} Message \\ Predictability\ Index \end{matrix} = \frac{T(citing, cited)}{Constant\ Message\ Predictability} = \frac{0.9244}{5} = 0.1849 = 18.49\%$$

The difference between predictable cited patterns under COAM given by U(cited | citing) and IWEA respectively is 30.4% -

18.49% which results in a cited or **sender predictability differential** equal to 11.91% or 0.12. The cited, for example, a reference or storage location such as a database technically represents intelligence which by expectation does not constitute new information since it is already known and so invokes data erasure. By comparison, the cited predictability differential computed above is found to lie within the limits of the crossover probability error. This implies that the predictable cited patterns acting as information sender does indeed undergo data erasure and so represents no effective information change. Similarly, the difference between predictable citing patterns under COAM given by U(citing | cited) and IWEA is respectively 27.9% - 18.49% which results in a citing or **receiver predictability differential** equal to 9.41% or 0.09. The citing, for example a research paper in a journal or search engine, in this scenario represents a phase interaction of creativity and intelligence. While the cited represents an intelligence phase, the citing technically represents creativity phase whose derived information is new. Thus, the computed citing predictability differential must be compared with the intelli-creative crossover probability error. Subsequent comparison shows that the computed citing predictability differential lies outside the limits of the intelli-creative crossover probability error. Hence, the change in predictable citing patterns acting as information receiver does not experience any data erasure and so represents an effective information change.

Big Data and Differential Modeling of Brain Network

The human brain filters enormous volumes of data (equivalently big data scenario) it receives via good algorithms without accessing all. This enables it to use only a millionth of the energy that powerful computers will use to achieve the same goal. Duplicating such algorithm to create better computers will require the understanding of how the brain works.

In order to ascertain how the complex human brain works as a system of neurons, a team of researchers led by Marianne Fyhn of University of Oslo (Fyhn et al., 2015) have opted to use differential equations (mathematical descriptions of changes over time) to model the its plasticity (ability to learn and store information) at multiple levels. These said levels which span how individual nerve cells interact via molecular activities (microscopic level) to its related effect on the entire network of brain cells (macroscopic level), will by linkage form a multiscale model. The multiscale model of the brain is divided into levels namely

1. Atomic level understanding of the brain.
2. Electrochemical machinery in a brain cell.
3. Simulation of a single nerve cell with branches.
4. Linkage between nerve cells and their communications via synapses.
5. Group activity of nerve cells.

To achieve said multiscale model, computational researchers have envisaged that the description of how each nerve cell propagates information in the network of brain neurons must be represented by a differential equation. This leads to approximately 100 billion of differential equations (maximum) that would need enormous computer power to solve. Furthermore, signals of individual brain cells can be noisy and imprecise. However, the existence of inter-neural cell recognition (verifiable via multiphoton imaging) leads to lower noise signal and inter-communication reliability (Smith et al., 2015). This necessitates the combination of thousands to millions of neurons in order to achieve a more accurate and effective neural communication. Invariably, the respective application of informatics wave equation fed by requisite meta-data derived from each of the above multiscale levels, easily leads to desired sub-models which can be combined to form said multiscale model of how the large complex network of neurons precisely work.

CHAPTER 16

INFORMATION AS THE BUILDING BLOCK OF THE PHYSICAL UNIVERSE

The fact that in an atom no two orbital electrons can have the same four electronic quantum numbers in accordance with Pauli Exclusion Principle (quantum mechanical principle), matter-energy is at least reasonably reduced to binary information consisting of up and down spin values. This insinuates an extricated fundamental purview of the physical universe wherein its fundamental paradigm is about information and information processing thereof making it a self-computer controlled physical system. According to the contention of Alan Guth (founder of inflationary theory) who sees information and matter-energy as almost identical fundamental building blocks of the physical universe, for information to be the ultimate constituent for the construction of the physical universe which acts essentially as a cosmic computer with reality as its perfect cosmic simulation, its pristine application should exhibit the attainment of all of the following fundamental objectives. In principle

1. It should be theoretically feasible to simulate whole worlds on future supercomputers using information.
2. There should be ways of using information to improve the Standard Model of fundamental physics – a theoretical

framework that describes interactions between elementary building blocks of matter (quarks and leptons) and the force carriers (bosons) of the physical universe.

3. It should confirm that space is not smooth and continuous but grid-like and discrete like information.
4. It should also confirm that the physical universe is like a hologram (3D projection from a 2D source).

As a consequence, confirmation of a simulated universe will transitively confirm reductionism (basic simplification of the complex). And so, phenomenon like consciousness is reduced to physics. The application of boundary condition in the analysis of the Halting Problem acknowledges the basis of ontological reductionism - the belief that the whole of reality comprises of minimal number of parts. To achieve scientific explanations via information as a basic building block (methodological reductionism), new theories are needed to reduce seemingly conflicting theories of the physical universe in terms of information (theory reductionism). Hence, through mechanistic explanations propelled by the derivation of mathematical proofs in concert with supporting empirical evidences, the needed verbatim translation of the visage of information as the building block of the physical universe is unveiled.

By invocation of existing fundamental similarity between networks of any kind and the basis of information as a mathematical description of a generalized communication system

(via informatics wave equation analysis IWEA), the aforementioned fundamental objectives are shown to be inexorably attestable through analysis of information.

CHAPTER 17

SEMANTIC PROCESSING AND ITS SOLE HUMAN AGENT

The lack of semantic processing involves a process that lacks the logic relating the conditions in which a system or theory can be said to be true. Thus, the semantic processing

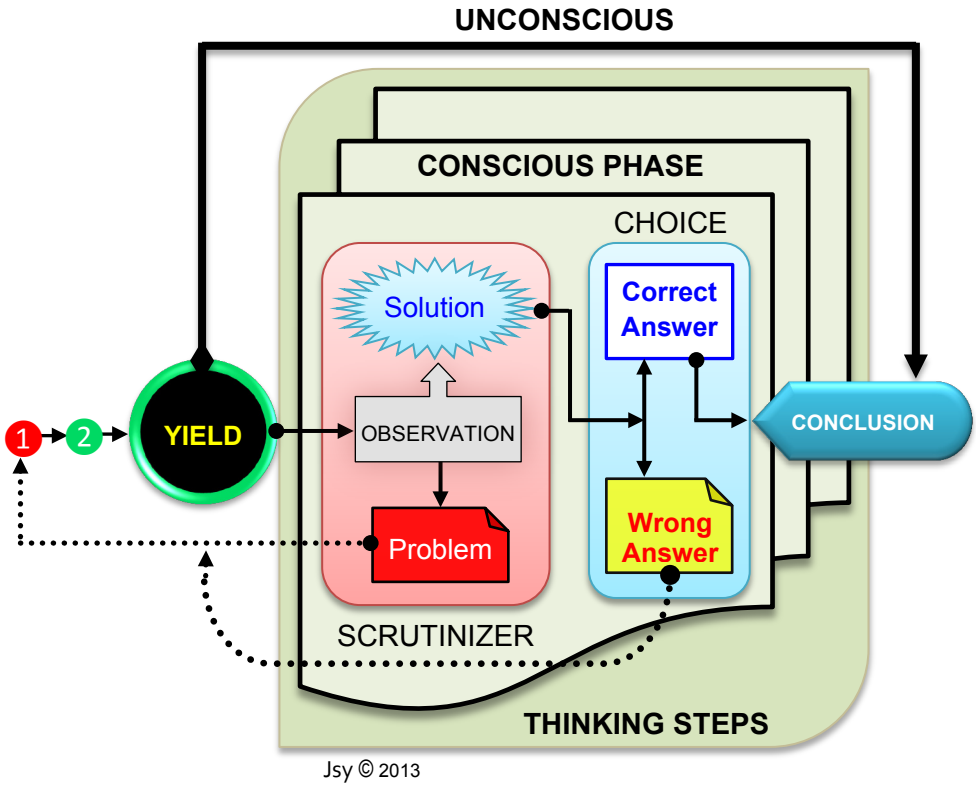

Figure 49. The basic thinking steps underlying semantic process.

phase of the pristine problem-solving process is one engulf within thinking steps which is shown in figure 49. It is unlike

the simple semantic activities (like the identification of missing or excessive semi colons, braces and the likes) that compilers are able to do during compilation of a computer program.

Distinguishing Between Problem and Solution

Hitherto, the ending of the processing of any problem was viewed to yield a solution – which could be right or wrong. As was shown earlier on, this is not even true with numerical computations. A closer look at a problem and solution relation reveals that a problem is a composite of numerical terms, mathematical operation(s) and desired answer. On the other hand, a solution would have the same composition but without a desired answer.

Unlike computational mathematics that deals with numerical scrutiny of problems, it will be difficult for mathematical logic which is a form of reasoning with symbolic statements in a language to make a clear distinction between a problem structure and a solution structure. This is because both problem and solution structures in logic are in sentential forms. Consequently, humans have to be responsible for the activity of the semantic processing phase of the pristine problem-solving process. The role of the thinking faculty and consciousness (the ability to recognize self) in the semantic processing can be deduced by asking the following pertinent question: Could a machine be able to do the same as humans in the semantic

processing phase? A reasonable answer to this is given using the following comatose analogy. Any true thinking process (organic or not) must thrive on conscious entity. In other words, the ability to think will require the presence of consciousness to operate but the reverse is not necessary true. Put another way, a thinker must be conscious. But the converse of the latter statement is not true. An empirical case in point is a patient who is in coma. Such a patient is not only experiencing unconsciousness but lacks thinking. Upon recovery, the patient will have no clue as to what went on. The gaining of consciousness rejuvenates not only the thinking faculty but also others that have, for example, to deal with language. Consciousness is the key to the correct identification of the process of thinking. It must however be noted that thinking is not the consequence of consciousness. Consciousness is the platform for cultivating thought activities which are aided by logical reasoning through the use of a language. This being the case, how can a machine be able to think? It would first of all have to be conscious in order to be considered as possibly being able to think. Are today's computers conscious or will they in the future? It is "obviously" true none of these materials namely plastics, metals and ceramics is a conscious entity. And none of them do we know thinks. And so is the computer! It has no grounds or platform (consciousness) for cultivating a thinking process.

What man has been able to do in the past several years is to mechanically mimic some processes that are akin to thinking process. This is a pseudo-thinking process at best because of the absence of consciousness. Conclusively, man is the solely important role player in deciding the presence of a solution yield during semantic processing phase in a problem-solving process.

Quantum Mechanics and Consciousness

Using De Broglie's equation which applies to all matter, it can fundamentally be established that

$$\mathbb{C} = hf$$

where $\mathbb{C}$ is consciousness, h Planck constant and f the frequency. If probability is expressed as consciousness, the information necessary to describe the current moment or probability amplitude of consciousness embodies the arrow of time. Also, any neural circuit can be seen as a vector with direction, underpinning cognitive dissonance and interference or resonance within consciousness. Consequently, artificial awareness (which occurs after actions) will require a network of independent processors instead of a linear sequence of complex algorithms.

As a product of widespread cross-network communication, consciousness according to research (Godwin, Barry, & Marois, 2014) seems to emergently define the property of how executable information is propagated all through the brain leading to an

integration that presents as a singular world. There generally exist two competing ideas namely focal and global approaches to modern theories of the neural basis of consciousness. But a study (Godwin, Barry, & Marois, 2014) focused on network approach to brain analysis via comparison of aware and unaware trials using conventional fMRI analyses that assess the amplitude of brain activity suggests (on the basis of an integrated or unified experience) that

1. The breakdown of brain neural networks seemingly exists by virtue of broad increase in their functional connectivity with awareness.
2. By way of widespread cross-network communication, it appears that information is spread throughout the brain via an emergent property called consciousness.

Reasonably, the above findings fundamentally underscore the needed interpretative answer to explain defined problem(s) in an environment via problem-solution cycle (PSC) as a conscious thought process (see figure 49). As a guarded conclusion, it is reasonable to suggest that the shortcut neural structure(s) identified in the brain as spontaneously facilitating creative processes through thought catalysis, thought inhibition and thought promotion, support(s) subconscious activities. The claustrum (area deep in the brain) is:

1. Known to play a strong role in communication (language) between left and right hemispheres of the brain (Smith & Alloway, 2010).
2. Suggestively involved in neural processes sub-serving perceptual binding (Crick & Koch, 2005).
3. Comprised of separate single mode processing regions (Remedios, Logothetis, & Kayser, 2010).

Capable of taking (via language or communication) and processing problem-solution cycle modalities, that is characteristics based on particular encoded thought representation formats namely intelligence, imagination and creativity, claustrum reasonably serves as the switch that turns off consciousness and turns on the sub-consciousness.

CHAPTER 18

CONCLUSION

The accuracy and precision of given theoretical proofs and empirically confirmations in support of the vital role of human thought process through the vein of problem-solution cycle(PSC) reasonably affirm the importance of multi-computational skills (brain traits) namely creativity, imagination and intelligence. To this effect, the tower of computer programming languages which essentially function as inherent communication linkage within multi-computational skills have been shown to be the vital source of current dismal performance of software production industry worldwide. As evinced, the attainment of an 'immediate' incremental efficiency to a maximal tune of 33.33% is possible if a reasonable reduction in the number of programming languages occurs. Until this silver bullet is implemented, software construction industry will continue to function at best close to 66.67% efficiency and so continue to wallow in its dismal performance. Left unaddressed, any push by software production industry will merely make up for 5.2% basic human error. What is therefore earnestly needed is the implementation of a policy-backed universal standardization that encompasses very minimal programming languages together with supporting operating systems

and development tools. Only then, would the estimated 3 to 6.2 trillion US dollars annual world-wide wastage caused by the global impact of IT failures be stopped. No amount of quality assurance measures can ever cure this dilemma.

On the other hand, the thought flow of human thought process (HTP) can be effectively analyzed using informatics wave equation analysis (IWEA). Its computer-generated eigen thermogram and eigen chromatogram (graphical outputs) facilitates effective analysis of information flow within any network or network systems. In particular, the messaging line spectra derived from eigen chromatogram unravels hidden system characteristics. Using message spectrum modeled after Journal-to-journal citation of 13 major chemistry journals, the prevailing metrics of its assured operational (citation) efficiencies can be easily identified. As a useful analytic tool, IWEA simulation provides enabling differential improvement of a thought flow system's maximal operational efficiency in areas such as dynamic network analysis (DNA) and Analytics (activities of data mining, big data, etc.). In the quest for computers that mimic human brain, the general mapping of HTP through problem-solution cycle (PSC), does provide new insights for artificial intelligence (AI) within the purview of future quantum and/or neuromorphic computers. The development of neuromorphic hardware based on HTP is a reasonable way to leverage the unique capabilities of neural networks in the future. Also, the fundamental insight into the interpretation of

complex neuronal maps can be ascertained using HTP provisions. This will make it possible, via neuromorphic computing, for the latter to be mimicked and thus allow scientists to explore the link between low-level and high-level brain circuitry functions within the complex network of brain circuitries via message line spectra derived through eigen-chromatography.

On the basis of simplicity, the fundamentals of HTP – the very bedrock of all human activities or existence – is framed in truth and its solution interpretation brings understanding to the human mind. The correct interpretations of solutions to problems borne out of finding the missing links are not really new but acts of truth-theoretic recognitions existing within environs of said problems which act as solution repositories. What therefore remains is the free will of humanity to exercise truth in deliberations of life activities. A life that is riddled with seemingly unending problems and solutions that together warp through space-time to form the very fabric of our existence. Only if we would choose rightly, then perhaps wisdom will be exulted.

Questions pertaining to HTP's front-end and back-end have been raised. Subsequently, future line of research on halting problem with a view to re-analyzed the solution of Kurt Gödel's incompleteness theorem(s) for truth-theoretic interpretation will be pursued.

As a general logical theory composed of a set of well-formed formulas and/or strings of symbols forming true sentences,

the question of decidability of PSC with halting problem as its defined decision problem over a Turing machine (TM) will be investigated. This means that the question as to whether an effective algorithm with decisive capability exists such that given texts representing arbitrary program and input in the programming language of PSC, it is viable to decide if it halts or not will be sort. In accordance with the core condition of Alan Turing's 1936 assertion, a general algorithm (if it exists) must solve the halting problem for all possible program-input pairs. Thus, a valid verification of halting problem needs infinite programs and data for successive verification. To instill credence in the logical arguments pertaining to halting problem, a complete infinity condition in agreement with modern mathematical infinity as advanced by Greorg Cantor must be holistically upheld. While infinite sets of program and input pairs can be created for TM's initial state by invoking Cantor's diagonal argument, a consistent one-to-one mapping order must be present within TM's program code (description number) during its transition state. Failure to do these will render any conclusion thereof invalid.

Finally, in the light of evolutionary algorithm (EA) such as genetic programming and gene algorithm in which computer programs evolve, a novel concept of a halting decision boundary will be advanced to practically optimize decidability of PSC's halting problem within polynomial time.

APPENDIX A

OVERALL GLOBAL CREATIVITY INDEX RANKING 2010

Table 28

Part I of Global Creativity Index (GCI) 2010 Data Spanning Countries Round the World

TOTAL RANK	COUNTRY	TECHNOLOGY	TALENT	TOLERANCE	3T MEANS	GLOBAL CREATIVITY INDEX	STRATIFIED RANDOM SAMPLING OF MEANS
1	Sweden	5	2	7	4.67	0.923	
2	United States	3	8	8	6.33	0.902	
3	Finland	1	1	19	7.00	0.894	
4	Denmark	7	4	14	8.33	0.878	
5	Australia	15	7	5	9.00	0.87	7.00
6	New Zealand	19	5	4	9.33	0.866	
7	Canada	11	17	1	9.67	0.862	
8	Norway	12	6	11	9.67	0.862	
9	Singapore	10	3	17	10.00	0.858	
10	Netherlands	17	11	3	10.33	0.854	
11	Belgium	16	12	13	13.67	0.813	
12	Ireland	20	21	2	14.33	0.805	9.67
13	United Kingdom	18	19	10	15.67	0.789	
14	Switzerland	6	22	20	16.00	0.785	
15	France	14	23	16	17.67	0.764	
16	Germany	9	26	18	17.67	0.764	
17	Spain	24	28	6	19.33	0.744	
18	Taiwan	—	32	21		0.737	
19	Italy	26	18	23	22.33	0.707	16.00
20	Hong Kong	22	37	12	23.67	0.691	
21	Austria	13	30	35	26.00	0.663	
22	Greece	38	9	37	28.00	0.638	
23	Slovenia	23	10	51	28.00	0.638	
24	Serbia	28	35	27	30.00	0.614	
24	Israel	4	20	66	30.00	0.614	30.00
26	Hungary	33	25	34	30.67	0.606	
27	Republic of Korea	8	24	62	31.33	0.598	
28	Portugal	32	34	33	33.00	0.577	
29	Czech Republic	25	31	49	35.00	0.553	
30	Japan	2	45	61	36.00	0.541	
31	Russian Federation	21	13	74	36.00	0.541	33.00
32	Costa Rica	43	42	26	37.00	0.528	
32	Estonia	27	15	69	37.00	0.528	
34	Latvia	39	14	60	37.67	0.52	
35	Croatia	29	39	46	38.00	0.516	
36	United Arab Emirates	—	49	38		0.513	
37	Uruguay	63	46	9	39.33	0.5	
38	Argentina	55	36	31	40.67	0.484	37.00

NOTE: Countries in red not used in analysis.

Table 29

Part II of Global Creativity Index (GCI) 2010 Data Spanning Countries Round the World

TOTAL RANK	COUNTRY	TECHNOLOGY	TALENT	TOLERANCE	3T MEANS	GLOBAL CREATIVITY INDEX	STRATIFIED RANDOM SAMPLING OF MEANS
39	Lithuania	31	16	75	40.67	0.484	
40	Bulgaria	40	38	45	41.00	0.48	
41	Slovakia	36	33	55	41.33	0.476	
42	Poland	37	29	58	41.33	0.476	
43	Nicaragua	—	69	24		0.474	
44	Cyprus	59	43	25	42.33	0.463	
45	South Africa	45	68	15	42.67	0.459	40.67
46	Brazil	41	66	22	43.00	0.455	
47	Chile	48	54	28	43.33	0.451	
48	Malaysia	54	50	29	44.33	0.439	
49	Ukraine	34	27	77	46.00	0.419	
50	India	42	75	30	49.00	0.382	
51	Panama	65	52	39	52.00	0.346	44.33
52	Romania	49	63	44	52.00	0.346	
53	Macedonia	61	47	48	52.00	0.346	
54	Philippines	52	64	41	52.33	0.341	
55	Armenia	46	61	50	52.33	0.341	
56	Kazakhstan	60	40	57	52.33	0.341	
57	Georgia	47	48	63	52.67	0.337	52.67
58	China	30	76	—		0.327	
59	Ecuador	72	58	32	54.00	0.321	
60	Bolivia	66	44	53	54.33	0.319	
61	Mexico	62	65	36	54.33	0.317	
62	Egypt	—	41	76		0.316	
63	Sri Lanka	69	55	42	55.33	0.305	
64	Trinidad & Tobago	53	70	43	55.33	0.305	
65	Kyrgyzstan	50	53	65	56.00	0.297	54.33
66	Peru	56	62	53	57.00	0.287	
67	Uganda	35	79	59	57.67	0.276	
68	Turkey	51	59	64	58.00	0.272	
69	Mongolia	—	51	73		0.27	
70	Azerbaijan	44	67	72	61.00	0.236	
71	El Salvador	67	73	47	62.33	0.22	
72	Thailand	64	56	67	62.33	0.22	58.00
73	Jamaica	57	60	71	62.67	0.215	
74	Honduras	58	77	56	63.67	0.203	
75	Madagascar	70	82	40	64.00	0.199	
76	Saudi Arabia	—	57	79		0.191	
77	Paraguay	71	72	54	65.67	0.179	
78	Iran	—	71	68		0.171	
79	Viet Nam	68	78	70	72.00	0.102	
80	Pakistan	73	74	81	76.00	0.053	63.67
81	Indonesia	74	80	78	77.33	0.037	
82	Cambodia	75	81	80	78.67	0.02	

NOTE: Countries in red not used in analysis.

Source: www.martinprosperity.org; 2010.

APPENDIX B

LINKING QUANTUM AND THERMODYNAMIC ARROW OF TIME

In reality, a free proton and electron cannot normally react to form a free neutron. However, the process can take place in a larger nucleus of an atom as an isolated system. This is made possible by a process called electron capture which is a form of radioactivity. For radioactive isotopes sufficient energy, electron capture is another mode to decay by positron emission. During an electron capture, an electron normally from the K or L electron shell (see light blue regions in figure 50) whose probabilistic path is described by Schrödinger's wave equation is captured by one of the protons in the nucleus of said atom to an irreversibly form neutron. An electron neutrino is emitted as a result. The ensuing microscopic level interactions is expressible in the following nuclear reaction equation

$$p^{+} + e^{-} \rightarrow n + \upsilon_{e}$$

The newly formed neutron increases the number of neutrons in the nucleus of the said atom but reduces its number of protons by 1. The said nucleon changes do not alter the atomic mass number (number of neutrons and protons) but rather the atomic number

(number of protons). This reduction in atomic number as a result of electron capture transforms the nucleus of the said atom into a new elemental atom in an excited state. Eventually, an outer shell electron in a higher energy state

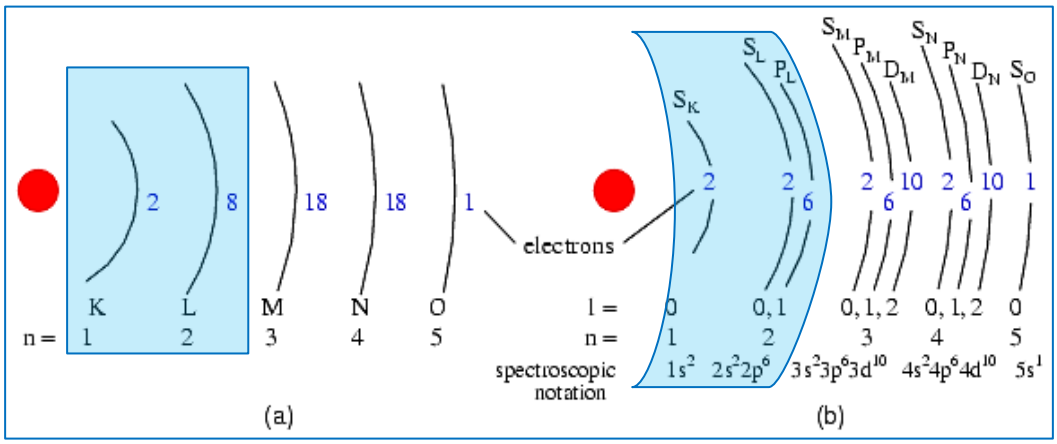

Figure 50. Electron shells in an atom designated by letter and a principal quantum number n. Left a: Maximum number of electrons per shell is given by $2n^2$. Right b: Electron configuration of an atom showing its electronic energy levels in spectroscopic notation. Adapted from *Angular Momentum Quantum Number*, retrieved June, 2014, from http://www.vias.org/feee/theory_03_quantumnumbers_02.html

transition to a lower energy state thereby giving off electromagnetic radiation. This creates disorderliness in the electron cloud system (orbital electron). Also, other orbital electrons may in the process emit Auger electrons (see figure 51). Thus, in time the orbital electrons moved into a more disorderly state as energy is released.

On the other hand, at the macroscopic level the different ways said isolated atomic system can achieve a particular macrostate is through the description of its number of particles, volume and energy. Thus, the nucleus of said atom and its newly

transformed excited atom describe two different chemical elements with different chemical properties. While the number of particles in terms of mass number (except for atomic number) and

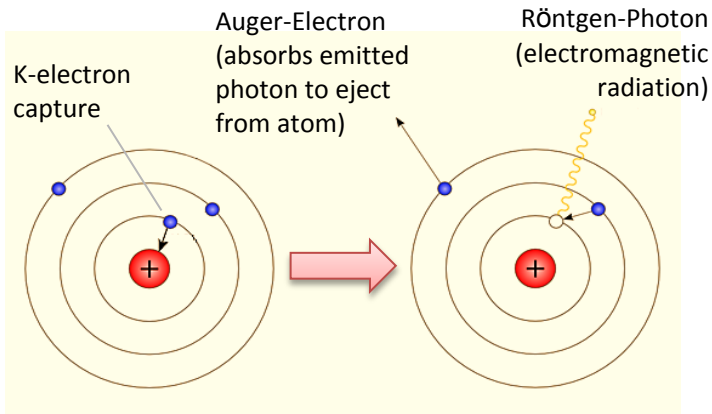

Figure 51. A general illustration of the process of electron capture by a nucleus. Adapted from Electron capture, in *Wikipedia, the free encyclopedia*, retrieved August, 2014, from https://en.wikipedia.org/wiki/Electron_capture

volume of the nucleus are practically invariant in the electron capture process before and after, the excited nucleus however undergoes transition to its ground energy state. The subsequent gamma ray energy which is emitted represents a form of increased disorderliness of the agitated nucleus. In support of this nuclear disorderliness is the nuclear bond energy that is sustained as a result of said mass defect.

Generally, the correlation of increment in entropy (degree of disorderliness) with the passage of time is supported by the fact that all natural processes are irreversible. This is based on the fact that particles of a system (e.g. subatomic particles, atoms, molecules) do work externally and also do internal work on

each other. Thus, the existence of internal inter-particulate opposing force such as friction is accounted for by entropy. Consider the case where an isolated nuclear system spontaneously undergoes an electron capture which involves an electron and a proton's quark combination (up, up, down). Then the ensuing nuclear bond which maintains the reacting proton's newly acquired three quark combination of a neutron (up, down, down) from its weak nuclear interaction must do internal work to sustain an irreversible transformation process. During the weak interaction between electron and proton, the up quark in the proton is changed into a down quark to give a neutron and the resulting W^+ boson emitted is absorbed by the electron to become an electron neutrino.

$$uud + e^- \rightarrow udd + W^+ + e^- \rightarrow udd + \bar{v}_e$$

An alternate path is for the electron to emit W^- boson to become an electron neutrino and the proton's up quark absorbs the W^- boson to become a down quark thereby converting the proton into a neutron.

$$uud + e^- \rightarrow uud + \bar{v}_e + W^- \rightarrow udd + \bar{v}_e$$

Inside the nucleus, the newly formed down quack together with other two quarks in new neutron exist like balls fixed on elastic string (gluons) and held together by their colour charges to facilitate any opposition via stretching by existing electric charge repulsion between them. Thus, an opposing force is provided by said "elastic" opposition in similitude to that of a

frictional force naturally accounted for by thermodynamic entropy. While thermodynamic entropy accounts for the existence of inter-molecular opposing force (friction), quantum entropy similarly accounts for the existence of inter-quack opposing force. Observe that since the down quark has more rest mass than top quark, the newly formed neutron is heavier than the original proton. As a result, the link of quantum arrow of time to thermodynamic arrow of time is mass defect. This means that the arrow of time associated with weak nuclear force is equivalent to the thermodynamic arrow of time. Therefore, thermodynamic arrow of time is indeed generally related to all other arrows of time.

Using a similar setup (see figure 52) to that used by Carnot, Clapeyron and Clausius to analyze entropy as a basis of the second law of thermodynamics, the following mathematical deductions for quantum arrow of time via entropy as a consequence of thermodynamic arrow of time can reasonably be done. Generally, by definition, the released energy Q of a nuclear reaction is given by

$$Q = KE_{final} - KE_{initial} = \left(m_{initial} - m_{final}\right)c^2$$

where KE is the kinetic energy, m the rest mass and c the velocity of light in vacuum. This means the decay of a neutron at rest in a time reversal manner to form a proton, electron and an electron antineutrino which is expressed as

$$n \rightarrow p + e + \bar{\nu}_e$$

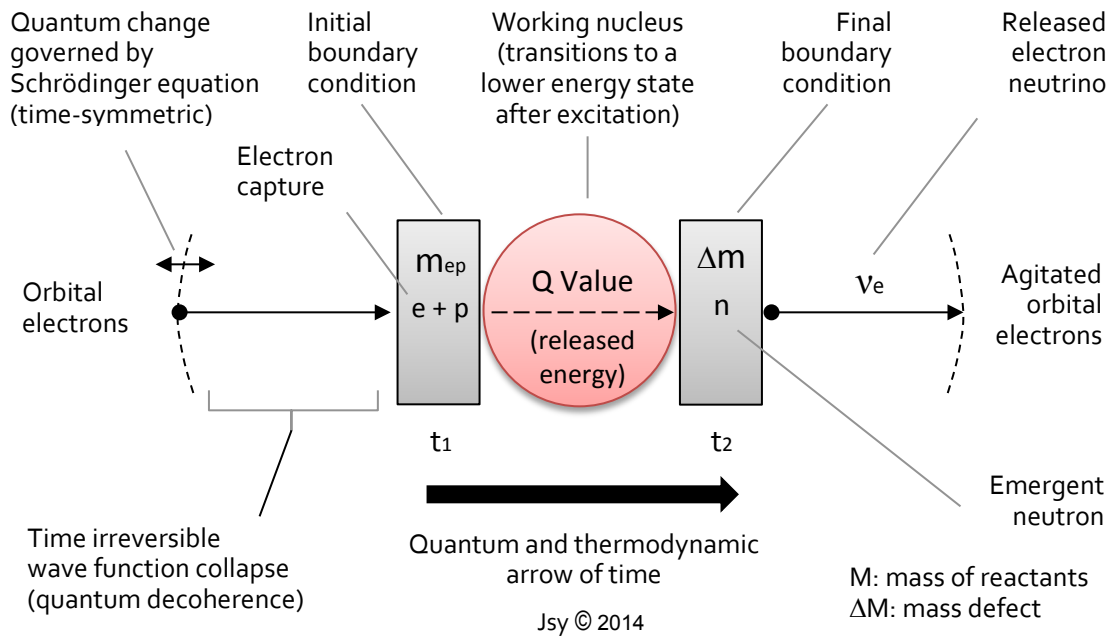

Figure 52. Illustration of quantum and thermodynamic changes occurring during a nuclear process via an orbital electron capture.

has a Q value given by

$$Q = (m_n - m_p - m_{\bar{\nu}} - m_e)c^2$$

where m_n is the mass of the neutron, m_p is the mass of the proton, m_ν is the mass of the electron antineutrino and m_e is the mass of the electron. As shown in figure 52, the entropy S involved in the channeling of Q value (released nuclear energy) from the agitated nucleus as its proton interacts with an orbital electron at time t_1 and produces a neutron at time t_2 can be defined as a function to measure nuclear irreversibility of the electron capture process. This means the initial entropy S_1 between the capture electron and proton from the nucleus at time t_1 is given

by the captured electron's binding energy while at time t_2 the final entropy S_2 of the closed nuclear system is given by newly formed neutron's binding energy E_{nb}. So, from the thermodynamic definition of entropy

$$S = \frac{Q}{T}$$

where Q is the amount of heat energy and T the temperature the following equivalent quantum definition for entropy can reasonably be put forth. The neutron binding energy E_{nb} of the newly formed neutron, in accordance with the energy-mass equation, is given by

$$E_{nb} = (m_{ep} - m_n)c^2 = \Delta mc^2$$

where m_n is the mass of neutron and c the velocity of light in vacuum. To find the kinetic temperature equivalence of this energy use is made of the following equation.

While temperature is generally associated with random motion of atoms or molecules in great amounts such as in a gas, the concept of kinetic temperature (expressed in electron volts) surfaces when consideration is given to the energy of an individual particle. To correlate the increase in quantum entropy with the passage of time, the energy of the mass defect Δm must be expressed in terms of kinetic temperature in order to facilitate an equivalent thermodynamic definition of entropy. By definition, comparison of the ideal gas law to the average molecular kinetic energy KE_{avg} leads to an expression for

temperature T referred to as kinetic temperature. This is given by

$$KE_{avg} = \overline{\frac{1}{2}mv^2} = \frac{3}{2}kT$$

where m is the mass of the particle, v is the velocity and k the Boltzmann's constant. Hence, one can write

$$\Delta mc^2 = \frac{3}{2}kT$$

which gives the temperature at t_2 as

$$T = \frac{2}{3k}\Delta mc^2$$

Hence, the entropy at time t_2 is given by

$$S_2 = \frac{Q}{T_2} = \frac{3kQ}{2\Delta mc^2}$$

A nucleus capturing an electron is generally equivalent to a hydrogen-like ion (two-particle system) whose interaction depends only on the distance between its two its nucleus and orbiting electron. Subsequently, the accurately predicting Bohr theory in the case of energy levels for one-electron atoms such as H, He^+, Li^{2+} and B^{4+} can be applied to determine the electron binding energy (i.e. first ionization energy IE) of the equivalent two-particle atomic system. It must be noted that Schrödinger's quantum mechanical theory which is more accurate confirms the correctness of Bohr's energy level equation for one-electron atoms. Also, the electron binding energy equivalently is the thermodynamic work done by supplying minimum amount of energy to

remove the only available or nearest electron from an equivalent two-particle atomic system to infinity.

In accordance with Bohr's theory, the energy of an electron in the nth energy level is given by

$$E_n = -\frac{Z^2 e^4 m_e}{8\varepsilon_o^2 h^2 n^2} = -(2.178 \times 10^{-18}\text{J})\left(\frac{Z^2}{n^2}\right)$$

where Z is the nuclear charge, -e is the electron charge, m_e the mass of the electron, ε_o the permittivity of free space, n the principal quantum number and h Planck's constant. This gives the electron binding energy for the nuclear system under scrutiny at time t_1 as

$$E_n = -(2.178 \times 10^{-18}\text{J})\left(\frac{Z^2}{n^2}\right)$$

This means the kinetic temperature at time t_1 is

$$-(2.178 \times 10^{-18}\text{J})\left(\frac{Z^2}{n^2}\right) = \frac{3}{2}kT$$

which gives

$$T = -\frac{2(2.178 \times 10^{-18}\text{J})}{3}\left(\frac{Z^2}{kn^2}\right)$$

Therefore the entropy at time t_1 is given by

$$S_1 = \frac{Q}{T_1} = -\frac{3kQ}{2(2.178 \times 10^{-18}\text{J})}\left(\frac{n}{Z}\right)^2$$

Consequently, the quantum entropy change given by

$$\Delta S = S_2 - S_1 = \frac{3kQ}{2\Delta mc^2} + \frac{3kQ}{2(2.178 \times 10^{-18}\text{J})}\left(\frac{n}{Z}\right)^2$$

But by definition, the Q value of the nuclear transformation is given in terms of the mass defect as

$$Q = \Delta mc^2$$

Subsequently, the change in quantum entropy can be expressed as

$$\Delta S = \frac{3k}{2} + \frac{3k\Delta m}{2(2.178 \times 10^{-18}\text{J})}\left(\frac{cn}{Z}\right)^2$$

This can be written as

$$\boxed{\Delta S = \frac{3k}{2}\left(1 + (0.459 \times 10^{18}\text{J})\left(\frac{cn}{Z}\right)^2\right)}$$

Notice that for any particular equivalent two-particle atomic system, the quantum entropy change is not only quantized but a constant for each type of particle. The quantum entropy change is therefore a statement of conservation of quantum mechanical entropy which is equal to the sum of a particle's potential entropy and its kinetic entropy. The kinetic entropy S_k is equal to

$$\boxed{S_k = 0.459 \times 10^{18}\text{J} \times \frac{3k}{2}\left(\frac{cn}{Z}\right)^2}$$

while the potential entropy S_p is given by

$$\boxed{S_P = \frac{3k}{2} = \frac{3}{2} \times 1.380662 \times 10^{-23} = 2.070992 \times 10^{-23}\, J/K}$$

which is a constant for all particles. By definition, the status quo definition of mechanical entropy relates to energy transfer through work interaction and therefore seen as complementary to thermal entropy (Palazzo, 2012).

Origin of the Arrow of Time

It is imperative that the origin of the arrow to time is understood. Such an understanding would pave the way for unraveling questions relating why entropy in general increases universally in terms of correlation, randomness, energy and most importantly in terms of information.

The core of quantum mechanics to some degree is seen in the phenomenon of quantum entanglement which is the result of quantum uncertainty. It is the basis for quantum cryptography, quantum teleportation and most importantly quantum computing. According to Popescu (Linden et al., 2009), within an infinite amount of time objects become quantum mechanically entangled with their surroundings and attain a state of uniform energy distribution /equilibrium. In other words, there exists a general flow of time towards equilibrium where the loss of information of objects through quantum entanglement leads them to equilibrate with their surrounding environments and correspondingly the various surrounding environments also moves towards equilibrium with the rest of the universe. Generally, entanglement is seen to cause objects to evolve towards equilibrium.

In a park analogy given by Popescu (Linden et al., 2009), entanglement is seen as starting next to the gate of a park far from equilibrium. By entering said gate, the vastness of the place gets one lost never to return to the said gate (Linden et

al., 2009). Notably, one of the aspects of the arrow of time that is unsolved is reflected in the lack of reason for in the first place appearing at the gate in the given part analogy. Answer(s) to such fundamental question must elucidate ones understanding of the origin and flow of the arrow of time and the flow of entropy as a whole. To answer this pertinent question, the follow explanations are given.

A particle in the universe is particulate because it exists with a mass. Its existence relatively started at a **zeroth point time** which is the origin of its time arrow. At that zeroth point time, the fundamental existence of a particle possessing mass energy is indicative of a non-spontaneous transformation of energy but a spontaneous appearance of mass during an emergent energy-mass transformation in accordance with Einstein's mass-energy equation. This mass is equivalently the start gate of the particle. It initiates its existence. Without it, the particle will not exist. Consequently, the reason for the universe's initial state being far from equilibrium can be simply explained using the following analogy of floating ping pong balls. Imagine a number of ping pong balls tied close to the bottom of a container (representing space) filled with water (representing energy) as shown in figure 53. A ball is randomly released and it rises up to the surface of the water (equivalently as a form energy-mass transformation process). The 'popped' ball (equivalent to created mass) causes the undisturbed surface water (in a pure state) to wave with a uniform mechanical energy

distribution which is its pure state of equilibrium. This in turn causes the ball to wave in like manner (see A of figure 53). The newly acquired bobbing (mechanical wave energy) from the water environment represents the ball's initial or pure state information. It is equivalent to its invariant potential entropy. Upon release of a second ball (see B of figure 53), the situation at the surface of the water will be one of interacting water waves from both balls is reminiscent to entanglement (see C of figure 53). Here, the pure state information of ball 1 affects that of ball 2 at a distance and vice versa. However, both balls will have the same entropic potential which affirms their respective existing masses. If the system is an isolated one, the pure state information of both balls will eventually

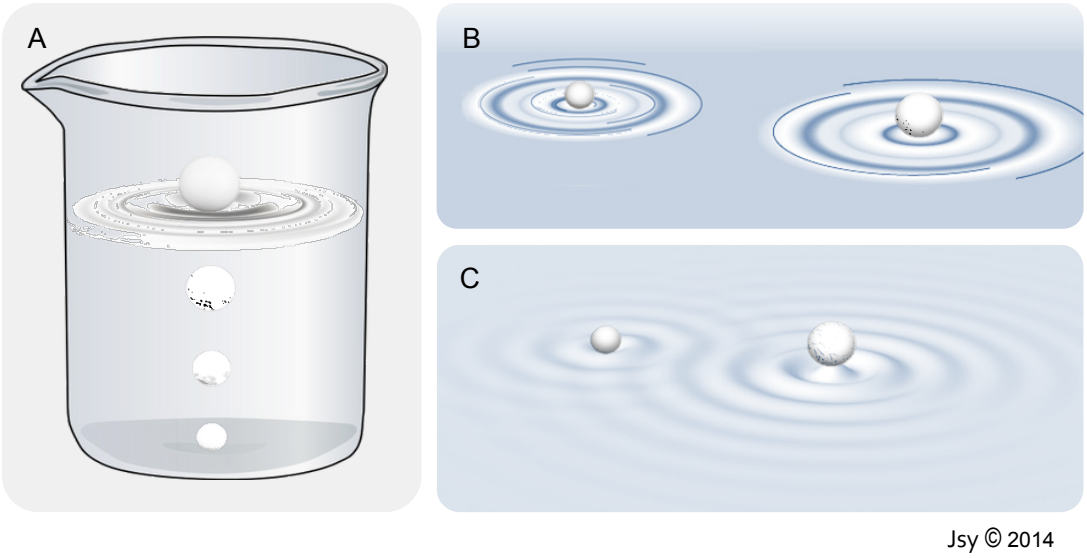

Figure 53. An illustration of floating ping pong balls analogy depicting effect of a popped ball on undisturbed water surface (A) and how the existence of another ball at the surface (B) causes respective water waves to entangle (interact) until the energy of the water waves is uniform or at equilibrium (C).

approach a final equilibrium state (a state of uniform energy distribution) where the vibrations of both balls would be the same but different from their individual pure states. At this point, though the total energy is increased, the entropy (degree of disorderliness) of the isolated system will remain the same. The entanglement phenomenon occurs due to the energy possessed by particles in the environment by virtue of their existence. This assertion is supported by the fact that if the vibrating system of floating ping pong balls is allowed to persist for some time, it will come to a non-vibrating or zero energy state. The dissipated wave energy has two important implications. Firstly, it means that the system is not an isolated system and secondly it means energy (vibrating) is a necessity for entanglement phenomenon. In general, the change or loss in the pure states of information of respective balls through entangled water waves occurs with the passage of time (arrow of time) as the varied wave energies get transformed or equilibrate with each other. Though quantum uncertainty, which results in quantum entanglement, is believed to be the cause of the arrow of time, (Wolchover, 2014) the result of the quantum entropy analysis provided earlier on renders such assertion an offshoot effect. Rather, the relative origin of time's arrow is consequentially rooted in a particle's zeroth point time of existence as a universal reference point of pure energy or information state. The thermodynamic view of time's arrow is one of a steady flow of energy that increases the overall entropy of the universe. Thus,

thermodynamic entropy is proportional to the marginal entropy of uncorrelated microstates. As microstate particles became correlated, the change in mutual entropy (entropy of correlation) is what can only be measured but not the mutual entropy of a microstate (Gull, 1989). This means that the thermodynamic time arrow fundamentally lacks an origin as it is a measure between changes between to changes of a microstate with time. On the other hand, the current quantum view rather asserts that information diffuses to a non-zero value in which case the universe's entropy remains invariantly zero (Wolchover, 2014). Hence, increasing correlation depicts the flow of arrow of time.

In comparison, the quantum basis for a zeroth point time of existence establishes a definite origin of time arrow relative to the absolute energy changes of a particle. By definition, the thermodynamic entropy change ΔS is given by

$$\Delta S = Q\frac{1}{T_2} - \frac{1}{T_1}$$

where T_1 and T_2 are the initial and final temperature of the isolated system. While thermodynamic entropy change which is effectively a difference process, the quantum entropy change on the other hand is effectively an additive process between the initial and final time of transformation. By adding entropies of an isolated system at any point in time, the total quantum mechanical entropy is determined. The entropy difference between states of an isolated system depicted by change in thermodynamic

entropy is in effect a measure of the inter-state entropy change of an isolated system. Of the two, quantum entropy change is more fundamental by being absolute. Surely, there exists a link between quantum and thermodynamics entropies. The quantum arrow of time is a fundamental time arrow. In quantum terms, a particle's potential entropy which has order in relation to other particles via constant potential entropy is less than its kinetic entropy which results in more disorderliness in the environment. Similarly in thermodynamic terms, the mutual entropy (entropy of correlation) of an isolated system is less than the marginal entropy of its uncorrelated particles. For by definition, thermodynamic entropy of an isolated system which is always increasing is proportional to its marginal entropy (Gull, 1989). These explain why the universe had such low entropy in the past which resulted in the distinction between the past and future and the second law of thermodynamics.

Within space-time continuum, the state of human brain is able to correlate objects in the three dimensions of space. However, the perception of a flowing time (nature of time) seems so different to the human thought process. The reason is that the flow of time is rooted in the zeroth point time of existence. As such, like existence it is extenuatingly (less seriously) perceived in such a manner reminiscent of sub-consciousness of the human brain.

APPENDIX C

Summation of two ΔIs

Sum of two ΔIs for row and column for each element k of a square matrix must be larger than or equal to zero.

Proof:

I_S have to be positive (cf. Theil 1972: 59f.) both for groups and for subgroups. ΔIs can be negative as an effect of normalization. However, I_{journal} can be obtained from the ΔIs for row and columns by appropriate normalization.

Let n_q and n_p be the margin totals for row k and column k, and N be the grand sum of the matrix; q and p are relative frequencies of the cells belonging to the respective row and column in terms of the grand sum of the matrix. Normalization relative to the margin totals for the respective row and column is achieved by multiplication of q by (N/n_q) and of p by (N/n_p)

Therefore:

$$I_{journal} = \sum \{q * (N/n_q)\} \log \frac{q * (N/n_q)}{p * (N/n_p)}$$
$$= \sum \{q * (N/n_q)\} \{\log(q/p) - \log(n_q/n_p)\}$$

Since $I_{journal} \geqq 0$:

$$\sum \{\log(q/p) - \log(n_q/n_p)\} \geqq 0$$

$$\sum \log(q/p) \geqq \log(n_q/n_p)$$

$$\sum q \ \log(q/p) \geqq n_q \log(n_q/n_p)$$

However:

$$\sum q \ \log(q/p) = \Delta I_{(q:p)}$$

and therefore:

$$\Delta I_{(q:p)} \geqq n_q \log(n_q/n_p)$$

Analogously:

$$\Delta I_{(p:q)} \geqq n_p \log(n_p/n_q)$$

and therefore:

$$\Delta I_{(q:p)} + \Delta I_{(p:q)} \ \geqq n_q \log(n_q/n_p) + n_p \log(n_p/n_q)$$

$$\geqq (n_q - n_p) \log(n_q/n_p)$$

For $n_q > n_p$, this is a product of two positive factors; hence, > 0; for $n_q = n_p$, this product is zero; for $n_q < n_p$, this is a product of two negative factors; hence, > 0. Q.e.d.

BIBLIOGRAPHY

2007 IT Project Success Rates Survey Results. (2007, August). *Dr. Dobb's Journal (DDJ)*. Retrieved November, 2013, from http://www.ambysoft.com/surveys/success2007.html

2010 IT Project Success Rates. (2010, August). *Dr. Dobb's World of Software Development*. Retrieved October, 2013, from http://www.drdobbs.com/architecture-and-design/2010-it-project-success-rates/226500046

2011 IT Project Success Rates Survey Results. (2011). Dr. Dobb's Journal(DDJ). Retrieved November, 2013, from http://www.ambysoft.com/surveys/success2011.html

Altman, D. G. (2005). Why we need confidence intervals. *World J Surg*; 29:554-6.

Ambler, S. W. (2009). Software Development Success Rates. Retrieved November, 2013, from http://www.drdobbs.com/architecture-and-design/software-development-success-rates/216600177

Appleby, D.M.; A. Ericsson & C. A. Fuchs (2011). Properties of QBist state spaces. *Foundations of Physics*, *41*(3), 564–79.

Atchley, R. A., Keeney, M. & Burgess, C. (1999). Cerebral hemispheric mechanisms linking ambiguous word meaning retrieval and creativity. *Brain Cogn*. 40, 479–499.

Atkins, P.W. (1977). Molecular Quantum Mechanics Parts I and II: An Introduction to Quantum Chemistry. Vol. 1. Oxford University Press.

Bae, Byoung-Il et al. (2014). Evolutionarily Dynamic Alternative Splicing of GPR56 Regulates Regional Cerebral Cortical Patterning. *Science*, p.764.

Bailey, D. H.; Borwein, J. M.; Calkin, N. J.; Girgensohn, R.; Luke, D. R.; and Moll, V. H. (2007). *Experimental Mathematics in Action*. Wellesley, MA: A K Peters, 36-38 and 265-266.

Borda, Monica (2011). Fundamentals in Information Theory and Coding. *Springer*. p. 11.

Bressler, S. L., & Menon, V. (2010). Large-scale brain networks in cognition: emerging methods and principles. *Trends Cogn. Sci*. 14, 277–290.

Brooks, Frederick P. (1995). The mythical man-month: Essays on Software Engineering. Anniversary Edition (2nd Edition), Boston: Addison-Wesley, p.181-182 ISBN 0-201-83595-9.

Buckner, R. L., et al. (2009). Cortical hubs revealed by intrinsic functional connectivity: mapping, assessment of stability, and relation to Alzheimer's disease. *J. Neurosci*. 29, 1860–1873.

Carlsson, G., et al. (1994). Verbal and non-verbal function of children with right- versus left-hemiplegic cerebral palsy of pre- and perinatal origin. *Dev. Med. Child Neurol*. 36, 503–512.

Crick, Francis; Koch, Christof. (2005). What is the function of the claustrum?. Philosophical Transactions of the Royal Society B: Biological Sciences 360(1458): 1271–9.

Coombs, C. H., Dawes, R. M. & Tversky, A. (1970). Mathematical Psychology: An Elementary Introduction. Englewood Cliffs, New Jersey: Prentice-Hall.

Cover, T. M. & Thomas, J. A. (2006). Elements of Information Theory. John Wiley & Sons, New York.

Craft, A. (2005). Creativity in Schools: tensions and dilemmas. Routledge.

Davey, B. A. & Priestley, H. A. (2002). Maps between ordered sets. *Introduction to Lattices and Order* (2nd ed.). New York: Cambridge University Press. 23–24.

Deary, I. J., Johnson, W., & Houlihan, L. M. (2009). Genetic foundations of human intelligence. Hum Genet 126, 215–232.

Deutsch, David. (2012, October). The very laws of physics imply that artificial intelligence must be possible. What's holding us up? Aeon. Retrieved October, 2014, from http://aeon.co/magazine/technology/david-deutsch-artificial-intelligence/

Dietrich, A. (2004). The cognitive neuroscience of creativity. Psychon. *Bull. Rev*. 11, 1011–1026.

Dodge, Y. (2003). Entry for admissible decision function. *The Oxford Dictionary of Statistical Terms*. OUP. ISBN 0-19-920613-9

Edwards, W., Lindman, H., & Savage, L.J. (1963). Bayesian statistical inference in statistical research. *Psychological Review*, *70*, 193-242.

Einstein, Albert & Infeld, Leopold. (1938). *The evolution of physics*. Cambridge: Cambridge University Press. p. 92.

Engel, K. (1997). *Sperner theory*. Cambridge: Cambridge Univ. Press.

Engel, K. (n.d.). Sperner theorem. *Encyclopedia of Mathematics.* Retrieved June, 2014, from http://www.encyclopediaofmath.org/index.php?title=Sperner_theorem&oldid=12799

Estimated IQ's of Famous Geniuses. (2014). Genius. CSE Emory University. Retrieved July, 2014, from http://www.cse.emory.edu/sciencenet/mismeasure/genius/research04.html

Failure Rate: Statistics over IT projects failure rate. *IT Cortex*. Retrieved November, 2014, from http://www.it-cortex.com/Stat_Failure_Rate.htm

Field, Andy. (2013). *Discovering statistics using SPSS*. London: SAGE.

Fink, A., & Benedek, M. (2012). EEG alpha power and creative ideation. *Neurosci. Biobehav. Rev.* pii: S0149-7634(12)00211-4. doi: 10.1016/j.neubiorev.2012.12.002

Floridi, Luciano. (2010). Information: A Very Short Introduction. Oxford: Oxford University Press, ISBN 0-19-160954-4.

Fyhn, Marianne et al. (2015). Mathematics to reveal the secrets of the brain. University of Oslo. Retrieved February, 2015, from http://medicalxpress.com/partners/university-of-oslo/

Galambos, Janos & Simonelli, Italo. (2004). *Products of Random Variables: Applications to Problems of Physics and to Arithmetical Functions*. Vol.268. Marcel Dekker, Theorem 3.5. ISSN 0079-8177.

Galorath, D. (2012, June). Software Project Failure Costs Billions..Better Estimation & Planning Can Help. *Galorath*. Retrieved February, 2014, from http://www.galorath.com/wp/software-project-failure-costs-billions-better-estimation-planning-can-help.php

Global IT Project Management Survey. (2005). *KPMG International*. Retrieved May, 2014, from www.kpmg.com.au/Portals/0/irmpmqa-global-it-pm-Survey2005.pdf

Godwin, D., Barry, Robert L. and Marois, R. (2014), Breakdown of the brain's functional network modularity with awareness, Proceedings of the National Academy of Sciences, DOI: 10.1073/pnas.1414466112.

Gull, S. F. (1989). Some Misconceptions about Entropy. Retrieved April, 2014, from http://www.ucl.ac.uk/~ucesjph/reality/entropy/text.html

Halliwell, J. J. et al. (1994). Physical Origins of Time Asymmetry. *Cambridge*, 35-38.

Hoppe, C; Stojanovic J. (2008). High-aptitude minds: the neurological roots of genius. *Scientific American*. Retrieved August, 2013, from http://www.scientificamerican.com/article/high-aptitude-minds/

Human brain, Internet, and cosmology: Similar laws at work? (2012,November). Sciencedaily/University of California, San Diego. Retrieved June, 2015 from http://www.sciencedaily.com/releases/2012/11/121119140545.htm#

Ihara, Shunsuke. (1993). Information theory for continuous systems. *World Scientific*. p. 2.

Intelligence. (2013). *Merriam-Webster online dictionary*. Retrieved June, 2013, from http://www.merriam-webster.com/

Intellectual giftedness. (2015). In *Wikipedia, the free encyclopedia*. Retrieved March, 2014, from https://en.wikipedia.org/wiki/Intellectual_giftedness Mifflin.

Jackson, Joab. (2014, December). MIT unifies Web dev into a single,speedy new language –Ur/Web. Retrieved December 24, 2014, from http://www.computerworld.com/article/2863069/application-development/mit-unifies-web-dev-into-a-single-speedy-new-language-urweb.html

Jaynes, E.T. (1986). Bayesian Methods: General Background. Cambridge:Cambridge Univ. Press.

Jech, Thomas. (2008). *The Axiom of Choice*. New York: Dover Publications.

Jia Qi et al. (2014). A glutamatergic reward input from the dorsal raphe to ventral tegmental area dopamine neurons. *Nature Communications*, *5*(5390).

Jung, R. E., Segall, J. M., Jeremy Bockholt, H., Flores, R. A., Smith, S. M., Chavez, R. S., et al. (2010). Neuroanatomy of creativity. *Hum. Brain Mapp*. 31, 398–409.

Jung, R. E., Gasparovic, C., Chavez, R. S., Caprihan, A., Barrow, R., & Yeo, R. A. (2009). Imaging intelligence with proton magnetic resonance spectroscopy. *Intelligence* 37, 192–198.

Justice, J. H. (1986). *In Maximum-Entropy and Bayesian Methods in Applied Statistics*. Cambridge: Cambridge Univ. Press.

Kahan, William. (1987). Branch cuts for complex elementary functions, or Much ado about nothing's sign bit. In *The State of the Art in Numerical Analysis* (eds. Iserles and Powell), Oxford: Clarendon Press.

Kaufman, S. B. (2014, December). The Messy Minds of Creative People. *Beautiful Minds*. Retrieved April, 2014, from http://blogs.scientificamerican.com/beautiful-minds/2014/12/ 24/the-messy-minds-of-creative-people/#ixzz3NOSEKKON

Kennard, E. H. (1927). Zur Quantenmechanik einfacher Bewegungstypen. *Zeitschrift für Physik*, *44*(4–5), 326.

Krigsman, M. (2011, March). CIO analysis: Why 37 percent of projects fail. Retrieved October, 2013 from http://www.zdnet.com/blog/projectfailures/cio-analysis-why-37-percent-of-projects-fail/12565

Krioukov, D., Kitsak, M., Sinkovits, R. S, Rideout, D., Meyer, D. & Marián Boguñá, M. (2012). Network Cosmology. *Nature's Scientific Reports 2*, Article number: 793, doi: 10.1038/srep00793.

Krishnamoorthy, Kalimuthu. (2006). *Handbook of Statistical Distributions with Applications*. Chapman & Hall/CRC. P.127.

Ihara, Shunsuke. (1993). Information theory for continuous systems. *World Scientific*. p. 2.

Lackenby, M. (2000). Word hyperbolic Dehn surgery, Invent. *Math*. *140*(2), 243–282.

Lee, H., Devlin J. T., Shakeshaft, C., Stewart, L. H., Brennan, A., Glensman, J., Pitcher, K., Crinion, J., Mechelli, A., Frackowiak, R. S., Green, D. W, Price, C. J. (2007). "Anatomical traces of vocabulary acquisition in the adolescent brain". *J Neurosci 27*(5): 1184–9.

Lee, P. M. (1997). *Bayesian Statistics: An Introduction*. Arnold. ISBN 0-340-67785-6.

Leydesdorff, Leot.(1991). The Static and Dynamic Analysis of Network Data using Information Theory. *Social Networks*, North-Holland, 13, p. 6, 306-310, 312.

Liu, S., et al.(2012). Neural correlates of lyrical improvisation: an FMRI study of freestyle rap. *Sci. Rep*. 2:834.

Linden, N., Popescu, S., Short, Anthony J., and Winter, A. (2009). Quantum mechanical evolution towards thermal equilibrium. *Phys. Rev. E* 79, 061103.

Limb, C. J., and Braun, A. R. (2008). Neural substrates of spontaneous musical performance: an FMRI study of jazz improvisation. *PLoS ONE 3*:e1679.

Lord Kelvin. (1883). Electrical units of measurement. *PLA*, vol. 1.

Luders, E.; Narr, K. L.; Thompson, P. M.; Toga, A. W. (2008). "Neuroanatomical Correlates of Intelligence". *Intelligence* 37(2): 156–163.

Lukacs, Eugene & King, Edgar P. (1954). A Property of Normal Distribution. *The Annals of Mathematical Statistics*, *25*(2), 389–394.

Malone, D. & Sullivan W. (2004). 'Guesswork and Entropy'. IEEE Transactions On Information Theory, 50:525 - 526.

Malone, D. & Sullivan, W. (2005). Guesswork is not a Substitute for Entropy. *Proceedings of the Information Technology & Telecommunications Conference*. Retrieved March 31, 2014, from http://www.maths.tcd.ie/~dwmalone/p/itt05.pdf

Mapping structural and functional connections in the human brain. (2014). *Human Connectome Project*. Retrieved June, 2014, from http://www.humanconnectome.org/about/project/pulse-sequences.html

Massey, J. L. (1994). Guessing and entropy. Paper presented at the *Information Theory, 1994. Proceedings*., 1994 *IEEE International Symposium* on, pp. 204. doi:10.1109/ISIT.1994.394764.

McDaniel, Michael (2005). Big-brained people are smarter. *Intelligence* 33: 337–346.

Mesulam, M. M. (1998). From sensation to cognition. *Brain* 121, 1013–1052.

Mohr, P. J.; Taylor, B. N. & Newell, D. B. (2011, June). The 2010 CODATA Recommended Values of the Fundamental Physical Constants. Web Version 6.0. *National Institute of Standards and Technology*. Retrieved May, 2014, from http://physics.nist.gov

Moore, W. J. (1992). Schrödinger: Life and Thought. Cambridge University Press.

Normal distribution. (2014). *In Wikipedia, the free encyclopedia*. Retrieved March, 2014, from http://en.wikipedia.org/wiki/Normal_distribution

Norwich, Kenneth H. (2003). *Information, Sensation and Perception*. Biopsychology.org. Esteban Barrull: Academic Press, p. 82.

Palazzo, Pierfrancesco. (2012). Thermal and mechanical aspect of entropy-exergy relationship. *International Journal of Energy and Environmental Engineering*, 3:4 doi:10.1186/2251-6832-3-4.

Patel, Jagdish K. & Read, Campbell B. (1996). *Handbook of the Normal Distribution* (2nd ed.). CRC Press, [2.3.6].

Peckham, Matt. (2012, November). Universe, human brain and Internet have similar structures. *Time*. Retrieved October, 2014, from http://techland.time.com/2012/11/28/your-brain-the-internet-and-the-universe-have-something-fascinating-in-common/

Peters, L. J., & Tripp, L. L.(1976). Is Software Design Wicked? *Datamation*, *22*(5), 127 – 136.

Plomin, R., DeFries, J. C., Knopik, V. S., Neiderhiser, J. M. (2013). Behavioral genetics 6th edn. Worth Publishers: New York.

Press, William H.; Flannery, Brian P.; Teukolsky, Saul A. & Vetterling, William T. (1992). Numerical Recipes: the Art of Scientific Computing (3rd ed.). Cambridge University Press. p. 761.

Preuss, D. H. (2006, August). Interview: Jim Johnson of the Standish Group. Retrieved Febuary, 2014, from http://www.infoq.com/articles/Interview-Johnson-Standish-CHAOS

Quine, M. P. (1993). On three characterisations of the normal distribution. *Probability and Mathematical Statistics*, *14*(2), 257-263.

Raichle, M. E. & Snyder, A. Z. (2007). A default mode of brain function: a brief history of an evolving idea. *Neuroimage* 37, 1083–1090.

Remedios, R.; Logothetis, N. K. & Kayser, C. (2010). Unimodal Responses Prevail within the Multisensory Claustrum. *Journal of Neuroscience* 30(39): 12902–7.

Renzulli, J. (1978, November). "What Makes Giftedness? Reexamining a Definition". *Phi Delta Kappan* 60 (3): 180–84, 261.

Rice, John. (1995). Mathematical Statistics and Data Analysis (Seconded.). Duxbury Press.

Rich, Barnett & Sandchmidt, Philip. (2004). *Schaum's Outline of Theory and Problems of Elementary Algebra*. The McGraw-Hill Companies. Chapter 13 §4.4, p. 291. ISBN 0-07-141083-X.

Rosado, J. I. (2011). Representation of quantum states as points in a probability simplex associated to a SIC-POVM. *Foundations of Physics*, *41*(3), 1200–13.

Rozema, L. A.; Darabi, A.; Mahler, D. H.; Hayat, A.; Soudagar, Y.; Steinberg, A. M. (2012). Violation of Heisenberg's Measurement-Disturbance Relationship by Weak Measurements. *Physical Review Letters*, *109*(10).

Smith, Gordon B., Sederberg, A., Elyada, Yishai M., Van Hooser, Stephen D., Kaschube, Matthias & Fitzpatrick, D. (2015). The development of cortical circuits for motion discrimination. *Nature Neuroscience*, 18 (252–261).

Smith, J. B. & Alloway, K. D. (2010). Functional Specificity of Claustrum Connections in the Rat: Interhemispheric Communication between Specific Parts of Motor Cortex. *Journal of Neuroscience*, 30(50): 16832–44.

Saggar, Manish et al. (2015). Pictionary-based fMRI paradigm to study the neural correlates of spontaneous improvisation and figural creativity. *Scientific Reports*, 5(10894).

Saunders, Arpiar et al. (2015). A direct GABAergic output from the basal ganglia to frontal cortex. *Nature*, doi: 10.1038/nature14179.

Stairs, Allen (2011). A loose and separate certainty: Caves, Fuchs and Schack on quantum probability one. *Studies In History and Philosophy of Science Part B: Studies In History and Philosophy of Modern Physics*, *42*(3), 158–166.

Swaminathan, Nikhil. (2008). Why Does the Brain Need So Much Power? *Scientific American*. Retrieved August, 2013, from http://www.scientificamerican.com/article/why-does-the-brain-need-s/

Takeuchi, H., et al. (2012). The Association between Resting Functional Connectivity and Creativity. *Cerebral Cortex*, 22:2921± 2929.

Thorme, Christian et al. (2014). Axon-Carrying Dendrites Convey Privileged Synaptic Input in Hippocampal Neurons. *Neuron*, *83*(6), 1418–1430.

Tuisku, P., Pernu, and T.K., Annila, A. (2009). In the light of time. *Proceedings of the Royal Society A* 465: 1173–1198.

Universe, human brain and Internet have similar structures. (1998-2015). *Z news*. Retrieved October, 2014, from http://zeenews.india.com/news/net-news/universe-human-brain-and-internet-have-similar-structures_812821.html

What Goes Into the Making of a Genius? (2014). *IQ Test Experts*. Retrieved July, 2014, from http://www.iqtestexperts.com/making-genius.php

Weyl, H. (1928). *Gruppentheorie und Quantenmechanik*, Leipzig: Hirzel. Claude Cohen-Tannoudji, Bernard Diu, Franck Laloë. (1996). *Quantum mechanics*. Wiley-Interscience: Wiley, 231–233.

White, Jim; Steingold, Sam and Fournelle, Connie. (2004). Performance Metrics for Group-Detection Algorithms. *Interface*. Retrieved May, 2014, from http://www.interfacesymposia.org/I04/I2004Proceedings/WhiteJim/WhiteJi m.presentation.pdf

Why Projects Fail? (2012). *McKinsey & University of Oxford. Calleam Consulting Ltd*. Retrieved October, 2013, from http://calleam.com/WTPF/?page_id=1445

Wicker, Stephen B. and Kim, Saejoon. (2003). Fundamentals of Codes,Graphs, and Iterative Decoding. *Springer*. pp. 1 ff. ISBN 1-4020-7264-3.

Wolchover, Natalie. (2014), Time's Arrow Traced to Quantum Source. *Quanta Magazine*. Retrieved April, 2014, from http://www.simonsfoundation.org/quanta/20140416-times-arrow-traced-to-quantum-source/

Wolf, U., Rapoport, M. J., Schweizer, T. A. (2009). Evaluating the affective component of the cerebellar cognitive affective syndrome. *J. Neuropsychiatry Clin. Neurosci.*, *21*(3), 245–53.

Zar, J.H. (1984). *Biostatistical Analysis.* Prentice Hall International, New Jersey. 43–45.

Zuev, Konstantin; Boguñá, Marián ; Bianconi, Ginestra & Krioukov, Fuchs, C. A.; Schack, R. (2011). A Quantum-Bayesian route to quantum-state space. *Foundations of Physics*, *41*(3), 345–56.